# HYPOXIA IN KIDNEY DISEASE

EDITED BY: Maarten Koeners and Fredrik Palm
PUBLISHED IN: Frontiers in Physiology

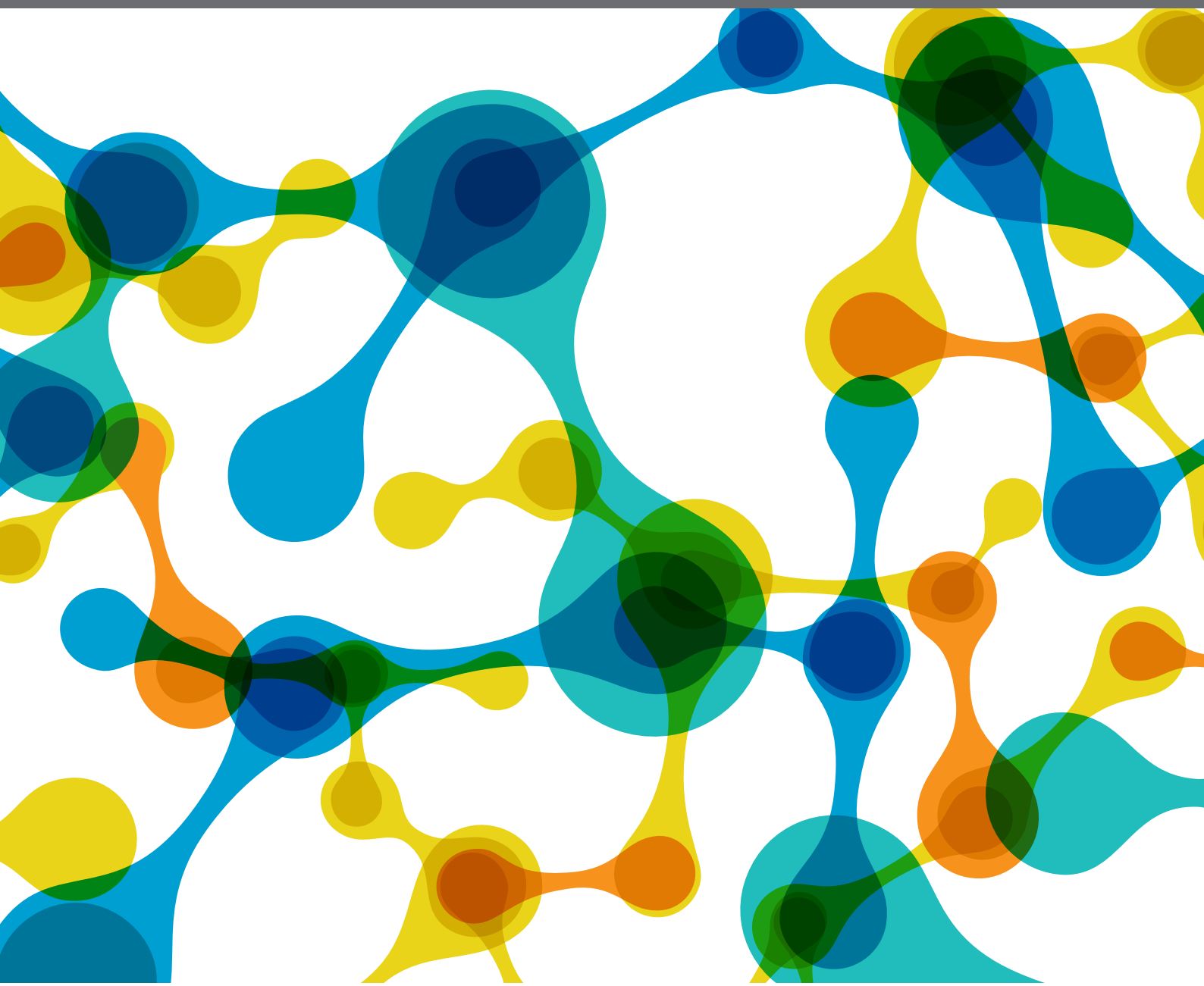

frontiers Research Topics

ISSN 1664-8714
ISBN 978-2-88945-617-8
DOI 10.3389/978-2-88945-617-8

## About Frontiers

Frontiers is more than just an open-access publisher of scholarly articles: it is a pioneering approach to the world of academia, radically improving the way scholarly research is managed. The grand vision of Frontiers is a world where all people have an equal opportunity to seek, share and generate knowledge. Frontiers provides immediate and permanent online open access to all its publications, but this alone is not enough to realize our grand goals.

## Frontiers Journal Series

The Frontiers Journal Series is a multi-tier and interdisciplinary set of open-access, online journals, promising a paradigm shift from the current review, selection and dissemination processes in academic publishing. All Frontiers journals are driven by researchers for researchers; therefore, they constitute a service to the scholarly community. At the same time, the Frontiers Journal Series operates on a revolutionary invention, the tiered publishing system, initially addressing specific communities of scholars, and gradually climbing up to broader public understanding, thus serving the interests of the lay society, too.

## Dedication to Quality

Each Frontiers article is a landmark of the highest quality, thanks to genuinely collaborative interactions between authors and review editors, who include some of the world's best academicians. Research must be certified by peers before entering a stream of knowledge that may eventually reach the public - and shape society; therefore, Frontiers only applies the most rigorous and unbiased reviews.
Frontiers revolutionizes research publishing by freely delivering the most outstanding research, evaluated with no bias from both the academic and social point of view. By applying the most advanced information technologies, Frontiers is catapulting scholarly publishing into a new generation.

## What are Frontiers Research Topics?

Frontiers Research Topics are very popular trademarks of the Frontiers Journals Series: they are collections of at least ten articles, all centered on a particular subject. With their unique mix of varied contributions from Original Research to Review Articles, Frontiers Research Topics unify the most influential researchers, the latest key findings and historical advances in a hot research area! Find out more on how to host your own Frontiers Research Topic or contribute to one as an author by contacting the Frontiers Editorial Office: researchtopics@frontiersin.org

# HYPOXIA IN KIDNEY DISEASE

Topic Editors:
**Maarten Koeners,** University of Bristol, United Kingdom
**Fredrik Palm,** Uppsala University, Sweden

**Citation:** Koeners, M., Palm, F., eds (2018). Hypoxia in Kidney Disease. Lausanne: Frontiers Media. doi: 10.3389/978-2-88945-617-8

# Table of Contents


*04* ***Editorial: Hypoxia in Kidney Disease***
Fredrik Palm and Maarten P. Koeners

*07* ***Cooperative Oxygen Sensing by the Kidney and Carotid Body in Blood Pressure Control***
Daniela Patinha, Wioletta Pijacka, Julian F. R. Paton and Maarten P. Koeners

*20* ***Multiparametric Renal Magnetic Resonance Imaging: Validation, Interventions, and Alterations in Chronic Kidney Disease***
Eleanor F. Cox, Charlotte E. Buchanan, Christopher R. Bradley, Benjamin Prestwich, Huda Mahmoud, Maarten Taal, Nicholas M. Selby and Susan T. Francis

*35* ***Renal Oxygenation in the Pathophysiology of Chronic Kidney Disease***
Zhi Zhao Liu, Alexander Bullen, Ying Li and Prabhleen Singh

*44* ***Innovative Perspective: Gadolinium-Free Magnetic Resonance Imaging in Long-Term Follow-Up After Kidney Transplantation***
Mick J. M. van Eijs, Arjan D. van Zuilen, Anneloes de Boer, Martijn Froeling, Tri Q. Nguyen, Jaap A. Joles, Tim Leiner and Marianne C. Verhaar

*56* ***Mitochondrial Reactive Oxygen Species and Kidney Hypoxia in the Development of Diabetic Nephropathy***
Tomas A. Schiffer and Malou Friederich-Persson

*68* ***Circadian Rhythm in Kidney Tissue Oxygenation in the Rat***
Tonja W. Emans, Ben J. Janssen, Jaap A. Joles and C. T. Paul Krediet

*75* ***Blood Pressure Increase During Oxygen Supplementation in Chronic Kidney Disease Patients Is Mediated by Vasoconstriction Independent of Baroreflex Function***
René van der Bel, Müşerref Çalişkan, Robert A. van Hulst, Johannes J. van Lieshout, Erik S. G. Stroes and C. T. Paul Krediet

*83* ***Renal Hypoxia in CKD; Pathophysiology and Detecting Methods***
Yosuke Hirakawa, Tetsuhiro Tanaka and Masaomi Nangaku

*93* ***Stress Signal Network Between Hypoxia and ER Stress in Chronic Kidney Disease***
Hiroshi Maekawa and Reiko Inagi

*98* ***Blood Oxygenation Level-Dependent MRI to Assess Renal Oxygenation in Renal Diseases: Progresses and Challenges***
Menno Pruijm, Bastien Milani and Michel Burnier

*105* ***Hyperpolarized Renal Magnetic Resonance Imaging: Potential and Pitfalls***
Christoffer Laustsen

frontiers in Physiology

EDITORIAL
published: 03 May 2018
doi: 10.3389/fphys.2018.00485

# Editorial: Hypoxia in Kidney Disease

*Fredrik Palm*[1] *and Maarten P. Koeners*[2,3]*

[1] Department of Medical Cell Biology, Uppsala University, Uppsala, Sweden, [2] Institute of Biomedical and Clinical Science, University of Exeter Medical School, University of Exeter, Exeter, United Kingdom, [3] School of Physiology, Pharmacology and Neuroscience, Biomedical Sciences, University of Bristol, Bristol, United Kingdom

**Keywords: kidney hypoxia, chronic kidney disease, hypertension, magnetic resonance imaging, mitochondrial uncoupling, telemetry, kidney transplantation, sympathetic nerve activity**

**Editorial on the Research Topic**

**Hypoxia in Kidney Disease**

## INTRODUCTION

Oxygen was first described by Carl Wilhelm Scheele as "Fire air" since it supported combustion. He obtained oxygen by heating mercuric oxide, silver carbonate, and nitrate salts. Scheele communicated his findings to Lavoisier, who realized the significance of this finding. Scheele's discovery of oxygen (ca. 1771) was chronologically earlier than the corresponding work of Priestley and Lavoisier, but he did not publish this discovery until 1777, after both of his rivals had already published their findings (West, 2014). Because others generally are accredited for the discovery of oxygen, and a number of other discoveries, he was nicknamed "hard-luck Scheele."

Oxygen is essential for aerobic metabolism, a fundamental mechanism for energy production. The delivery of optimal levels of oxygen to tissues is tightly regulated as both hypoxia and hyperoxia are detrimental for cellular function. Indeed, tissue hypoxia has been found during pathological conditions such as cancer (Liu et al., 2016), diabetes (Palm et al., 2003), hypertension (Welch et al., 2001), chronic kidney disease (CKD) (Milani et al., 2016), and stroke (Ferdinand and Roffe, 2016). In the 90's Fine et al. proposed kidney hypoxia as a mediator of progressive kidney disease (Fine et al., 1998). Since then, experimental and clinical studies have solidified the view that kidney hypoxia plays a critical role during the genesis and progression of both acute and CKD. This research field is currently at the beginning of integrating pre-clinical with clinical research in which kidney hypoxia related mechanisms are quantified by non-invasive imaging. In combination with the fact that some key questions remain unanswered, this offers exciting new research perspectives that are waiting to be explored. With this Frontiers Research Topic we discuss and identify potential mediators/controllers of hypoxia in kidney disease. If we understand more about the sequence of events leading to kidney hypoxia, its regulation and consequences in renal disease, we might be able to have a major impact in clinical practice. I.e., more accurate and earlier diagnosis, novel treatment targets, and novel therapies.

## HYPOXIA IN KIDNEY DISEASE

Liu et al. describes the alterations in renal oxygenation (delivery, consumption and tissue oxygen tension) in pre-clinical and clinical studies in diabetic and hypertensive CKD along with the underlying mechanisms and potential therapeutic options. The novel hypothesis by Patinha et al. on the cooperative oxygen sensing by the kidney and carotid body in blood pressure control, could further explain the role of kidney hypoxia in hypertension. This is relevant for the pursuit of novel ways to treat associated with sympathetic overdrive. Indeed, Hering et al. reduced sympathetic

OPEN ACCESS

***Edited and reviewed by:***
*Matthew A. Bailey, University of Edinburgh, United Kingdom*

***Correspondence:**
*Maarten P. Koeners*
*m.p.koeners@exeter.ac.uk*

***Specialty section:***
*This article was submitted to Renal and Epithelial Physiology, a section of the journal Frontiers in Physiology*

***Received:*** *07 March 2018*
***Accepted:*** *16 April 2018*
***Published:*** *03 May 2018*

***Citation:***
*Palm F and Koeners MP (2018) Editorial: Hypoxia in Kidney Disease. Front. Physiol. 9:485. doi: 10.3389/fphys.2018.00485*

nerve activity and lowered blood pressure in CKD patients using 100% oxygen (Hering et al., 2007). Furthermore, van der Bel et al. assessed the underlying hemodynamic modulation and found that oxygen supplementation in CKD patients caused a non-baroreflex-mediated increase in vascular resistance and blood pressure. Conceivably, within their experimental set-up, the effects of oxygen on systemic vasoconstriction (leading to baroreflex deactivation with reduction in sympathetic tone) did not allow for the detection of any possible subtle effects of kidney specific oxygenation on sympathetic outflow.

Maekawa et al. describes that elevated levels of the uremic toxin indoxyl sulfate (IS) in CKD can induce endoplasmatic reticulum (ER) stress and subsequent hypoxia through suppression of erythropoiesis and exacerbation of tubular fibrosis. They propose that the removal of IS, blockage of aryl hydrocarbon receptor (mediator of IS-induced suppression of erythropoietin production), inhibition of hepcidin production (controls iron homeostasis) and mediation of the ER unfolded protein pathway could be therapeutic targets in ameliorating hypoxia and subsequent CKD progression. Preserving mitochondrial uncoupling might be a potential treatment target. Indeed, kidney hypoxia *per se*, caused by mitochondrial uncoupling, without confounding factors such as uraemia, hyperglycaemia or hypertension results in albuminuria and tubulointerstitial damage (Friederich-Persson et al., 2013). Schiffer et al. proposes that diabetic nephropathy is likely a joint mechanism of mitochondrial reactive oxygen species production, which include altered mitophagy, mitochondrial dynamics, mitochondrial uncoupling, and signaling through AMP-activated protein kinase and hypoxia-inducible factors. Therefore, prevention or correction of mitochondrial dysfunction might be pivotal in treating diabetic kidney disease.

## HYPOXIA QUANTIFICATION IN KIDNEY DISEASE

Hirakawa et al. addresses the pathophysiological importance of renal hypoxia with a focus on hypoxia detection and quantification. Although kidney tissue oxygenation has been studied for a long time, recent advances have made it possible to achieve continuous measurements, non-invasive oxygen assessments, and intracellular oxygen assessments. Using oxygen tension telemetry Emans et al. demonstrate circadian variation in kidney tissue oxygenation with maximal values during the lights-off period, when renal excretion of electrolytes was highest. These type of experiments will allow long-term investigation of kidney oxygenation in relation to disease development, including the investigation of circadian influence on normal physiology and disease development (Adamovich et al., 2017). Blood Oxygenation-Level Dependent (BOLD) magnetic resonance imaging (MRI) allows for non-invasive estimation of kidney oxygenation in humans, without the need for administration of exogenous contrast agents. Pruijm et al. summarizes the growing knowledge of factors that influence the BOLD-signal and how this has led to better standardization, refinements, and reproducibility. BOLD, alone or in combination with other MRI modalities, could therefore contribute to patient stratification, earlier diagnosis, and improve long-term follow up. Indeed, Eijs et al. report that functional MRI (including BOLD) has the potential to detect several pathophysiological mechanisms involved in kidney allograft dysfunction, making it a promising tool in long-term follow-up of kidney transplantation patients. In addition, Cox et al. showed in a pilot study that multiparametric MRI could assess renal structure, hemodynamics and oxygenation in healthy participants and CKD patients. Renal blood flow and renal cortex perfusion was lower in CKD patients compared with healthy participants. Longitudinal relaxation time ($T_1$ values), an MRI parameter that increases with reduced perfusion/filtration and/or progressive scarring, were increased in both renal cortex and medulla compared to healthy participants, though primarily in cortex, resulting in a loss of corticomedullary differentiation. Finally, Laustsen describes how the introduction of dissolution dynamic nuclear polarization technology has enabled a new paradigm for renal MRI. They describe the utility of hyperpolarized MRI in preclinical research in which the real-time interrogation of metabolic turnover has already aided the physiological and pathophysiological metabolic and functional effects in *ex vivo* and *in vivo* models, and discus its potential translation to renal patients.

## CONCLUSION

This research topic highlights the important role of hypoxia in kidney disease and what progress has been made to address its importance. We conclude that it is imperative to further advance our understanding about the sequence of events leading to intrarenal tissue hypoxia, its regulation and consequences in both acute and CKD. If we do that, we might be able to end Scheele's "hard-luck" and have a major impact of patient care and reduce the poor quality of life often associated with kidney disease.

## AUTHOR CONTRIBUTIONS

MK: conceived the content and drafted the manuscript; MK and FP: revised and approved the final manuscript.

## ACKNOWLEDGMENTS

This work was supported by the British Heart Foundation (FS/14/2/30630), the European Union, Seventh Framework Programme, Marie Curie Actions (CARPEDIEM - No 612280), the Swedish Research Council and the Swedish Diabetes Foundation.

## REFERENCES


Adamovich, Y., Ladeuix, B., Golik, M., Koeners, M. P., and Asher, G. (2017). Rhythmic oxygen levels reset circadian clocks through HIF1alpha. *Cell Metab.* 25, 93–101. doi: 10.1016/j.cmet.2016.09.014

Ferdinand, P., and Roffe, C. (2016). Hypoxia after stroke: a review of experimental and clinical evidence. *Exp. Transl. Stroke Med.* 8, 9. doi: 10.1186/s13231-016-0023-0

Fine, L. G., Orphanides, C., and Norman, J. T. (1998). Progressive renal disease: the chronic hypoxia hypothesis. *Kidney Int. Suppl.* 65, S74–S78.

Friederich-Persson, M., Thörn, E., Hansell, P., Nangaku, M., Levin, M., and Palm, F. (2013). Kidney hypoxia, attributable to increased oxygen consumption, induces nephropathy independently of hyperglycemia and oxidative stress. *Hypertension* 62, 914–919. doi: 10.1161/HYPERTENSIONAHA.113.01425

Hering, D., Zdrojewski, Z., Król, E., Kara, T., Kucharska, W., Somers, V. K., et al. (2007). Tonic chemoreflex activation contributes to the elevated muscle sympathetic nerve activity in patients with chronic renal failure. *J. Hypertens.* 25, 157–161. doi: 10.1097/HJH.0b013e3280102d92

Liu, L., Zhao, X., Zou, H., Bai, R., Yang, K., and Tian, Z. (2016). Hypoxia promotes gastric cancer malignancy partly through the HIF-1alpha dependent transcriptional activation of the long non-coding RNA GAPLINC. *Front. Physiol.* 7:420. doi: 10.3389/fphys.2016.00420

Milani, B., Ansaloni, A., Sousa-Guimaraes, S., Vakilzadeh, N., Piskunowicz, M., Pruijm, B., et al. (2016). Reduction of cortical oxygenation in chronic kidney disease: evidence obtained with a new analysis method of blood oxygenation level-dependent magnetic resonance imaging. *Nephrol. Dial. Transplant.* 32, 2097–2105. doi: 10.1093/ndt/gfw362

Palm, F., Cederberg, J., Hansell, P., Liss, P., and Carlsson, P. O. (2003). Reactive oxygen species cause diabetes-induced decrease in renal oxygen tension. *Diabetologia* 46, 1153–1160. doi: 10.1007/s00125-003-1155-z

Welch, W. J., Baumgärtl, H., Lübbers, D., and Wilcox, C. S. (2001). Nephron $pO_2$ and renal oxygen usage in the hypertensive rat kidney. *Kidney Int.* 59, 230–237. doi: 10.1046/j.1523-1755.2001.00483.x

West, J. B. (2014). Carl Wilhelm Scheele, the discoverer of oxygen, and a very productive chemist. *Am. J. Physiol. Lung Cell. Mol. Physiol.* 307, L811–L816. doi: 10.1152/ajplung.00223.2014


**Conflict of Interest Statement:** The authors declare that the research was conducted in the absence of any commercial or financial relationships that could be construed as a potential conflict of interest.

frontiers in Physiology

HYPOTHESIS AND THEORY
published: 04 October 2017
doi: 10.3389/fphys.2017.00752

# Cooperative Oxygen Sensing by the Kidney and Carotid Body in Blood Pressure Control

*Daniela Patinha*[1,2], *Wioletta Pijacka*[1], *Julian F. R. Paton*[1]* and *Maarten P. Koeners*[1,2]*

[1] School of Physiology, Pharmacology and Neuroscience, Biomedical Sciences, University of Bristol, Bristol, United Kingdom,
[2] Institute of Biomedical and Clinical Science, University of Exeter Medical School, University of Exeter, Exeter, United Kingdom

Oxygen sensing mechanisms are vital for homeostasis and survival. When oxygen levels are too low (hypoxia), blood flow has to be increased, metabolism reduced, or a combination of both, to counteract tissue damage. These adjustments are regulated by local, humoral, or neural reflex mechanisms. The kidney and the carotid body are both directly sensitive to falls in the partial pressure of oxygen and trigger reflex adjustments and thus act as oxygen sensors. We hypothesize a cooperative oxygen sensing function by both the kidney and carotid body to ensure maintenance of whole body blood flow and tissue oxygen homeostasis. Under pathological conditions of severe or prolonged tissue hypoxia, these sensors may become continuously excessively activated and increase perfusion pressure chronically. Consequently, persistence of their activity could become a driver for the development of hypertension and cardiovascular disease. Hypoxia-mediated renal and carotid body afferent signaling triggers unrestrained activation of the renin angiotensin-aldosterone system (RAAS). Renal and carotid body mediated responses in arterial pressure appear to be synergistic as interruption of either afferent source has a summative effect of reducing blood pressure in renovascular hypertension. We discuss that this cooperative oxygen sensing system can activate/sensitize their own afferent transduction mechanisms via interactions between the RAAS, hypoxia inducible factor and erythropoiesis pathways. This joint mechanism supports our view point that the development of cardiovascular disease involves afferent nerve activation.

**Keywords: hypoxia, kidney, carotid body, hypertension, angiotensin II**

OPEN ACCESS

***Edited by:***
*Marcelo D. Carattino, University of Pittsburgh, United States*

***Reviewed by:***
*Heather Drummond, University of Mississippi Medical Center School of Dentistry, United States*
*Ignacio Gimenez, Aragon's Health Sciences Institute, Spain*

***Correspondence:**
*Julian F. R. Paton*
*Julian.F.R.Paton@bristol.ac.uk*
*Maarten P. Koeners*
*M.P.Koeners@exeter.ac.uk*

***Specialty section:***
*This article was submitted to Renal and Epithelial Physiology, a section of the journal Frontiers in Physiology*

***Received:*** *07 April 2017*
***Accepted:*** *15 September 2017*
***Published:*** *04 October 2017*

***Citation:***
*Patinha D, Pijacka W, Paton JFR and Koeners MP (2017) Cooperative Oxygen Sensing by the Kidney and Carotid Body in Blood Pressure Control. Front. Physiol. 8:752. doi: 10.3389/fphys.2017.00752*

## INTRODUCTION

Oxygen is essential for aerobic metabolism, a fundamental mechanism for energy production. However, the delivery of optimal levels of oxygen to tissues must be highly regulated as both insufficient (hypoxia) or excessive oxygen levels (hyperoxia) are highly detrimental. Indeed, tissue oxygenation has been found to be reduced during pathological conditions such as cancer (Liu et al., 2016), diabetes (Palm et al., 2003), hypertension (Welch et al., 2001), chronic kidney disease (Milani et al., 2016), and stroke (Ferdinand and Roffe, 2016). We will explore the idea that an inappropriate activation of some of the signaling pathways that counteract hypoxia can contribute to the development of hypertension and cardiovascular disease through activation of the sympathetic nervous system.

Adaptation to low partial pressure of oxygen, for instance at high altitude, triggers a protective mechanism that includes an increase in sympathetic activity, vascular resistance, and blood pressure (Hainsworth and Drinkhill, 2007). The kidney and carotid body both participate in this adaptation for the maintenance of systemic oxygen levels and blood flow (Marshall, 1994; Dunn et al., 2007; Jelkmann, 2011). For example, within the kidney the number of erythropoietin-producing cells increases proportionally to the degree of hypoxia, which correlates directly with the concentration of erythropoietin in blood (Koury and Haase, 2015), ensuring higher blood oxygen carrying capacity (Marshall, 1994; Dunn et al., 2007; Jelkmann, 2011). In comparison, the carotid body triggers reflex increases ventilation and sympathetic activity to maintain oxygen tension and delivery (Marshall, 1994). Interestingly the kidney and the carotid body are both innervated by efferent and afferent nerve fibers and are both targets and modulators of sympathetic activity. Hypoxic-hypoperfusion of the kidney and carotid body is a likely trigger for increased reflex sympathetic activity (Koeners et al., 2016) and aberrant afferent drive from these organs is implicated in the etiology of neurogenic hypertension (Fisher and Paton, 2012; Narkiewicz et al., 2016; Silva et al., 2016; Osborn and Foss, 2017).

We wish to explore whether there is cooperative oxygen sensing between the kidney and the carotid body that plays a role in homeostasis. We will consider this notion under physiological conditions where it counteracts moderate or brief tissue hypoxia over an acute short time scale (minutes to hours). We will also assess the long term (days) cooperative oxygen sensing where hypoxia afferent signaling from these organs persists and drives the progression of cardiovascular disease. We initiate our discussion by examining the effect of short and long term hypoxia on the kidney and carotid body.

## HYPOXIA, AFFERENT NERVE ACTIVATION/SENSITIZATION AND HYPERTENSION

### Hypoxia

Oxygen delivery to different organs is a product of cardiac output and arterial oxygen content per unit of time (Habler and Messmer, 1997; Leach and Treacher, 2002). The majority of oxygen transported throughout the body is reversibly bound to hemoglobin, and its diffusion to the cell is dependent on the local tissue partial pressure gradient. Oxygen consumption in a given tissue is the volume of oxygen consumed per unit of time, which in aerobic conditions corresponds to the metabolic rate [adenosine triphosphate (ATP) formation/consumption] (Habler and Messmer, 1997; Leach and Treacher, 2002). Each organ has a different metabolic rate, and hence a different oxygen demand. Every organ has the capacity of altering their metabolic rate (except skin), as part of the local dynamics which, in most cases, directly influences local blood flow. Due to an oxygen reserve, oxygen consumption is independent of oxygen delivery within a wide range of delivered oxygen. In addition, organs have different oxygen extraction ratios (fraction of oxygen delivery) and different oxygen reserves. Organs that have a lower oxygen extraction, such as the skin, have a higher oxygen venous reserve. Conversely, the heart and the brain have a limited oxygen reserve due to the high oxygen extraction (Habler and Messmer, 1997). In case of systemic low oxygen delivery or systemic high oxygen demand, blood can be redistributed to sustain high extraction organs, without compromising oxygen supply to the ones with higher oxygen reserves. However, increases in oxygen consumption or decreases in oxygen delivery will increase oxygen extraction to maintain aerobic metabolism. When the critical oxygen delivery limit is reached, any increase in oxygen consumption or decrease in oxygen delivery will lead to tissue hypoxia, as reviewed in Leach and Treacher (2002).

The term hypoxia represents a reduced partial pressure of oxygen and deoxygenation of tissue. Such a condition triggers a series of responses that manifest themselves over different sequential time frames: First, acute systemic reduction of tissue oxygen partial pressure stimulates peripheral chemoreceptors that triggers respiratory and cardiovascular responses to elevate oxygen uptake and delivery to bodily organs (Lahiri et al., 1980; Marshall, 1994; Blessing et al., 1999). Second, persistent subacute hypoxia activates cellular pathways through the stabilization of hypoxia inducible factor (HIF)-1 and HIF-2 complexes (Greer et al., 2012). HIF-1 is understood to be the most important regulator of cellular responses to hypoxia. This long term adaptation is triggered in order to enhance the oxygen delivery capacity and maintain organ function, including glycolysis, angiogenesis, erythropoiesis, iron metabolism, pH regulation, apoptosis, cell proliferation as well as cell-cell, and cell-matrix interactions (Haase, 2006; Greer et al., 2012). Examples of classic HIF target genes are phosphoglycerate kinase-1, glucose transporter-1, vascular endothelial growth factor, and erythropoietin. Pathologic conditions like renal disease and diabetic nephropathy have shown to impede this adaptation via, for example, desensitization of renal erythropoietin-producing cells by uremic toxins (Chiang et al., 2012) or direct inhibition of HIF activity (Nordquist et al., 2015; Tanaka et al., 2016). Indeed, treatment which increased HIF activity corrected abnormal renal metabolism (oxygen consumption, efficiency) and hemodynamics (renal blood flow, glomerular filtration) in a rat model of chronic kidney disease (Deng et al., 2010). Interestingly these effects were similar to RAAS inhibition but involved a significantly different molecular pathway. Third, chronic sustained tissue hypoxia can result from stenosis/partial occlusion of conduit arteries that may be of congenital or atherosclerotic origin. In case of obstruction of blood flow ischemic injury will follow due to the reduced nutrient and oxygen supply. As proposed previously (Koeners et al., 2016), hypoxic-hypoperfusion may trigger aberrant renal and/or carotid body afferent tonicity and initiate/amplify sympathetic hyperactivity accentuating arteriolar vasoconstriction and further compounding blood flow and oxygen delivery; this results in hypertension.

### Renal Oxygenation

Renal oxygenation is tightly regulated (both short and long term) to maintain the balance between oxygen supply and demand. Under normal conditions, but under anesthesia, renal partial

pressure of oxygen varies from 15 to 50 mmHg in the cortex and 5–25 mmHg in the renal medulla (Evans et al., 2008; Carreau et al., 2011). Due to the unique anatomy of the kidney, the renal medulla is believed to receive the minimum level of oxygen needed to support normal cell function, and hence might be very susceptible to reductions of the partial pressure of oxygen.

The heterogeneous oxygenation within the renal parenchyma is a result of the different tasks performed along the nephron and is mainly associated with: (1) the high energy demand necessary to reabsorb $Na^+$, (2) the arteriovenous oxygen shunt, and (3) the requirements to perform the countercurrent mechanism that permits urine concentration. Almost all of the renal oxygen consumption is coupled with active $Na^+$ transport through Na-K-ATPase (Mandel and Balaban, 1981). To put this in perspective, the energy required to reabsorb 1 mol $Na^+$ is ∼7 kj, which corresponds to lifting 1 mol $Na^+$ (∼20 g) to a height of 70 km (Hansell et al., 2013). In addition, the development of a $Na^+$ gradient allows the transport of other molecules such as glucose, amino-acids, other solutes, and water. Since the reabsorption of $Na^+$ depends on the glomerular filtration rate, increasing the blood flow to the kidney will increase the filtered $Na^+$ load and further deplete renal oxygen due to a higher oxygen consumption (Hansell et al., 2013). Another factor contributing to the oxygen content in the renal tissue is the arteriovenous oxygen shunt. The renal arteries and veins run in close proximity, oxygen can diffuse in such a way that the oxygen content in the veins is higher than that in the glomerular capillaries and efferent arterioles (Schurek et al., 1990; Welch et al., 2001; Evans et al., 2008). This is especially important when considering that the renal medullary peritubular capillaries arise from the efferent arterioles of the juxtamedullary glomeruli. This vessel network also has a low blood flow to maintain the gradients necessary for the countercurrent mechanism that allows urine concentration (Brezis and Rosen, 1995; Fry et al., 2014). Furthermore, the close proximity of the ascending and descending medullary vasa recta may theoretically promote more arteriovenous oxygen diffusion (Zhang and Edwards, 2002). Hence, the renal medulla has a relative low partial pressure of oxygen and is highly susceptible to ischemic/hypoxic injury.

As already indicated above the kidney contributes to long-term (days) hypoxic adaptation. It has a primordial role in maintaining systemic oxygen content through hypoxia-induced erythropoietin production from the renal interstitial fibroblast-like cells. Under hypoxia, HIF-α is no longer hydroxylated, and HIF-α subunits can accumulate to activate HIF-1-dependent genes like erythropoietin and many others (Haase, 2006). Erythropoietin acts on bone marrow to increase red blood cell production (Dunn et al., 2007; Jelkmann, 2011) which will increase the oxygen carrying capacity. Therefore, the kidney serves as one of the most important physiological oxygen sensors and detectors of systemic hypoxia.

## Renal Hypoxia, Afferent Nerve Activation/Sensitization, and Hypertension

Chronic hypoxia has been confirmed in different kidney disease models such as diabetic nephropathy (Palm et al., 2003) and hypertension (Welch et al., 2001). Long term renal hypoxia is an increasingly recognized common pathway for the development of chronic kidney disease (Hansell et al., 2013; Kawakami et al., 2014), but it can also generate renal injury. Friederich-Persson et al showed that increasing kidney oxygen metabolism, using a mitochondrial uncoupler, reduces the cortical partial pressure of oxygen and causes proteinuria in otherwise healthy rats (Friederich-Persson et al., 2013).

Acute renal hypoxia may also be involved in the activation of renal afferent pathways that leads to the establishment and maintenance of elevated blood pressure. The cell bodies of the renal afferent nerve fibers are located in the dorsal root ganglia and project to the ipsilateral dorsal horn where they synapse with neurons projecting to sites associated with cardiovascular regulation such as the nucleus tractus solitarii and the rostral ventral medulla (Solano-Flores et al., 1997; Ciriello and de Oliveira, 2002; Kopp, 2015) where integration with other inputs will occur and reflex sympathetic responses can be generated. Indeed, perfusion of the kidney with hypoxic blood ($PaO_2$: 36 mmHg) is enough to increase femoral perfusion pressure by >30 mmHg. This response is mediated by renal afferent nerves as it was abolished after denervating the kidney (Ashton et al., 1994). However, whether there is a threshold, or graded thresholds of renal tissue partial oxygen pressure for renal afferent nerve activation is unknown. Furthermore, performing the same experiment using normoxic blood and ischemic metabolites such as bradykinin, prostaglandin E2, and adenosine elicits similar rises in blood pressure (Ashton et al., 1994). This demonstrates that both low partial pressure of oxygen and ischemic metabolites can directly and/or indirectly stimulate renal sensory nerve fibers, promoting reflex increase of the sympathetic nerve activity, and blood pressure (Katholi et al., 1985).

In the two-kidney one clip model of hypertension, denervation of the hypoperfused (clipped) kidney reduced arterial blood pressure, noradrenaline plasma concentration and peripheral sympathetic nerve activity (Katholi et al., 1982). Similarly, in the one-kidney, one-clip model of renovascular hypertension, dorsal root rhizotomy ipsilateral to the clipped kidney attenuated the evoked hypertension (Wyss et al., 1986). Importantly, even a small lesion in the kidney that results in an area(s) of ischemia (hypoperfusion) not necessarily affecting renal function, e.g., by intrarenal injection of phenol, can cause neurogenic hypertension via activation of hypoxia-sensitive renal afferent mechanisms (Ye et al., 2002; Koeners et al., 2014). In this phenol model of renal neurogenic hypertension there is a rapid (within 5 min) and sustained increase in blood pressure that is abolished by nephrectomy or denervation of the injured kidney (Ye et al., 2002; Koeners et al., 2014). These studies support the concept that hypoxia-induced renal afferent activation contributes to hypertension by increasing sympathetic nerve activity through reflex pathways. Similarly, in patients with renovascular hypertension, restoration of renal perfusion reduces muscle sympathetic nerve activity and blood pressure (Miyajima et al., 1991) and renal nerve ablation can reduce blood pressure and muscle sympathetic nerve activity in some patients with resistant hypertension (Hering et al., 2014). Finally, given the change in set-point of sympathetic activity and blood

pressure it is perhaps not surprising that the baroreceptor reflex is reset and gain improved following renal denervation in a rat model of chronic kidney disease (Chen et al., 2016).

We suggest that the aforementioned renal afferent reflex pathway impinging on the nucleus tractus solitarii is a likely nodal point for modulation of the baroreflex. Taken together, both acute or chronic renal hypoxia and hypoperfusion (associated with macro- or microvascular disease) may cause/sustain hypertension through activation of renal afferent chemosensory fibers (Campese et al., 2006; Johns et al., 2011; Foss et al., 2015; Banek et al., 2016). This has parallels with sustained activation of the peripheral chemoreceptors, which are considered next.

## Carotid Body Oxygenation

Carotid bodies are distinct organs located bilaterally at the bifurcation of the common carotid arteries. They have the highest blood flow per tissue weight when compared to any other organ in the body and play an important role in the monitoring and maintenance of physiological levels of blood gases through reflex activation of respiration (Lahiri et al., 1980). The carotid body consists of glomus or type I cells, which are the primary oxygen sensing cells, and supporting or type II cells. Blood supply to the carotid body originates mostly from the carotid artery. The carotid body vasculature is innervated by postganglionic sympathetic fibers from the superior cervical ganglion and by parasympathetic fibers originating from intraglomic ganglion cells. With larger blood vessels having predominantly parasympathetic innervation and smaller blood vessels having predominantly sympathetic innervation, as reviewed by Kumar and Prabhakar (2012). Hence, the arterioles that are in close contact with the type I and type II cells are predominantly innervated with sympathetic fibers, thus more prone to vasoconstriction/hypoperfusion that promotes chemoreceptor activation.

The blood supply to the carotid body is very high given the total metabolic demand, with <3% of oxygen consumed (De Burgh Daly et al., 1954). Of interest, tissue partial pressure of oxygen is lower than that measured in the venous blood, suggesting the existence of an arteriovenous shunt, with potentially a large amount of blood bypassing the chemosensory cells (Acker et al., 1971; Acker and O'Regan, 1981; O'Regan et al., 1990). Despite the very low total organ oxygen consumption, type I cells have a very high metabolic rate with an oxygen consumption at rest approaching the maximum (Duchen and Biscoe, 1992). This very high oxygen consumption makes type I cells very sensitive to reductions in partial pressure of oxygen.

The microvascular partial pressure of oxygen in the carotid body is around 50–70 mmHg in the anesthetized cat (Whalen et al., 1973; Rumsey et al., 1991). It has been shown that changes in oxygenation below this level results in a powerful increase in carotid body afferent activity (Vidruk et al., 2001). Neurosecretion from the glomus cells within the carotid body in response to acute hypoxia is fundamental to chemosensation and involves release of a variety of molecules including acetylcholine, dopamine, ATP, and neuropeptides such as substance P or enkephalins have been investigated. Recently, evidence for gas signaling molecules such as nitric oxide and carbon monoxide have been highlighted in the carotid body for oxygen sensing (Prabhakar, 2000; Nurse and Piskuric, 2013). These transmitters all activate the terminals of afferent fibers at the glomus cell-afferent junction. Anatomical studies on the cat carotid region revealed that glomus cells are innervated both by sensory and autonomic fibers mostly from the carotid sinus nerve but also by superior cervical ganglion and occasionally the ganglio-glomerular nerves (Eyzaguirre and Uchizono, 1961; Knoche and Kienecker, 1977).

## Carotid Body Hypoxia, Afferent Nerve Activation/Sensitization, and Hypertension

Chemoreceptor activation typically occurs after a change in arterial partial oxygen pressure from ∼95 to ∼50 mmHg for a single unit chemoreceptor *in vitro* (Vidruk and Dempsey, 1980), and to ∼35 mmHg for a whole nerve *in vivo* (Vidruk et al., 2001). However, chemoreceptor afferent fibers show huge variability in their threshold of activation to hypoxia permitting graded responses (Vidruk et al., 2001) and therefore is likely to overlap with renal afferent threshold(s). It has also been proposed that carotid body glomus cells and associated sensory fibers have reflex specific circuits that account for different patterns of response evoked by different stimulants or different levels of hypoxia (acute or chronic) (Paton et al., 2013). Importantly, the afferent nerves of the different sub-populations of glomus cells may project into compartmentalized sites of the nucleus tractus solitarii that regulate cardiac, respiratory, sympathetic as well has higher brain functions (Paton et al., 2013). Carotid body chemoreceptor activation leads to an increased sympathetic tone through glutamatergic excitatory signaling in the nucleus tractus solitarii, rostral ventrolateral medulla, and the paraventricular nucleus resulting in increased blood pressure (Marshall, 1994; Blessing et al., 1999).

The carotid chemoreflex plays a powerful role in the blood pressure regulation including modulation of renal function. For example, carotid chemoreflex activation using autologous venous blood, while maintaining carotid sinus pressure constant, reduced renal blood flow, and glomerular filtration rate through increased renal nerve activation in dogs (Karim et al., 1987). For a long time it has been considered that carotid bodies only change blood pressure over seconds. However, recently an increasing amount of evidence suggests that persistent stimulation of the carotid body might play a role in long-term blood pressure control. In hypertensive animals and humans, chemo-sensory fibers are continuously activated causing increased vasomotor sympathetic activity and hypertension in animals and humans (Sinski et al., 2014; Pijacka et al., 2016b). To demonstrate carotid body tonicity, the carotid sinus nerves were resected and this was found to attenuate the developmental increase in the blood pressure in young spontaneously hypertensive animals (Abdala et al., 2012). In addition, carotid sinus denervation performed in adult spontaneously hypertensive rats reduced blood pressure and sympathetic activity chronically; it also led to increased aortic baroreflex sensitivity (Abdala et al., 2012; McBryde et al., 2013).

These animal studies were translated into a first human study with similar results in some hypertensive patients (Narkiewicz et al., 2016).

This evidence suggests that excessive afferent signaling from carotid bodies may lead to the development of pathological conditions such as hypertension in animals and human. However, what triggers carotid body tonicity is still poorly understood but it is unlikely to be *systemic* hypoxia. The possibility that the carotid body is chronically hypoxic, perhaps due to hypoperfusion secondary to either increased sympathetic vasomotor tone or circulating angiotensin II is plausible, at least in hypertension.

## KIDNEY AND CAROTID BODY: COOPERATIVE OXYGEN SENSORS

As outlined above acute and chronic hypoxia is sensed by both the kidney and the carotid body that activates afferent nerve signaling promoting reflex increases in sympathetic nerve activity triggering hypertension (Katholi et al., 1982; Tafil-Klawe et al., 1985; Somers et al., 1988; Ashton et al., 1994; Ye et al., 2002; Campese et al., 2006; Tan et al., 2010; Johns et al., 2011; Abdala et al., 2012; Sinski et al., 2012; McBryde et al., 2013; Paton et al., 2013; Koeners et al., 2014; Foss et al., 2015; Banek et al., 2016; Pijacka et al., 2016a,b). We hypothesize that the response to systemic hypoxia is based on both local renal and carotid body specific chronic hypoxia sensing which act cooperatively (see **Box 1**). Given the greater sensitivity of the kidney to hypoxia (see above) we propose that this organ responds first to falls in arterial oxygen tension. As oxygen tension falls further signals cascading from the kidney activate the carotid body that once recruited acts cooperatively to ensure sustained long term sympathoexcitation. Evidence for this cooperative mechanism comes from the additive blood pressure lowering effect after renal denervation is performed in combination with carotid body de-afferentation/resection (McBryde et al., 2013, 2017; Pijacka et al., 2016a). The carotid sinus and the renal afferent nerves converge in multiple central cardiovascular regulation areas, providing an anatomical basis for interaction such as the nucleus tractus solitarii and the rostral ventrolateral medulla (Johns et al., 2011).

**Box 1 | Novel insights of the cooperative oxygen sensing by the kidney and carotid body in blood pressure control.**

- Integration of renal and carotid body afferent activity act together to regulate blood pressure during both acute and chronic hypoxia.
- The interaction between the kidney and the carotid body is cooperative—not facilitatory or occlusive.
- The afferent systems of the kidney and the carotid body may have overlapping thresholds for detecting reduced tissue oxygen partial pressure.
- Given the postulated overlap in thresholds, there may be a temporal sequence to the reflex responses elicited between the two organs.
- The cooperative oxygen sensing by the kidney and carotid body could be of great relevance in the pursuit of novel ways to treat diseases in which there is sympathetic overdrive.

## Lines of Communication: Kidney to Carotid Body

Given their relative sensitivities to acute and chronic hypoxia it would seem logical to postulate a communication cascade from the kidney to the carotid body (**Figure 1**). This might include the RAAS. The RAAS plays a key role in cardiovascular and renal physiology and is primarily activated as a functional response to maintain organ perfusion. Most of the RAAS effects arise from angiotensin II $AT_1$ receptor activation and include direct vasoconstriction, increased tubular sodium reabsorption, activation of sympathetic nervous system and increased aldosterone release, fibrosis, reactive oxygen species production and cell proliferation (Balakumar and Jagadeesh, 2014). Accordingly, the RAAS is currently the main pharmacological target of anti-hypertensive therapy (Romero et al., 2015). The mechanism of action of RAAS blockade seems to be straightforward: reduce or block angiotensin II and aldosterone, thereby preventing the deleterious cardiovascular effects. Strikingly, RAAS inhibition is also effective in patients with medium-to low plasma RAAS activity (Te Riet et al., 2015). Moreover, in some cases, after inhibiting angiotensin II/aldosterone receptors, plasma levels of these two hormones returns to normal or even rise above pre-treatment levels: the so-called angiotensin II escape/ refractory hyperaldosteronism (Te Riet et al., 2015). Nonetheless, RAAS inhibition remains partially anti-hypertensive (Te Riet et al., 2015), which may be related to locally generated and regulated RAAS. Experimental evidence shows that intra-renal RAAS is compartmentalized from systemic RAAS; for example, intrarenal RAAS is not adequately inhibited by plasma concentrations of RAAS inhibition in currently used dosages (Nishiyama et al., 2002). Whether this RAAS compartmentalization occurs in other organs, like the carotid body, and is immune to systemic RAAS antagonists is unknown.

If the carotid body is an additional source of afferent drive contributing to sympathetic excess in conditions of hypertension, then what drives it? Certainly, all the components of the RAAS have been identified in the carotid body, except renin (Allen, 1998; Lam and Leung, 2002, 2003). Interestingly a high density of angiotensin II AT1 receptors are located on the primary chemoreceptor element, the glomus cell (Allen, 1998) and their expression and function is upregulated when exposed to chronic hypoxia (Leung et al., 2000). We hypothesize that this forms a line of communication to amplify the generation of sympathetic activity. We do not rule out that in renovascular hypertension heightened sympathetic activity to the carotid body itself (causing vasoconstriction, hypoperfusion) results in enhanced carotid body discharge and elevated systemic RAAS activity. We will address the proposed role of RAAS and cooperative oxygen sensing in the kidney and carotid body.

### Hypoxia and Renal Renin-Angiotensin Aldosterone System in Hypertension

Renal sympathetic activation constricts the renal vasculature thus reducing renal blood flow and glomerular filtration rate, increases sodium retention, and activates the RAAS through increased

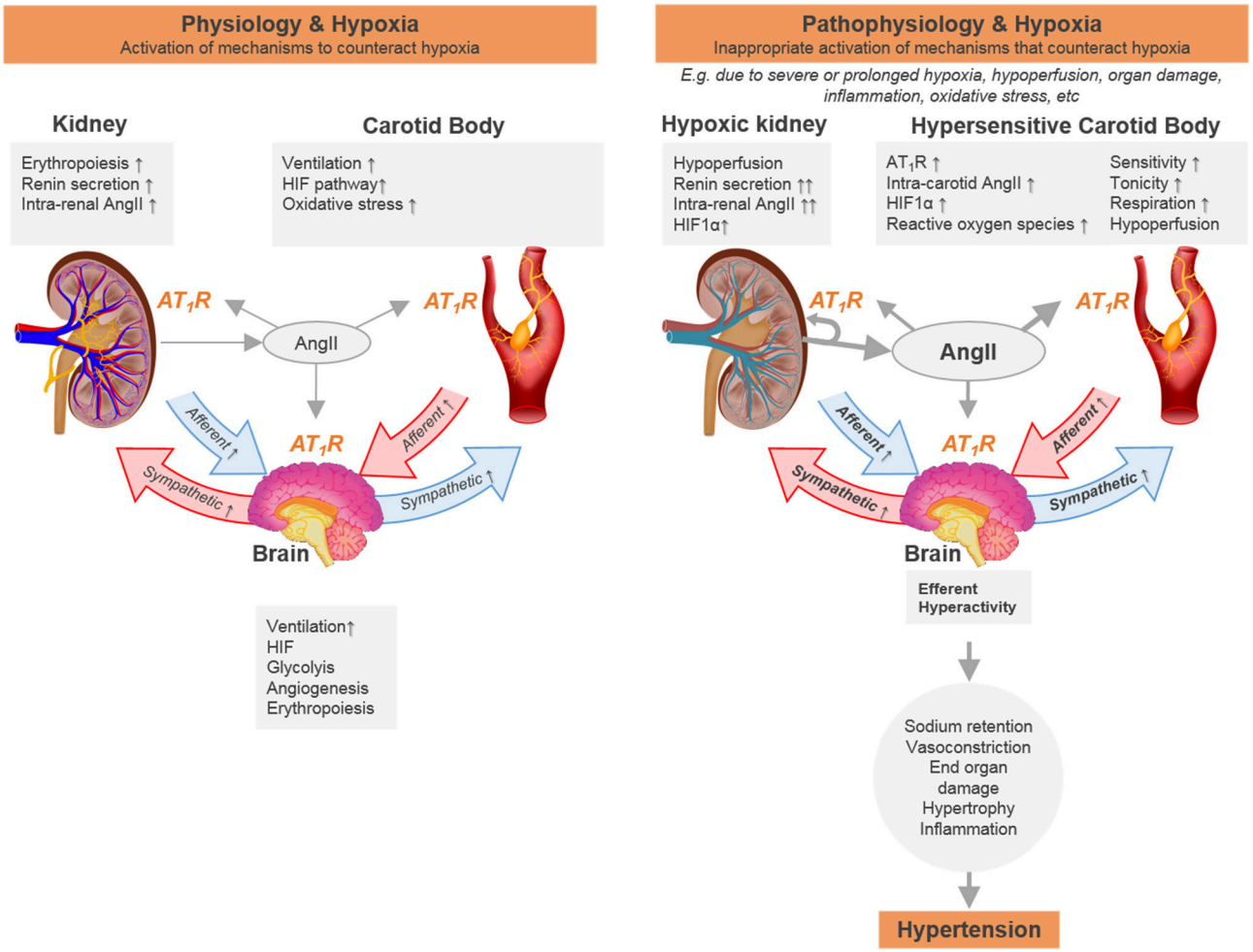


**FIGURE 1 |** Schematic representation of the hypothesis that chronic hypoxia sensed by carotid body and kidney is essential for physiological adaptation and when over-activated can contribute to cardiovascular disease due to positive cross-organ interactive feedback mechanisms. We propose a temporal sequence to the reflex responses elicited between the two organs. One potential way of how the transition from one state to the other would occur includes the inability of the kidney to overcome tissue hypoxia during pathological conditions related to hypoperfusion and/or increased metabolic rate (e.g., vasoconstriction, mitochondrial dysfunction, hyperfiltration). Signals cascading from the hypoxic kidney activate the carotid body that acts cooperatively to ensure sustained (and in the end aberrant) long term sympathoexcitation. Furthermore, the renin angiotensin system is activated in both organs in response to low blood flow/hypoxia. This chronic low blood flow/hypoxia together with the activation of the renin angiotensin system forms a non-functional positive feedback loop that leads to tissue damage. Increasing the renin angiotensin system will lead to activation of different pathways to ensure proper oxygen delivery, including hypoxia inducible factor and erythropoiesis, that may also contribute to the dysfunctional sympathetic activation in hypertension.

renin release from the juxtaglomerular cells (DiBona, 2000; Johns et al., 2011). Angiotensin II $AT_1$ receptor activation affects oxygen availability in the kidney by acting on both its delivery (vasoconstriction) and consumption (increased metabolic rate, decreased efficiency, or both). Angiotensin II-induced reduction in renal blood flow is associated with the reduction of partial pressure of oxygen in the renal cortex (Welch et al., 2005; Emans et al., 2016). Interestingly, in the two kidney one clip model of renovascular hypertension, renal angiotensin II is increased in both kidneys from the first week post clipping (Sadjadi et al., 2002). This suggests that the induced hypoxic-hypoperfusion in the ipsi-lateral kidney also activates the RAAS in the contra-lateral kidney (perhaps via a renorenal reflex) in the development of renovascular hypertension in this model.

By increasing angiotensin II within the kidney, HIF, and erythropoiesis pathways may be triggered to increase oxygen delivery systemically. This in line with the fact that angiotensin II infusion reduces cortical partial pressure of oxygen (Welch et al., 2005; Emans et al., 2016) and increases erythropoietin production in the kidney (Gossmann et al., 2001; Jelkmann, 2011; Calo et al., 2015). Once active, the HIF and erythropoiesis pathways act as feedforward mechanisms. For instance, the increased renal angiotensin II further exaggerates the efferent sympathetic input and sodium retention by abolishing the renorenal reflex, as reviewed by Johns et al. (2011). We

cannot exclude that aldosterone also plays a role in our hypothesized cooperative oxygen sensing and blood pressure control. Increased aldosterone secretion is associated with hypertension (Laragh et al., 1960; Mackenzie and Connell, 2006). Clinical studies have shown that aldosterone blockade is the most effective add-on drug (step 4 treatment in the NICE guidelines; www.nice.org.uk/Guidance/CG127) for the treatment of resistant hypertension (Epstein and Duprez, 2016). However, the role of the mineralcorticoid receptor in relation with cooperative sensing of hypoxia by the kidney and carotid body is completely unknown.

Taken together, activation of renal afferents (discussed previously) and the RAAS act as two distinct feedback systems during acute and chronic hypoxia sensing by the kidney. As hypoxia is relative to physiological tissue oxygen pressure these feedback systems are likely to have overlapping hypoxia thresholds for their activation and play intricate roles in both acute and/or chronic changes in tissue oxygenation.

### Carotid Body and Renin-Angiotensin Aldosterone System in Hypertension

Locally generated angiotensin II increases carotid body afferent discharge (Lam and Leung, 2002) and increases the intracellular calcium levels via activation of $AT_1$ receptors in carotid body type I (Fung et al., 2001) and type II (Murali et al., 2014) cells. Murali and coworkers hypothesized that angiotensin II $AT_1$ receptor-mediated pannexin-1 channel dependent ATP release in type II cells serves as a boost for carotid body excitation (Murali et al., 2014), which may be specially relevant in conditions where local angiotensin II is elevated such as chronic heart failure (Li et al., 2006), sleep apnea (Lam et al., 2014), and in the hypertensive state. Chronic hypoxia induces angiotensin II $AT_1$ receptor expression in the carotid body (Lam et al., 2014). Blockade of angiotensin II $AT_1$ receptors prevents chronic intermittent hypoxia-mediated reactive oxygen species production in the carotid body (Lam et al., 2014) and the development of hypertension (Fletcher et al., 1999). In fact, angiotensin II $AT_1$ receptor activation has been shown to induce sensory long term facilitation of the carotid body via NADPHoxidase (Peng et al., 2011b). Importantly, in chronic intermittent hypoxia, carotid body afferent nerve activation is also mediated by angiotensin II $AT_1$ receptors (Marcus et al., 2010). Moreover, reducing the blood flow (hypoxic-hypoperfusion) to carotid body by carotid artery occlusion elevated angiotensin II $AT_1$ receptor expression in carotid body and increased chemoreceptor activity in the rabbit (Ding et al., 2011). Activation of angiotensin II $AT_1$ receptor *in vitro* (hence independently of vasoconstriction) by AngII activated afferent chemoreceptor activity (Allen, 1998). Importantly, blocking angiotensin II $AT_1$ receptor receptors in isolated carotid body blunts angiotensin II $AT_1$ receptor - dependent carotid body sensitivity (Li et al., 2007).

Many mechanisms govern carotid body signaling, including ATP-gated ion channels (called purinergic P2X receptors), specifically the C-fiber-localized, P2X3-receptor subtypes, which are commonly associated with afferent sensitization and might contribute to hyper-reflexic disease states in a variety of organs. We found that in spontaneously hypertensive rats P2X3 receptors are upregulated and that blockade of P2X3 receptors was effective at reducing blood pressure and sympathetic activity in the spontaneously hypertensive rats but had no effect in normotensive control rats (Pijacka et al., 2016b). Interestingly chronic angiotensin II infused hypertensive rats have upregulated intrarenal P2X1 receptors (Franco et al., 2011).

Taken together this underlines the important role RAAS in carotid body can play in hypoxia sensing, possibly via purineric signaling. Potentially the kidney could trigger the carotid body via RAAS activation, compounding renal sympathetic activity (driving renal afferents) which will exaggerate RAAS activity. If this is true a continued carotid body drive could be deleterious to the kidney causing over excitation of renal afferents, genomic changes, resulting in a double wind up of the systems and ultimately cause persistent hypertension.

## COMMONALITY IN THE HIF PATHWAY AND ITS ROLE IN COOPERATIVE OXYGEN SENSING BY THE KIDNEY AND CAROTID BODY

When tissue oxygen levels drop chronically, expression of the HIF-1α and−1β subunits increase. The HIF-1 α/β heterodimer binds and activates expression of various genes including those encoding glycolytic enzymes (for anaerobic metabolism), vascular endothelial growth factor (for angiogenesis), inducible nitric oxide synthase and heme oxygenase-1 (for production of vasodilators), erythropoietin (for erythropoiesis), and possibly tyrosine hydroxylase (for dopamine production to increase breathing) (Guillemin and Krasnow, 1997). These genes help the cell survive at low oxygen and act to restore normal oxygen levels.

In the normal, fully developed kidney, HIF-1α is expressed in most cell types, whereas HIF-2α is mainly found in renal interstitial fibroblast-like cells and endothelial cells. The HIF pathway has been implicated with renal development, normal kidney function, and disease (Haase, 2006). Recently HIF-1α mRNA has been suggested to be a potential biomarker in chronic kidney disease, and comes primarily from cells of renal origin (Movafagh et al., 2017). Interestingly, the carotid body glomus cells constitutively overexpress HIFs and certain HIF transcriptional targets that are normally part of the counteractive mechanism against the negative impacts of sustained hypoxia (Zhou et al., 2016). Specifically, the glomus cells transcriptionally upregulate atypical mitochondrial electron transfer chain components, suggesting unique mitochondria are present in the carotid body and may be responsible for oxygen sensing (Zhou et al., 2016).

A few years ago, Gassmann and Soliz postulated that there was a crosstalk between the ventilatory and erythropoietin responses and suggested that the chemoreflex pathway may be activated by circulating erythropoietin (Brines et al., 2004; Gassmann and Soliz, 2009). In fact, circulating erythropoietin, acting on its receptors present in the carotid body improves the hypoxic ventilatory response (Soliz et al., 2005) suggesting a key role of erythropoietin for hypoxia adaption beyond

the classical regulation of erythropoiesis (Pichon et al., 2016). Interestingly, in models of chronic and intermittent hypoxia, erythropoietin and its receptor are upregulated in the carotid body which may promote enhanced excitability and contribute to the pathophysiology of breathing disorders (Lam et al., 2009).

Balanced expression of the HIF-α isoforms is essential for the correct functioning of oxygen sensing in the carotid body (Yuan et al., 2013; Prabhakar and Semenza, 2016). HIF-1α is expressed in both type I and type II cells of the carotid body, while HIF-2α is only expressed in type I cells (Roux et al., 2005). The carotid body chemoreflex response to acute and chronic hypoxia is blunted when HIF-1α expression is reduced (Kline et al., 2002; Yuan et al., 2011, 2013). Conversely, acute and chronic hypoxic sensitivity is enhanced when HIF-2α is reduced (Nanduri et al., 2009; Peng et al., 2011a; Yuan et al., 2013). The balance between the two isoforms may be implicated in the genesis of aberrant signaling during pathology. For instance, intermittent hypoxia in rodents is associated with increased HIF-1α and reduced HIF-2α protein in the carotid body (Nanduri et al., 2009). In these conditions, carotid body chemoreceptor signaling to the adrenal medulla selectively upregulates HIF-1α expression, inducing catecholamine secretion and blood pressure rise (Peng et al., 2014; Kumar et al., 2015), the latter is eliminated by adrenal demedullation (Bao et al., 1997). Restoring the levels of HIF-2α also prevents oxidative stress and blood pressure increase during intermittent hypoxia exposure (Nanduri et al., 2009). This demonstrates the contribution of HIF-1α pathway in the carotid body and its influence in increasing blood pressure.

As angiotensin II stimulates the HIF-1α pathway (see for example, Imanishi et al., 2014; Luo et al., 2015) RAAS activation could potentially cause an imbalance between HIF-α isoforms in the carotid body. This is supported by the fact that carotid body sensitivity is reduced when angiotensin II $AT_1$ receptors are blocked (see discussion above) (Li et al., 2007). Whether there is a direct link between HIF and erythropoiesis pathways with the cooperative oxygen sensing by the kidney and carotid body, is unknown and will be off great interest to be studied in further detail.

## CLINICAL PERSPECTIVE

Our hypothesis on the cooperative oxygen sensing by the kidney and carotid body in blood pressure control could be of great relevance in the pursuit of novel ways to treat hypertension and cardiovascular disease (see **Box 1**). Reducing or eliminating the activity of the carotid body specifically is emerging as a viable target in diseases in which there is autonomic imbalance such as hypertensive conditions. Potentially, in resistant hypertensive patients that do not respond to renal denervation, concomitant elimination of carotid body activity could have a therapeutic benefit, as proposed by McBryde et al. (2017). Currently, surgical removal of the carotid body is the only way to reduce carotid body activity chronically in humans. Targeting aberrant hypoxia-mediated activation of renal and carotid body afferent activity would be potentially highly effective clinically.

Hydrogen sulfide, $H_2S$, a gaseous endogenous signaling molecule, is increasingly identified to be involved in numerous cardiovascular (patho)physiology (Snijder et al., 2014, 2015; Xie et al., 2016; Huang et al., 2017; Merz et al., 2017). In the kidney, $H_2S$ exerts significant diuretic, natriuretic and kaliuretic effects by raising glomerular filtration rate and inhibiting tubular sodium re-absorption (Xia et al., 2009). In the renal medulla, $H_2S$ acts as an oxygen sensor where its accumulation in hypoxic conditions helps to restore oxygen balance by increasing medullary blood flow, reducing energy requirements for $Na^+$ transport, and directly inhibiting mitochondrial respiration (Beltowski, 2010). Interestingly both low $H_2S$ levels and mitochondrial dysfunction have been found in humans (Granata et al., 2009; Perna and Ingrosso, 2012) and in animal models (Aminzadeh and Vaziri, 2012; Perna and Ingrosso, 2012; Gong et al., 2016) with cardiovascular disease. However, it remains to be established if intervention aimed to improve $H_2S$ levels, e.g., AP39, which proved to specifically increase $H_2S$ in the mitochondria (Ahmad et al., 2016; Chatzianastasiou et al., 2016) can alleviate tissue hypoxia and reduce blood pressure.

Pre-clinical and clinical evidence suggests that Finerenone, a next-generation non-steroidal dihydropyridine-based aldosterone antagonist, may achieve equivalent organ-protective effects with fewer adverse effects and reduced levels of electrolyte disturbance (Kolkhof et al., 2014; Bramlage et al., 2016). The latter is important for its potential applicability for patient with impaired renal function. This in combination with the above mentioned unknowm relation of the mineralcorticoid receptor with cooperative sensing of hypoxia by the kidney and carotid body invites for further pre-clinical research of Finerenone for the treatment of cardiovascular and renal hypertensive disease.

The argument can be made that pharmacological intervention that mimics and enhances natural, physiological response to disease may be preferable to single protein regulation. A promising approach to protect organisms against hypoxia, is upregulation of HIFs, which results in a broad and coordinated downstream reaction, possibly increasing cellular tolerance to hypoxia and thereby alleviating the double windup of RAAS and sympathetic hyperactivity that is responsible to the hypertensive state. Indeed, pre-conditioning by HIFα protein stabilization conferred protection in several models of acute renal ischemia (Bernhardt et al., 2009; Jarmi and Agarwal, 2009; Yang et al., 2009; Wang et al., 2012; Koeners et al., 2014). Furthermore, HIF stabilizing compounds are currently being investigated in clinical trials as a treatment for anemia (Besarab et al., 2016; Holdstock et al., 2016; Pergola et al., 2016). However, a major concern for clinical use includes the "broad pharmacology" of HIF stabilization due to the upregulation of many genes, including proteins that have been targeted for inhibition by marketed drugs (e.g., vascular endothelial growth factor, cyclooxygenase−2), in all tissues some of which may not be hypoxic. A potential way to circumvent unwanted effects of systemic HIF stabilization is to develop novel hypoxia activated pro-drugs, which are currently under development for targeting hypoxia in cancer therapy (Wilson and Hay, 2011). Hypothetically these pro-drugs will only be activated in specifically targeted hypoxic tissues like kidney and/or carotid body and thereby being able to alleviate

hypoxia-mediated renal and carotid body afferent signaling, unrestrained RAAS activation and hence reduce blood pressure in hypertension.

Theoretically, all these therapies are effective only in patients whose have prolonged and/or severe tissue hypoxia. We know that, for example in the kidney, tissue oxygenation can vary wildly within and between individuals and follows a diurnal pattern. The latter, possibly due to variations in oxygen delivery, which is known to be determined by renal blood flow and peaks in the active phase (Emans et al., 2017), can act as cue for circadian clock genes via the HIF pathway (Adamovich et al., 2017). Thus, it is important to identify patients with tissue hypoxia, i.e., more responsive to hypoxia-oriented therapies. We believe that Magnetic Resonance Imaging (MRI) like blood oxygenation-level dependent (BOLD) MRI (Pruijm et al., 2016) and hyperpolarized MRI (Laustsen, 2016; Laustsen et al., 2016) represent very exciting tools to help us to elucidate the role of tissue oxygen metabolism in hypertension and other cardiovascular diseases.

## AUTHOR CONTRIBUTIONS

DP and MK drafted manuscript; DP, WP, JP, and MK edited and revised manuscript, approved final version of manuscript, and ensured integrity.

## FUNDING

This work was supported by the British Heart Foundation (FS/14/2/30630, RG/12/6/29670 and PG/15/68/31717) and the European Union, Seventh Framework Programme, Marie Curie Actions (CARPEDIEM—No 612280).

## ACKNOWLEDGMENTS

We would like to acknowledge the outstanding art work provided by Michel Cekalovic (www.moviesandgraphics.com) used in the schematic.

## REFERENCES

Abdala, A. P., McBryde, F. D., Marina, N., Hendy, E. B., Engelman, Z. J., Fudim, M., et al. (2012). Hypertension is critically dependent on the carotid body input in the spontaneously hypertensive rat. *J. Physiol.* 590, 4269–4277. doi: 10.1113/jphysiol.2012.237800

Acker, H., and O'Regan, R. G. (1981). The effects of stimulation of autonomic nerves on carotid body blood flow in the cat. *J. Physiol.* 315, 99–110. doi: 10.1113/jphysiol.1981.sp013735

Acker, H., Lubbers, D. W., and Purves, M. J. (1971). The distribution of oxygen tension in the carotid body of the cat. *J. Physiol.* 216, 78–79.

Adamovich, Y., Ladeuix, B., Golik, M., Koeners, M. P., and Asher, G. (2017). Rhythmic oxygen levels reset circadian clocks through HIF1alpha. *Cell Metab.* 25, 93–101. doi: 10.1016/j.cmet.2016.09.014

Ahmad, A., Olah, G., Szczesny, B., Wood, M. E., Whiteman, M., and Szabo, C. (2016). AP39, A mitochondrially targeted hydrogen sulfide donor, exerts protective effects in renal epithelial cells subjected to oxidative stress *in vitro* and in acute renal injury *in vivo*. *Shock* 45, 88–97. doi: 10.1097/SHK.0000000000000478

Allen, A. M. (1998). Angiotensin AT(1) receptor-mediated excitation of rat carotid body chemoreceptor afferent activity. *J. Physiol.* 510(Pt 3), 773–781. doi: 10.1111/j.1469-7793.1998.773bj.x

Aminzadeh, M. A., and Vaziri, N. D. (2012). Downregulation of the renal and hepatic hydrogen sulfide ($H_2S$)-producing enzymes and capacity in chronic kidney disease. *Nephrol. Dial. Transplant.* 27, 498–504. doi: 10.1093/ndt/gfr560

Ashton, N., Clarke, C. G., Eddy, D. E., and Swift, F. V. (1994). Mechanisms involved in the activation of ischemically sensitive, afferent renal nerve mediated reflex increases in hind-limb vascular resistance in the anesthetized rabbit. *Can. J. Physiol. Pharmacol.* 72, 637–643. doi: 10.1139/y94-090

Balakumar, P., and Jagadeesh, G. (2014). A century old renin-angiotensin system still grows with endless possibilities: AT1 receptor signaling cascades in cardiovascular physiopathology. *Cell. Signal.* 26, 2147–2160. doi: 10.1016/j.cellsig.2014.06.011

Banek, C. T., Knuepfer, M. M., Foss, J. D., Fiege, J. K., Asirvatham-Jeyaraj, N., Van Helden, D., et al. (2016). Resting afferent renal nerve discharge and renal inflammation: elucidating the role of afferent and efferent renal nerves in deoxycorticosterone acetate salt hypertension. *Hypertension* 68, 1415–1423. doi: 10.1161/HYPERTENSIONAHA.116.07850

Bao, G., Metreveli, N., Li, R., Taylor, A., and Fletcher, E. C. (1997). Blood pressure response to chronic episodic hypoxia: role of the sympathetic nervous system. *J. Appl. Physiol.* 83:95.

Beltowski, J. (2010). Hypoxia in the renal medulla: implications for hydrogen sulfide signaling. *J. Pharmacol. Exp. Ther.* 334, 358–363. doi: 10.1124/jpet.110.166637

Bernhardt, W. M., Gottmann, U., Doyon, F., Buchholz, B., Campean, V., Schodel, J., et al. (2009). Donor treatment with a PHD-inhibitor activating HIFs prevents graft injury and prolongs survival in an allogenic kidney transplant model. *Proc. Natl. Acad. Sci. U.S.A.* 106, 21276–21281. doi: 10.1073/pnas.0903978106

Besarab, A., Chernyavskaya, E., Motylev, I., Shutov, E., Kumbar, L. M., Gurevich, K., et al. (2016). Roxadustat (FG-4592): correction of anemia in incident dialysis patients. *J. Am. Soc. Nephrol.* 27, 1225–1233. doi: 10.1681/ASN.2015030241

Blessing, W. W., Yu, Y., and Nalivaiko, E. (1999). Medullary projections of rabbit carotid sinus nerve. *Brain Res.* 816, 405–410. doi: 10.1016/S0006-8993(98)01147-0

Bramlage, P., Swift, S. L., Thoenes, M., Minguet, J., Ferrero, C., and Schmieder, R. E. (2016). Non-steroidal mineralocorticoid receptor antagonism for the treatment of cardiovascular and renal disease. *Eur. J. Heart Fail.* 18, 28–37. doi: 10.1002/ejhf.444

Brezis, M., and Rosen, S. (1995). Hypoxia of the renal medulla–its implications for disease. *N. Engl. J. Med.* 332, 647–655. doi: 10.1056/NEJM199503093321006

Brines, M., Grasso, G., Fiordaliso, F., Sfacteria, A., Ghezzi, P., Fratelli, M., et al. (2004). Erythropoietin mediates tissue protection through an erythropoietin and common beta-subunit heteroreceptor. *Proc. Natl. Acad. Sci. U.S.A.* 101, 14907–14912. doi: 10.1073/pnas.0406491101

Calo, L. A., Davis, P., A., Maiolino, G., Pagnin, E., Ravarotto, V., Naso, A., et al. (2015). Assessing the relationship of angiotensin II type 1 receptors with erythropoietin in a human model of endogenous angiotensin ii type 1 receptor antagonism. *Cardiorenal Med.* 6, 16–24. doi: 10.1159/000439183

Campese, V. M., Mitra, N., and Sandee, D. (2006). Hypertension in renal parenchymal disease: why is it so resistant to treatment? *Kidney Int.* 69, 967–973. doi: 10.1038/sj.ki.5000177

Carreau, A., B., El Hafny-Rahbi, Matejuk, A., Grillon, C., and Kieda, C. (2011). Why is the partial oxygen pressure of human tissues a crucial parameter? Small molecules and hypoxia. *J. Cell. Mol. Med.* 15, 1239–1253. doi: 10.1111/j.1582-4934.2011.01258.x

Chatzianastasiou, A., Bibli, S., I., Andreadou, I., Efentakis, P., Kaludercic, N., Papapetropoulos, A., et al. (2016). Cardioprotection by $H_2S$ donors: nitric oxide-dependent and independent mechanisms. *J. Pharmacol. Exp. Ther.* 358, 431–440. doi: 10.1124/jpet.116.235119

Chen, H. H., Cheng, P. W., Ho, W. Y., Lu, P. J., Lai, C. C., Tseng, Y. M., et al. (2016). Renal denervation improves the baroreflex and GABA system in chronic kidney disease-induced hypertension. *Sci. Rep.* 6:38447. doi: 10.1038/srep38447

Chiang, C. K., Tanaka, T., and Nangaku, M. (2012). Dysregulated oxygen metabolism of the kidney by uremic toxins: review. *J. Ren. Nutr.* 22, 77–80. doi: 10.1053/j.jrn.2011.10.028

Ciriello, J., and de Oliveira, C. V. (2002). Renal afferents and hypertension. *Curr. Hypertens. Rep.* 4, 136–142. doi: 10.1007/s11906-002-0038-x

De Burgh Daly, M., Lambertsen, C. J., and Schweitzer, A. (1954). Observations on the volume of blood flow and oxygen utilization of the carotid body in the cat. *J. Physiol.* 125, 67–89. doi: 10.1113/jphysiol.1954.sp005143

Deng, A., Arndt, M. A., Satriano, J., Singh, P., Rieg, T., Thomson, S., et al. (2010). Renal protection in chronic kidney disease: hypoxia-inducible factor activation vs. angiotensin II blockade. *Am. J. Physiol. Renal. Physiol.* 299, F1365–F1373. doi: 10.1152/ajprenal.00153.2010

DiBona, G. F. (2000). Nervous kidney: interaction between renal sympathetic nerves and the renin-angiotensin system in the control of renal function. *Hypertension* 36, 1083–1088. doi: 10.1161/01.HYP.36.6.1083

Ding, Y., Li, Y. L., and Schultz, H. D. (2011). Role of blood flow in carotid body chemoreflex function in heart failure. *J. Physiol.* 589(Pt 1), 245–258. doi: 10.1113/jphysiol.2010.200584

Duchen, M. R., and Biscoe, T. J. (1992). Mitochondrial function in type I cells isolated from rabbit arterial chemoreceptors. *J. Physiol.* 450, 13–31. doi: 10.1113/jphysiol.1992.sp019114

Dunn, A., Lo, V., and Donnelly, S. (2007). The role of the kidney in blood volume regulation: the kidney as a regulator of the hematocrit. *Am. J. Med. Sci.* 334, 65–71. doi: 10.1097/MAJ.0b013e318095a4ae

Emans, T. W., Janssen, B. J., Joles, J. A., and Krediet, C. T. P. (2017). Circadian rhythm in kidney tissue oxygenation in the rat. *Front. Physiol.* 8:205. doi: 10.3389/fphys.2017.00205

Emans, T. W., Janssen, B. J., Pinkham, M. I., Ow, C. P., Evans, R. G., Joles, J. A., et al. (2016). Exogenous and endogenous angiotensin-II decrease renal cortical oxygen tension in conscious rats by limiting renal blood flow. *J. Physiol.* 594, 6287–6300. doi: 10.1113/JP270731

Epstein, M., and Duprez, D. A. (2016). Resistant hypertension and the pivotal role for mineralocorticoid receptor antagonists: a clinical update 2016. *Am. J. Med.* 129, 661–666. doi: 10.1016/j.amjmed.2016.01.039

Evans, R. G., Gardiner, B. S., Smith, D. W., and O'Connor, P. M. (2008). Intrarenal oxygenation: unique challenges and the biophysical basis of homeostasis. *Am. J. Physiol. Renal Physiol.* 295, F1259–F1270. doi: 10.1152/ajprenal.90230.2008

Eyzaguirre, C., and Uchizono, K. (1961). Observations on the fibre content of nerves reaching the carotid body of the cat. *J. Physiol.* 159, 268–281. doi: 10.1113/jphysiol.1961.sp006807

Ferdinand, P., and Roffe, C. (2016). Hypoxia after stroke: a review of experimental and clinical evidence. *Exp. Transl. Stroke Med.* 8:9. doi: 10.1186/s13231-016-0023-0

Fisher, J. P., and Paton, J. F. (2012). The sympathetic nervous system and blood pressure in humans: implications for hypertension. *J. Hum. Hypertens.* 26, 463–475. doi: 10.1038/jhh.2011.66

Fletcher, E. C., Bao, G., and Li, R. (1999). Renin activity and blood pressure in response to chronic episodic hypoxia. *Hypertension* 34, 309–314. doi: 10.1161/01.HYP.34.2.309

Foss, J. D., Wainford, R. D., Engeland, W. C., Fink, G. D., and Osborn, J. W. (2015). A novel method of selective ablation of afferent renal nerves by periaxonal application of capsaicin. *Am. J. Physiol. Regul. Integr. Comp. Physiol.* 308, R112–R122. doi: 10.1152/ajpregu.00427.2014

Franco, M., Bautista, R., Tapia, E., Soto, V., Santamaria, J., Osorio, H., et al. (2011). Contribution of renal purinergic receptors to renal vasoconstriction in angiotensin II-induced hypertensive rats. *Am. J. Physiol. Renal Physiol.* 300, F1301–F1309. doi: 10.1152/ajprenal.00367.2010

Friederich-Persson, M., Thorn, E., Hansell, P., Nangaku, M., Levin, M., and Palm, F. (2013). Kidney hypoxia, attributable to increased oxygen consumption, induces nephropathy independently of hyperglycemia and oxidative stress. *Hypertension* 62, 914–919. doi: 10.1161/HYPERTENSIONAHA.113.01425

Fry, B. C., Edwards, A., Sgouralis, I., and Layton, A., T. (2014). Impact of renal medullary three-dimensional architecture on oxygen transport. *Am. J. Physiol. Renal Physiol.* 307, F263–F272. doi: 10.1152/ajprenal.00149.2014

Fung, M. L., Lam, S. Y., Chen, Y., Dong, X., and Leung, P. S. (2001). Functional expression of angiotensin II receptors in type-I cells of the rat carotid body. *Pflugers Arch.* 441, 474–480. doi: 10.1007/s004240000445

Gassmann, M., and Soliz, J. (2009). Erythropoietin modulates the neural control of hypoxic ventilation. *Cell. Mol. Life Sci.* 66, 3575–3582. doi: 10.1007/s00018-009-0142-z

Gong, W., Mao, S., Yu, J., Song, J., Jia, Z., Huang, S., et al. (2016). NLRP3 deletion protects against renal fibrosis and attenuates mitochondrial abnormality in mouse with 5/6 nephrectomy. *Am. J. Physiol. Renal Physiol.* 310, F1081–F1088. doi: 10.1152/ajprenal.00534.2015

Gossmann, J., Burkhardt, R., Harder, S., Lenz, T., Sedlmeyer, A., Klinkhardt, U., et al. (2001). Angiotensin II infusion increases plasma erythropoietin levels via an angiotensin II type 1 receptor-dependent pathway. *Kidney Int.* 60, 83–86. doi: 10.1046/j.1523-1755.2001.00773.x

Granata, S., Zaza, G., Simone, S., Villani, G., Latorre, D., Pontrelli, P., et al. (2009). Mitochondrial dysregulation and oxidative stress in patients with chronic kidney disease. *BMC Genomics* 10:388. doi: 10.1186/1471-2164-10-388

Greer, S. N., Metcalf, J. L., Wang, Y., and Ohh, M. (2012). The updated biology of hypoxia-inducible factor. *EMBO J.* 31, 2448–2460. doi: 10.1038/emboj.2012.125

Guillemin, K., and Krasnow, M. A. (1997). The hypoxic response: huffing and HIFing. *Cell* 89, 9–12. doi: 10.1016/S0092-8674(00)80176-2

Haase, V. H. (2006). Hypoxia-inducible factors in the kidney. *Am. J. Physiol. Renal Physiol.* 291, F271–F281. doi: 10.1152/ajprenal.00071.2006

Habler, O. P., and Messmer, K. F. (1997). The physiology of oxygen transport. *Transfus. Sci.* 18, 425–435. doi: 10.1016/S0955-3886(97)00041-6

Hainsworth, R., and Drinkhill, M. J. (2007). Cardiovascular adjustments for life at high altitude. *Respir. Physiol. Neurobiol.* 158, 204–211. doi: 10.1016/j.resp.2007.05.006

Hansell, P., Welch, W. J., Blantz, R. C., and Palm, F. (2013). Determinants of kidney oxygen consumption and their relationship to tissue oxygen tension in diabetes and hypertension. *Clin. Exp. Pharmacol. Physiol.* 40, 123–137. doi: 10.1111/1440-1681.12034

Hering, D., Marusic, P., Walton, A. S., Lambert, E. A., Krum, H., Narkiewicz, K., et al. (2014). Sustained sympathetic and blood pressure reduction 1 year after renal denervation in patients with resistant hypertension. *Hypertension* 64, 118–124. doi: 10.1161/HYPERTENSIONAHA.113.03098

Holdstock, L., Meadowcroft, A. M., Maier, R., Johnson, B. M., Jones, D., Rastogi, A., et al. (2016). Four-week studies of oral hypoxia-inducible factor-prolyl hydroxylase inhibitor GSK1278863 for treatment of anemia. *J. Am. Soc. Nephrol.* 27, 1234–1244. doi: 10.1681/ASN.2014111139

Huang, P., Shen, Z., Yu, W., Huang, Y., Tang, C., Du, J., et al. (2017). Hydrogen sulfide inhibits high-salt diet-induced myocardial oxidative stress and myocardial hypertrophy in dahl rats. *Front. Pharmacol.* 8:128. doi: 10.3389/fphar.2017.00128

Imanishi, M., Tomita, S., Ishizawa, K., Kihira, Y., Ueno, M., Izawa-Ishizawa, Y., et al. (2014). Smooth muscle cell-specific Hif-1alpha deficiency suppresses angiotensin II-induced vascular remodelling in mice. *Cardiovasc. Res.* 102, 460–468. doi: 10.1093/cvr/cvu061

Jarmi, T., and Agarwal, A. (2009). Heme oxygenase and renal disease. *Curr. Hypertens. Rep.* 11, 56–62. doi: 10.1007/s11906-009-0011-z

Jelkmann, W. (2011). Regulation of erythropoietin production. *J. Physiol.* 589(Pt 6), 1251–1258. doi: 10.1113/jphysiol.2010.195057

Johns, E. J., Kopp, U. C., and DiBona, G. F. (2011). Neural control of renal function. *Compr. Physiol.* 1, 731–767. doi: 10.1002/cphy.c100043

Karim, F., Poucher, S. M., and Summerill, R. A. (1987). The effects of stimulating carotid chemoreceptors on renal haemodynamics and function in dogs. *J. Physiol.* 392, 451–462. doi: 10.1113/jphysiol.1987.sp016790

Katholi, R. E., McCann, W. P., and Woods, W. T. (1985). Intrarenal adenosine produces hypertension via renal nerves in the one-kidney, one clip rat. *Hypertension* 7(3 Pt 2), I88–I93. doi: 10.1161/01.HYP.7.3_Pt_2.I88

Katholi, R. E., Whitlow, P. L., Winternitz, S. R., and Oparil, S. (1982). Importance of the renal nerves in established two-kidney, one clip Goldblatt hypertension. *Hypertension* 4(3 Pt 2), 166–174.

Kawakami, T., Mimura, I., Shoji, K., Tanaka, T., and Nangaku, M. (2014). Hypoxia and fibrosis in chronic kidney disease: crossing at pericytes. *Kidney Int. Suppl. (2011)* 4, 107–112. doi: 10.1038/kisup.2014.20

Kline, D. D., Peng, Y. J., Manalo, D. J., Semenza, G. L., and Prabhakar, N. R. (2002). Defective carotid body function and impaired ventilatory responses to chronic hypoxia in mice partially deficient for hypoxia-inducible factor 1 alpha. *Proc. Natl. Acad. Sci. U.S.A.* 99, 821–826. doi: 10.1073/pnas.022634199

Knoche, H., and Kienecker, E. W. (1977). Sympathetic innervation of the carotid bifurcation in the rabbit and cat: blood vessels, carotid body and carotid sinus. A fluorescence and electron microscopic study. *Cell Tissue Res.* 184, 103–112. doi: 10.1007/BF00220530

Koeners, M. P., Lewis, K. E., Ford, A. P., and Paton, J. F. (2016). Hypertension: a problem of organ blood flow supply-demand mismatch. *Future Cardiol.* 12, 339–349. doi: 10.2217/fca.16.5

Koeners, M. P., Vink, E. E., Kuijper, A., Gadellaa, N., Rosenberger, C., Mathia, S., et al. (2014). Stabilization of hypoxia inducible factor-1α ameliorates acute renal neurogenic hypertension. *J. Hypertens.* 32, 587–597. doi: 10.1097/HJH.0000000000000060

Kolkhof, P., Delbeck, M., Kretschmer, A., Steinke, W., Hartmann, E., Barfacker, L., et al. (2014). Finerenone, a novel selective nonsteroidal mineralocorticoid receptor antagonist protects from rat cardiorenal injury. *J. Cardiovasc. Pharmacol.* 64, 69–78. doi: 10.1097/FJC.0000000000000091

Kopp, U. C. (2015). Role of renal sensory nerves in physiological and pathophysiological conditions. *Am. J. Physiol. Regul. Integr. Comp. Physiol.* 308, R79–R95. doi: 10.1152/ajpregu.00351.2014

Koury, M. J., and Haase, V. H. (2015). Anaemia in kidney disease: harnessing hypoxia responses for therapy. *Nat. Rev. Nephrol.* 11, 394–410. doi: 10.1038/nrneph.2015.82

Kumar, G. K., Peng, J.-Y, Nanduri, J., and Prabhakar, N. R. (2015). Carotid body chemoreflex mediates intermittent hypoxia-induced oxidative stress in the adrenal medulla. *Adv. Exp. Med. Biol.* 860, 195–199. doi: 10.1007/978-3-319-18440-1_21

Kumar, P., and Prabhakar, N. R. (2012). Peripheral chemoreceptors: function and plasticity of the carotid body. *Compr. Physiol.* 2, 141–219. doi: 10.1002/cphy.c100069

Lahiri, S., Nishino, T., Mulligan, E., and Mokashi, A. (1980). Relative latency of responses of chemoreceptor afferents from aortic and carotid bodies. *J. Appl. Physiol. Respir. Environ. Exerc. Physiol.* 48, 362–369.

Lam, S. Y., and Leung, P. S. (2002). A locally generated angiotensin system in rat carotid body. *Regul. Pept.* 107, 97–103. doi: 10.1016/S0167-0115(02)00068-X

Lam, S. Y., and Leung, P. S. (2003). Chronic hypoxia activates a local angiotensin-generating system in rat carotid body. *Mol. Cell. Endocrinol.* 203, 147–153. doi: 10.1016/S0303-7207(03)00087-X

Lam, S. Y., Liu, Y., Ng, K. M., Liong, E. C., Tipoe, G. L., Leung, P. S., et al. (2014). Upregulation of a local renin-angiotensin system in the rat carotid body during chronic intermittent hypoxia. *Exp. Physiol.* 99, 220–231. doi: 10.1113/expphysiol.2013.074591

Lam, S. Y., Tipoe, G. L., and Fung, M. L. (2009). Upregulation of erythropoietin and its receptor expression in the rat carotid body during chronic and intermittent hypoxia. *Adv. Exp. Med. Biol.* 648, 207–214. doi: 10.1007/978-90-481-2259-2_24

Laragh, J. H., Ulick, S., Januszewicz, V., Deming, Q. B., Kelly, W. G., and Lieberman, S. (1960). Aldosterone secretion and primary and malignant hypertension. *J. Clin. Invest.* 39, 1091–1106. doi: 10.1172/JCI104124

Laustsen, C. (2016). Hyperpolarized renal magnetic resonance imaging: potential and pitfalls. *Front. Physiol.* 7:72. doi: 10.3389/fphys.2016.00072

Laustsen, C., Stokholm Norlinger, T., Christoffer Hansen, D., Qi, H., Mose Nielsen, P., Bonde Bertelsen, L. J., et al. (2016). Hyperpolarized (13) C urea relaxation mechanism reveals renal changes in diabetic nephropathy. *Magn. Reson. Med.* 75, 515–518. doi: 10.1002/mrm.26036

Leach, R. M., and Treacher, D. F. (2002). The pulmonary physician in critical care * 2: oxygen delivery and consumption in the critically ill. *Thorax* 57, 170–177. doi: 10.1136/thorax.57.2.170

Leung, P. S., Lam, S. Y., and Fung, M. L. (2000). Chronic hypoxia upregulates the expression and function of AT(1) receptor in rat carotid body. *J. Endocrinol.* 167, 517–524. doi: 10.1677/joe.0.1670517

Li, Y. L., Gao, L., Zucker, I. H., and Schultz, H. D. (2007). NADPH oxidase-derived superoxide anion mediates angiotensin II-enhanced carotid body chemoreceptor sensitivity in heart failure rabbits. *Cardiovasc. Res.* 75, 546–554. doi: 10.1016/j.cardiores.2007.04.006

Li, Y. L., Xia, X. H., Zheng, H., Gao, L., Li, Y. F., Liu, D., et al. (2006). Angiotensin II enhances carotid body chemoreflex control of sympathetic outflow in chronic heart failure rabbits. *Cardiovasc. Res.* 71, 129–138. doi: 10.1016/j.cardiores.2006.03.017

Liu, L., Zhao, X., Zou, H., Bai, R., Yang, K., and Tian, Z. (2016). Hypoxia promotes gastric cancer malignancy partly through the HIF-1α dependent transcriptional activation of the long non-coding RNA GAPLINC. *Front. Physiol.* 7:420. doi: 10.3389/fphys.2016.00420

Luo, R., Zhang, W., Zhao, C., Zhang, Y., Wu, H., Jin, J., et al. (2015). Elevated endothelial hypoxia-inducible factor-1α contributes to glomerular injury and promotes hypertensive chronic kidney disease. *Hypertension* 66, 75–84. doi: 10.1161/HYPERTENSIONAHA.115.05578

Mackenzie, S. M., and Connell, J. (2006). Hypertension and the expanding role of aldosterone. *Curr. Hypertens. Rep.* 8, 255–261. doi: 10.1007/s11906-006-0059-y

Mandel, L. J., and Balaban, R. S. (1981). Stoichiometry and coupling of active transport to oxidative metabolism in epithelial tissues. *Am. J. Physiol.* 240, F357–F371.

Marcus, N. J., Li, Y. L., Bird, C. E., Schultz, H. D., and Morgan, B. J. (2010). Chronic intermittent hypoxia augments chemoreflex control of sympathetic activity: role of the angiotensin II type 1 receptor. *Respir. Physiol. Neurobiol.* 171, 36–45. doi: 10.1016/j.resp.2010.02.003

Marshall, J. M. (1994). Peripheral chemoreceptors and cardiovascular regulation. *Physiol. Rev.* 74, 543–594.

McBryde, F. D., Abdala, A. P., Hendy, E. B., Pijacka, W., Marvar, P., Moraes, D. J., et al. (2013). The carotid body as a putative therapeutic target for the treatment of neurogenic hypertension. *Nat. Commun.* 4:2395. doi: 10.1038/ncomms3395

McBryde, F. D., Hart, E. C., Ramchandra, R., and Paton, J. F. (2017). Evaluating the carotid bodies and renal nerves as therapeutic targets for hypertension. *Auton. Neurosci.* 204, 126–130. doi: 10.1016/j.autneu.2016.08.002

Merz, T., Stenzel, T., Nussbaum, B., Wepler, M., Szabo, C., Wang, R., et al. (2017). Cardiovascular disease and resuscitated septic shock lead to the downregulation of the $H_2S$-producing enzyme cystathionine-gamma-lyase in the porcine coronary artery. *Intensive Care Med. Exp.* 5:17. doi: 10.1186/s40635-017-0131-8

Milani, B., Ansaloni, A., Sousa-Guimaraes, S., Vakilzadeh, N., Piskunowicz, M., Vogt, B., et al. (2016). Reduction of cortical oxygenation in chronic kidney disease: evidence obtained with a new analysis method of blood oxygenation level-dependent magnetic resonance imaging. *Nephrol. Dial. Transplant.* doi: 10.1093/ndt/gfw362. [Epub ahead of print].

Miyajima, E., Yamada, Y., Yoshida, Y., Matsukawa, T., Shionoiri, H., Tochikubo, O., et al. (1991). Muscle sympathetic nerve activity in renovascular hypertension and primary aldosteronism. *Hypertension* 17(6 Pt 2), 1057–1062. doi: 10.1161/01.HYP.17.6.1057

Movafagh, S., Raj, D., Sanaei-Ardekani, M., Bhatia, D., Vo, K., Mahmoudieh, M., et al. (2017). Hypoxia inducible factor 1: a urinary biomarker of kidney disease. *Clin. Transl. Sci.* 10, 201–207. doi: 10.1111/cts.12445

Murali, S., Zhang, M., and Nurse, C. A. (2014). Angiotensin II mobilizes intracellular calcium and activates pannexin-1 channels in rat carotid body type II cells via AT1 receptors. *J. Physiol.* 592, 4747–4762. doi: 10.1113/jphysiol.2014.279299

Nanduri, J., Wang, N., Yuan, G., Khan, S. A., Souvannakitti, D., Peng, Y. J., et al. (2009). Intermittent hypoxia degrades HIF-2alpha via calpains resulting in oxidative stress: implications for recurrent apnea-induced morbidities. *Proc. Natl. Acad. Sci. U.S.A.* 106, 1199–1204. doi: 10.1073/pnas.0811018106

Narkiewicz, K., Ratcliffe, L. E. K., Hart, E. C., Briant, L. J. B., Chrostowska, M., Wolf, J., et al. (2016). Unilateral carotid body resection in resistant hypertension: a safety and feasibility trial. *JACC Basic Transl. Sci.* 1, 313–324. doi: 10.1016/j.jacbts.2016.06.004

Nishiyama, A., Seth, D. M., and Navar, L. G. (2002). Renal interstitial fluid concentrations of angiotensins I and II in anesthetized rats. *Hypertension* 39, 129–134. doi: 10.1161/hy0102.100536

Nordquist, L., Friederich-Persson, M., Fasching, A., Liss, P., Shoji, K., Nangaku, M., et al. (2015). Activation of hypoxia-inducible factors prevents diabetic nephropathy. *J. Am. Soc. Nephrol.* 26, 328–338. doi: 10.1681/ASN.2013090990

Nurse, C. A., and Piskuric, N. A. (2013). Signal processing at mammalian carotid body chemoreceptors. *Semin. Cell Dev. Biol.* 24, 22–30. doi: 10.1016/j.semcdb.2012.09.006

O'Regan, R. G., Ennis, S., and Kennedy, M. (1990). "Calibre of arteriovenous blood vessels in the cat carotid body: an assessment using latex microspheres," in *Arterial Chemoreception*, eds C. Eyzaguirre, S. J. Fidone, R. S. Fitzgerald, S. Lahiri, and D. M. McDonald (New York, NY: Springer), 309–315.

Osborn, J. W., and Foss, J. D. (2017). Renal nerves and long-term control of arterial pressure. *Compr. Physiol.* 7, 263–320. doi: 10.1002/cphy.c150047

Palm, F., Cederberg, J., Hansell, P., Liss, P., and Carlsson, P. O. (2003). Reactive oxygen species cause diabetes-induced decrease in renal oxygen tension. *Diabetologia* 46, 1153–1160. doi: 10.1007/s00125-003-1155-z

Paton, J. F., Ratcliffe, L., Hering, D., Wolf, J., Sobotka, P. A., and Narkiewicz, K. (2013). Revelations about carotid body function through its pathological role in resistant hypertension. *Curr. Hypertens. Rep.* 15, 273–280. doi: 10.1007/s11906-013-0366-z

Paton, J. F., Sobotka, P. A., Fudim, M., Engelman, Z. J., Hart, E. C., McBryde, F. D., et al. (2013). The carotid body as a therapeutic target for the treatment of sympathetically mediated diseases. *Hypertension* 61, 5–13. doi: 10.1161/HYPERTENSIONAHA.111.00064

Peng, Y. J., Nanduri, J., Khan, S. A., Yuan, G., Wang, N., Kinsman, B., et al. (2011a). Hypoxia-inducible factor 2α (HIF-2α) heterozygous-null mice exhibit exaggerated carotid body sensitivity to hypoxia, breathing instability, and hypertension. *Proc. Natl. Acad. Sci. U.S.A.* 108, 3065–3070. doi: 10.1073/pnas.1100064108

Peng, Y. J., Raghuraman, G., Khan, S. A., Kumar, G. K., and Prabhakar, N. R. (2011b). Angiotensin II evokes sensory long-term facilitation of the carotid body via NADPH oxidase. *J. Appl. Physiol. (1985)* 111, 964–970. doi: 10.1152/japplphysiol.00022.2011

Peng, Y. J., Yuan, G., Khan, S., Nanduri, J., Makarenko, V. V., Reddy, V. D., et al. (2014). Regulation of hypoxia-inducible factor-alpha isoforms and redox state by carotid body neural activity in rats. *J. Physiol.* 592, 3841–3858. doi: 10.1113/jphysiol.2014.273789

Pergola, P. E., Spinowitz, B. S., Hartman, C. S., Maroni, B. J., and Haase V. H. (2016). Vadadustat, a novel oral HIF stabilizer, provides effective anemia treatment in nondialysis-dependent chronic kidney disease. *Kidney Int.* 90, 1115–1122. doi: 10.1016/j.kint.2016.07.019

Perna, A. F., and Ingrosso, D. (2012). Low hydrogen sulphide and chronic kidney disease: a dangerous liaison. *Nephrol. Dial. Transplant.* 27, 486–493. doi: 10.1093/ndt/gfr737

Pichon, A., Jeton, F., El Hasnaoui-Saadani, R., Hagström, L., Launay, T., Beaudry, M., et al. (2016). Erythropoietin and the use of a transgenic model of erythropoietin-deficient mice. *Hypoxia* 4, 29–39. doi: 10.2147/HP.S83540

Pijacka, W., McBryde, F. D., Marvar, P. J., Lincevicius, G. S., Abdala, A. P., Woodward, L., et al. (2016a). Carotid sinus denervation (CSD) ameliorates renovascular hypertension in adult Wistar rats. *J. Physiol.* 594, 6255–6266. doi: 10.1113/JP272708

Pijacka, W., Moraes, D. J., Ratcliffe, L. E., Nightingale, A. K., Hart, E. C., da Silva, M. P., et al. (2016b). Purinergic receptors in the carotid body as a new drug target for controlling hypertension. *Nat. Med.* 22, 1151–1159. doi: 10.1038/nm.4173

Prabhakar, N. R. (2000). Oxygen sensing by the carotid body chemoreceptors. *J. Appl. Physiol. (1985)* 88, 2287–2295.

Prabhakar, N. R., and Semenza, G. L. (2016). Regulation of carotid body oxygen sensing by hypoxia-inducible factors. *Pflugers Arch.* 468, 71–75. doi: 10.1007/s00424-015-1719-z

Pruijm, M., Milani, B., and Burnier, M. (2016). Blood oxygenation level-dependent MRI to assess renal oxygenation in renal diseases: progresses and challenges. *Front. Physiol.* 7:667. doi: 10.3389/fphys.2016.00667

Romero, C. A., Orias, M., and Weir, M. R. (2015). Novel RAAS agonists and antagonists: clinical applications and controversies. *Nat. Rev. Endocrinol.* 11, 242–252. doi: 10.1038/nrendo.2015.6

Roux, J. C., Brismar, H., Aperia, A., and Lagercrantz, H. (2005). Developmental changes in HIF transcription factor in carotid body: relevance for $O_2$ sensing by chemoreceptors. *Pediatr. Res.* 58, 53–57. doi: 10.1203/01.PDR.0000163390.78239.EA

Rumsey, W. L., Iturriaga, R., Spergel, D., Lahiri, S., and Wilson, D. F. (1991). Optical measurements of the dependence of chemoreception on oxygen pressure in the cat carotid body. *Am. J. Physiol.* 261(4 Pt 1), C614–C622.

Sadjadi, J., Puttaparthi, K., Welborn, M. B. III., Rogers, T. E., Moe, O., Clagett, G. P., et al. (2002). Upregulation of autocrine-paracrine renin-angiotensin systems in chronic renovascular hypertension. *J. Vasc. Surg.* 36, 386–392. doi: 10.1067/mva.2002.125016

Schurek, H. J., Jost, U., Baumgartl, H., Bertram, H., and Heckmann, U. (1990). Evidence for a preglomerular oxygen diffusion shunt in rat renal cortex. *Am. J. Physiol.* 259(6 Pt 2), F910–F915.

Silva, J. D., Costa, M., Gersh, B. J., and Goncalves, L. (2016). Renal denervation in the era of HTN-3. Comprehensive review and glimpse into the future. *J. Am. Soc. Hypertens.* 10, 656–670. doi: 10.1016/j.jash.2016.05.009

Sinski, M., Lewandowski, J., Przybylski, J., Bidiuk, J., Abramczyk, P., Ciarka, A., et al. (2012). Tonic activity of carotid body chemoreceptors contributes to the increased sympathetic drive in essential hypertension. *Hypertens. Res.* 35, 487–491. doi: 10.1038/hr.2011.209

Sinski, M., Lewandowski, J., Przybylski, J., Zalewski, P., Symonides, B., Abramczyk, P., et al. (2014). Deactivation of carotid body chemoreceptors by hyperoxia decreases blood pressure in hypertensive patients. *Hypertens. Res.* 37, 858–862. doi: 10.1038/hr.2014.91

Snijder, P. M., Frenay, A. R., de Boer, R. A., Pasch, A., Hillebrands, J. L., Leuvenink, H. G., et al. (2015). Exogenous administration of thiosulfate, a donor of hydrogen sulfide, attenuates angiotensin II-induced hypertensive heart disease in rats. *Br. J. Pharmacol.* 172, 1494–1504. doi: 10.1111/bph.12825

Snijder, P. M., Frenay, A. R., Koning, A., M., Bachtler, M., Pasch, A., Kwakernaak, A. J., et al. (2014). Sodium thiosulfate attenuates angiotensin II-induced hypertension, proteinuria and renal damage. *Nitric Oxide* 42, 87–98. doi: 10.1016/j.niox.2014.10.002

Solano-Flores, L. P., Rosas-Arellano, M. P., and Ciriello, J. (1997). Fos induction in central structures after afferent renal nerve stimulation. *Brain Res.* 753, 102–119. doi: 10.1016/S0006-8993(96)01497-7

Soliz, J., Joseph, V., Soulage, C., Becskei, C., Vogel, J., Pequignot, J. M., et al. (2005). Erythropoietin regulates hypoxic ventilation in mice by interacting with brainstem and carotid bodies. *J. Physiol.* 568(Pt 2), 559–571. doi: 10.1113/jphysiol.2005.093328

Somers, V. K., Mark, A. L., and Abboud, F. M. (1988). Potentiation of sympathetic nerve responses to hypoxia in borderline hypertensive subjects. *Hypertension* 11(6 Pt 2), 608–612. doi: 10.1161/01.HYP.11.6.608

Tafil-Klawe, M., Trzebski, A., Klawe, J., and Palko, T. (1985). Augmented chemoreceptor reflex tonic drive in early human hypertension and in normotensive subjects with family background of hypertension. *Acta Physiol. Pol.* 36, 51–58.

Tan, Z. Y., Lu, Y., Whiteis, C. A., Simms, A. E., Paton, J. F., Chapleau, M. W., et al. (2010). Chemoreceptor hypersensitivity, sympathetic excitation, and overexpression of ASIC and TASK channels before the onset of hypertension in SHR. *Circ. Res.* 106, 536–545. doi: 10.1161/CIRCRESAHA.109.206946

Tanaka, S., Tanaka, T., and Nangaku, M. (2016). Hypoxia and hypoxia-inducible factors in chronic kidney disease. *Renal Replace. Ther.* 2:25. doi: 10.1186/s41100-016-0038-y

Te Riet, L., van Esch, J. H., Roks, A. J., A. H., van den Meiracker, and Danser, A. H. (2015). Hypertension: renin-angiotensin-aldosterone system alterations. *Circ. Res.* 116, 960–975. doi: 10.1161/CIRCRESAHA.116.303587

Vidruk, E. H., and Dempsey, J. A. (1980). Carotid body chemoreceptor activity as recorded from the petrosal ganglion in cats. *Brain Res.* 181, 455–459. doi: 10.1016/0006-8993(80)90629-0

Vidruk, E. H., Olson, E., B. Jr., Ling, L., and Mitchell, G. S. (2001). Responses of single-unit carotid body chemoreceptors in adult rats. *J. Physiol.* 531(Pt 1), 165–170. doi: 10.1111/j.1469-7793.2001.0165j.x

Wang, Z., Schley, G., Turkoglu, G., Burzlaff, N., Amann, K. U., Willam, C., et al. (2012). The protective effect of prolyl-hydroxylase inhibition against renal ischaemia requires application prior to ischaemia but is superior to EPO treatment. *Nephrol. Dial. Transplant.* 27, 929–936. doi: 10.1093/ndt/gfr379

Welch, W. J., Baumgartl, H., Lubbers, D., and Wilcox, C. S. (2001). Nephron $pO_2$ and renal oxygen usage in the hypertensive rat kidney. *Kidney Int.* 59, 230–237. doi: 10.1046/j.1523-1755.2001.00483.x

Welch, W. J., Blau, J., Xie, H., Chabrashvili, T., and Wilcox, C. S. (2005). Angiotensin-induced defects in renal oxygenation: role of oxidative stress. *Am. J. Physiol. Heart Circ. Physiol.* 288, H22–H28. doi: 10.1152/ajpheart.00626.2004

Whalen, W. J., Savoca, J., and Nair, P. (1973). Oxygen tension measurements in carotid body of the cat. *Am. J. Physiol.* 225, 986–991.

Wilson, W. R., and Hay, M. P. (2011). Targeting hypoxia in cancer therapy. *Nat. Rev. Cancer* 11, 393–410. doi: 10.1038/nrc3064

Wyss, J. M., Aboukarsh, N., and Oparil, S. (1986). Sensory denervation of the kidney attenuates renovascular hypertension in the rat. *Am. J. Physiol.* 250(1 Pt 2), H82–H86.

Xia, M., Chen, L., Muh, R. W., Li, P. L., and Li, N. (2009). Production and actions of hydrogen sulfide, a novel gaseous bioactive substance, in the

kidneys. *J. Pharmacol. Exp. Ther.* 329, 1056–1062. doi: 10.1124/jpet.108.149963

Xie, L., Gu, Y., Wen, M., Zhao, S., Wang, W., Ma, Y., et al. (2016). Hydrogen sulfide induces Keap1 S-sulfhydration and suppresses diabetes-accelerated atherosclerosis via Nrf2 activation. *Diabetes* 65, 3171–3184. doi: 10.2337/db16-0020

Yang, C. C., Lin, L. C., Wu, M. S., Chien, C. T., and Lai, M. K. (2009). Repetitive hypoxic preconditioning attenuates renal ischemia/reperfusion induced oxidative injury via upregulating HIF-1 alpha-dependent bcl-2 signaling. *Transplantation* 88, 1251–1260. doi: 10.1097/TP.0b013e3181b4a07

Ye, S., Zhong, H., Yanamadala, V., and Campese, V. M. (2002). Renal injury caused by intrarenal injection of phenol increases afferent and efferent renal sympathetic nerve activity. *Am. J. Hypertens.* 15, 717–724. doi: 10.1016/S0895-7061(02)02959-X

Yuan, G., Khan, S. A., Luo, W., Nanduri, J., Semenza, G. L., and Prabhakar, N. R. (2011). Hypoxia-inducible factor 1 mediates increased expression of NADPH oxidase-2 in response to intermittent hypoxia. *J. Cell. Physiol.* 226, 2925–2933. doi: 10.1002/jcp.22640

Yuan, G., Peng, Y. J., Reddy, V. D., Makarenko, V. V., Nanduri, J., Khan, S. A., et al. (2013). Mutual antagonism between hypoxia-inducible factors 1α and 2α regulates oxygen sensing and cardio-respiratory homeostasis. *Proc. Natl. Acad. Sci. U.S.A.* 110, E1788–E1796. doi: 10.1073/pnas.1305961110

Zhang, W., and Edwards, A. (2002). Oxygen transport across vasa recta in the renal medulla. *Am. J. Physiol. Heart Circ. Physiol.* 283, H1042–H1055. doi: 10.1152/ajpheart.00074.2002

Zhou, T., Chien, M. S., Kaleem, S., and Matsunami, H. (2016). Single cell transcriptome analysis of mouse carotid body glomus cells. *J. Physiol.* 594, 4225–4251. doi: 10.1113/JP271936

**Conflict of Interest Statement:** The authors declare that the research was conducted in the absence of any commercial or financial relationships that could be construed as a potential conflict of interest.

frontiers in Physiology

ORIGINAL RESEARCH
published: 14 September 2017
doi: 10.3389/fphys.2017.00696

# Multiparametric Renal Magnetic Resonance Imaging: Validation, Interventions, and Alterations in Chronic Kidney Disease

*Eleanor F. Cox[1], Charlotte E. Buchanan[1], Christopher R. Bradley[1], Benjamin Prestwich[1], Huda Mahmoud[2], Maarten Taal[2], Nicholas M. Selby[2] and Susan T. Francis[1]**

[1] Sir Peter Mansfield Imaging Centre, University of Nottingham, Nottingham, United Kingdom, [2] Centre for Kidney Research and Innovation, Royal Derby Hospital, University of Nottingham, Derby, United Kingdom

**Background:** This paper outlines a multiparametric renal MRI acquisition and analysis protocol to allow non-invasive assessment of hemodynamics (renal artery blood flow and perfusion), oxygenation (BOLD $T_2$*), and microstructure (diffusion, $T_1$ mapping).

**Methods:** We use our multiparametric renal MRI protocol to provide (1) a comprehensive set of MRI parameters [renal artery and vein blood flow, perfusion, $T_1$, $T_2$*, diffusion (ADC, D, D*, $f_p$), and total kidney volume] in a large cohort of healthy participants (127 participants with mean age of 41 ± 19 years) and show the MR field strength (1.5 T vs. 3 T) dependence of $T_1$ and $T_2$* relaxation times; (2) the repeatability of multiparametric MRI measures in 11 healthy participants; (3) changes in MRI measures in response to hypercapnic and hyperoxic modulations in six healthy participants; and (4) pilot data showing the application of the multiparametric protocol in 11 patients with Chronic Kidney Disease (CKD).

**Results:** Baseline measures were in-line with literature values, and as expected, $T_1$-values were longer at 3 T compared with 1.5 T, with increased $T_1$ corticomedullary differentiation at 3 T. Conversely, $T_2$* was longer at 1.5 T. Inter-scan coefficients of variation (CoVs) of $T_1$ mapping and ADC were very good at <2.9%. Intra class correlations (ICCs) were high for cortex perfusion (0.801), cortex and medulla $T_1$ (0.848 and 0.997 using SE-EPI), and renal artery flow (0.844). In response to hypercapnia, a decrease in cortex $T_2$* was observed, whilst no significant effect of hyperoxia on $T_2$* was found. In CKD patients, renal artery and vein blood flow, and renal perfusion was lower than for healthy participants. Renal cortex and medulla $T_1$ was significantly higher in CKD patients compared to healthy participants, with corticomedullary $T_1$ differentiation reduced in CKD patients compared to healthy participants. No significant difference was found in renal $T_2$*.

**Conclusions:** Multiparametric MRI is a powerful technique for the assessment of changes in structure, hemodynamics, and oxygenation in a single scan session. This protocol provides the potential to assess the pathophysiological mechanisms in various etiologies of renal disease, and to assess the efficacy of drug treatments.

**Keywords: magnetic resonance imaging, hemodynamics, oxygenation, renal function, arterial spin labeling**

OPEN ACCESS

***Edited by:***
*Maarten Koeners, University of Bristol, United Kingdom*

***Reviewed by:***
*Samuel Heyman, Hadassah Hebrew University Hospitals, Israel*
*Menno Pruijm, Centre Hospitalier Universitaire Vaudois (CHUV), Switzerland*

****Correspondence:***
*Susan T. Francis*
*susan.francis@nottingham.ac.uk*

***Specialty section:***
*This article was submitted to Renal and Epithelial Physiology, a section of the journal Frontiers in Physiology*

***Received:*** *15 February 2017*
***Accepted:*** *30 August 2017*
***Published:*** *14 September 2017*

***Citation:***
*Cox EF, Buchanan CE, Bradley CR, Prestwich B, Mahmoud H, Taal M, Selby NM and Francis ST (2017) Multiparametric Renal Magnetic Resonance Imaging: Validation, Interventions, and Alterations in Chronic Kidney Disease. Front. Physiol. 8:696. doi: 10.3389/fphys.2017.00696*

## INTRODUCTION

Magnetic Resonance Imaging (MRI) offers the possibility to non-invasively assess the structure of the kidney as well as renal function in a single scan session. This article outlines the development of a quantitative functional multiparametric renal MRI protocol to probe hemodynamics (total and regional blood flow, perfusion), oxygenation [Blood Oxygen Level Dependent (BOLD) $T_2$* imaging], and microstructure (diffusion weighted imaging, longitudinal relaxation time $T_1$ mapping) and describes associated analysis methods. This multiparametric MRI protocol is applied in healthy participants, to assess both reproducibility and the field strength dependence of MRI parameters between 1.5 and 3 Tesla (T). In addition, studies are performed in healthy participants to evaluate the possibility of using hypercapnia and hyperoxia to monitor changes in renal BOLD and $T_1$ reactivity. Finally, pilot data demonstrating the feasibility of this multiparametric protocol in Chronic Kidney Disease (CKD) is shown.

The kidney is an intricate organ which regulates electrolytes, acid-base balance, and blood pressure and filters blood to remove water soluble waste products (Skorecki et al., 2016). Regulation of renal tissue oxygenation is complex, because renal blood flow is not only needed to prevent hypoxic injury but is inextricably linked to the requirement for glomerular filtration. The kidney's response to hypoxia cannot simply be an increase in renal blood flow, as this would also increase oxygen demand; a number of hemodynamic mechanisms are required to regulate the fine balance between oxygen delivery and consumption, and these can be measured using multiparametric MRI.

Oxygen delivery is determined by arterial blood flow, which is regulated by arterial blood pressure and intrarenal vascular resistance, local tissue perfusion and blood oxygen content (Evans et al., 2008). Arterial blood is supplied to the kidney via the renal artery, and blood flow can be estimated from phase contrast MR. The renal artery sequentially divides into segmental, interlobar, arcuate, and interlobular arteries before finally reaching the afferent arterioles that supply the glomeruli. The renal microcirculation varies depending on the location of each nephron within the cortex. In the outer cortex, glomerular efferent arterioles give rise to a capillary network that surrounds the tubules, important for reabsorption of water and electrolytes. In contrast, the efferent arterioles supply the medulla and give rise to the vasa recta, the long unbranched capillary loops that run into the inner medulla associated with the loop of Henle, as well as capillaries in the outer medulla. This facilitates concentration of urine in the medulla, but also has consequences for oxygenation.

The majority of arterial blood delivered to the kidney is directed toward the renal cortex, which primarily is responsible for filtration and tubular reabsorption; 5–15% is delivered to the medulla, whose purpose is concentration of the urine by maintaining a hypertonic environment. Despite the much lower proportional blood flow, the absolute blood flow to the medulla is still significant, reflecting large total renal blood flow (∼20% of cardiac output), and a number of physiological and pathological conditions can produce significant redistribution of renal blood flow. However, a significant cortico-medullary oxygen gradient exists, with the inner medulla having a tissue oxygenation ($pO_2$) as low as 10 mmHg, compared to 50 mmHg in the cortex. MR potentially provides a non-invasive method to assess this change in tissue oxygenation.

Tubular epithelial transport allows the kidney to regulate volume and composition of urine, but has significant energy and oxygen requirements. Reabsorption of sodium is the main determinant of oxygen consumption (Blantz et al., 2007; Thomson and Blantz, 2008), so that oxygen consumption is related to renal function, with reductions in glomerular filtration rate (GFR) resulting in a lower filtered load and lower requirement for sodium reabsorption. Renal perfusion is driven primarily by the need to maintain glomerular filtration rather than oxygenation, and therefore arteriovenous shunting of oxygen occurs to prevent hyperoxic tissue injury (via peri-glomerular shunts and between arterial and venous limbs of the vasa recta).

Although the kidney can reduce oxygen consumption in response to hypoxia, the lower $pO_2$ in the medulla increases its propensity to ischemic damage, which is considered a key pathogenic event in acute kidney injury (AKI) and CKD (Venkatachalam et al., 2010). Since multiple interacting mechanisms operate in concert to provide tight regulation of intrarenal oxygenation, dysfunction of these mechanisms may contribute to the pathogenesis of kidney disease. For example, vascular morphologic changes may occur such as, capillary rarefaction as well as factors that affect regional blood flow and oxygen diffusion e.g., upregulation of the renin-angiotensin or sympathetic nervous systems (Adler et al., 2004). Alternatively, other changes may impact regional oxygen utilization such as alterations in global and single nephron GFR, drugs interfering with glomerular hemodynamics or tubular transport and hydration status. In addition to the complexity of kidney function, renal diseases such as CKD are diverse in terms of pathophysiological processes, etiology and outcomes, highlighting the need for multiparametric MRI measures. Renal perfusion and tissue oxygenation appear central integrating factors in kidney disease, highlighting the need to perform a combined assessment of these parameters, and regardless of the nature of initial insult, fibrosis is the final common pathway.

The potential use of complementary MRI techniques to non-invasively assess multiple parameters to provide a wealth of information on renal blood flow and regional perfusion, tissue oxygenation, and degree of fibrosis, as well as behavior in low or high oxygen or carbon dioxide, will undoubtedly aid the understanding of kidney disease. Prior to the use of MRI in kidney disease, the reproducibility of MRI measures and their dependence on different factors must be understood in normal tissue.

Here, we assess the inter-subject variability, repeatability, and field strength dependence of multiparametric MRI measures in healthy participants. Physiological modulations such as, hyperoxia and hypercapnia are performed, and pilot data are shown to illustrate the feasibility of detecting changes in MR measures in CKD.

# MATERIALS AND METHODS

## Study Design

Studies were carried out according to the principles of the Declaration of Helsinki. Healthy participant studies were approved by the Local Ethics Committee and patient studies were approved by the East Midlands Research Ethics Committee. Written informed consent was obtained from all participants.

Imaging was performed on either a 1.5 or 3 T Philips whole body MR scanner. Data is presented from studies that use the multiparametric renal MRI protocol, comprising quantification of renal blood flow and perfusion, renal oxygenation, and markers of renal microstructural change due to fibrosis/inflammation. All data was collected with subjects fasted for at least 2 h prior to their scan.

### Variability, Repeatability, and Field Strength Dependence in Healthy Participants

Here, we evaluate the variation in MRI measures within normal tissue of a healthy participant cohort, specifically we assess renal artery and renal vein blood flow [as measured with phase contrast (PC)-MRI], kidney perfusion [as measured with arterial spin labeling (ASL)], $T_1$ measures [and a comparison of readout schemes: spin echo–echo planar imaging (SE-EPI) and balanced fast field echo (bFFE)], tissue oxygenation (from BOLD $T_2$*), diffusion weighted imaging (DWI), and total kidney volume. Data collated across a number of studies are first shown, giving a cohort of 127 participants (88 male) with mean age of 41 ± 19 years. This data is then divided into two groups comprising healthy participants <40 years and >40 years [see Section Application in Chronic Kidney Disease (CKD)]. In addition the field strength dependence of MR relaxation times is assessed. Since clinical MR scanners at both 1.5 and 3 T are now widely available, the field dependence of MR relaxation time measures of $T_1$ (using both SE-EPI and bFFE) and $T_2$* for renal cortex and renal medulla was assessed.

A subset of 11 participants (age 20–28 years, body mass index 20–26 kg/m$^2$) had two/three repeat 3 T scans at the same time of day and after an overnight fast to limit diurnal and dietary variability. To determine the between session repeatability of MRI measures, the intra-subject Coefficient of Variation (CoV; defined as the standard deviation/mean) and intra class correlation (ICC, average measures, two-way random, absolute agreement) were assessed.

### Physiological Modulation in Healthy Participants

Physiological modulations, such as gas enrichment by hypercapnia, hyperoxia, or carbogen (hypercapnic-hyperoxia; Milman et al., 2013) may provide a more sensitive marker to assess changes in renal oxygenation and microcirculation reactivity and functionality, and changes in these parameters associated with pathology. Here, we assess the change in MRI parameters in healthy participants in response to hypercapnia and hyperoxia. We induced hypercapnia and hyperoxia using a sequential gas delivery breathing circuit and a prospective, feed-forward gas delivery system (Respiract$^{TM}$, Thornhill Research Inc., Toronto, Canada) to control and monitor end-tidal oxygen ($P_{ET}O_2$) and carbon dioxide ($P_{ET}CO_2$) partial pressures. Hypercapnia was targeted at $P_{ET}CO_2$ ∼6 mmHg above the subjects' baseline value whilst keeping $P_{ET}O_2$ constant at the subjects' resting value, the paradigm comprised 5 min normoxia and 5 min of hypercapnia. Hyperoxia was targeted at $P_{ET}O_2$ ∼500 mmHg with $P_{ET}CO_2$ targeted to remain constant at the subjects' resting value. The paradigm comprised 5 min normoxia and 5 min of hyperoxia, $P_{ET}O_2$ was increased/decreased over a 1 min transition period.

BOLD $T_2$* was measured at 3 T using a multi-gradient echo Fast Field Echo (mFFE) sequence in six healthy participants (3 male, mean age 25 years, range 22–28 years) during the hyperoxia and hypercapnia challenge. $T_1$ was measured during a hyperoxic challenge in five healthy participants (3 male, mean age 26 years, range 22–31 years) using an inversion recovery sequence with modified respiratory triggering and a bFFE readout at 3 T.

### Application in Chronic Kidney Disease (CKD)

To demonstrate the feasibility of use of the multiparametric MR protocol in patients, 11 patients with CKD Stage 3 or 4 were scanned (inclusion criteria: estimated GFR 15–66 ml/min/1.73 m$^2$, age 18–85 years). Baseline blood pressure and estimated GFR of the patients was recorded. The complete multiparametric protocol was performed comprising of localizer scans, PC-MRI, ASL, $T_1$, $T_2$*, and DWI data as described below. All scans were acquired in approximately 45 min.

## The Multiparametric MRI Protocol

**Figure 1** outlines the key MRI parameters within the multiparametric protocol, these measures can all be performed within a 45 min scan session. All mapping data are collected with matched geometry with slices in a coronal-oblique plane through the long axis of the kidneys, allowing automated interrogation of the resulting multiparametric maps. All data is acquired using respiratory triggering or an end-expiration breath hold to ensure data is acquired at the same point in the respiratory cycle. Each of the parameters within this protocol are outlined below.

### Localizers and Kidney Volume Assessment

Balanced turbo field echo (bTFE) scans are acquired in three orthogonal planes (30 slices of 1.75 × 1.75 × 7 mm$^3$ resolution, data collected in single breath hold per orientation). These scans provide a localizer to allow accurate planning of subsequent images, and segmentation of these images yields total kidney volume.

### Phase Contrast (PC)-MRI to Assess Renal Artery and Vein Blood Flow

Prior to the PC-MRI acquisition, an angiogram is acquired to plan the placement of the PC-MRI renal artery slice to ensure that it is positioned prior to any bifurcations of the artery.

PC-MRI is then used for the measurement of blood flow in the renal arteries and veins (Debatin et al., 1994; Schoenberg et al., 1997; Bax et al., 2005; Park et al., 2005; Dambreville et al., 2010). PC-MRI is performed using a single slice TFE image placed perpendicular to the vessel of interest. Multiple phases are collected across the cardiac cycle when imaging the renal

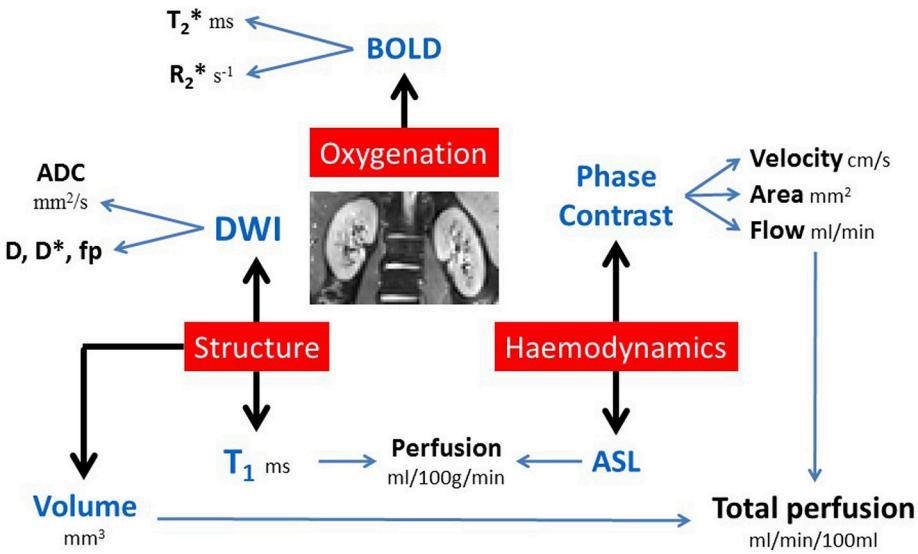


**FIGURE 1 |** Multiparametric non-invasive renal MRI protocol.

artery (20 phases) and renal vein (15 phases). Imaging parameters use a flip angle of 25°, reconstructed resolution 1.2 × 1.2 × 6 $mm^3$, and velocity encoding of 100/50 cm/s for renal artery and vein, respectively. Each measurement is acquired during a single 15–20 s breath hold, dependent on the subjects' heart rate.

## Arterial Spin Labeling (ASL) to Assess Renal Cortex Perfusion

ASL uses magnetically labeled water protons in blood that act as a diffusible tracer, providing an internal endogenous contrast. By subtracting labeled images (radiofrequency magnetic labeling) from control images (no labeling applied), perfusion maps can be quantified using a kinetic model (Buxton et al., 1998). Renal tissue perfusion assessed by ASL has been implemented in healthy (Karger et al., 2000; Martirosian et al., 2004; Boss et al., 2005; Kiefer et al., 2009; Gardener and Francis, 2010; Cutajar et al., 2012, 2014; Park et al., 2013; Gillis et al., 2014; Tan et al., 2014; Hammon et al., 2016), transplanted (Artz et al., 2011a,b; Niles et al., 2016) and diseased (Michaely et al., 2004; Boss et al., 2005; Fenchel et al., 2006; Ritt et al., 2010; Rossi et al., 2012; Dong et al., 2013; Heusch et al., 2013; Tan et al., 2014) kidneys.

To measure renal cortex perfusion, we have implemented a respiratory-triggered FAIR (Flow-sensitive Alternating Inversion Recovery) ASL scheme. For imaging, we use either a SE-EPI or bFFE readout. Typical imaging parameters at 3 T are a post label delay (PLD) time of 1,800 ms (depending on choice of readout scheme and field strength Buchanan et al., 2015), 40 label/control pairs, 288 × 288 mm field of view, 3 × 3 × 5 $mm^3$ voxel resolution. A SE-EPI readout provides good spatial coverage, allowing multiple slices to be acquired in a short acquisition time over the ASL signal curve (five slices in ∼ 300 ms at 3 T). A bFFE readout provides the benefit of high spatial resolution, typically 1.5 mm in-plane spatial resolution and 5 mm slice thickness, however this can limit slice coverage due to the increased acquisition time per slice (∼ 250 ms slice spacing at 3 T). Since ASL is a subtraction technique, we use respiratory triggering to minimize the effects of respiratory motion leading to misalignment or blurring. It is important to take into account the arrival time of the blood to the tissue when quantifying perfusion, particularly in disease where the arrival time can be increased, resulting in an apparent reduction in perfusion. A separate scan to assess the arrival time of the blood to the tissue is acquired, by collecting ∼4 label/control pairs at shorter PLD times (500, 700, 900, 1,100 ms). A base equilibrium $M_0$ scan and $T_1$ map are also required for accurate perfusion quantification. Depending on respiratory rate, scan time for 40 label/control pairs of ASL data is approximately 6 min, with a further 2 min for assessment of arrival time and collection of a base $M_0$ scan.

## Longitudinal Relaxation Time $T_1$ Mapping

The assessment of the longitudinal relaxation time $T_1$ of tissue is essential for the quantification of ASL perfusion. Recently, $T_1$ mapping alone has been shown to provide an important parameter by which to evaluate fibrosis (due to the association of collagen with supersaturated hydrogel) or inflammation (interstitial edema, cellular swelling). $T_1$ has been shown to correlate well with fibrosis and edema in the myocardium (Iles et al., 2008; Jellis and Kwon, 2014), liver (Hoad et al., 2015; Tunnicliffe et al., 2017), and more recently in the kidney (Friedli et al., 2016).

Here, an inversion recovery sequence with a modified respiratory triggering scheme (**Figure 2**) has been developed to minimize respiratory-induced abdominal motion between images of differing contrast collected across the range of inversion times required to compute a $T_1$ map. The respiratory trigger is applied at the peak of inspiration in the respiratory cycle and the image is then acquired at a constant time following this trigger, during the flat end-expiration period of the respiratory

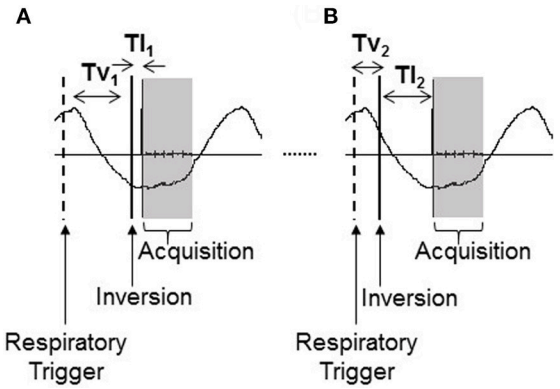


**FIGURE 2 |** Modified respiratory triggered inversion recovery sequence shown for **(A)** short ($TI_1$) and **(B)** long ($TI_2$) inversion time. By altering the variable delay, Tv, each image acquisition is collected at a constant time (Tv + TI) following the respiratory trigger. First arrow indicates the respiratory trigger ("Respiratory Trigger"), second the inversion pulse ("Inversion"), and the shaded block indicates the image acquisition readout ("Acquisition").

cycle. A variable delay, Tv, is introduced between the respiratory trigger and the inversion pulse which is followed by the inversion time, TI, between the inversion pulse and image acquisition. By holding the total time period Tv + TI constant, this results in all image readouts for all inversion times being collected at a constant time of (Tv + TI) following the respiratory trigger and as such all images are aligned across the inversion times. The time (Tv + TI) is chosen to be at the end-expiration period of the respiratory cycle to minimize any potential motion artifacts.

Here, we use either a SE-EPI or bFFE readout scheme for $T_1$ mapping. In general, the same readout scheme as is used for the ASL acquisition is chosen. Importantly, the chosen image readout scheme has an impact on the measured $T_1$ value. A SE-EPI readout scheme provides a "true" $T_1$ value, whereas a bFFE readout scheme results in an "apparent" $T_1$, shorter than the "true" $T_1$ due to the influence of transverse relaxation rates ($T_2/T_2^*$; Schmitt et al., 2004). At 3 T, we typically collect 13 inversion times of 200, 300, 400, 500, 600, 700, 800, 900, 1,000, 1,100, 1,200, 1,300, and 1,500 ms in a total scan time of <3 min. For a multi-slice bFFE readout, the temporal slice spacing is longer (∼250 ms at 3 T) than for a SE-EPI (∼60 ms at 3 T) readout, and therefore the dynamic range of TIs can be increased by acquiring the scans ascend, descend and interleaved slice order.

An alternative scheme for $T_1$ mapping is to use a modified look-locker inversion recovery (MOLLI) sequence originally developed for cardiac $T_1$ mapping. This typically involves the acquisition of a cardiac-gated single-shot MOLLI sequence using a bFFE readout [23] with a 3(3)3(3)5 sampling pattern collected in a breath hold. However, this acquisition scheme is not best suited to the kidney, since it is cardiac triggered, requires a number of breath holds for complete coverage of the kidneys, and does not match the ASL acquisition readout scheme, and so it is not implemented in our multiparametric protocol.

### Diffusion Weighted Imaging (DWI)

DWI assesses the thermally induced Brownian motion of water within tissues, which can be quantified from the Apparent Diffusion Coefficient (ADC). ADC may also be affected by factors such as tubular flow and capillary perfusion, which can be better distinguished using the IntraVoxel Incoherent Motion (IVIM) model to quantify pure diffusion (D; Le Bihan et al., 1988). In DWI, at least two single-shot echo-planar images are acquired without and with diffusion weighting gradients (b-values) from which molecular diffusion can be quantified and spatially mapped. It is important to note that the quantification of the ADC is affected by the b-values acquired. In this multiparametric protocol, DWI data is acquired with a SE-EPI readout at multiple b-values (for example, 11 b-values of 0, 5, 10, 20, 30, 50, 100, 200, 300, 400, 500 s/mm$^2$). The highest b-value is chosen such that the echo time (TE) does not become so long as to limit the signal-to-noise ratio (SNR) of the image. Typically a 288 × 288 mm field of view is used with 3 × 3 × 5 mm$^3$ voxel resolution which has a minimum TE of 56 ms. This sequence is acquired with respiratory triggering such that the image readouts are collected at the end-expiration period. For 11 b-values, the acquisition time is approximately 8 min.

### Blood Oxygenation Level Dependent (BOLD) Imaging to Assess Tissue Oxygenation

BOLD MRI exploits the paramagnetic properties of deoxygenated blood, which acts to shorten the transverse relaxation time constant ($T_2^*$)—alternatively expressed as the relaxation rate $R_2^*$ ($1/T_2^*$)—a measure which provides an indirect non-invasive assessment of oxygen content. Higher $R_2^*$ (or lower $T_2^*$) is an indicator of lower tissue $pO_2$. BOLD MRI is more sensitive at detecting changes in medullary compared to cortical $pO_2$ due to their relative positions on the oxygen dissociation curve—cortical $pO_2$ lies near the plateau of the hemoglobin oxygenation curve and medullary $pO_2$ lies on the linear part of the curve, thus a large change in local $pO_2$ is needed to cause a similar change in $R_2^*$ for the cortex compared to the medulla. The use of BOLD MRI to measure renal oxygenation has been extensively studied. However, it should be highlighted that a number of other factors, such as, hydration status, dietary sodium intake, and susceptibility effects also alter BOLD $R_2^*$ (Pruijm et al., 2017), this can make it difficult to draw definite conclusions from its independent use. For a review of this technique, see Pruijm et al. (2017). In this multiparametric protocol, BOLD $T_2^*$ data is acquired using a mFFE sequence with multiple slices. Typical imaging parameters are 1.5 mm in-plane resolution, 5 mm slice thickness, initial TE 5 ms, TE spacing 3 ms, 12 echoes, flip angle 30°. Each measurement is acquired in a single ∼17 s breath hold.

## Analysis of Multiparametric MRI

### Kidney Volume Assessment

Analyze9 software (AnalyzeDirect, Overland Park, KS) is used to define a region of interest around the kidneys on each bTFE localizer image slice. Total kidney volume can then be calculated by summing across all slices, typically the coronal slices are

used for organ volume measures. Analysis time is approximately 10 min.

### PC-MRI Renal Blood Flow Assessment

A region of interest is placed over the vessel using Q-flow software (Philips Medical Systems, Best, NL). Mean flow velocity (cm/s), mean cross-sectional area of the lumen ($mm^2$), and hence mean bulk renal blood flow (ml/s) over the cardiac cycle, are calculated for each vessel. Total perfusion of each kidney can then be calculated by correcting the renal blood flow to kidney volume. Analysis time is approximately 2 min per vessel.

### Multiparametric Interpretation

Combining multiparametric MRI maps adds considerable insight into the underlying physiology. We have developed a multiparametric image analysis program (MATLAB, The Mathworks Inc., Natick, MA) that generates and combines the parametric ASL perfusion, $T_1$, diffusion, and BOLD $T_2$* maps in the same data space. The multiparametric maps can then be used to perform multivariate analysis of structural and hemodynamic measures in automated regions of interest in the cortex and medulla.

#### *Mapping perfusion from ASL data*

Individual perfusion weighted difference images (control-label) are calculated, inspected for motion (exclude >1 voxel movement) or realigned, and averaged to create a single perfusion-weighted ($\Delta M$) map. $\Delta M$, $T_1$ maps (see below), and $M_0$ maps are then used in a kinetic model (Equation 1; Buxton et al., 1998) to calculate tissue perfusion ($f$) maps (in ml/100 g tissue/min). $T_{1,blood}$ is assumed to be 1.55 s at 3 T and 1.36 s at 1.5 T (Dobre et al., 2007), whilst $\lambda$, the blood-tissue partition coefficient, is assumed to be 0.8 ml/g for kidney. Analysis time is approximately 10 min.

$$\Delta M\,(PLD) = 2M_0 \frac{f}{\lambda} \frac{e^{PLD/T_{1,app-e}}\; PLD/T_{1,blood}}{1/T_{1,blood} - 1/T_{1,app}} \text{ where}$$
$$1/T_{1,app} = 1/T_1 + f/\lambda \quad (1)$$

#### *Longitudinal relaxation time ($T_1$) mapping*

Inversion recovery data is fit on a voxel-by-voxel basis to Equation (2) to generate a "true" $T_1$ map for the SE-EPI readout, for the bFFE readout an "apparent" $T_1$ map is obtained. Analysis time is approximately 3 min of user intervention, and up to 1 h processing time on a standard pc.

$$S\,(\mathrm{TI}) = S_0\left(1 - 2e^{-\mathrm{TI}/T_1}\right) \quad (2)$$

#### *Mapping ADC, D, D*, and $f_p$ from DWI data*

DWI data are fit to form ADC maps (in $mm^2/s$) by taking the log of the exponential signal decay (Equation 3). In addition, since the DWI data is collected at a number of b-values, it is possible to model the bi-exponential IVIM model (Equation 4). In the IVIM model, D (in $mm^2/s$) is the pure tissue molecular diffusion coefficient representing the diffusion coefficient of slow or non-perfusion-based molecular diffusion, D* (in $mm^2/s$) is the pseudodiffusion coefficient which is the fast or perfusion-based molecular diffusion representing intravoxel microcirculation or perfusion, and $f_p$ is the perfusion fraction (%) of the voxel (Le Bihan et al., 1988; Koh et al., 2011). To fit data to the IVIM model, D was first fit to Equation (3) for b-values of >200 $s/mm^2$, this assumes that the pseudodiffusion component D* can be neglected above this value. Second, $f_p$ was determined from the zero intercept of this fit. Finally, D* was obtained from the monoexponential fit using the precalculated values of D and $f_p$ (Suo et al., 2015). Analysis time is approximately 5 min of user intervention, and up to 5 min processing time on a standard pc.

$$S(b) = S_0 e^{-b.ADC} \quad (3)$$
$$S\,(b) = f_p S_0 e^{-b.D^*} + (1 - f_p)\, S_0 e^{-b.D} \quad (4)$$

#### *BOLD MRI to map $T_2$*/$R_2$**

mFFE data are fit voxelwise using a weighted echo time (TE) fit to form $T_2$*/$R_2$* maps from the log of the exponential signal decay (Equation 5). Analysis time is approximately 5 min.

$$S(TE) = S_0 e^{-TE/T_2^*} \quad (5)$$

#### *Interpretation of multiparametric maps*

Binary whole kidney masks are formed from the manual segmentation of the base equilibrium $M_0$ scan or $T_1$ map. To distinguish renal cortex and medulla, a histogram of $T_1$ values across both kidneys is formed (with a bin size of 20 ms). Two peaks in the histogram, originating from the renal cortex and medulla, can be identified from which to form separate renal cortex and renal medulla masks. This segmentation procedure is illustrated for both a healthy participant and CKD patient in **Figure 3**. It should be noted that $T_1$ values are elevated in CKD [see Section Application in Chronic Kidney Disease (CKD)], but sufficient corticomedullary differentiation remains to segment the cortex from medulla. These binary cortex and medulla masks can then be applied to each parametric map (perfusion, $T_1$, ADC, D, D*, and $f_p$) to interrogate identical regions of interest in which to assess mean values of each parameter. Importantly, to assess heterogeneity of measures and remove bias, a Gaussian curve fit can be applied to the histogram to determine both the mode and full-width-at-half-maximum (FWHM) of renal cortex and medulla parameter values across one or both kidneys (Rossi et al., 2012). The assessment of corticomedullary differentiation (medulla-cortex) in MRI parameters also provides important information. Analysis time is approximately 10 min.

## RESULTS

All results given are the mean and standard deviation across participants.

## Variability, Repeatability, and Field Strength Dependence in Healthy Participants

**Figure 4** shows example multiparametric MRI maps for a single healthy participant collected at 3 T, illustrating that the maps can be combined in the same data space and allow assessment of heterogeneity across the kidney. **Table 1** provides the mean

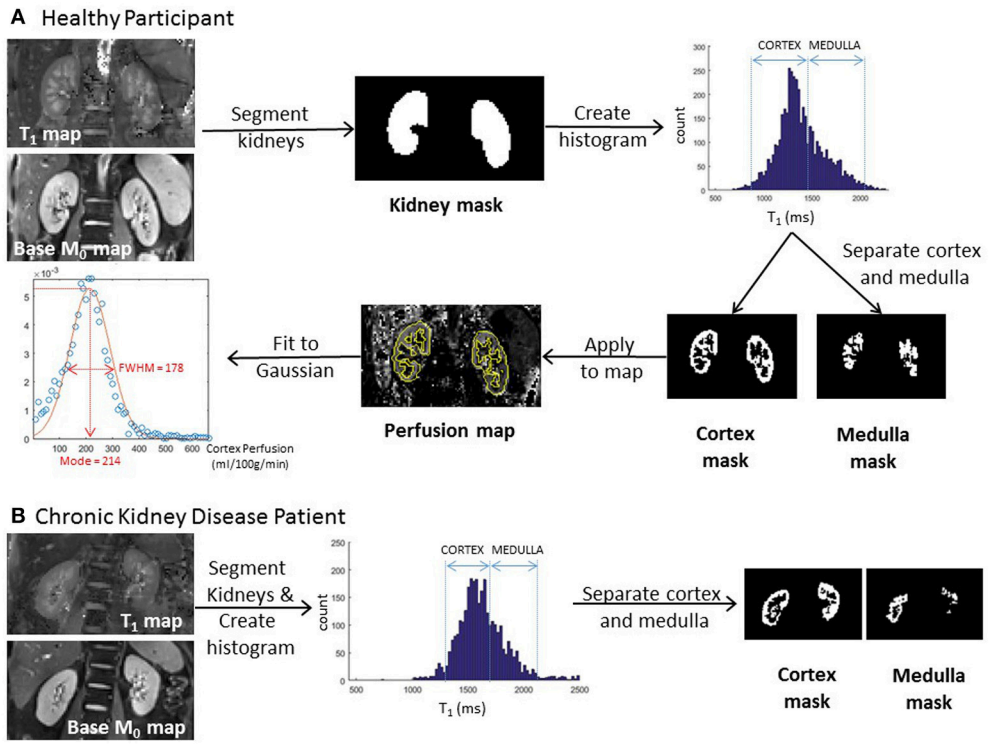


**FIGURE 3 | (A)** Example image analysis for a healthy participant indicating segmentation of the kidneys from the $T_1$ map, definition of cortex and medulla masks from the histogram, and the application of the renal cortex mask to an arterial spin labeling perfusion map allowing the interrogation of a histogram [for mode and full-width-at-half-maximum (FWHM)] of renal cortex perfusion values. **(B)** Example image analysis for a chronic kidney disease patient indicating definition of cortex and medulla masks from the $T_1$ histogram of the kidneys.

and associated standard deviation for MRI parameters collected across the cohort of healthy participants, with the number of subjects included in each analysis provided, and a comparison to literature values.

**Table 2** shows the field strength dependence of longitudinal ($T_1$) and transverse ($T_2$*) relaxation times. As expected, $T_1$-values are longer at 3 T compared with 1.5 T for both the SE-EPI and bFFE readout schemes. It should be noted that the "apparent" $T_1$ measured using a bFFE readout scheme is shorter than the "true" $T_1$ measured using a SE-EPI readout. The corticomedullary differentiation of $T_1$ can be seen to be greater at 3 T compared with 1.5 T. Conversely, the transverse relaxation time ($T_2$*) is longer at 1.5 T.

**Table 3** provides the CoV and ICCs for the repeatability study at 3 T. The CoV is low for $T_1$ (< 2.9%), ADC (2.9%), $T_2$* (4.1%), and kidney volume (4.2%). The ICCs were high for cortex perfusion (0.801), cortex and medulla $T_1$ (0.848 and 0.997 using SE-EPI), renal artery flow (0.844) and total kidney volume (0.985).

## Physiological Modulation in Healthy Participants

**Figure 5A** shows the $T_2$* mode and FWHM in renal cortex and medulla at normoxia and during hypercapnia or during hyperoxia. During hypercapnia, there was a trend for a decrease in the $T_2$* mode in the renal cortex ($P = 0.098$, paired $t$-test), but the $T_2$* FWHM did not change. The $T_2$* mode in the renal medulla did not change, but the $T_2$* FWHM was found to increase ($P = 0.02$, paired $t$-test). During hyperoxia, there was no change in $T_2$* mode or FWHM in either the renal cortex or renal medulla.

**Figure 5B** shows the "apparent" $T_1$ mode and FWHM for renal cortex and medulla at normoxia and during hyperoxia. During hyperoxia, there was no significant change in the "apparent" $T_1$ mode of renal cortex or medulla, but the FWHM increased in the renal cortex ($P = 0.009$, paired $t$-test) and medulla ($P = 0.092$, paired $t$-test).

## Application in Chronic Kidney Disease (CKD)

All 11 CKD patients had glomerular kidney disease, **Table 4** provides demographic details of the patients and divides the healthy participants into young (<40 years) and older (>40 years) age groups for comparison. **Table 5** provides the MRI results for each of these groups.

Renal artery blood flow was significantly reduced in the older healthy participants compared to the young healthy participants, though no difference is seen between the older participants and CKD patients. In CKD, renal cortex perfusion and renal vein

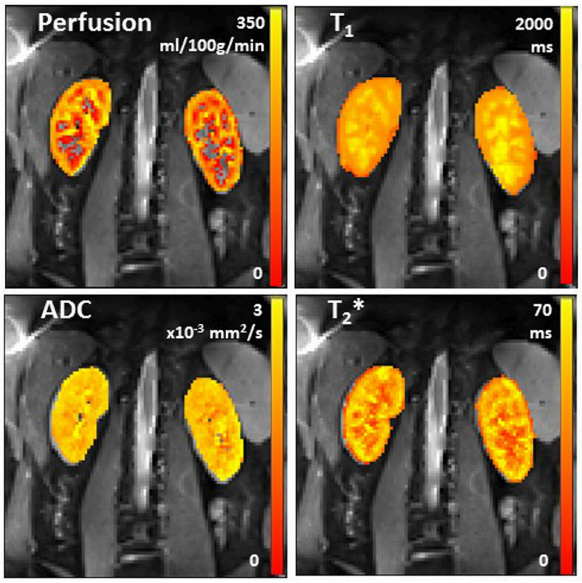


**FIGURE 4 |** Example arterial spin labeling perfusion, longitudinal relaxation time $T_1$, ADC (apparent diffusion coefficient), and transverse relaxation time $T_2$* maps in a healthy participant.

blood flow were lower than in older healthy participants. $T_1$ SE-EPI in the renal cortex was significantly higher in CKD patients compared to older healthy participants, and corticomedullary $T_1$ differentiation was reduced in CKD patients compared to older healthy participants. $T_2$* measured in the renal cortex and medulla was not significantly different in CKD patients compared with healthy participants. In this patient cohort, renal cortex ADC, D and total kidney volume in CKD patients were also not significantly different to healthy participants.

## DISCUSSION

This article has demonstrated acquisition and analysis methods to perform multiparametric assessment of the kidneys in healthy participants and CKD patients.

### Variability, Repeatability, and Field Strength Dependence in Healthy Participants

We provide a comprehensive summary of MRI parameter values for healthy participants, results are in agreement with values reported across separate studies in the literature (**Table 1**). When comparing $T_1$ measures for the renal cortex and medulla to literature values, it is important to consider the MR field strength and readout scheme used for the image acquisition. Here, we show the expected $T_1$ increase with field strength (**Table 2**). Further, the computed $T_1$ value is dependent on the image readout scheme, with a shorter "apparent" $T_1$ measured for a bFFE readout compared to a SE-EPI readout, due to the influence of transverse relaxation on the bFFE readout. The $T_1$ of the medulla was higher than that of the cortex, resulting in clearly visualized corticomedullary differentiation.

The CoV of $T_1$ measures is very low, <3% for cortex and medulla (**Table 3**). Cutajar et al. reported CoVs of between 0.3 and 11.5% for repeatability of renal cortex $T_1$ measures on the same day (Cutajar et al., 2012). Gillis et al. showed no significant difference between visits for repeated measures of renal cortex $T_1$ using a MOLLI method (Gillis et al., 2014). However, MOLLI has some compromises, it is a cardiac gated scheme which provides poor sampling of the inversion recovery curve, requires a breath hold per slice, and since it uses a bFFE readout, its "apparent" $T_1$ value is also affected by tissue fat content at 3 T (Mozes et al., 2016).

PC-MRI measures of renal artery and vein blood flow have a reasonably high CoV, as previously described (Bax et al., 2005; Khatir et al., 2014). This is likely a result of placement of the imaging slice. In contrast, ASL renal cortex perfusion is a voxel-wise measure and this is shown to have a low CoV and high ICC. Cutajar et al. reported CoVs of between 1.8 and 12.1% for repeatability of renal cortex perfusion measures on the same day (Cutajar et al., 2012) and Chowdhury et al. reported a within session CoV of 3.3% (Chowdhury et al., 2012), but to our knowledge there have been no CoVs reported for measures collected between visits. Gillis et al. showed no significant differences between visits for repeated measures of renal cortex perfusion (Gillis et al., 2014).

Thoeny et al. showed that the measured value of ADC is affected by the choice of b-values (Thoeny et al., 2005). Using only low b-values (0–100 s/mm$^2$) will result in a high calculated ADC, whilst high b-values (500–1,000 s/mm$^2$) will result in a low calculated ADC. Using a wide range of b-values provides the least variation in ADC between healthy participants. Here, we use b-values of between 0 and 500 s/mm$^2$ and show comparable results to Thoeny et al. (2005). Cutajar et al. found no significant difference in ADC between sessions, their ADC values were higher than we report, likely due to their acquisition using only two b-values (Cutajar et al., 2011). The value of both ADC and D had a low CoV, whilst D* and $f_p$ had poor repeatability.

A wide range of renal cortex and medulla $T_2$* ($R_2$*) values are reported in the literature. $T_2$* decreases with increasing field strength and is longer in the renal cortex compared to the renal medulla, indicating the hypoxic state of the medulla. The $T_2$*/$R_2$* values we present are in agreement with several studies (Li et al., 2004a; Ding et al., 2013; Khatir et al., 2014; Piskunowicz et al., 2015; van der Bel et al., 2016), whilst others give lower (Simon-Zoula et al., 2006; Park et al., 2012) or higher (Li et al., 2004b) $R_2$*-values. Khatir et al. (2014) measured similar between session CoVs to those we present here.

### Physiological Modulations in Healthy Participants

Here, we assess the change in $T_2$* on hypercapnia and on hyperoxia, and the change in $T_1$ in response to hyperoxia. $T_2$* and $T_1$ relaxation times of tissues have been suggested to be a potential biomarker for renal tissue oxygenation (Jones et al., 2002; O'Connor et al., 2009; Winter et al., 2011; Donati et al., 2012; Khatir et al., 2014; Ganesh et al., 2016). Changes in $T_2$* arise from local field inhomogeneities created

**TABLE 1 |** Between-subject variability for multiparametric MRI measures in healthy participants and associated literature values.

| Parameter | | Between subject variability | | Literature values |
|---|---|---|---|---|
| | | Mean ± std. dev. | Number of subjects | |
| Single renal artery flow | | 373 ± 105 ml/min | 73 | 583 ± 164 ml/min (Bax et al., 2005)<br>443 (404–481) ml/min (Khatir et al., 2015)<br>365 ± 119 ml/min (Khatir et al., 2014)<br>0.48 ± 0.13 L/min (Steeden and Muthurangu, 2015) |
| Single renal vein flow | | 410 ± 134 ml/min | 28 | |
| Total perfusion to single kidney | | 222 ± 60 ml/min/100 ml | 11 | 3.6 (3.2–4.0) ml/min/$cm^3$ (Khatir et al., 2015) |
| Cortex perfusion | | 255 ± 70 ml/100 g/min | 85 | 204 ml/min/100 g (Cutajar et al., 2012)<br>355 ± 71 ml/100 g/min (Gardener and Francis, 2010)<br>321 ± 63 ml/min/100 g (Gillis et al., 2014)<br>200–260 ml/100 g/min (Martirosian et al., 2004)<br>367 ± 41 ml/100 g/min (Wang et al., 2012) |
| Cortex $T_1$ (at 3 T) | SE-EPI | 1367 ± 79 ms | 21 | 1,376 ± 104 ms (MOLLI) (Gillis et al., 2014) |
| | bFFE | 1124 ± 114 ms | 26 | 1,142 ± 154 ms (FSE) (de Bazelaire et al., 2004) |
| Medulla $T_1$ (at 3 T) | SE-EPI | 1655 ± 76 ms | 20 | 1,651 ± 86 ms (MOLLI) (Gillis et al., 2014) |
| | bFFE | 1389 ± 126 ms | 25 | 1,545 ± 142 ms (FSE) (de Bazelaire et al., 2004) |
| Cortex $T_2^*$ (at 3 T) | | 49.6 ± 6.6 ms ($R_2$* 20.6 ± 3.3 $s^{-1}$) | 18 | 51 ± 8 ms (Ding et al., 2013)<br>21.8 ± 1.2 $s^{-1}$ (Li et al., 2004b)<br>11.1 ± 3.8 $s^{-1}$ (Park et al., 2012)<br>18.2 ± 1.7 $s^{-1}$ (Piskunowicz et al., 2015)<br>17.4 ± 1.1 $s^{-1}$ (van der Bel et al., 2016) |
| Medulla $T_2^*$ (at 3T) | | 29.7 ± 5.4 ms ($R_2$* 34.9 ± 6.9 $s^{-1}$) | 18 | 37.4 ± 1.2 $s^{-1}$ (Li et al., 2004b)<br>36 ± 7 ms (Ding et al., 2013) |
| Cortex ADC | | 2.3 ± 0.3 ×$10^{-3}$ $mm^2$/s | 39 | 2.4 ± 0.1 ×$10^{-3}$ $mm^2$/s (Zhang et al., 2010)<br>2.63 ± 0.08 × $10^{-3}$ $mm^2$/s (Cutajar et al., 2011)<br>2.4 ± 0.2 × $10^{-3}$ $mm^2$/s (Sigmund et al., 2012)<br>2.00 ± 0.07 × $10^{-3}$ $mm^2$/s (Thoeny et al., 2005)<br>2.4 ± 0.1 × $10^{-3}$ $mm^2$/s (Wittsack et al., 2010) |
| Cortex D | | 1.7 ± 0.3 ×$10^{-3}$ $mm^2$/s | 38 | 1.8 ± 0.1 × $10^{-3}$ $mm^2$/s (Zhang et al., 2010)<br>1.96 ± 0.09 × $10^{-3}$ $mm^2$/s (Sigmund et al., 2012)<br>1.5 ± 0.1 × $10^{-3}$ $mm^2$/s (Wittsack et al., 2010)<br>2.44 ± 0.12 × $10^{-3}$ $mm^2$/s (Notohamiprodjo et al., 2015) |
| Cortex D* | | 10.7 ± 4.5 × $10^{-3}$ $mm^2$/s | 29 | 14.2 ± 0.8 × $10^{-3}$ $mm^2$/s (Zhang et al., 2010)<br>24.56 ± 6.10 × $10^{-3}$ $mm^2$/s (Sigmund et al., 2012)<br>13.1 ± 2.2 × $10^{-3}$ $mm^2$/s (Wittsack et al., 2010)<br>22.7 ± 10.6 × $10^{-3}$ $mm^2$/s (Notohamiprodjo et al., 2015) |
| Cortex $f_p$ | | 28 ± 10% | 29 | 31 ± 2% (Zhang et al., 2010)<br>18.7 ± 3.5% (Sigmund et al., 2012)<br>52 ± 10% (Wittsack et al., 2010)<br>26.6 ± 6.1% (Notohamiprodjo et al., 2015) |
| Total kidney volume | | 367 ± 58 ml (Mean 184 ± 29 ml) | 22 | Mean across kidneys:<br>141.6 ± 28.5 ml (Seuss et al., 2017)<br>167 (97–307) ml (Cohen et al., 2009)<br>196 (136–295) ml (van den Dool et al., 2005) |

*$T_1$, longitudinal relaxation time; SE-EPI, spin echo-echo planar imaging; bFFE, balanced fast field echo; $T_2$*, transverse relaxation time; ADC, Apparent Diffusion Coefficient; D, pure Diffusion coefficient; D*, pseudodiffusion coefficient; $f_p$, perfusion fraction.*

**TABLE 2 |** Field strength variability in $T_1$ and $T_2$*/$R_2$* in renal cortex and renal medulla, and corticomedullary differentiation (medulla-cortex) for healthy participants.

| Parameter | Field strength (T) | Renal cortex | | Renal medulla | | Corticomedullary differentiation (medulla-cortex) | |
|---|---|---|---|---|---|---|---|
| | | Mean ± std.dev. | Number of subjects | Mean ± std.dev. | Number of subjects | Mean ± std.dev. | Number of subjects |
| $T_1$ SE-EPI | 1.5 | 1,024 ± 71 ms | 8 | 1,272 ± 140 ms | 8 | 248 ± 68 ms | 8 |
| | 3 | 1,367 ± 79 ms | 21 | 1,655 ± 76 ms | 20 | 286 ± 58 ms | 20 |
| $T_1$ bFFE | 1.5 | 1,053 ± 72 ms | 58 | 1,318 ± 98 ms | 38 | 265 ± 38 ms | 38 |
| | 3 | 1,124 ± 114 ms | 26 | 1,388 ± 126 ms | 25 | 268 ± 80 ms | 25 |
| $T_2$* | 1.5 | 70.7 ± 2.4 ms | 8 | 40.7 ± 2.8 ms | 8 | −30.0 ± 5.2 ms | 8 |
| | 3 | 49.6 ± 6.6 ms | 18 | 29.7 ± 5.4 ms | 18 | −19.9 ± 5.1 ms | 18 |
| $R_2$* | 1.5 | 14.2 ± 0.5 $s^{-1}$ | 8 | 24.6 ± 1.7 $s^{-1}$ | 2 | 10.5 ± 2.2 $s^{-1}$ | 8 |
| | 3 | 20.6 ± 3.3 $s^{-1}$ | 18 | 34.9 ± 6.9 $s^{-1}$ | 18 | 14.3 ± 5.0 $s^{-1}$ | 18 |

*$T_1$, longitudinal relaxation time; SE-EPI, spin echo-echo planar imaging; bFFE, balanced fast field echo; $T_2$*, transverse relaxation time; $R_2$*, transverse relaxation rate.*

**TABLE 3 |** Intra subject repeatability for the multiparametric MRI measures in healthy participants.

| Parameter | | Repeatability measures | | | |
|---|---|---|---|---|---|
| | | CoV (%) | ICC | Number of subjects | Number of visits |
| Single renal artery flow | | 14.4 ± 4.3 | 0.844 | 11 | 3 |
| Single renal vein flow | | 18.8 ± 10.3 | 0.649 | 11 | 3 |
| Total perfusion to single kidney | | 14.9 ± 3.8 | 0.611 | 10 | 3 |
| Cortex perfusion | | 9.3 ± 4.4 | 0.801 | 11 | 3 |
| Cortex $T_1$ (at 3 T) | SE-EPI | 2.0 ± 1.5 | 0.848 | 9 | 2 |
| | bFFE | 2.3 ± 1.3 | 0.616 | 11 | 3 |
| Medulla $T_1$ (at 3 T) | SE-EPI | 1.8 ± 1.5 | 0.997 | 9 | 2 |
| | bFFE | 2.9 ± 2.4 | 0.239 | 11 | 3 |
| Cortex $T_2$* (at 3 T) | | 4.1 ± 3.0 | 0.718 | 4 | 2 |
| Cortex ADC | | 2.9 ± 2.0 | 0.745 | 10 | 3 |
| Cortex D | | 9.5 ± 4.8 | 0.307 | 10 | 3 |
| Cortex D* | | 38.8 ± 19.6 | 0.210 | 10 | 3 |
| Cortex $f_p$ | | 21.5 ± 10.6 | 0.102 | 10 | 3 |
| Total kidney volume | | 4.2 ± 2.6 | 0.985 | 11 | 3 |

*CoV, coefficient of variation; ICC, intra class correlation; $T_1$, longitudinal relaxation time; SE-EPI, spin echo-echo planar imaging; bFFE, balanced fast field echo; $T_2$*, transverse relaxation time; ADC, apparent diffusion coefficient; D, pure diffusion coefficient; D*, pseudodiffusion coefficient; $f_p$, perfusion fraction.*

by deoxyhemoglobin (Hb) molecules. Increasing the inspired oxygen increases the ratio of diamagnetic oxyhemoglobin to paramagnetic deoxyhemoglobin ($HbO_2$/Hb) leading to longer $T_2$*. Increasing inspired carbon dioxide reduces the oxygen affinity of hemoglobin, thus leading to increases in the levels of deoxygenated Hb in venous blood and a reduction in $T_2$* (Milman et al., 2013). Changes in $T_1$ arise from changes in levels of dissolved $O_2$ in plasma and tissue, since oxygen is weakly paramagnetic (Young et al., 1981), thus increasing levels of oxygen acts to shorten $T_1$.

There is discrepancy in the literature of the effect of breathing 100% oxygen on $T_2$*. Some studies have shown no change in $T_2$* in the renal cortex (Jones et al., 2002; O'Connor et al., 2009; Khatir et al., 2014; Niendorf et al., 2015) or medulla (Jones et al., 2002), whilst a small number of studies show a small increase in $T_2$* in the renal cortex (Winter et al., 2011; Ganesh et al., 2016) and medulla (Donati et al., 2012; Khatir et al., 2014). At normal levels of inspired oxygen, the body maintains hemoglobin levels in arterial blood near to saturation level. During hyperoxia, a higher fraction of $HbO_2$/Hb and a reduction in blood volume could both be expected to contribute to a small increase in $T_2$*. As an alternative, hypercapnic-hyperoxia has been shown to cause a marked 50% increase in renal $T_2$*-weighted signal intensity, suggesting this method provides enhanced sensitivity (Milman et al., 2013).

For $T_1$, previous studies have shown a decrease in the renal cortex on breathing 100% oxygen, which is equivalent to ∼600 mmHg (Jones et al., 2002; O'Connor et al., 2007, 2009; Ganesh et al., 2016). Here, we used our modified respiratory triggered scheme to measure $T_1$ and independently controlled end-tidal concentrations of oxygen and carbon dioxide (constant to ∼0.1 mmHg). No significant difference in the mode of $T_1$ was found between hypercapnia and normoxia. The controlled gas delivery was equivalent to breathing ∼80% oxygen, and this may explain the smaller $T_1$ change seen in our data. It should be noted that breathing 100% oxygen can lead to hypocapnia (Becker et al., 1996) resulting in a reduction in flow.

To our knowledge, no studies of human kidneys have used hypercapnia. Winter et al. showed no change in $T_2$* at 1.5 T in the rabbit renal cortex when inspiring 10% carbon dioxide (balance air; Winter et al., 2011), whilst Ganesh et al. show a decrease in $T_2$* at 3 T when inspiring 10–30% carbon dioxide (21% oxygen, balance nitrogen; Ganesh et al., 2016). Milman et al. showed that hypercapnia induced by 5% $CO_2$ inhalation caused a marked decline in hemodynamic response imaging maps, based on changes in the signal intensity of a $T_2$*-weighted image, resembling results of studies in the liver (Milman et al., 2013). The level of inspired carbon dioxide in this work is significantly lower than 10%, this may explain why our $T_2$* decrease did not reach significance.

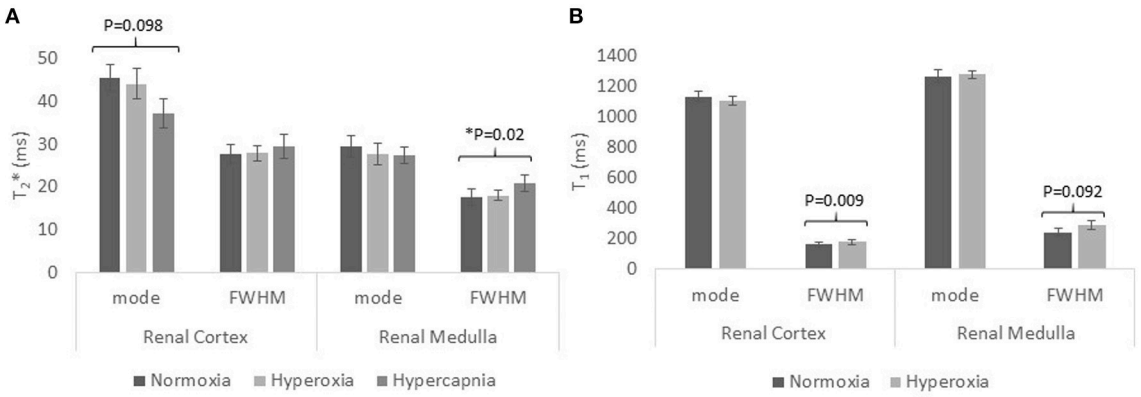


**FIGURE 5 |** The mode and FWHM (full-width-at-half-maximum) in the renal cortex and medulla of healthy participants for **(A)** transverse relaxation time $T_2^*$ during normoxia, hyperoxia, and hypercapnia; **(B)** longitudinal relaxation time $T_1$ during normoxia and hyperoxia.

**TABLE 4 |** Characteristics of healthy participants, split according to age, <40 years and >40 years, and the chronic kidney disease patient cohort.

| | Healthy participants <40 years | Healthy participants >40 years | CKD |
|---|---|---|---|
| Male/Female | 53/16 | 34/24 | 8/3 |
| Age (years) | 25 ± 4 | 60 ± 9 | 52 ± 14 |
| Height (m) | 1.76 ± 0.09 | 1.71 ± 0.09 | 1.74 ± 0.06 |
| Weight (kg) | 72.4 ± 10.0 | 76.0 ± 11.7 | 89.7 ± 10.5 |
| BMI (kg/m$^2$) | 23 ± 2 | 26 ± 3 | 30 ± 4 |
| eGFR (ml/min/1.73 m$^2$) | – | – | 51 ± 15 |
| Systolic BP (mmHg) | – | – | 132 ± 8 |
| Diastolic BP (mmHg) | – | – | 82 ± 8 |
| Hypertension Medication yes/no | – | – | 8/3 |

*CKD, Chronic Kidney Disease; BMI, body mass index; eGFR, estimated glomerular filtration rate; BP, blood pressure.*

Alternative mechanisms of physiological modulation to assess renal oxygenation and microcirculation reactivity and functionality include water loading, sodium loading, or drug administration (e.g., angiotensin, furosemide, saline). Studies have shown that water loading results in an increase in BOLD $T_2^*$ in the medulla (Prasad et al., 1996; Prasad and Epstein, 1999; Tumkur et al., 2006a; Vivier et al., 2013; Ding et al., 2015), this is thought to be due to the production of endogenous prostaglandin PGE2 in the medulla which decreases deoxyhemoglobin (Hb) levels, but it is not possible to distinguish between changes in oxygen supply and oxygen consumption. Similar more pronounced results have been shown following administration of furosemide (a sodium pump inhibitor; Prasad et al., 1996; Li et al., 2004a; Tumkur et al., 2006b; Vivier et al., 2013), coupled with a larger increase in urinary output (Vivier et al., 2013). Interestingly, $T_2^*$ is not altered in older subjects after water loading (Prasad and Epstein, 1999) or furosemide administration (Epstein and Prasad, 2000).

## Chronic Kidney Disease

The standard clinical assessment of renal function is the estimated GFR (eGFR) calculated from serum creatinine concentration. However, this is a late marker of renal dysfunction, is often discordant with tissue damage, is subject to hemodynamic fluctuation, and cannot be used to assess individual kidney function. Kidney biopsy has sampling error associated with the small specimen size, and comes with associated risks of an invasive procedure. This pilot study has assessed the use of multiparametric MRI in CKD patients, potentially providing a number of techniques by which to assess kidney structure and function. Renal blood flow and renal cortex perfusion was lower in CKD patients compared with healthy participants. $T_1$ values were increased in both renal cortex and medulla compared to healthy participants, though primarily in cortex, resulting in a loss of corticomedullary differentiation.

There have been a number of previous studies assessing changes in individual MRI parameters related to hemodynamics and structure in CKD patients (Inoue et al., 2011; Michaely et al., 2012; Xin-Long et al., 2012; Khatir et al., 2014, 2015; Milani et al., 2016). Studies have compared perfusion in CKD patients with healthy participants and found perfusion to be lower in CKD patients (Rossi et al., 2012; Tan et al., 2014). Gillis et al. showed that the $T_1$ relaxation time was longer in CKD patients compared to healthy participants (Gillis et al., 2016). Further, ADC values have been shown to be reduced in CKD compared to healthy participants (Goyal et al., 2012). A recent study using DWI and $T_1$ mapping has demonstrated changes in both kidney ADC and $T_1$ in animal models and humans with CKD (Friedli et al., 2016). Prior studies have shown conflicting changes in measures of oxygenation in CKD, with some groups reporting a reduction in oxygenation in CKD, whilst others report no differences in cortical or medullary $R_2^*$ (Pruijm et al., 2014). Khatir et al. showed similar cortical and medulla $R_2^*$ values at baseline between patients and controls. But on inspiring 100% oxygen, $R_2^*$ significantly decreased in the renal cortex of CKD patients with no change in $R_2^*$ was observed in healthy participants. Medullary $R_2^*$ increased in both patients and controls on

**TABLE 5 |** Multiparametric MRI measures in healthy participants split according to age and Chronic Kidney Disease patients.

| Parameter | Healthy participants <40 years | | Healthy participants >40 years | | CKD mean ± SD ($N = 11$) | *P*-value | | |
|---|---|---|---|---|---|---|---|---|
| | Mean ± SD | N | Mean ± SD | N | | ANOVA between groups | <40 years vs. >40 years | >40 years vs. CKD |
| Renal artery flow (ml/min) | 427 ± 117 | 33 | 329 ± 69 | 40 | 314 ± 148 | 0.0001 | <0.0001 | ns |
| Renal vein flow (ml/min) | 437 ± 142 | 21 | 334 ± 76 | 7 | 212 ± 90 | 0.0002 | 0.0773 | 0.0134 |
| Cortex perfusion (ml/100 g/min) | 279 ± 75 | 42 | 232 ± 57 | 43 | 83 ± 68 | <0.0001 | 0.0019 | <0.0001 |
| SE-EPI $T_1$ (ms) (at 3 T) Cortex | 1,347 ± 65 | 13 | 1,399 ± 93 | 8 | 1,530 ± 99 | <0.0001 | ns | 0.0099 |
| Medulla | 1,635 ± 66 | 12 | 1,685 ± 84 | 8 | 1,726 ± 78 | 0.0254 | ns | ns |
| $\Delta T_1$ | 286 ± 28 | 12 | 286 ± 89 | 8 | 196 ± 45 | 0.0006 | ns | 0.0095 |
| $T_2^*$ (ms) (at 3 T) Cortex | 48.9 ± 7.4 | 10 | 50.4 ± 5.8 | 8 | 54.6 ± 7.7 | 0.0860 | ns | ns |
| Medulla | 29.8 ± 5.4 | 10 | 29.5 ± 5.7 | 8 | 33.0 ± 9.0 | ns | ns | ns |
| Cortex ADC ($\times 10^{-3}$ $mm^2/s$) | 2.3 ± 0.4 | 23 | 2.4 ± 0.2 | 16 | 2.1 ± 0.3 | ns | ns | ns |
| Cortex D ($\times 10^{-3}$ $mm^2/s$) | 1.7 ± 0.2 | 23 | 1.6 ± 0.4 | 15 | 1.8 ± 0.4 | ns | ns | ns |
| Total kidney volume (ml) | 361 ± 62 | 15 | 382 ± 51 | 7 | 409 ± 153 | ns | ns | ns |
| Kidney volume, BSA corrected ($ml/m^2$) | 184 ± 29 | 15 | 190 ± 25 | 7 | 202 ± 86 | ns | ns | ns |

*CKD, Chronic Kidney Disease; $T_1$, longitudinal relaxation time; SE-EPI, spin echo-echo planar imaging; $T_2^*$, transverse relaxation time; ADC, apparent diffusion coefficient; D pure diffusion coefficient; BSA body surface area; ns, not significant.*

inspiring 100% oxygen (Khatir et al., 2015). Pruijm et al. (2014) assessed patients with CKD and arterial hypertension (Pruijm et al., 2014), no difference in $R_2^*$ was seen between the patient group and healthy participants at baseline. However, following administration of furosemide, a blunted $R_2^*$ decrease was seen in patients compared with healthy participants. Xin-Long et al. (2012) measured the corticomedullary differentiation in $R_2^*$ in healthy participants and CKD patients and found an increased differentiation in CKD patients compared to healthy participants (Xin-Long et al., 2012).

## Limitations

It is important to consider the different factors which can impact on reported MR measures. Inconsistent BOLD results have been widely documented between published studies, whilst Michaely et al. showed that in a study of 280 subjects, $R_2^*$ correlated poorly with eGFR (Michaely et al., 2012). This is likely since $R_2^*$ is only an estimator of oxygenation, and is confounded by many other factors, with it being suggested that changes in the blood volume fraction considerably influences renal $T_2^*$ (Niendorf et al., 2015). Estimates of total renal blood flow need to consider kidney volume to also compute total perfusion, and in CKD patients the shrinkage of the kidney should be considered, which can mean that blood flow per kidney is preserved. However, this correction does not take into account that the cortex and medulla may not lose volume at the same rate.

ICC's are high for some MRI parameters presented—$T_1$, perfusion, renal artery flow and ADC—but other values are relatively low, presently hampering the introduction of these methods in clinical practice. Currently, MRI is expensive and multiple breath hold methods cannot be used in older, frail patients. Here, our multiparametric protocol includes a limited number of breath holds, with ASL, $T_1$, and DWI data collected using respiratory triggered acquisitions. In this study, inter-observer variability was not assessed since the post-processing is automated, including ROI placement. Further automation of this pipeline could be included and with the introduction of greater processing power, maps could be computed online at the scanner. In future, functional sodium technology to provide information on renal concentrating capacity will provide a further additional measure for multiparametric protocols (Maril et al., 2006). At this point, studies showing that MRI parameters can predict hard outcomes, such as, end stage renal disease, death or rapid decline of kidney function are necessary. For ultimate use in the clinic, MRI protocols need to be time efficient, and so it will be important to define key MRI parameters of high ICC which can be used for clinical assessment.

## CONCLUSIONS

This paper has outlined a multiparametric MRI acquisition and analysis protocol for assessment of renal structure, hemodynamics and oxygenation. No other modality can combine non-invasive techniques to provide such a comprehensive evaluation of renal function as MRI. Studies showing that MRI has added value to simply monitoring serum creatinine and proteinuria in kidney disease, and that MRI can provide similar information as a kidney biopsy are now eagerly awaited. The ability of early identification of patients at risk of progressing to end-stage kidney disease and protocols to assess the efficacy of treatments would improve clinical outcome, be of cost benefit for society and improve life quality for the patients.

## AUTHOR CONTRIBUTIONS

EC: study design, acquisition, analysis and interpretation of data, statistical analysis, drafting of manuscript, final

approval of manuscript, accountable for all aspects of the work; CEB: study design, acquisition, analysis and interpretation of data, critical revision of manuscript, final approval of manuscript, accountable for all aspects of the work; CRB: acquisition, analysis and interpretation of data, critical revision of manuscript, final approval of manuscript, accountable for all aspects of the work; BP: acquisition, analysis and interpretation of data, final approval of manuscript, accountable for all aspects of the work; HM: study design, interpretation of data, final approval of manuscript, accountable for all aspects of the work; MT: study design, interpretation of data, final approval of manuscript, accountable for all aspects of the work; NS: study design, interpretation of data, critical revision of manuscript, final approval of manuscript, accountable for all aspects of the work; SF: study design, acquisition, analysis and interpretation of data, drafting of manuscript, final approval of manuscript, accountable for all aspects of the work.

## FUNDING

The authors acknowledge the financial support from the National Institute for Health Research Nottingham Digestive Diseases Biomedical Research Unit, Nottingham University Hospitals NHS Trust and University of Nottingham, the Medical Research Council Confidence in Concept Award and the Dr. Hadwen Trust. The Dr. Hadwen Trust (DHT) is the UK's leading non-animal biomedical research charity that exclusively funds and promotes human-relevant research that replaces the use of animals whilst supporting the progress of medicine.

## ACKNOWLEDGMENTS

The authors acknowledge the support of the Sir Peter Mansfield Imaging Centre (SPMIC), the NIHR Nottingham Digestive Diseases Biomedical Research Unit (NDDBRU) and the Centre for Kidney Research and Innovation (CKRI), University of Nottingham.

## REFERENCES

Adler, S., Huang, H., Wolin, M. S., and Kaminski, P. M. (2004). Oxidant stress leads to impaired regulation of renal cortical oxygen consumption by nitric oxide in the aging kidney. *J. Am. Soc. Nephrol.* 15, 52–60. doi: 10.1097/01.ASN.0000101032.21097.C5

Artz, N. S., Sadowski, E. A., Wentland, A. L., Djamali, A., Grist, T. M., Seo, S., et al. (2011a). Reproducibility of renal perfusion MR imaging in native and transplanted kidneys using non-contrast arterial spin labeling. *J. Magn. Reson. Imaging* 33, 1414–1421. doi: 10.1002/jmri.22552

Artz, N. S., Sadowski, E. A., Wentland, A. L., Grist, T. M., Seo, S., Djamali, A., et al. (2011b). Arterial spin labeling MRI for assessment of perfusion in native and transplanted kidneys. *Magn. Reson. Imaging* 29, 74–82. doi: 10.1016/j.mri.2010.07.018

Bax, L., Bakker, C. J., Klein, W. M., Blanken, N., Beutler, J. J., and Mali, W. P. (2005). Renal blood flow measurements with use of phase-contrast magnetic resonance imaging: normal values and reproducibility. *J. Vasc. Intervent. Radiol.* 16, 807–814. doi: 10.1097/01.RVI.0000161144.98350.28

Becker, H. F., Polo, O., McNamara, S. G., Berthon-Jones, M., and Sullivan, C. E. (1996). Effect of different levels of hyperoxia on breathing in healthy subjects. *J. Appl. Physiol.* 81, 1683–1690.

Blantz, R. C., Deng, A., Miracle, C. M., and Thomson, S. C. (2007). Regulation of kidney function and metabolism: a question of supply and demand. *Trans. Am. Clin. Climatol. Assoc.* 118, 23–43.

Boss, A., Martirosian, P., Graf, H., Claussen, C. D., Schlemmer, H. P., and Schick, F. (2005). High resolution MR perfusion imaging of the kidneys at 3 Tesla without administration of contrast media. *RoFo* 177, 1625–1630. doi: 10.1055/s-2005-858761

Buchanan, C. E., Cox, E. F., and Francis, S. T. (eds.). (2015). *Evaluation of Readout Schemes for Arterial Spin Labelling in the Human Kidney*. Toronto, ON: Int Soc Mag Reson.

Buxton, R. B., Frank, L. R., Wong, E. C., Siewert, B., Warach, S., and Edelman, R. R. (1998). A general kinetic model for quantitative perfusion imaging with arterial spin labeling. *Magn. Reson. Med.* 40, 383–396. doi: 10.1002/mrm.1910400308

Chowdhury, A. H., Cox, E. F., Francis, S. T., and Lobo, D. N. (2012). A randomized, controlled, double-blind crossover study on the effects of 2-L infusions of 0.9% saline and plasma-lyte(R) 148 on renal blood flow velocity and renal cortical tissue perfusion in healthy volunteers. *Ann. Surg.* 256, 18–24. doi: 10.1097/SLA.0b013e318256be72

Cohen, E. I., Kelly, S. A., Edye, M., Mitty, H. A., and Bromberg, J. S. (2009). MRI estimation of total renal volume demonstrates significant association with healthy donor weight. *Eur. J. Radiol.* 71, 283–287. doi: 10.1016/j.ejrad.2008.03.006

Cutajar, M., Clayden, J. D., Clark, C. A., and Gordon, I. (2011). Test-retest reliability and repeatability of renal diffusion tensor MRI in healthy subjects. *Eur. J. Radiol.* 80, e263–e268. doi: 10.1016/j.ejrad.2010.12.018

Cutajar, M., Thomas, D. L., Banks, T., Clark, C. A., Golay, X., and Gordon, I. (2012). Repeatability of renal arterial spin labelling MRI in healthy subjects. *Magma* 25, 145–153. doi: 10.1007/s10334-011-0300-9

Cutajar, M., Thomas, D. L., Hales, P. W., Banks, T., Clark, C. A., and Gordon, I. (2014). Comparison of ASL and DCE MRI for the non-invasive measurement of renal blood flow: quantification and reproducibility. *Eur. Radiol.* 24, 1300–1308. doi: 10.1007/s00330-014-3130-0

Dambreville, S., Chapman, A. B., Torres, V. E., King, B. F., Wallin, A. K., Frakes, D. H., et al. (2010). Renal arterial blood flow measurement by breath-held MRI: accuracy in phantom scans and reproducibility in healthy subjects. *Magn. Reson. Med.* 63, 940–950. doi: 10.1002/mrm.22278

de Bazelaire, C. M., Duhamel, G. D., Rofsky, N. M., and Alsop, D. C. (2004). MR imaging relaxation times of abdominal and pelvic tissues measured *in vivo* at 3.0 T: preliminary results. *Radiology* 230, 652–659. doi: 10.1148/radiol.2303021331

Debatin, J. F., Ting, R. H., Wegmuller, H., Sommer, F. G., Fredrickson, J. O., Brosnan, T. J., et al. (1994). Renal artery blood flow: quantitation with phase-contrast MR imaging with and without breath holding. *Radiology* 190, 371–378. doi: 10.1148/radiology.190.2.8284383

Ding, J., Xing, W., Wu, D., Chen, J., Pan, L., Sun, J., et al. (2015). Evaluation of renal oxygenation level changes after water loading using susceptibility-weighted imaging and T2* mapping. *Korean J. Radiol.* 16, 827–834. doi: 10.3348/kjr.2015.16.4.827

Ding, Y., Mason, R. P., McColl, R. W., Yuan, Q., Hallac, R. R., Sims, R. D., et al. (2013). Simultaneous measurement of tissue oxygen level-dependent (TOLD) and blood oxygenation level-dependent (BOLD) effects in abdominal tissue oxygenation level studies. *J. Magn. Reson. Imaging* 38, 1230–1236. doi: 10.1002/jmri.24006

Dobre, M. C., Ugurbil, K., and Marjanska, M. (2007). Determination of blood longitudinal relaxation time (T1) at high magnetic field strengths. *Magn. Reson. Imaging* 25, 733–735. doi: 10.1016/j.mri.2006.10.020

Donati, O. F., Nanz, D., Serra, A. L., and Boss, A. (2012). Quantitative BOLD response of the renal medulla to hyperoxic challenge at 1.5 T and 3.0 T. *NMR Biomed.* 25, 1133–1138. doi: 10.1002/nbm.2781

Dong, J., Yang, L., Su, T., Yang, X., Chen, B., Zhang, J., et al. (2013). Quantitative assessment of acute kidney injury by noninvasive arterial spin labeling perfusion MRI: a pilot study. *Sci. China Life Sci.* 56, 745–750. doi: 10.1007/s11427-013-4503-3

Epstein, F. H., and Prasad, P. (2000). Effects of furosemide on medullary oxygenation in younger and older subjects. *Kidney Int.* 57, 2080–2083. doi: 10.1046/j.1523-1755.2000.00057.x

Evans, R. G., Gardiner, B. S., Smith, D. W., and O'Connor, P. M. (2008). Intrarenal oxygenation: unique challenges and the biophysical basis of homeostasis. *Am. J. Physiol. Renal Physiol.* 295, F1259–F1270. doi: 10.1152/ajprenal.90230.2008

Fenchel, M., Martirosian, P., Langanke, J., Giersch, J., Miller, S., Stauder, N. I., et al. (2006). Perfusion MR imaging with FAIR true FISP spin labeling in patients with and without renal artery stenosis: initial experience. *Radiology* 238, 1013–1021. doi: 10.1148/radiol.2382041623

Friedli, I., Crowe, L. A., Berchtold, L., Moll, S., Hadaya, K., de Perrot, T., et al. (2016). New Magnetic resonance imaging index for renal fibrosis assessment: a comparison between diffusion-weighted imaging and T1 mapping with histological validation. *Sci. Rep.* 6:30088. doi: 10.1038/srep30088

Ganesh, T., Estrada, M., Duffin, J., and Cheng, H. L. (2016). T2* and T1 assessment of abdominal tissue response to graded hypoxia and hypercapnia using a controlled gas mixing circuit for small animals. *J. Magn. Reson. Imaging* 44, 305–316. doi: 10.1002/jmri.25169

Gardener, A. G., and Francis, S. T. (2010). Multislice perfusion of the kidneys using parallel imaging: image acquisition and analysis strategies. *Magn. Reson. Med.* 63, 1627–1636. doi: 10.1002/mrm.22387

Gillis, K. A., McComb, C., Foster, J. E., Taylor, A. H., Patel, R. K., Morris, S. T., et al. (2014). Inter-study reproducibility of arterial spin labelling magnetic resonance imaging for measurement of renal perfusion in healthy volunteers at 3 Tesla. *BMC Nephrol.* 15:23. doi: 10.1186/1471-2369-15-23

Gillis, K. A., McComb, C., Patel, R. K., Stevens, K. K., Schneider, M. P., Radjenovic, A., et al. (2016). Non-contrast renal magnetic resonance imaging to assess perfusion and corticomedullary differentiation in health and chronic kidney disease. *Nephron* 133, 183–192. doi: 10.1159/000447601

Goyal, A., Sharma, R., Bhalla, A. S., Gamanagatti, S., and Seth, A. (2012). Diffusion-weighted MRI in assessment of renal dysfunction. *Indian J. Radiol. Imaging* 22, 155–159. doi: 10.4103/0971-3026.107169

Hammon, M., Janka, R., Siegl, C., Seuss, H., Grosso, R., Martirosian, P., et al. (2016). Reproducibility of kidney perfusion measurements with arterial spin labeling at 1.5 Tesla MRI combined with semiautomatic segmentation for differential cortical and medullary assessment. *Medicine* 95:e3083. doi: 10.1097/MD.0000000000003083

Heusch, P., Wittsack, H. J., Heusner, T., Buchbender, C., Quang, M. N., Martirosian, P., et al. (2013). Correlation of biexponential diffusion parameters with arterial spin-labeling perfusion MRI: results in transplanted kidneys. *Invest. Radiol.* 48, 140–144. doi: 10.1097/RLI.0b013e318277bfe3

Hoad, C. L., Palaniyappan, N., Kaye, P., Chernova, Y., James, M. W., Costigan, C., et al. (2015). A study of T(1) relaxation time as a measure of liver fibrosis and the influence of confounding histological factors. *NMR Biomed.* 28, 706–714. doi: 10.1002/nbm.3299

Iles, L., Pfluger, H., Phrommintikul, A., Cherayath, J., Aksit, P., Gupta, S. N., et al. (2008). Evaluation of diffuse myocardial fibrosis in heart failure with cardiac magnetic resonance contrast-enhanced T1 mapping. *J. Am. Coll. Cardiol.* 52, 1574–1580. doi: 10.1016/j.jacc.2008.06.049

Inoue, T., Kozawa, E., Okada, H., Inukai, K., Watanabe, S., Kikuta, T., et al. (2011). Noninvasive evaluation of kidney hypoxia and fibrosis using magnetic resonance imaging. *J. Am. Soc. Nephrol.* 22, 1429–1434. doi: 10.1681/ASN.2010111143

Jellis, C. L., and Kwon, D. H. (2014). Myocardial T1 mapping: modalities and clinical applications. *Cardiovasc. Diagn. Ther.* 4, 126–137. doi: 10.3978/j.issn.2223-3652.2013.09.03

Jones, R. A., Ries, M., Moonen, C. T., and Grenier, N. (2002). Imaging the changes in renal T1 induced by the inhalation of pure oxygen: a feasibility study. *Magn. Reson. Med.* 47, 728–735. doi: 10.1002/mrm.10127

Karger, N., Biederer, J., Lusse, S., Grimm, J., Steffens, J., Heller, M., et al. (2000). Quantitation of renal perfusion using arterial spin labeling with FAIR-UFLARE. *Magn. Reson. Imaging* 18, 641–647. doi: 10.1016/S0730-725X(00)00155-7

Khatir, D. S., Pedersen, M., Jespersen, B., and Buus, N. H. (2014). Reproducibility of MRI renal artery blood flow and BOLD measurements in patients with chronic kidney disease and healthy controls. *J. Magn. Reson. Imaging* 40, 1091–1098. doi: 10.1002/jmri.24446

Khatir, D. S., Pedersen, M., Jespersen, B., and Buus, N. H. (2015). Evaluation of renal blood flow and oxygenation in CKD using magnetic resonance imaging. *Am. J. Kidney Dis.* 66, 402–411. doi: 10.1053/j.ajkd.2014.11.022

Kiefer, C., Schroth, G., Gralla, J., Diehm, N., Baumgartner, I., and Husmann, M. (2009). A feasibility study on model-based evaluation of kidney perfusion measured by means of FAIR prepared true-FISP arterial spin labeling (ASL) on a 3-T MR scanner. *Acad. Radiol.* 16, 79–87. doi: 10.1016/j.acra.2008.04.024

Koh, D. M., Collins, D. J., and Orton, M. R. (2011). Intravoxel incoherent motion in body diffusion-weighted MRI: reality and challenges. *Am. J. Roentgenol.* 196, 1351–1361. doi: 10.2214/AJR.10.5515

Le Bihan, D., Breton, E., Lallemand, D., Aubin, M. L., Vignaud, J., and Laval-Jeantet, M. (1988). Separation of diffusion and perfusion in intravoxel incoherent motion MR imaging. *Radiology* 168, 497–505. doi: 10.1148/radiology.168.2.3393671

Li, L. P., Storey, P., Pierchala, L., Li, W., Polzin, J., and Prasad, P. (2004a). Evaluation of the reproducibility of intrarenal R2* and DeltaR2* measurements following administration of furosemide and during waterload. *J. Magn. Reson. Imaging* 19, 610–616. doi: 10.1002/jmri.20043

Li, L. P., Vu, A. T., Li, B. S., Dunkle, E., and Prasad, P. V. (2004b). Evaluation of intrarenal oxygenation by BOLD MRI at 3.0 T. *J. Magn. Reson. Imaging* 20, 901–904. doi: 10.1002/jmri.20176

Maril, N., Margalit, R., Rosen, S., Heyman, S. N., and Degani, H. (2006). Detection of evolving acute tubular necrosis with renal 23Na MRI: studies in rats. *Kidney Int.* 69, 765–768. doi: 10.1038/sj.ki.5000152

Martirosian, P., Klose, U., Mader, I., and Schick, F. (2004). FAIR true-FISP perfusion imaging of the kidneys. *Magn. Reson. Med.* 51, 353–361. doi: 10.1002/mrm.10709

Michaely, H. J., Metzger, L., Haneder, S., Hansmann, J., Schoenberg, S. O., and Attenberger, U. I. (2012). Renal BOLD-MRI does not reflect renal function in chronic kidney disease. *Kidney Int.* 81, 684–689. doi: 10.1038/ki.2011.455

Michaely, H. J., Schoenberg, S. O., Ittrich, C., Dikow, R., Bock, M., and Guenther, M. (2004). Renal disease: value of functional magnetic resonance imaging with flow and perfusion measurements. *Invest. Radiol.* 39, 698–705. doi: 10.1097/00004424-200411000-00008

Milani, B., Ansaloni, A., Sousa-Guimaraes, S., Vakilzadeh, N., Piskunowicz, M., Vogt, B., et al. (2016). Reduction of cortical oxygenation in chronic kidney disease: evidence obtained with a new analysis method of blood oxygenation level-dependent magnetic resonance imaging. *Nephrol. Dial. Transplant.* doi: 10.1093/ndt/gfw362. [Epub ahead of print].

Milman, Z., Heyman, S. N., Corchia, N., Edrei, Y., Axelrod, J. H., Rosenberger, C., et al. (2013). Hemodynamic response magnetic resonance imaging: application for renal hemodynamic characterization. *Nephrol. Dial. Transplant.* 28, 1150–1156. doi: 10.1093/ndt/gfs541

Mozes, F. E., Tunnicliffe, E. M., Pavlides, M., and Robson, M. D. (2016). Influence of fat on liver T1 measurements using modified Look-Locker inversion recovery (MOLLI) methods at 3T. *J. Magn. Reson. Imaging* 44, 105–111. doi: 10.1002/jmri.25146

Niendorf, T., Pohlmann, A., Arakelyan, K., Flemming, B., Cantow, K., Hentschel, J., et al. (2015). How bold is blood oxygenation level-dependent (BOLD) magnetic resonance imaging of the kidney? Opportunities, challenges and future directions. *Acta Physiol.* 213, 19–38. doi: 10.1111/apha.12393

Niles, D. J., Artz, N. S., Djamali, A., Sadowski, E. A., Grist, T. M., and Fain, S. B. (2016). Longitudinal assessment of renal perfusion and oxygenation in transplant donor-recipient pairs using arterial spin labeling and blood oxygen level-dependent magnetic resonance imaging. *Invest. Radiol.* 51, 113–120. doi: 10.1097/RLI.0000000000000210

Notohamiprodjo, M., Chandarana, H., Mikheev, A., Rusinek, H., Grinstead, J., Feiweier, T., et al. (2015). Combined intravoxel incoherent motion and diffusion tensor imaging of renal diffusion and flow anisotropy. *Magn. Reson. Med.* 73, 1526–1532. doi: 10.1002/mrm.25245

O'Connor, J. P., Jackson, A., Buonaccorsi, G. A., Buckley, D. L., Roberts, C., Watson, Y., et al. (2007). Organ-specific effects of oxygen and carbogen gas inhalation on tissue longitudinal relaxation times. *Magn. Reson. Med.* 58, 490–496. doi: 10.1002/mrm.21357

O'Connor, J. P., Naish, J. H., Jackson, A., Waterton, J. C., Watson, Y., Cheung, S., et al. (2009). Comparison of normal tissue R1 and R2* modulation by oxygen and carbogen. *Magn. Reson. Med.* 61, 75–83. doi: 10.1002/mrm.21815

Park, J. B., Santos, J. M., Hargreaves, B. A., Nayak, K. S., Sommer, G., Hu, B. S., et al. (2005). Rapid measurement of renal artery blood flow with ungated spiral phase-contrast MRI. *J. Magn. Reson. Imaging* 21, 590–595. doi: 10.1002/jmri.20325

Park, S. H., Wang, D. J., and Duong, T. Q. (2013). Balanced steady state free precession for arterial spin labeling MRI: initial experience for blood flow mapping in human brain, retina, and kidney. *Magn. Reson. Imaging* 31, 1044–1050. doi: 10.1016/j.mri.2013.03.024

Park, S. Y., Kim, C. K., Park, B. K., Huh, W., Kim, S. J., and Kim, B. (2012). Evaluation of transplanted kidneys using blood oxygenation level-dependent MRI at 3 T: a preliminary study. *Am. J. Roentgenol.* 198, 1108–1114. doi: 10.2214/AJR.11.7253

Piskunowicz, M., Hofmann, L., Zuercher, E., Bassi, I., Milani, B., Stuber, M., et al. (2015). A new technique with high reproducibility to estimate renal oxygenation using BOLD-MRI in chronic kidney disease. *Magn. Reson. Imaging* 33, 253–261. doi: 10.1016/j.mri.2014.12.002

Prasad, P. V., and Epstein, F. H. (1999). Changes in renal medullary pO2 during water diuresis as evaluated by blood oxygenation level-dependent magnetic resonance imaging: effects of aging and cyclooxygenase inhibition. *Kidney Int.* 55, 294–298. doi: 10.1046/j.1523-1755.1999.00237.x

Prasad, P. V., Edelman, R. R., and Epstein, F. H. (1996). Noninvasive evaluation of intrarenal oxygenation with BOLD MRI. *Circulation* 94, 3271–3275. doi: 10.1161/01.CIR.94.12.3271

Pruijm, M., Hofmann, L., Piskunowicz, M., Muller, M. E., Zweiacker, C., Bassi, I., et al. (2014). Determinants of renal tissue oxygenation as measured with BOLD-MRI in chronic kidney disease and hypertension in humans. *PLoS ONE* 9:e95895. doi: 10.1371/journal.pone.0095895

Pruijm, M., Milani, B., and Burnier, M. (2017). Blood oxygenation level-dependent MRI to assess renal oxygenation in renal diseases: progresses and challenges. *Front. Physiol.* 7:667. doi: 10.3389/fphys.2016.00667

Ritt, M., Janka, R., Schneider, M. P., Martirosian, P., Hornegger, J., Bautz, W., et al. (2010). Measurement of kidney perfusion by magnetic resonance imaging: comparison of MRI with arterial spin labeling to para-aminohippuric acid plasma clearance in male subjects with metabolic syndrome. *Nephrol. Dial.* 25, 1126–1133. doi: 10.1093/ndt/gfp639

Rossi, C., Artunc, F., Martirosian, P., Schlemmer, H. P., Schick, F., and Boss, A. (2012). Histogram analysis of renal arterial spin labeling perfusion data reveals differences between volunteers and patients with mild chronic kidney disease. *Invest. Radiol.* 47, 490–496. doi: 10.1097/RLI.0b013e318257063a

Schmitt, P., Griswold, M. A., Jakob, P. M., Kotas, M., Gulani, V., Flentje, M., et al. (2004). Inversion recovery TrueFISP: quantification of T1, T2, and spin density. *Magn. Reson. Med.* 51, 661–667. doi: 10.1002/mrm.20058

Schoenberg, S. O., Just, A., Bock, M., Knopp, M. V., Persson, P. B., and Kirchheim, H. R. (1997). Noninvasive analysis of renal artery blood flow dynamics with MR cine phase-contrast flow measurements. *Am. J. Physiol.* 272, H2477–H2484.

Seuss, H., Janka, R., Prummer, M., Cavallaro, A., Hammon, R., Theis, R., et al. (2017). Development and evaluation of a semi-automated segmentation tool and a modified ellipsoid formula for volumetric analysis of the kidney in non-contrast T2-weighted MR images. *J. Digit. Imaging* 30, 244–254. doi: 10.1007/s10278-016-9936-3

Sigmund, E. E., Vivier, P. H., Sui, D., Lamparello, N. A., Tantillo, K., Mikheev, A., et al. (2012). Intravoxel incoherent motion and diffusion-tensor imaging in renal tissue under hydration and furosemide flow challenges. *Radiology* 263, 758–769. doi: 10.1148/radiol.12111327

Simon-Zoula, S. C., Hofmann, L., Giger, A., Vogt, B., Vock, P., Frey, F. J., et al. (2006). Non-invasive monitoring of renal oxygenation using BOLD-MRI: a reproducibility study. *NMR Biomed.* 19, 84–89. doi: 10.1002/nbm.1004

Skorecki, K., Chertow, G. M., Marsden, P. A., Taal, M. W., and Yu, A. S. L. (2016). *Brenner and Rector's The Kidney, 10th Edn*. Philadelphia, PA: Elsevier.

Steeden, J. A., and Muthurangu, V. (2015). Investigating the limitations of single breath-hold renal artery blood flow measurements using spiral phase contrast MR with R-R interval averaging. *J. Magn. Reson. Imaging* 41, 1143–1149. doi: 10.1002/jmri.24638

Suo, S., Lin, N., Wang, H., Zhang, L., Wang, R., Zhang, S., et al. (2015). Intravoxel incoherent motion diffusion-weighted MR imaging of breast cancer at 3.0 Tesla: comparison of different curve-fitting methods. *J. Magn. Reson. Imaging* 42, 362–370. doi: 10.1002/jmri.24799

Tan, H., Koktzoglou, I., and Prasad, P. V. (2014). Renal perfusion imaging with two-dimensional navigator gated arterial spin labeling. *Magn. Reson. Med.* 71, 570–579. doi: 10.1002/mrm.24692

Thoeny, H. C., De Keyzer, F., Oyen, R. H., and Peeters, R. R. (2005). Diffusion-weighted MR imaging of kidneys in healthy volunteers and patients with parenchymal diseases: initial experience. *Radiology* 235, 911–917. doi: 10.1148/radiol.2353040554

Thomson, S. C., and Blantz, R. C. (2008). Glomerulotubular balance, tubuloglomerular feedback, and salt homeostasis. *J. Am. Soc. Nephrol.* 19, 2272–2275. doi: 10.1681/ASN.2007121326

Tumkur, S. M., Vu, A. T., Li, L. P., Pierchala, L., and Prasad, P. V. (2006a). Evaluation of intra-renal oxygenation during water diuresis: a time-resolved study using BOLD MRI. *Kidney Int.* 70, 139–143. doi: 10.1038/sj.ki.5000347

Tumkur, S., Vu, A., Li, L., and Prasad, P. V. (2006b). Evaluation of intrarenal oxygenation at 3.0 T using 3-dimensional multiple gradient-recalled echo sequence. *Invest. Radiol.* 41, 181–184. doi: 10.1097/01.rli.0000187166.43871.fb

Tunnicliffe, E. M., Banerjee, R., Pavlides, M., Neubauer, S., and Robson, M. D. (2017). A model for hepatic fibrosis: the competing effects of cell loss and iron on shortened modified Look-Locker inversion recovery T1 (shMOLLI-T1) in the liver. *J. Magn. Reson. Imaging* 45, 450–462. doi: 10.1002/jmri.25392

van den Dool, S. W., Wasser, M. N., de Fijter, J. W., Hoekstra, J., and van der Geest, R. J. (2005). Functional renal volume: quantitative analysis at gadolinium-enhanced MR angiography–feasibility study in healthy potential kidney donors. *Radiology* 236, 189–195. doi: 10.1148/radiol.2361021463

van der Bel, R., Coolen, B. F., Nederveen, A. J., Potters, W. V., Verberne, H. J., Vogt, L., et al. (2016). Magnetic resonance imaging-derived renal oxygenation and perfusion during continuous, steady-state angiotensin-II infusion in healthy humans. *J. Am. Heart Assoc.* 5:e003185. doi: 10.1161/JAHA.115.003185

Venkatachalam, M. A., Griffin, K. A., Lan, R., Geng, H., Saikumar, P., and Bidani, A. K. (2010). Acute kidney injury: a springboard for progression in chronic kidney disease. *Am. J. Physiol. Renal Physiol.* 298, F1078–F1094. doi: 10.1152/ajprenal.00017.2010

Vivier, P. H., Storey, P., Chandarana, H., Yamamoto, A., Tantillo, K., Khan, U., et al. (2013). Renal blood oxygenation level-dependent imaging: contribution of R2 to R2* values. *Invest. Radiol.* 48, 501–508. doi: 10.1097/RLI.0b013e3182823591

Wang, J., Zhang, Y., Yang, X., Wang, X., Zhang, J., Fang, J., et al. (2012). Hemodynamic effects of furosemide on renal perfusion as evaluated by ASL-MRI. *Acad. Radiol.* 19, 1194–1200. doi: 10.1016/j.acra.2012.04.021

Winter, J. D., Estrada, M., and Cheng, H. L. (2011). Normal tissue quantitative T1 and T2* MRI relaxation time responses to hypercapnic and hyperoxic gases. *Acad. Radiol.* 18, 1159–1167. doi: 10.1016/j.acra.2011.04.016

Wittsack, H. J., Lanzman, R. S., Mathys, C., Janssen, H., Modder, U., and Blondin, D. (2010). Statistical evaluation of diffusion-weighted imaging of the human kidney. *Magn. Reson. Med.* 64, 616–622. doi: 10.1002/mrm.22436

Xin-Long, P., Jing-Xia, X., Jian-Yu, L., Song, W., and Xin-Kui, T. (2012). A preliminary study of blood-oxygen-level-dependent MRI in patients with chronic kidney disease. *Magn. Reson. Imaging* 30, 330–335. doi: 10.1016/j.mri.2011.10.003

Young, I. R., Clarke, G. J., Bailes, D. R., Pennock, J. M., Doyle, F. H., and Bydder, G. M. (1981). Enhancement of relaxation rate with paramagnetic contrast agents in NMR imaging. *J. Comput. Tomogr.* 5, 543–547. doi: 10.1016/0149-936X(81)90089-8

Zhang, J. L., Sigmund, E. E., Chandarana, H., Rusinek, H., Chen, Q., Vivier, P. H., et al. (2010). Variability of renal apparent diffusion coefficients: limitations of the monoexponential model for diffusion quantification. *Radiology* 254, 783–792. doi: 10.1148/radiol.09090891

**Conflict of Interest Statement:** The authors declare that the research was conducted in the absence of any commercial or financial relationships that could be construed as a potential conflict of interest.

frontiers in Physiology

MINI REVIEW
published: 28 June 2017
doi: 10.3389/fphys.2017.00385

# Renal Oxygenation in the Pathophysiology of Chronic Kidney Disease

*Zhi Zhao Liu, Alexander Bullen, Ying Li and Prabhleen Singh **

*Division of Nephrology-Hypertension, University of California San Diego School of Medicine, VA San Diego Healthcare System, San Diego, CA, United States*

Chronic kidney disease (CKD) is a significant health problem associated with high morbidity and mortality. Despite significant research into various pathways involved in the pathophysiology of CKD, the therapeutic options are limited in diabetes and hypertension induced CKD to blood pressure control, hyperglycemia management (in diabetic nephropathy) and reduction of proteinuria, mainly with renin-angiotensin blockade therapy. Recently, renal oxygenation in pathophysiology of CKD progression has received a lot of interest. Several advances have been made in our understanding of the determinants and regulators of renal oxygenation in normal and diseased kidneys. The goal of this review is to discuss the alterations in renal oxygenation (delivery, consumption and tissue oxygen tension) in pre-clinical and clinical studies in diabetic and hypertensive CKD along with the underlying mechanisms and potential therapeutic options.

**Keywords: hypoxia, renal oxygen consumption, hypoxia inducible factor (HIF), AMPK, chronic kidney disease pathophysiology**

OPEN ACCESS

***Edited by:***
*Fredrik Palm,*
*Uppsala University, Sweden*

***Reviewed by:***
*Jaap Joles,*
*Utrecht University, Netherlands*
*Reiko Inagi,*
*University of Tokyo, Japan*

****Correspondence:***
*Prabhleen Singh*
*p1singh@ucsd.edu*

***Specialty section:***
*This article was submitted to Renal and Epithelial Physiology, a section of the journal Frontiers in Physiology*

***Received:*** *15 March 2017*
***Accepted:*** *23 May 2017*
***Published:*** *28 June 2017*

***Citation:***
*Liu ZZ, Bullen A, Li Y and Singh P (2017) Renal Oxygenation in the Pathophysiology of Chronic Kidney Disease. Front. Physiol. 8:385. doi: 10.3389/fphys.2017.00385*

## INTRODUCTION

Chronic kidney disease (CKD) is a worldwide public health problem. In the United States, 14% of adults suffer from CKD (Coresh et al., 2007). Besides its impact on health, CKD and end-stage renal disease (ESRD) require substantial healthcare resources (Honeycutt et al., 2013). Despite the resources committed to the treatment of CKD and improvements in the quality of dialysis therapy, CKD patients continue to experience significant mortality and morbidity and a reduced quality of life. Numerous studies have elucidated the underlying mechanisms of CKD and identified new therapeutic targets, but success in clinical translation has been limited. Among various pathways, imbalance between oxygen delivery and consumption leading to tissue hypoxia has been recognized as an important contributor to CKD development and progression (Fine et al., 1998; Norman and Fine, 2006; O'Connor, 2006; Mimura and Nangaku, 2010). The aim of this review is to discuss the role of renal oxygenation (oxygen delivery, consumption and tissue oxygen tension) in CKD progression and potential therapeutic options based on recent literature.

## TUBULAR TRANSPORT

The major function of kidney is to remove waste products and excess fluid from the body to maintain homeostasis. The kidneys filter about 180 liters of fluid daily. Nearly 99% of the of filtered sodium is reabsorbed and this is the primary energy consuming process in the kidneys powered

by the Na- and K-ATPase (sodium-potassium pump) in the basolateral membranes of tubular cells in the kidney. About 60–70% of total sodium reabsorption takes place in the proximal tubule, and another 25–30% in the thick ascending limb of the loop of Henle, and less than 10% in the distal convoluted tubule and collecting duct (Palmer and Schnermann, 2015). The sodium-potassium pump transports three sodium atoms out of the cell and two potassium atoms into the cell with the cost of hydrolyzing one ATP molecule (Mandel and Balaban, 1981). To retrieve nearly 99% of filtered Na, a continuously large amount of ATP ($>1.7 \times 10^{24}$ molecules) is required.

## RENAL OXYGENATION

Both oxidative and glycolytic pathways produce ATP. Compared to 2 molecules of ATP production in glycolysis per molecule of glucose, oxidative phosphorylation, generating 30–36 molecules of ATP, is more efficient (Soltoff, 1986). Hence, sufficient oxygen delivery to the kidney is needed to generate the required ATP via mitochondrial oxidative phosphorylation. Renal blood flow in the kidney is inhomogeneous, with cortex being well-perfused, but only 10–15% of perfusion directed to medulla to preserve osmotic gradients and enhance urinary concentration (Chou et al., 1990). Moreover, the arterial-to-venous oxygen shunting in medulla, which results from a counter-current exchange of oxygen before arterial blood reaches the renal microcirculation, decreases oxygen availability in this region (Evans et al., 2008). Lastly, the high metabolic requirements of the thick ascending limbs also contribute to hypoxia particularly in the outer medullary region, where the transport-related oxygen demand is high, while the delivery is lower than the cortex (Aukland and Krog, 1960; Mandel and Balaban, 1981; O'Connor, 2006). These particular features of tubular transport and metabolism can aggravate outer medullary hypoxia.

There is a close relation between GFR, renal sodium reabsorption, and oxygen consumption (Kiil et al., 1961; Blantz et al., 2007). In most organs, an increased demand of oxygen is met by an increased blood flow to increase oxygen delivery. However, an increase in blood flow to the kidney results in a simultaneously increased tubular sodium load due to increased GFR. Since sodium reabsorption is the major determinant of renal oxygen consumption (Lassen et al., 1961; Torelli et al., 1966), increased renal blood flow besides increasing oxygen supply also increases oxygen demand attributed to increased reabsorptive sodium load. It has been shown that renal oxygen extraction remains stable over a wide range of renal blood flow (Levy, 1960), indicating the increased oxygen delivery by renal blood flow is directly counteracted by increased oxygen consumption. So, maneuvers that increase GFR and thus the tubular sodium load also increase oxygen consumption and the effect on renal oxygenation is not always predictable.

## RENAL OXYGENATION IN DIABETIC CKD

According to the data from National Institute of Diabetes and Digestive and Kidney Diseases, as of 2014, nearly 10% of the US population has diabetes (Diabetes-NIDDK[1]). Diabetic nephropathy develops in nearly 40% of patients with diabetes and is the leading cause of CKD in patients with ESRD (Reutens, 2013). There has been significant advances in our understanding of the various pathways in the pathogenesis of diabetic nephropathy: hyperglycemia, glomerular hyperfiltration, activation of the polyol, renin-angiotensin and the protein kinase C pathways, advanced glycation end products, and genetic susceptibility (Brownlee, 2005). However, clinical translation to successful therapeutics for diabetic nephropathy has been limited. Since Fine et al. proposed kidney hypoxia as a mediator of progressive kidney disease (Fine et al., 1998), numerous experimental and clinical studies have provided evidence in support of chronic hypoxia being a common pathway for various progressive kidney diseases including diabetic nephropathy (Nangaku, 2006; Palm, 2006; Singh et al., 2008a, 2013; Mimura and Nangaku, 2010; Palm and Nordquist, 2011).

In experimental streptozotocin-induced diabetes, Ries et al. demonstrated that hypoxia was present in all compartments of the diabetic kidney, particularly in the outer medulla, using blood oxygen level-dependent (BOLD) MRI and diffusion-weighted imaging (Ries et al., 2003). Palm et al. showed a decrease in renal oxygen tension in the diabetic kidney, particular in medulla, due to the augmented oxygen consumption (Palm et al., 2003). Intrarenal microcirculation was not changed, but deoxyhemoglobin signals rose in diabetic kidney and oxygen consumption by tubular cells was significantly enhanced (Palm et al., 2003, 2004). Later the same group confirmed their findings using BOLD imaging (Edlund et al., 2009). Another study, demonstrated that hypoxic changes can be detected as early as 2 days in the diabetic kidney (dos Santos et al., 2007). Subsequently, Rosenberger et al. provided information on cellular localization of hypoxia in thick ascending limbs and a lesser extent in the collecting ducts using immunohistochemical staining with pimonidazole, a molecular hypoxia probe, and hypoxia inducible factor (HIF) (Rosenberger et al., 2008).

Recent studies have demonstrated the presence of tissue hypoxia before the presence of markers of kidney injury in diabetes. Friederich-Persson et al. reported kidney hypoxia resulting from increased mitochondrial oxygen consumption, independent of hyperglycemia and oxidative stress, was associated with tubulointerstitial damage, proteinuria and infiltration of inflammatory cells (Friederich-Persson et al., 2013). They concluded that kidney tissue hypoxia, *per se*, may be sufficient to initiate the development of nephropathy. Others have demonstrated the presence of tissue hypoxia in the kidney before the onset of albuminuria in diabetic mice (Franzén et al., 2016). Functional MRI imaging techniques have also been used to assess intrarenal oxygenation in humans, specifically in diabetic patients. Inoue et al. demonstrated parenchymal hypoxia and fibrosis in the renal cortex of CKD patients with or without diabetes using BOLD MRI and diffusion-weighted MRI, respectively (Inoue et al., 2011). Yin et al. reported reduced cortical and medullary oxygenation in patients with type 2

[1]Diabetes-NIDDK. National Institute of Diabetes and Digestive and Kidney Diseases. https://wwwniddknihgov/health-information/diabetes (accessed 2017).

diabetes with nephropathy (Yin et al., 2012). Medullary hypoxia was more prominent and present at earlier stages, with cortical hypoxia becoming more apparent with worsening renal function in diabetic patients. Pruijm studied the role renin-angiotensin system (RAS) in renal oxygenation in early stage type 2 diabetic patients with evidence of nephropathy (albuminuria and/or hypertension) (Pruijm et al., 2013). Short-term RAS blockade with ace-inhibitor or angiotension receptor blocker did not increase renal tissue oxygenation. Although not specifically examined in diabetes, animal studies have demonstrated an increase renal oxygenation in both normal and remnant rat kidney with RAS inhibition (Norman et al., 2003; Deng et al., 2009). Short duration of RAS blockade or modest changes in oxygenation not detected by BOLD MRI may explain the discrepancy.

Other studies have examined renal oxygenation in diabetes before any evidence of nephropathy and found similar baseline renal oxygenation in cortical and medullary oxygenation in diabetes compared to controls with BOLD MRI (Epstein et al., 2002; Economides et al., 2004). However, remarkably in both studies, patients with diabetes and even those at risk of diabetes did not show any improvement in medullary oxygenation with water diuresis, which was observed in healthy controls. This suggests an early impairment of adaptive vasodilation in the renal medulla in diabetes. Conversely, in a study in patients with moderate to severe diabetic nephropathy, no differences in cortical oxygenation but higher medullary oxygenation compared to controls was observed (Wang et al., 2011). The authors speculate that hypoxia noted in other studies in early stages of diabetes may be due to high oxygen consumption to support increased tubular reabsorption during the stage of glomerular hyperfiltration. In their study, reduced GFR and the associated decrease in tubular sodium reabsorption may result in lower oxygen consumption and the apparent increase in medullary oxygenation. The other possibility may be related to the technical aspects of BOLD MRI measurements. BOLD MRI measures tissue oxygenation indirectly by the changes in the deoxyhemoglobin concentration in the capillaries supplying the tissue. In advanced nephropathy, tissue fibrosis, reduction in peritubular capillaries, and changes in tissue oxygen extraction may lead to discrepancies between capillary deoxyhemoglobin concentrations and tissue oxygenation. Technical aspects of BOLD MRI and standard protocols for these measurements have been extensively discussed in recent papers (Simon-Zoula et al., 2006; Pruijm et al., 2016; Hirakawa et al., 2017). Characteristics of the studies discussed is summarized in **Table 1**.

## RENAL OXYGENATION IN HYPERTENSION AND HYPERTENSIVE CKD

Nearly 30% of adults in the United States hypertension according to the National Health and Nutrition Examination Survey 2011–2012 (Ostchega et al., 2008). Hypertension can affect each renal compartment: vessels, glomeruli and tubulointerstitium (Meyrier, 2015). Hypertensive nephropathy is the second only to diabetic nephropathy as the most common cause of ESRD in the US (Udani et al., 2011). Franz Volhard and Theodor Fahr first introduced the term hypertensive nephrosclerosis in 1918 (Meyrier, 2015) and several studies investigating the pathophysiology and potential treatments have been published. Over the last two decades, the role of renal oxygenation in hypertensive nephrosclerosis has been investigated.

Welch et al. were the first to show that a lower tissue oxygenation in both the cortex and medulla in angiotensin II (Ang II)-infused or spontaneously hypertensive rats (Welch et al., 2001, 2003). They further demonstrated that oxygenation was restored with the administration of superoxide dismutase mimetic, tempol, or an angiotensin receptor blocker, candesartan. In spontaneously hypertensive rats, they also observed a reduction in the ratio of tubular sodium transport by oxygen consumption (TNa/QO2). In an acute hypertension model with intravenous infusion of Ang II, reduced the oxygenation in the cortex and isolated proximal tubules and reduced TNa/QO2 was observed (Welch et al., 2005). All the effects were reversed by tempol, demonstrating the role of oxidative stress in this model. Recently, Emans et al. studied the effects of Ang II on cortical pO2 by telemetry in conscious rats (Emans et al., 2016). Using exogenous Ang II intravenously or activated RAS in transgenic Cyp1a1Ren2 rats, they found reduced renal cortical PO2 preceding the development of tissue injury. Zhu et al. showed that chronic infusion of Ang II in uninephrectomized rats increased tissue hypoxia as measured by immunostaining with pimonidazole, as well as increased urinary albumin excretion and collagen accumulation (Zhu et al., 2011). The albuminuria and collagen accumulation was attenuated by gene silencing of HIF-1α, linking upregulation of HIF-1α with fibrosis in this model. In another model of hypertension, renal neurogenic hypertension, induced by intrarenal injection of phenol, was shown to renal increase HIF-1α expression (Koeners et al., 2014). Interestingly, pretreatment with cobalt chloride, known HIF-1α activator, attenuated the development of hypertension and renal vasoconstriction.

Subtotal nephrectomy (STN), by uninephrectomy and partial renal infarction in the contralateral kidney, is a well-established, representative model of hypertensive CKD. Increased oxygen consumption factored for sodium reabsorption or nephron number has been observed in this model. Harris et al. observed a threefold increase in oxygen consumption per nephron in STN kidney at 4 weeks (Harris et al., 1988). Similar results were observed by Nath et al. at 3 weeks in the STN kidney (Nath et al., 1990). We have extensively studied the early hemodynamic, transport and metabolic adaptations in the 1-week STN kidney (Deng et al., 2009, 2010; Singh et al., 2009, 2012; Singh and Thomson, 2014). A major adaptation to nephron loss in early STN is hyperfiltration in the remaining nephrons (Singh et al., 2009). Hyperfiltration in the remaining nephrons results in hyperreabsorption, and this is associated with increased oxygen consumption. Indeed, we have previously reported the high oxygen consumption factored for sodium reabsorption at 1 week after STN (Deng et al., 2009, 2010). We have also demonstrated improved renal oxygenation with RAS blockade and HIF-1α activation (Deng et al., 2009, 2010). Manotham

**TABLE 1 |** Characteristics of studies in diabetes/diabetic CKD.

| Species | Types of diabetes | Duration of diabetes | Blood glucose (mmol/l) | $HbA_{1c}$ (%) | GFR (ml/min) | eGFR (ml/min/1.73 $m^2$) | Urinary protein (mg/g uCr) | References |
|---|---|---|---|---|---|---|---|---|
| Rat | STZ induced diabetes | Up to 3 weeks | 47.8 ± 14 | | N/A | | N/A | Ries et al., 2003 |
| | | 14 days | 20.9 ± 1.0 | | | | | Edlund et al., 2009 |
| | | Up to 4 weeks | 24.5 ± 1.7 | | | | | dos Santos et al., 2007 |
| | | 4 weeks | 25.5 ± 1.2 | | 1.14 ± 0.06 | | | Palm et al., 2003 |
| | | 4 weeks | 25.1 ± 0.6 | | 1.01 ± 0.08 | | | Palm et al., 2004 |
| | | Up to 90 days | 23.0 ± 1.5 | | ≤ 1.97 ± 0.1 | | | Rosenberger et al., 2008 |
| Mouse | Alloxan induced diabetes | Up to 15 days | 23.8 ± 1.7 | | N/A | | Negative | Franzén et al., 2016 |
| Human | Diabetes* | N/A | N/A | 7.0 ± 1.2 | | 43.8 ± 27.7 | 980.0 ± 2229.1 | Inoue et al., 2011 |
| | Type 2 diabetes | 5.6 ± 5.5 years | 7.8–11.1 | 7.7 ± 1.8 | | N/A | 30-300 | Economides et al., 2004 |
| | | 7 ± 4.75 years | 8.4 ± 1.0 | 7.4 ± 0.46 | 133 ± 7 | | Negative | Epstein et al., 2002 |
| | | 7.85 ± 5.31 years | N/A | N/A | ≤88.45 | | ≤ 9989.55 | Yin et al., 2012 |
| | | | | | | ±22.29 | ±7421.91 | |
| | | 11 ± 7 years | 7.2 ± 3 | 7.8 ± 1.0 | 62 ± 22 | | Positive | Pruijm et al., 2013 |
| | Diabetes* | N/A | N/A | N/A | | ≤ 67 | Positive | Wang et al., 2011 |

*CKD, chronic kidney disease; STZ, streptozotocin; HbA1c, hemoglobin A1c; GFR, glomerular filtration rate; eGFR, estimated GFR; uCr, urinary creatinine; N/A, information not available. *Diabetes type not specified.*

et al. showed evidence of tissue hypoxia in the STN kidney as early as 4 days and more prominently at 7 days by using pimonidazole immunostaining (Manotham et al., 2004). Tissue hypoxia persisted until interstitial damage developed. Treatment with Ang II blocker, olmesartan, prevented vascular changes and ameliorated tubular hypoxia after nephron loss.

In terms of clinical evidence, Textor et al. showed that African-American, hypertensive patients had elevated renal medullary volumes and blood flow, and lower medullary oxygenation compared to white hypertensive patients (Textor et al., 2012). Pruijm et al. investigated the effect of sodium intake on renal oxygenation in normotensive and hypertensive subjects after 1 week of high sodium and 1 week of low-sodium diet using BOLD MRI (Pruijm et al., 2010). They found that low sodium intake was associated with an increased renal medullary oxygenation but no changes in renal cortical oxygenation in both normo- and hypertensive individuals. In hypertensive patients, medullary oxygenation correlated with 24-h sodium excretion but no correlation with segmental renal sodium reabsorption was seen as observed in normotensive group. They speculated that this may be due to enhanced proximal sodium reabsorption and salt sensitivity observed in hypertensive patients (Burnier et al., 2006).

Schachiger et al. studied the role of RAS activation in renal oxygenation in humans and showed an acute decrease in cortical oxygenation by BOLD MRI after Ang II bolus injection (Schachinger et al., 2006). Subsequently, another study demonstrated a dose-dependent decrease of renal blood flow accompanied by a minor decrease of oxygenation in the cortex, not in the medulla with continuous Ang II infusion in healthy humans (Bel et al., 2016). As discussed above, parenchymal hypoxia and fibrosis in the renal cortex of CKD patients using BOLD MRI and diffusion-weighted MRI has been shown (Inoue et al., 2011). Other recent studies have demonstrated increased renal oxygenation, particularly in the renal medulla, with RAS blockade in healthy subjects and in CKD patients (Stein et al., 2012; Siddiqi et al., 2014; Vink et al., 2015). Characteristics of the studies discussed is summarized in **Table 2**.

## PATHOPHYSIOLOGY OF HYPOXIA IN CKD

Tubulointerstitial injury, which encompasses tubular atrophy and interstitial fibrosis, is a hallmark of progressive CKD regardless of its cause. Several studies have validated the role of tissue hypoxia in the progression of kidney disease (Kang et al., 2002; Nangaku, 2006; Heyman et al., 2008; Singh et al., 2013). Compromised oxygen delivery due to structural and functional changes impairing blood flow has been demonstrated. Tubulointerstitial hypoxia in advanced CKD can result from glomerular injury and interstitial fibrosis (Heyman et al., 2008). Glomerulosclerosis decreases the blood flow to downstream peritubular capillaries leading to insufficient oxygen delivery. Interstitial fibrosis further impairs oxygen delivery from the peritubular capillaries to the tubules. Recent studies have demonstrated peritubular capillary dysfunction as an important factor in the initiation of renal hypoxia (Ohashi et al., 2000; Kang et al., 2002; Matsumoto et al., 2004; Kawakami et al., 2014). Animal and human biopsy

**TABLE 2 |** Characteristics of studies in hypertension/hypertensive CKD.

| Species | Model/type of hypertension | Duration of hypertension | GFR (ml/min) | eGFR (ml/min/1.73 $m^2$) | Urinary protein (mg/d) | References |
|---|---|---|---|---|---|---|
| Rat | STN | Up to 1 week | N/A | | $\leq 51.5 \pm 8.6$ | Manotham et al., 2004 |
| | | 1 week | $0.53 \pm 0.04$ | | N/A | Deng et al., 2010 |
| | | 8 days | $0.85 \pm 0.23$ | | | Singh et al., 2009 |
| | | 8 days | $1.05 \pm 0.20$ (low salt)<br>$0.95 \pm 0.19$ (high salt) | | | Singh and Thomson, 2014 |
| | | 3 weeks | $0.66 \pm 0.07$ | | | Nath et al., 1990 |
| | STN, unilateral nephrectomy | 1 week | N/A | | | Singh et al., 2012 |
| | Drug-induced | 19 days | No change compared to control | | | Emans et al., 2016 |
| Human | Essential | N/A | | $95 \pm 24$ | $120 \pm 293$ | Textor et al., 2012 |
| | Essential | N/A | | $106.9 \pm 15.6$ | Negative | Pruijm et al., 2010 |
| | Drug-induced | 1 day | | N/A | Negative | Schachinger et al., 2006 |
| | Drug-induced | 1 day | | $110 \pm 18$ | N/A | Bel et al., 2016 |
| | Essential and secondary | N/A | | $30 \pm 11$ | N/A | Siddiqi et al., 2014 |
| | Essential | N/A | | 75 | 2.2 mg/mmol, albumin/creatinine ratio | Vink et al., 2015 |

*CKD, chronic kidney disease; STN, subtotal nephrectomy; GFR, glomerular filtration rate; eGFR, estimated GFR; N/A, information not available.*

specimens in CKD have demonstrated that tubulointerstitial injury is preceded by rarefaction of the peritubular capillaries (Bohle et al., 1996; Choi et al., 2000; Babickova et al., 2017).

The significance of these structural changes aside, early hypoxia demonstrated in animal and human studies are likely due to altered hemodynamics and metabolism. As discussed above, alteration in renal oxygen consumption and tissue hypoxia has been demonstrated in both diabetic and non-diabetic CKD models prior to the development of structural changes (Ries et al., 2003; Manotham et al., 2004; dos Santos et al., 2007; Deng et al., 2009, 2010; Franzén et al., 2016). Moreover, kidney hypoxia resulting from increased mitochondrial oxygen consumption alone has been shown to induce kidney injury (Friederich-Persson et al., 2013). Hence, understanding of the determinants and regulation of renal oxygenation in early stages is valuable in preventing subsequent tissue injury.

Chronic hypoxia causes tissue damage via various cytokine and cell-signaling pathways including RAS, endothelin, plasmin activator inhibitor-1, adhesion molecules and growth factors (Heyman et al., 2008; Haase, 2013). Impaired nitric oxide availability has also been implicated in the pathophysiology of diabetic nephropathy (Palm et al., 2003; Prabhakar et al., 2007) and hypertensive nephropathy (Welch et al., 2003; Singh et al., 2008b; Deng et al., 2009). Nitric oxide can increase renal oxygenation by improving oxygen delivery via vasodilation and directly lowering oxygen consumption (Evans and Fitzgerald, 2005; Singh et al., 2008b). HIF, a key transcriptional regulator of cellular adaption to hypoxia, has also received significant attention. It induces various target genes that impact oxygen delivery via vasomotor regulation and cellular oxygen consumption via several pathways (Semenza, 2009). Downstream HIF target proteins include inducible NOS, heme oxygenase-1, vascular endothelial growth factor, glucose transproters, glycolytic enzymes as well as proteins involved in cell proliferation and survival (Nangaku and Eckardt, 2007; Gunaratnam and Bonventre, 2009). HIF activation induces a glycolytic phenotype by upregulating GLUT transporters to facilitate glucose entry and inducing glycolytic enzymes (Semenza, 2009). HIF also has significant effects on mitochondrial metabolism and improves efficiency of respiratory chain proteins in hypoxia (Wheaton and Chandel, 2011). It represses mitochondrial biogenesis and respiration (Papandreou et al., 2006). It also induces mitochondrial autophagy as an adaptive metabolic response in hypoxia (Zhang et al., 2008).

While HIF activation has been shown to be renoprotective role in acute kidney injury, its effect in CKD are conflicting (Nangaku and Eckardt, 2007; Haase, 2009). Pharmacological HIF activation improved renal oxygenation, function and morphology in streptozotocin-induced diabetic and in STN rats (Deng et al., 2010; Li et al., 2015; Nordquist et al., 2015). Other studies have also shown beneficial effects of systemic HIF activation with different pharmacological agents in experimental models characterized by hypoxia (Manotham et al., 2004; Tanaka et al., 2005; Song et al., 2010; Yu et al., 2012a). However, studies using genetic approaches have yielded conflicting results. HIF-1α gene silencing or HIF-1α knockout has been shown to attenuate albuminuria, collagen accumulation and the development of tubulointerstitial fibrosis (Welch et al., 2005; Wang et al., 2014). Proximal tubule specific

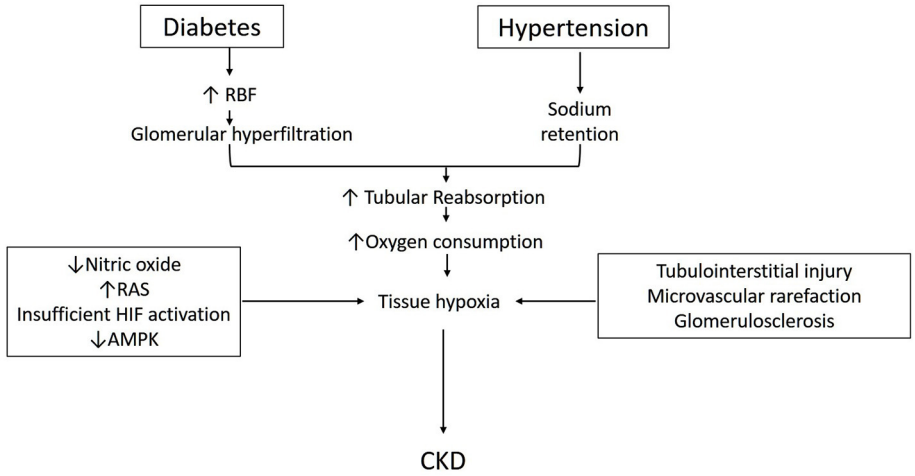


**FIGURE 1 |** Schematic describing pathophysiology for the development of CKD in diabetes and hypertension (see text for details).

overexpression of HIF-1α under normoxic conditions increased fibrosis while ablation ameliorated it (Higgins et al., 2007, 2008). Interestingly, the same group has subsequently shown that global activation of HIF-1α in all tubules ameliorated inflammation and fibrosis (Kobayashi et al., 2012). These results suggest that the outcomes of HIF activation are cell-specific, context-specific and timing-dependent in CKD (Yu et al., 2012b).

Lastly, the role AMP-activated kinase in the metabolism of diabetic and non-diabetic CKD is also receiving attention. AMPK is a ubiquitously expressed, highly conserved, key energy sensor and regulator of cellular metabolic activity (Hardie and Ashford, 2014). It is activated by cellular stressor such as nutrient deprivation, hypoxia or ischemia. AMPK facilitates metabolic adaptation by triggering ATP producing pathways, while inhibiting ATP consuming pathways (Gwinn et al., 2008). It stimulates mitochondrial biogenesis and cellular autophagy as survival mechanisms in low energy states (Steinberg and Kemp, 2009; Weinberg, 2011). Beneficial effects of AMPK activation in diabetes and high-fat diet induced kidney disease has been described (Lee et al., 2007; Hallows et al., 2010; Decleves et al., 2011). AMPK activation has also been shown to improve oxygen delivery and lower oxygen consumption and improve renal function and histology in STN (Satriano et al., 2013). We have also recently described the interactions between HIF and AMPK pathways in the regulation of cellular hypoxia adaptation in STN (Li et al., 2015). A schematic diagram incorporating some of the above discussed aspects in the pathophysiology of development of CKD is shown in **Figure 1**.

## CONCLUSION

CKD is a major healthcare burden, associated with significant comorbidities and progression to ESRD. Available therapies for diabetic and non-diabetic CKD are inadequate in halting or slowing the progression of disease. An increasing number of experimental and clinical studies indicate that renal tissue hypoxia, resulting from mismatch between oxygen delivery and consumption is a major contributor to CKD progression. Hence, it is imperative to understand the regulation of kidney oxygenation in CKD to identify novel therapeutic targets. Interventions to restore kidney tissue oxygenation has been shown to be beneficial in animal models of CKD. Clinical studies are limited and additional investigations into therapeutic targets to improve renal oxygenation in different forms of CKD are needed to improve clinical outcomes.

## AUTHOR CONTRIBUTIONS

ZZL: drafted, prepared, and edited the manuscript. AB and YL: reviewed and edited the manuscript. PS: reviewed, revised and edited the manuscript.

## ACKNOWLEDGMENTS

This work was supported by VA Merit BX002175 (PS), NIH-NIDDK R01 DK107852 (PS), NIH-NIDDK R03 DK101841 (PS), American Diabetes Association Grant #4-15-CKD-70 and UAB-UCSD O'Brien Center (NIH P30-DK 079337).

## REFERENCES

Aukland, K., and Krog, J. (1960). Renal oxygen tension. *Nature* 188:671. doi: 10.1038/188671a0

Babickova, J., Klinkhammer, B. M., Buhl, E. M., Djudjaj, S., Hoss, M., Heymann, F., et al. (2017). Regardless of etiology, progressive renal disease causes ultrastructural and functional alterations of peritubular capillaries. *Kidney Int.* 91, 70–85. doi: 10.1016/j.kint.2016.07.038

Bel, R., Coolen, B. F., Nederveen, A. J., Potters, W. V., Verberne, H. J., Vogt, L., et al. (2016). Magnetic resonance imaging–derived renal oxygenation and perfusion during continuous, steady-state angiotensin-II infusion in healthy humans. *J. Am. Heart Assoc.* 5:e003185. doi: 10.1161/JAHA.115.003185

Blantz, R. C., Deng, A., Miracle, C. M., and Thomson, S. C. (2007). Regulation of kidney function and metabolism: a question of supply and demand. *Trans. Am. Clin. Climatol. Assoc.* 118, 23–43.

Bohle, A., Mackensen-Haen, S., and Wehrmann, M. (1996). Significance of postglomerular capillaries in the pathogenesis of chronic renal failure. *Kidney Blood Press. Res.* 19, 191–195. doi: 10.1159/000174072

Brownlee, M. (2005). The pathobiology of diabetic complications: a unifying mechanism. *Diabetes* 54, 1615–1625. doi: 10.2337/diabetes.54.6.1615

Burnier, M., Bochud, M., and Maillard, M. (2006). Proximal tubular function and salt sensitivity. *Curr. Hypertens. Rep.* 8, 8–15. doi: 10.1007/s11906-006-0035-6

Choi, Y. J., Chakraborty, S., Nguyen, V., Nguyen, C., Kim, B. K., Shim, S. I., et al. (2000). Peritubular capillary loss is associated with chronic tubulointerstitial injury in human kidney: altered expression of vascular endothelial growth factor. *Hum. Pathol.* 31, 1491–1497. doi: 10.1053/hupa.2000.20373

Chou, S. Y., Porush, J. G., and Faubert, P. F. (1990). Renal medullary circulation: hormonal control. *Kidney Int.* 37, 1–13. doi: 10.1038/ki.1990.1

Coresh, J., Selvin, E., Stevens, L. A., Manzi, J., Kusek, J. W., Eggers, P., et al. (2007). Prevalence of chronic kidney disease in the United States. *JAMA* 298, 2038–2047. doi: 10.1001/jama.298.17.2038

Decleves, A. E., Mathew, A. V., Cunard, R., and Sharma, K. (2011). AMPK mediates the initiation of kidney disease induced by a high-fat diet. *J. Am. Soc. Nephrol.* 22, 1846–1855. doi: 10.1681/ASN.2011010026

Deng, A., Arndt, M. A. K., Satriano, J., Singh, P., Rieg, T., Thomson, S., et al. (2010). Renal protection in chronic kidney disease: hypoxia-inducible factor activation vs. angiotensin II blockade. *Am. J. Physiol. Ren. Physiol.* 299, F1365–F1373. doi: 10.1152/ajprenal.00153.2010

Deng, A., Tang, T., Singh, P., Wang, C., Satriano, J., Thomson, S. C., et al. (2009). Regulation of oxygen utilization by angiotensin II in chronic kidney disease. *Kidney Int.* 75, 197–204. doi: 10.1038/ki.2008.481

dos Santos, E. A., Li, L.-P., Ji, L., and Prasad, P. V. (2007). Early changes with diabetes in renal medullary hemodynamics as evaluated by fiberoptic probes and BOLD magnetic resonance imaging. *Invest. Radiol.* 42, 157–162. doi: 10.1097/01.rli.0000252492.96709.36

Economides, P. A., Caselli, A., Zuo, C. S., Sparks, C., Khaodhiar, L., Katsilambros, N., et al. (2004). Kidney oxygenation during water diuresis and endothelial function in patients with type 2 diabetes and subjects at risk to develop diabetes. *Metab. Clin. Exp.* 53, 222–227. doi: 10.1016/j.metabol.2003.09.019

Edlund, J., Hansell, P., Fasching, A., Liss, P., Weis, J., Glickson, J. D., et al. (2009). Reduced oxygenation in diabetic rat kidneys measured by T2∗ weighted magnetic resonance micro-imaging. *Adv. Exp. Med. Biol.* 645, 199–204. doi: 10.1007/978-0-387-85998-9_31

Emans, T. W., Janssen, B. J., Pinkham, M. I., Ow, C. P., Evans, R. G., Joles, J. A., et al. (2016). Exogenous and endogenous angiotensin-II decrease renal cortical oxygen tension in conscious rats by limiting renal blood flow. *J. Physiol.* 594, 6287–6300. doi: 10.1113/JP270731

Epstein, F. H., Veves, A., and Prasad, P. V. (2002). Effect of diabetes on renal medullary oxygenation during water diuresis. *Diabetes Care* 25, 575–578. doi: 10.2337/diacare.25.3.575

Evans, R. G., and Fitzgerald, S. M. (2005). Nitric oxide and superoxide in the renal medulla: a delicate balancing act. *Curr. Opin. Nephrol. Hypertens.* 14, 9–15. doi: 10.1097/00041552-200501000-00003

Evans, R. G., Gardiner, B. S., Smith, D. W., and O'Connor, P. M. (2008). Intrarenal oxygenation: unique challenges and the biophysical basis of homeostasis. *Am. J. Physiol. Ren. Physiol.* 295, F1259–F1270. doi: 10.1152/ajprenal.90230.2008

Fine, L. G., Orphanides, C., and Norman, J. T. (1998). Progressive renal disease: the chronic hypoxia hypothesis. *Kidney Int. Suppl.* 65, S74–S78.

Franzén, S., Pihl, L., Khan, N., Gustafsson, H., and Palm, F. (2016). Pronounced kidney hypoxia precedes albuminuria in type 1 diabetic mice. *Am. J. Physiol. Ren. Physiol.* 310, F807–F809. doi: 10.1152/ajprenal.00049.2016

Friederich-Persson, M., Thörn, E., Hansell, P., Nangaku, M., Levin, M., and Palm, F. (2013). Kidney hypoxia, attributable to increased oxygen consumption, induces nephropathy independently of hyperglycemia and oxidative stress. *Hypertension* 62, 914–919. doi: 10.1161/HYPERTENSIONAHA.113.01425

Gunaratnam, L., and Bonventre, J. V. (2009). HIF in kidney disease and development. *JASN* 20, 1877–1887. doi: 10.1681/ASN.2008070804

Gwinn, D. M., Shackelford, D. B., Egan, D. F., Mihaylova, M. M., Mery, A., Vasquez, D. S., et al. (2008). AMPK phosphorylation of raptor mediates a metabolic checkpoint. *Mol Cell.* 30, 214–226. doi: 10.1016/j.molcel.2008.03.003

Haase, V. H. (2009). Pathophysiological consequences of HIF activation: HIF as a modulator of fibrosis. *Ann. N. Y. Acad. Sci.* 1177, 57–65. doi: 10.1111/j.1749-6632.2009.05030.x

Haase, V. H. (2013). Mechanisms of hypoxia responses in renal tissue. *J. Am. Soc. Nephrol.* 24, 537–541. doi: 10.1681/ASN.2012080855

Hallows, K. R., Mount, P. F., Pastor-Soler, N. M., and Power, D. A. (2010). Role of the energy sensor AMP-activated protein kinase in renal physiology and disease. *Am. J. Physiol. Ren. Physiol.* 298, F1067–F1077. doi: 10.1152/ajprenal.00005.2010

Hardie, D. G., and Ashford, M. L. (2014). AMPK: regulating energy balance at the cellular and whole body levels. *Physiology* 29, 99–107. doi: 10.1152/physiol.00050

Harris, D. C., Chan, L., and Schrier, R. W. (1988). Remnant kidney hypermetabolism and progression of chronic renal failure. *Am. J. Physiol.* 254, F267–F276.

Heyman, S. N., Khamaisi, M., Rosen, S., and Rosenberger, C. (2008). Renal parenchymal hypoxia, hypoxia response and the progression of chronic kidney disease. *Am. J. Nephrol.* 28, 998–1006. doi: 10.1159/000146075

Higgins, D. F., Kimura, K., Bernhardt, W. M., Shrimanker, N., Akai, Y., Hohenstein, B., et al. (2007). Hypoxia promotes fibrogenesis *in vivo* via HIF-1 stimulation of epithelial-to-mesenchymal transition. *J. Clin. Invest.* 117, 3810–3820. doi: 10.1172/JCI30487

Higgins, D. F., Kimura, K., Iwano, M., and Haase, V. H. (2008). Hypoxia-inducible factor signaling in the development of tissue fibrosis. *Cell Cycle* 7, 1128–1132. doi: 10.4161/cc.7.9.5804

Hirakawa, Y., Tanaka, T., and Nangaku, M. (2017). Renal hypoxia in CKD; pathophysiology and detecting methods. *Front. Physiol.*8:99. doi: 10.3389/fphys.2017.00099

Honeycutt, A. A., Segel, J. E., Zhuo, X., Hoerger, T. J., Imai, K., and Williams, D. (2013). Medical costs of CKD in the medicare population. *J. Am. Soc. Nephrol.* 24, 1478–1483. doi: 10.1681/ASN.2012040392

Inoue, T., Kozawa, E., Okada, H., Inukai, K., Watanabe, S., Kikuta, T., et al. (2011). Noninvasive evaluation of kidney hypoxia and fibrosis using magnetic resonance imaging. *J. Am. Soc. Nephrol.* 22, 1429–1434. doi: 10.1681/ASN.2010111143

Kang, D.-H., Kanellis, J., Hugo, C., Truong, L., Anderson, S., Kerjaschki, D., et al. (2002). Role of the microvascular endothelium in progressive renal disease. *J. Am. Soc. Nephrol.* 13, 806–816. doi: 10.1097/01.ASN.0000034910.58454.FD

Kawakami, T., Mimura, I., Shoji, K., Tanaka, T., and Nangaku, M. (2014). Hypoxia and fibrosis in chronic kidney disease: crossing at pericytes. *Kidney Int. Suppl.* 4, 107–112. doi: 10.1038/kisup.2014.20

Kiil, F., Aukland, K., and Refsum, H. E. (1961). Renal sodium transport and oxygen consumption. *Am. J. Physiol.* 201, 511–516.

Kobayashi, H., Gilbert, V., Liu, Q., Kapitsinou, P. P., Unger, T. L., Rha, J., et al. (2012). Myeloid cell-derived hypoxia-inducible factor attenuates inflammation in unilateral ureteral obstruction-induced kidney injury. *J. Immunol.* 188, 5106–5115. doi: 10.4049/jimmunol.1103377

Koeners, M. P., Vink, E. E., Kuijper, A., Gadellaa, N., Rosenberger, C., Mathia, S., et al. (2014). Stabilization of hypoxia inducible factor-1alpha ameliorates acute renal neurogenic hypertension. *J. Hypertens.* 32, 587–597. doi: 10.1097/HJH.0000000000000060

Lassen, N. A., Munck, O., and Thaysen, J. H. (1961). Oxygen consumption and sodium reabsorption in the kidney. *Acta Physiol. Scand.* 51, 371–384. doi: 10.1111/j.1748-1716.1961.tb02147.x

Lee, M. J., Feliers, D., Mariappan, M. M., Sataranatarajan, K., Mahimainathan, L., Musi, N., et al. (2007). A role for AMP-activated protein kinase in diabetes-induced renal hypertrophy. *Am. J. Physiol. Ren. Physiol.* 292, F617–F627. doi: 10.4049/jimmunol.1103377

Levy, M. N. (1960). Effect of variations of blood flow on renal oxygen extraction. *Am. J. Physiol.* 199, 13–18.

Li, H., Satriano, J., Thomas, J. L., Miyamoto, S., Sharma, K., Pastor-Soler, N. M., et al. (2015). Interactions between HIF-1alpha and AMPK in the regulation of cellular hypoxia adaptation in chronic kidney disease. *Am. J. Physiol. Ren. Physiol.* 309, F414–F428. doi: 10.1152/ajprenal.00463.2014

Mandel, L. J., and Balaban, R. S. (1981). Stoichiometry and coupling of active transport to oxidative metabolism in epithelial tissues. *Am. J. Physiol.* 240, F357–F371.

Manotham, K., Tanaka, T., Matsumoto, M., Ohse, T., Miyata, T., Inagi, R., et al. (2004). Evidence of tubular hypoxia in the early phase in the remnant kidney model. *J. Am. Soc. Nephrol.* 15, 1277–1288. doi: 10.1097/01.ASN.0000125614.35046.10

Matsumoto, M., Tanaka, T., Yamamoto, T., Noiri, E., Miyata, T., Inagi, R., et al. (2004). Hypoperfusion of peritubular capillaries induces chronic hypoxia before progression of tubulointerstitial injury in a progressive model of rat glomerulonephritis. *J. Am. Soc. Nephrol.* 15, 1574–1581. doi: 10.1097/01.ASN.0000128047.13396.48

Meyrier, A. (2015). Nephrosclerosis: update on a centenarian. *Nephrol. Dial. Transplant.* 30, 1833–1841. doi: 10.1093/ndt/gfu366

Mimura, I., and Nangaku, M. (2010). The suffocating kidney: tubulointerstitial hypoxia in end-stage renal disease. *Nat. Rev. Nephrol.* 6, 667–678. doi: 10.1038/nrneph.2010.124

Nangaku, M. (2006). Chronic hypoxia and tubulointerstitial injury: a final common pathway to end-stage renal failure. *J. Am. Soc. Nephrol.* 17, 17–25. doi: 10.1681/ASN.2005070757

Nangaku, M., and Eckardt, K.-U. (2007). Hypoxia and the HIF system in kidney disease. *J. Mol. Med.* 85, 1325–1330. doi: 10.1007/s00109-007-0278-y

Nath, K. A., Croatt, A. J., and Hostetter, T. H. (1990). Oxygen consumption and oxidant stress in surviving nephrons. *Am. J. Physiol.* 258, F1354–F1362.

Nordquist, L., Friederich-Persson, M., Fasching, A., Liss, P., Shoji, K., Nangaku, M., et al. (2015). Activation of hypoxia-inducible factors prevents diabetic nephropathy. *J. Am. Soc. Nephrol.* 26, 328–338. doi: 10.1681/ASN.2013090990

Norman, J. T., and Fine, L. G. (2006). Intrarenal oxygenation in chronic renal failure. *Clin. Exp. Pharmacol. Physiol.* 33, 989–996. doi: 10.1111/j.1440-1681.2006.04476.x

Norman, J. T., Stidwill, R., Singer, M., and Fine, L. G. (2003). Angiotensin II blockade augments renal cortical microvascular pO2 indicating a novel, potentially renoprotective action. *Nephron Physiol.* 94, P39–P46. doi: 10.1159/000071289

O'Connor, P. M. (2006). Renal oxygen delivery: matching delivery to metabolic demand. *Clin. Exp. Pharmacol. Physiol.* 33, 961–967. doi: 10.1111/j.1440-1681.2006.04475.x

Ohashi, R., Kitamura, H., and Yamanaka, N. (2000). Peritubular capillary injury during the progression of experimental glomerulonephritis in rats. *J. Am. Soc. Nephrol.* 11, 47–56.

Ostchega, Y., Yoon, S. S., Hughes, J., and Louis, T. (2008). Hypertension awareness, treatment, and control–continued disparities in adults: United States, 2005–2006. *NCHS Data Brief.* 1–8.

Palm, F. (2006). Intrarenal oxygen in diabetes and a possible link to diabetic nephropathy. *Clin. Exp. Pharmacol. Physiol.* 33, 997–1001. doi: 10.1111/j.1440-1681.2006.04473.x

Palm, F., Cederberg, J., Hansell, P., Liss, P., and Carlsson, P. O. (2003). Reactive oxygen species cause diabetes-induced decrease in renal oxygen tension. *Diabetologia* 46, 1153–1160. doi: 10.1007/s00125-003-1155-z

Palm, F., Hansell, P., Ronquist, G., Waldenström, A., Liss, P., and Carlsson, P. O. (2004). Polyol-pathway-dependent disturbances in renal medullary metabolism in experimental insulin-deficient diabetes mellitus in rats. *Diabetologia* 47, 1223–1231. doi: 10.1007/s00125-004-1434-3

Palm, F., and Nordquist, L. (2011). Renal tubulointerstitial hypoxia: cause and consequence of kidney dysfunction. *Clin. Exp. Pharmacol. Physiol.* 38, 474–480. doi: 10.1111/j.1440-1681.2011.05532.x

Palmer, L. G., and Schnermann, J. (2015). Integrated control of Na transport along the nephron. *Clin. J. Am. Soc. Nephrol.* 10, 676–687. doi: 10.2215/CJN.12391213

Papandreou, I., Cairns, R. A., Fontana, L., Lim, A. L., and Denko, N. C. (2006). HIF-1 mediates adaptation to hypoxia by actively downregulating mitochondrial oxygen consumption. *Cell Metab.* 3, 187–197. doi: 10.1016/j.cmet.2006.01.012

Prabhakar, S., Starnes, J., Shi, S., Lonis, B., and Tran, R. (2007). Diabetic nephropathy is associated with oxidative stress and decreased renal nitric oxide production. *J. Am. Soc. Nephrol.* 18, 2945–2952. doi: 10.1681/ASN.2006080895

Pruijm, M., Hofmann, L., Maillard, M., Tremblay, S., Glatz, N., Wuerzner, G., et al. (2010). Effect of sodium loading/depletion on renal oxygenation in young normotensive and hypertensive men. *Hypertension* 55, 1116–1122. doi: 10.1161/HYPERTENSIONAHA.109.149682

Pruijm, M., Hofmann, L., Zanchi, A., Maillard, M., Forni, V., Muller, M.-E., et al. (2013). Blockade of the renin-angiotensin system and renal tissue oxygenation as measured with BOLD-MRI in patients with type 2 diabetes. *Diabetes Res. Clin. Pract.* 99, 136–144. doi: 10.1016/j.diabres.2012.11.004

Pruijm, M., Milani, B., and Burnier, M. (2016). Blood oxygenation level-dependent MRI to assess renal oxygenation in renal diseases: progresses and challenges. *Front. Physiol.* 7:667. doi: 10.3389/fphys.2016.00667

Reutens, A. T. (2013). Epidemiology of diabetic kidney disease. *Med. Clin. North Am.* 97, 1–18. doi: 10.1016/j.mcna.2012.10.001

Ries, M., Basseau, F., Tyndal, B., Jones, R., Deminière, C., Catargi, B., et al. (2003). Renal diffusion and BOLD MRI in experimental diabetic nephropathy. Blood oxygen level-dependent. *J. Magn. Reson. Imaging* 17, 104–113. doi: 10.1002/jmri.10224

Rosenberger, C., Khamaisi, M., Abassi, Z., Shilo, V., Weksler-Zangen, S., Goldfarb, M., et al. (2008). Adaptation to hypoxia in the diabetic rat kidney. *Kidney Internat.* 73, 34–42. doi: 10.1038/sj.ki.5002567

Satriano, J., Sharma, K., Blantz, R. C., and Deng, A. (2013). Induction of AMPK activity corrects early pathophysiological alterations in the subtotal nephrectomy model of chronic kidney disease. *Am. J. Physiol. Ren. Physiol.* 305, F727–F733. doi: 10.1152/ajprenal.00293.2013

Schachinger, H., Klarhöfer, M., Linder, L., Drewe, J., and Scheffler, K. (2006). Angiotensin II decreases the renal MRI blood oxygenation level-dependent signal. *Hypertension* 47, 1062–1066. doi: 10.1161/01.HYP.0000220109.98142.a3

Semenza, G. L. (2009). Regulation of oxygen homeostasis by hypoxia-inducible factor 1. *Physiology* 24, 97–106. doi: 10.1152/physiol.00045.2008

Siddiqi, L., Hoogduin, H., Visser, F., Leiner, T., Mali, W. P., and Blankestijn, P. J. (2014). Inhibition of the renin-angiotensin system affects kidney tissue oxygenation evaluated by magnetic resonance imaging in patients with chronic kidney disease. J *Clin. Hypertens.* 16, 214–218. doi: 10.1111/jch.12263

Simon-Zoula, S. C., Hofmann, L., Giger, A., Vogt, B., Vock, P., Frey, F. J., et al. (2006). Non-invasive monitoring of renal oxygenation using BOLD-MRI: a reproducibility study. *NMR Biomed.* 19, 84–89. doi: 10.1002/nbm.1004

Singh, D. K., Winocour, P., and Farrington, K. (2008a). Mechanisms of disease: the hypoxic tubular hypothesis of diabetic nephropathy. *Nat. Clin. Pract. Nephrol.* 4, 216–226. doi: 10.1038/ncpneph0757

Singh, P., Blantz, R. C., Rosenberger, C., Gabbai, F. B., Schoeb, T. R., and Thomson, S. C. (2012). Aberrant tubuloglomerular feedback and HIF-1α confer resistance to ischemia after subtotal nephrectomy. *J. Am. Soc. Nephrol.* 23, 483–493. doi: 10.1681/ASN.2011020130

Singh, P., Deng, A., Blantz, R. C., and Thomson, S. C. (2009). Unexpected effect of angiotensin AT1 receptor blockade on tubuloglomerular feedback in early subtotal nephrectomy. *Am. J. Physiol. Ren. Physiol.* 296, F1158–F1165. doi: 10.1152/ajprenal.90722.2008

Singh, P., Deng, A., Weir, M. R., and Blantz, R. C. (2008b). The balance of angiotensin II and nitric oxide in kidney diseases. *Curr. Opin. Nephrol. Hypertens.* 17, 51–56. doi: 10.1097/MNH.0b013e3282f29a8b

Singh, P., Ricksten, S.-E., Bragadottir, G., Redfors, B., and Nordquist, L. (2013). Renal oxygenation and hemodynamics in acute kidney injury and chronic kidney disease. *Clin. Exp. Pharmacol. Physiol.* 40, 138–147. doi: 10.1111/1440-1681.12036

Singh, P., and Thomson, S. C. (2014). Salt sensitivity of tubuloglomerular feedback in the early remnant kidney. *Am. J. Physiol. Ren. Physiol.* 306, F172–F180. doi: 10.1152/ajprenal.00431.2013

Soltoff, S. P. (1986). ATP and the regulation of renal cell function. *Annu. Rev. Physiol.* 48, 9–31. doi: 10.1146/annurev.ph.48.030186.000301

Song, Y. R., You, S. J., Lee, Y. M., Chin, H. J., Chae, D. W., Oh, Y. K., et al. (2010). Activation of hypoxia-inducible factor attenuates renal injury in rat remnant kidney. *Nephrol. Dial. Transplant.* 25, 77–85. doi: 10.1093/ndt/gfp454

Stein, A., Goldmeier, S., Voltolini, S., Setogutti, E., Feldman, C., Figueiredo, E., et al. (2012). Renal oxygen content is increased in healthy subjects after angiotensin-converting enzyme inhibition. *Clinics (Sao Paulo).* 67, 761–765. doi: 10.6061/clinics/2012(07)10

Steinberg, G. R., and Kemp, B. E. (2009). AMPK in health and disease. *Physiol. Rev.* 89, 1025–1078. doi: 10.1152/physrev.00011.2008

Tanaka, T., Kojima, I., Ohse, T., Ingelfinger, J. R., Adler, S., Fujita, T., et al. (2005). Cobalt promotes angiogenesis via hypoxia-inducible factor and protects tubulointerstitium in the remnant kidney model. *Lab. Invest.* 85, 1292–1307. doi: 10.1038/labinvest.3700328

Textor, S. C., Gloviczki, M. L., Flessner, M. F., Calhoun, D. A., Glockner, J., Grande, J. P., et al. (2012). Association of filtered sodium load with medullary volumes

and medullary hypoxia in hypertensive African Americans as compared with whites. *Am. J. Kidney Dis.* 59, 229–237. doi: 10.1053/j.ajkd.2011.09.023

Torelli, G., Milla, E., Faelli, A., and Costantini, S. (1966). Energy requirement for sodium reabsorption in the *in vivo* rabbit kidney. *Am. J. Physiol.* 211, 576–580.

Udani, S., Lazich, I., and Bakris, G. L. (2011). Epidemiology of hypertensive kidney disease. *Nat. Rev. Nephrol.* 7, 11–21. doi: 10.1038/nrneph.2010.154

Vink, E. E., de Boer, A., Hoogduin, H. J., Voskuil, M., Leiner, T., Bots, M. L., et al. (2015). Renal BOLD-MRI relates to kidney function and activity of the renin-angiotensin-aldosterone system in hypertensive patients. *J. Hypertens.* 33, 597–603. discussion: 603–594. doi: 10.1097/HJH.0000000000000436

Wang, Z. J., Kumar, R., Banerjee, S., and Hsu, C.-Y. (2011). Blood oxygen level-dependent (BOLD) MRI of diabetic nephropathy: preliminary experience. *J. Magn. Reson. Imaging* 33, 655–660. doi: 10.1002/jmri.22501

Wang, Z., Zhu, Q., Li, P.-L., Dhaduk, R., Zhang, F., Gehr, T. W., et al. (2014). Silencing of hypoxia-inducible factor-1α gene attenuates chronic ischemic renal injury in two-kidney, one-clip rats. *Amer. J. Physiol.* 306, F1236–F1242. doi: 10.1152/ajprenal.00673.2013

Weinberg, J. M. (2011). Mitochondrial biogenesis in kidney disease. *J. Am. Soc. Nephrol.* 22, 431–436. doi: 10.1681/ASN.2010060643

Welch, W. J., Baumgärtl, H., Lübbers, D., and Wilcox, C. S. (2001). Nephron pO2 and renal oxygen usage in the hypertensive rat kidney. *Kidney Int.* 59, 230–237. doi: 10.1046/j.1523-1755.2001.00483.x

Welch, W. J., Baumgärtl, H., Lübbers, D., and Wilcox, C. S. (2003). Renal oxygenation defects in the spontaneously hypertensive rat: role of AT1 receptors. *Kidney Int.* 63, 202–208. doi: 10.1046/j.1523-1755.2003.00729.x

Welch, W. J., Blau, J., Xie, H., Chabrashvili, T., and Wilcox, C. S. (2005). Angiotensin-induced defects in renal oxygenation: role of oxidative stress. *Am. J. Physiol. Heart Circ. Physiol.* 288, H22–H28. doi: 10.1152/ajpheart.00626.2004

Wheaton, W. W., and Chandel, N. S. (2011). Hypoxia. 2. Hypoxia regulates cellular metabolism. *Am. J. Physiol. Cell. Physiol.* 300, C385–C393. doi: 10.1152/ajpcell.00485.2010

Yin, W.-J., Liu, F., Li, X.-M., Yang, L., Zhao, S., Huang, Z.-X., et al. (2012). Noninvasive evaluation of renal oxygenation in diabetic nephropathy by BOLD-MRI. *Eur. J. Radiol.* 81, 1426–1431. doi: 10.1016/j.ejrad.2011.03.045

Yu, X., Fang, Y., Ding, X., Liu, H., Zhu, J., Zou, J., et al. (2012a). Transient hypoxia-inducible factor activation in rat renal ablation and reduced fibrosis with L-mimosine. *Nephrology (Carlton).* 17, 58–67. doi: 10.1111/j.1440-1797.2011.01498.x

Yu, X., Fang, Y., Liu, H., Zhu, J., Zou, J., Xu, X., et al. (2012b). The balance of beneficial and deleterious effects of hypoxia-inducible factor activation by prolyl hydroxylase inhibitor in rat remnant kidney depends on the timing of administration. *Nephrol. Dial. Transplant.* 27, 3110–3119. doi: 10.1093/ndt/gfr754

Zhang, H., Bosch-Marce, M., Shimoda, L. A., Tan, Y. S., Baek, J. H., Wesley, J. B., et al. (2008). Mitochondrial autophagy is an HIF-1-dependent adaptive metabolic response to hypoxia. *J. Biol. Chem.* 283, 10892–10903. doi: 10.1074/jbc.M800102200

Zhu, Q., Wang, Z., Xia, M., Li, P.-L., Van Tassell, B. W., Abbate, A., et al. (2011). Silencing of hypoxia-inducible factor-1α gene attenuated angiotensin II-induced renal injury in Sprague-Dawley rats. *Hypertension* 58, 657–664. doi: 10.1161/HYPERTENSIONAHA.111.177626

**Conflict of Interest Statement:** The authors declare that the research was conducted in the absence of any commercial or financial relationships that could be construed as a potential conflict of interest.

frontiers in Physiology

REVIEW
published: 16 May 2017
doi: 10.3389/fphys.2017.00296

# Innovative Perspective: Gadolinium-Free Magnetic Resonance Imaging in Long-Term Follow-Up after Kidney Transplantation

*Mick J. M. van Eijs[1], Arjan D. van Zuilen[1], Anneloes de Boer[2], Martijn Froeling[2], Tri Q. Nguyen[3], Jaap A. Joles[1], Tim Leiner[2] and Marianne C. Verhaar[1]**

[1] Department of Nephrology and Hypertension, University Medical Center Utrecht, Utrecht, Netherlands, [2] Department of Radiology, University Medical Center Utrecht, Utrecht, Netherlands, [3] Department of Pathology, University Medical Center Utrecht, Utrecht, Netherlands

Since the mid-1980s magnetic resonance imaging (MRI) has been investigated as a non- or minimally invasive tool to probe kidney allograft function. Despite this long-standing interest, MRI still plays a subordinate role in daily practice of transplantation nephrology. With the introduction of new functional MRI techniques, administration of exogenous gadolinium-based contrast agents has often become unnecessary and true non-invasive assessment of allograft function has become possible. This raises the question why application of MRI in the follow-up of kidney transplantation remains restricted, despite promising results. Current literature on kidney allograft MRI is mainly focused on assessment of (sub) acute kidney injury after transplantation. The aim of this review is to survey whether MRI can provide valuable diagnostic information beyond 1 year after kidney transplantation from a mechanistic point of view. The driving force behind chronic allograft nephropathy is believed to be chronic hypoxia. Based on this, techniques that visualize kidney perfusion and oxygenation, scarring, and parenchymal inflammation deserve special interest. We propose that functional MRI mechanistically provides tools for diagnostic work-up in long-term follow-up of kidney allografts.

**Keywords: magnetic resonance imaging, functional MRI, kidney transplantation follow-up, chronic allograft nephropathy, protocol kidney biopsy, chronic hypoxia theory**

OPEN ACCESS

***Edited by:***
*Christine Kranz, University of Ulm, Germany*

***Reviewed by:***
*Samuel Heyman, Hadassah Hebrew University Hospitals, Israel*
*Pottumarthi Vara Prasad, NorthShore University HealthSystem, USA*

****Correspondence:***
*Marianne C. Verhaar*
*m.c.verhaar@umcutrecht.nl*

***Specialty section:***
*This article was submitted to Renal and Epithelial Physiology, a section of the journal Frontiers in Physiology*

***Received:*** *09 January 2017*
***Accepted:*** *24 April 2017*
***Published:*** *16 May 2017*

***Citation:***
*van Eijs MJM, van Zuilen AD, de Boer A, Froeling M, Nguyen TQ, Joles JA, Leiner T and Verhaar MC (2017) Innovative Perspective: Gadolinium-Free Magnetic Resonance Imaging in Long-Term Follow-Up after Kidney Transplantation. Front. Physiol. 8:296. doi: 10.3389/fphys.2017.00296*

## INTRODUCTION

A rise in serum creatinine concentration (SCr) is often the first sign of kidney allograft dysfunction. It is only observed if considerable damage has occurred in the allograft, from which it follows that initial damage develops subclinically (Pascual et al., 2012). Various processes contribute to damage accumulating in kidney allografts over time, e.g., calcineurin inhibitor nephrotoxicity, chronic rejection, aging, and recurrent infections (Pascual et al., 2002). Early detection of allograft damage, preferably even before the actual onset of allograft fibrosis, is desirable, since it may improve long term allograft survival (Pascual et al., 2012). Currently the best method to monitor the course of such damage would be sequential protocol biopsies.

Protocol biopsy facilitates early diagnosis of *de novo* and recurrent kidney disease (Morozumi et al., 2014) and therefore one or sometimes multiple protocol biopsies several months to

a year after kidney transplantation are performed in several programs. Specific indications for protocol biopsies have been proposed (Racusen, 2006). Although pathology findings currently are leading for therapy initiation or alteration, benefits of protocol biopsies for the early detection of subclinical allograft damage are seriously questioned due to considerable burden (Tanabe, 2014). Especially in the absence of any clinical signs indicating allograft dysfunction, kidney biopsy comes with risks and drawbacks, including a logistic burden for nephrology departments, discomfort in patients, risk of allograft bleeding, and, albeit to a lesser extent, infectious complications (Corapi et al., 2012; Chung et al., 2014; Morgan et al., 2016). Finally, there is a risk of sampling error which may confound adequate assessment of biopsy samples, (Madaio, 1990) since allograft fibrosis develops from focal lesions (Cosio et al., 2008). In practice this strategy is therefore not universally applied on a regular basis. A non-invasive alternative test such as MRI would be a more convenient solution. However, centers that perform protocol biopsies are provided with the ideal opportunity of conducting longitudinal imaging studies that could also involve parallel assessment of kidney imaging and histological morphology. Such parallel assessment could possibly also contribute to improvement in evaluation of acute kidney injury (AKI) and chronic kidney disease (CKD) in native kidneys.

MRI has been suggested as a promising technique in clinical nephrology, but thus far has not been successfully implemented as a specific method of choice in follow-up of kidney transplant recipients (Michaely et al., 2007; Chandarana and Lee, 2009; Zhang et al., 2014a). Whereas previous reviews on renal imaging discussed applications of MRI in the entire domain of nephrology, (Ebrahimi et al., 2014; Grenier et al., 2016) this review will specifically address disease processes underlying kidney allograft damage, focusing on different aspects that can be assessed with MRI techniques. A brief description of the technical background of these techniques will be provided. Our main aim is to evaluate—from a mechanistic point of view—whether MRI has the potential to provide valuable diagnostic information in long-term follow-up of kidney transplant recipients.

# CONVENTIONAL VS. FUNCTIONAL MRI FOR THE ASSESSMENT OF SUBCLINICAL KIDNEY ALLOGRAFT DAMAGE

## Conventional MRI Techniques

A distinction must be made between functional MRI techniques on the one hand, and conventional, non-functional, or anatomic MRI techniques on the other. Functional MRI refers to techniques that aim to measure or visualize physiological variables in the kidney, whereas non-functional MRI renders images of kidney anatomy. Conventional imaging of the kidney (through $T_1$, $T_2$ and proton density weighted imaging) (Currie et al., 2013) can identify morphological abnormalities, for instance with magnetic resonance urography and angiography, and a sensitive, though non-specific loss of corticomedullary differentiation with increased $T_1$ relaxation times can be observed in kidneys with impaired function (Huang et al., 2011). Since $T_1$ imaging cannot identify the cause of kidney function impairment given its lack of specificity, this technique is probably of little value in evaluation of allograft function in transplantation patients.

## Functional MRI Techniques

In addition to assessment of kidney morphology investigators have often tried to assess single kidney renal function with dynamic contrast-enhanced MRI (DCE-MRI) (Zeng et al., 2015) but its advantage in kidney transplantation patients above eGFR is debatable, given that in this case total GFR depends almost entirely on allograft GFR. DCE-MRI depicts the passage of an intravenously injected gadolinium-based contrast agent (GBCA) through the vascular system and kidney parenchyma. DCE-MRI has been used for calculation of GFR (Eikefjord et al., 2015; Zeng et al., 2015) and to discriminate between acutely rejected and non-rejected kidney allografts (Khalifa et al., 2013). Although this technique is very promising, concerns about the long-term side effects of GBCAs by both clinicians as well as patients have stymied the adoption of DCE-MRI. It is also of note that detection of kidney pathology by assessment of a suspected decrease in GFR is of rather restricted use, since reduced GFR is in fact the final result of the entire chain of events in kidney disease.

Several other (patho)physiological processes in the kidney potentially relevant for kidney allograft follow-up have been visualized with non-contrast enhanced (functional) MRI to date (**Table 1**). The chronic hypoxia theory, first introduced by Fine et al. (1998) postulates that progressive development of fibrosis in chronic kidney disease is related to kidney allograft hypoxia (Fine and Norman, 2008). Indeed it was demonstrated in experimental diabetes that hypoxia had occurred at an early stage (dos Santos et al., 2007) before any histologic damage could be observed (Manotham et al., 2004). This has also been observed in experimental kidney transplantation (Papazova et al., 2015). Moreover, hypoxia-inducible factor-1alpha has been immunohistochemically detected in kidney allografts with (sub)clinical rejection at 3 months after transplantation and beyond (Rosenberger et al., 2007). There is, however, an unmet need for longitudinal functional imaging studies, both in experimental and clinical settings. These studies would contribute most to a better understanding of the role of hypoxia in the course of chronic allograft nephropathy (CAN).

The essence of the chronic hypoxia theory is shown in **Figure 1**, along with the MRI techniques that are proposed to unravel specific links in the pathophysiologic chain of CAN. Based on this theory, some (functional) techniques deserve special interest for their potential in long-term follow-up:

**Abbreviations:** ADC, Apparent diffusion coefficient; AKI, Acute kidney injury; ASL, Arterial spin labeling; BOLD, Blood oxygen level dependent; CAN, Chronic allograft nephropathy; CKD, Chronic kidney disease; DCE, Dynamic contrast-enhanced; (de)oxyHb; (De) oxyhemoglobin; DTI, Diffusion tensor imaging; DWI, Diffusion weighted imaging; (e)GFR, (Estimated) glomerular filtration rate; FA, Fractional anisotropy; GBCA, Gadolinium-based contrast agent; GMC, Glomerular macrophage count; IVIM, Intravoxel incoherent motion; MRE, Magnetic resonance elastography; MRI, Magnetic resonance imaging; SCr, Serum creatinine concentration; US, Ultrasound; USPIO, Ultrasmall superparamagnetic particles of iron oxide.

**TABLE 1 | Currently available techniques for kidney allograft imaging.**

| (Patho)physiological process | Imaging technique |
|---|---|
| Oxygenation | Blood oxygen level dependent (BOLD) imaging |
| Water diffusion and tubular flow | Diffusion weighted imaging (DWI)/Diffusion tensor imaging (DTI) |
| (Arterial) blood supply | Arterial spin labeling (ASL) |
| Scarring | $T_1$ in the rotating frame ($T_{1\rho}$) |
| | Magnetic resonance elastography (MRE) |
| | Diffusion weighted imaging (DWI)/Diffusion tensor imaging (DTI) |
| Inflammation | Ultrasmall superparamagnetic particles of iron oxide (USPIO) enhanced imaging |
| Vascular reactivity | Hemodynamic response imaging (HRI) |
| Maintenance of corticomedullary sodium gradient | $^{23}$Na-MRI |

*(Patho)physiological processes in the kidney that can be assessed with functional MRI to date. Although a lower corticomedullary sodium gradient has been demonstrated in kidney allografts in comparison to native kidneys, sodium imaging has neither been able to reflect kidney function in kidney transplantation patients (Moon et al., 2014), nor in healthy individuals with a variety of eGFRs (Haneder et al., 2013), and is therefore not discussed in detail. However, it must be pointed out that preliminary experimental results in other kidney disease states, such as acute tubular necrosis, have shown changes in sodium imaging (Maril et al., 2006; Atthe et al., 2009), Similar to sodium MRI, hemodynamic response imaging has only been applied in experimental settings in animals thus far (Milman et al., 2013, 2014).*

sequences that visualize (1) kidney perfusion and oxygenation, (2) parenchymal inflammation, and (3) kidney scarring. These techniques will be discussed in more detail later (Section Clinical experience with functional MRI in kidney allografts).

Thus far, the focus of interest has been on non-invasive diagnosis of the cause of acute allograft dysfunction. In this setting, non-functional MRI techniques possess unique qualities to assess morphologic abnormalities such as urinary obstruction (Kalb et al., 2008) and therefore better suit this application. Given the mechanisms underlying chronic kidney allograft dysfunction, we expect that the biggest gains with functional MRI can possibly be made in long-term follow-up.

In recent years, several existing and new gadolinium-free functional MRI techniques that measure various aspects of kidney function have advanced to the stage that they can be used in clinical practice. Below we discuss these in more detail.

# CLINICAL EXPERIENCE WITH FUNCTIONAL MRI IN KIDNEY ALLOGRAFTS

## Blood Oxygen Level Dependent (BOLD) MRI

BOLD MRI is used to obtain a measure for oxygenation (**Figure 2**). For a background of this imaging technique we refer to Pruijm et al. (2016) who have recently described renal BOLD MRI and its inherent limitations in detail in Frontiers in Physiology. BOLD MRI should be interpreted carefully, as also stated by Pruijm et al. (2016). Of special importance is the oxygen-hemoglobin dissociation curve. Since oxyHb releases oxygen more easily at lower oxygen levels, the amount of deoxyHb does not have a linear relationship with blood oxygenation (O'Connor et al., 2006; Leong et al., 2007). In the kidneys, BOLD MRI is therefore less sensitive to oxygenation changes in the highly oxygenated cortex (Prasad, 2006). Lastly, renal oxygenation can change due to increased consumption of oxygen by active processes in the kidney or decreased perfusion (Heyman et al., 2008). Strategies are now sought after that enable deduction of tissue $pO_2$s from $R_2^*$ values using mathematical models, e.g., the two-step model by Zhang et al. (2014b) Interestingly, hemodynamic changes should not only be considered as a confounder in interpretation of BOLD images. In hemodynamic response imaging (HRI) air composition is intentionally modified (hypercapnia, hypercapnia plus hyperoxia) while at the same time multiple BOLD images are acquired. In this way hemodynamic changes due to Bohr-effect and $CO_2$-induced vasodilation are provoked, for instance in the kidney, which enables evaluation of regional vascular reactivity. To date, only two studies in experimental animals have investigated kidney HRI (Milman et al., 2013, 2014).

Since the introduction of BOLD MRI in nephrology various researchers have investigated this technique in kidney transplant recipients (Sadowski et al., 2005, 2010; Djamali et al., 2006, 2007; Thoeny et al., 2006; Han et al., 2008; Park et al., 2012, 2014; Xiao et al., 2012; Liu et al., 2014). **Table 2** lists studies in which BOLD MRI was used to assess malfunctioning kidney allografts. There is ample evidence that medullary $R_2^*$ values decrease in allografts with acute impaired function, possibly indicating regional blood *hyperoxia*. However, as explained above, changes in perfusion and hemoglobin content (blood volume, hematocrit) can also explain the decrease in $R_2^*$. In one study medullary and cortical blood hyperoxia as measured with BOLD MRI were related to respectively medullary and cortical hypoperfusion (Sadowski et al., 2010) suggesting that decreased oxygen consumption is the main reason for the hyperoxia observed in kidney allograft dysfunction. The most probable explanation for this would be that the GFR is reduced due to hypoperfusion, with consequently reduced solute delivery to the nephron and thus reduced regional oxygen consumption. Observation of improved medullary oxygenation during controlled hypotension demonstrated by Brezis et al. supports this explanation (Brezis et al., 1994).

Moreover, significant differences in medullary $R_2^*$ ($MR_2^*$) values between acute rejection and acute tubular necrosis have been reported with BOLD MRI (**Table 2**). Differences in cortical $R_2^*$ ($CR_2^*$) values between native kidneys or allografts with normal function and allografts with impaired function are often not significant, which is remarkable given that sodium is mainly reabsorbed in the cortex. It would therefore be expected that this is reflected by BOLD parameters, since the cortex accounts for the major part of total oxygen consumption, as it receives most of total renal blood flow (Brezis et al., 1984). Possibly this is explained by the lower sensitivity of BOLD MRI to changes in the renal cortex, as explained above. However, signal intensity due to BOLD effects increases almost linearly to main field strength

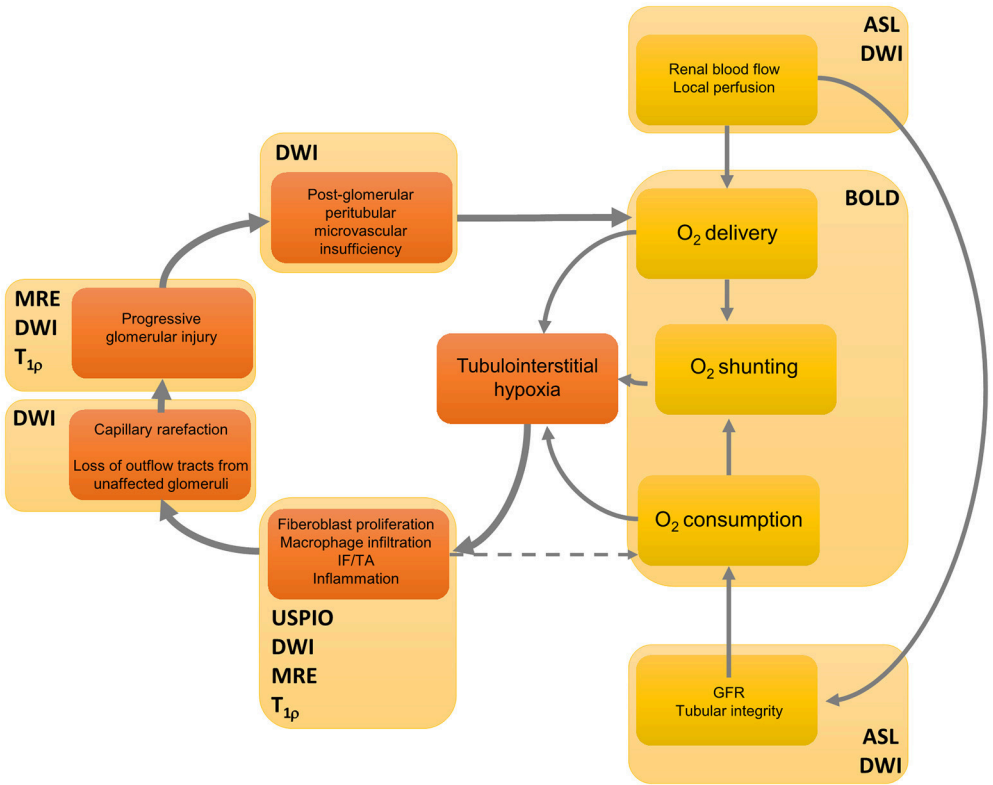


**FIGURE 1 | A feedforward loop in the hypothesized processes of the development of fibrosis in chronic kidney disease, and their non-invasive modes of detection.** Renal blood flow determines delivery of oxygen, but also the glomerular filtration rate and thus oxygen consumption. Moreover, arteriovenous shunting has an effect on total oxygen balance. The initial event that gives rise to kidney hypoxia and thus to scarring could have a specific etiology, yet increased oxygen consumption is also caused by a variety of factors such as mitochondrial uncoupling following reperfusion immediately after transplantation (Evans et al., 2015). Interstitial hypoxia results in active inflammation and fibroblast proliferation directly mediated through hypoxia by cytokines such as transforming growth factor β1, which leads to interstitial fibrosis and tubular atrophy (IF/TA) (Fine et al., 2000). Active inflammation also contributes to hypoxia since it consumes energy. Then fibrotic foci infiltrate neighboring structures, causing further damage to previously unaffected tissue, which eventually has a negative effect on oxygen supply. For several links in the chain of events MRI techniques are displayed that yield visual information at a given functional event. Although many steps of the process are likely sensitive to one or another technique, no technique is specific for a single event. Furthermore, there is currently no imaging technique that can directly display tubulo-interstitial hypoxia. See **Table 1** for denotation of abbreviations. DWI also encompasses DTI. This figure was modified from Fine and Norman (2008) (Elsevier) and Evans et al. (2013) (John Wiley and Sons) with permission from the publishers.

up to 7T (Seehafer et al., 2010). Hence, with current technology, it is conceivable that differences in $CR_2^*$s are invisible due to low signal-to-noise ratios. Advances in experimental settings in ultrahigh field scanners may establish better resolution of cortical pathophysiology.

As mentioned, experience in the chronic phase post-transplantation is very limited. Djamali et al. investigated $R_2^*$ parameters in 10 transplantation patients clinically diagnosed with CAN that were at least 12 months post-transplantation, and found decreased values for $CR_2^*$ and $MR_2^*$ compared to healthy volunteers (Djamali et al., 2007). However, one of the inclusion criteria in this study was that CAN patients suffered at least KDOQI stage 3, which implies that fibrosis was probably abundantly present in all allografts studied. It would be presumptive therefore to draw any conclusions from this study with regard to the role of hypoxia in development of CAN. Interestingly though, markers of oxidative stress in serum and urine correlated significantly with $R_2^*$ values in CAN patients. Furthermore, $MR_2^*$ was studied repeatedly in 15 transplanted kidneys. As compared with baseline readings, obtained before renal harvesting, $MR_2^*$ declined by 8.3% ($P = 0.06$) over 2 years follow-up (Niles et al., 2016). Since allograft GFR in these patients even improved during follow-up by 33.3% ($P < 0.01$) compared to corrected baseline GFR, these results suggest a role for disturbed oxygen balance in development of subclinical chronic damage. Continuous follow-up of these patients beyond 2 years would be interesting to further test this hypothesis. In contrast, results with BOLD MRI in CKD are inconsistent with the above, since most studies demonstrate no difference in $CR_2^*$ and $MR_2^*$ among CKD patients with different characteristics, such as disease stage (Neugarten and Golestaneh, 2014). However, this does not imply that the chronic hypoxia theory should be rejected, since incompletely understood oxygen balance and other reasons inherent to BOLD MRI already mentioned may confound interpretation of these results (Neugarten and Golestaneh, 2014).

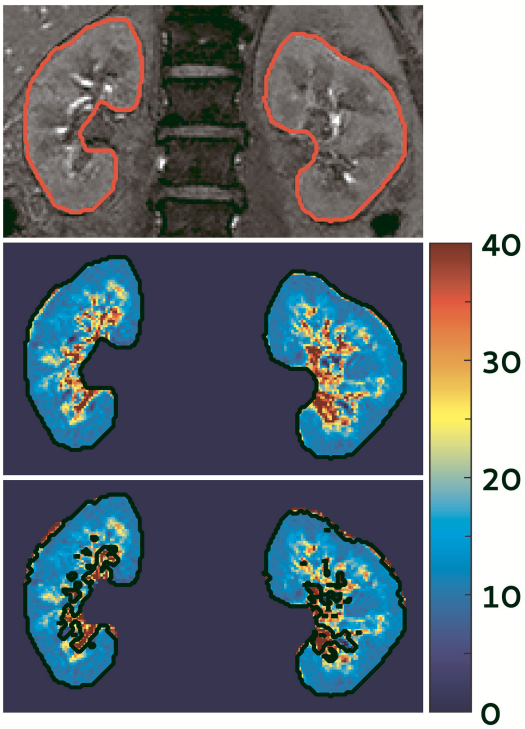


**FIGURE 2 | BOLD image of the kidney acquired at our center in a hypertensive subject (unpublished data). Top:** one of the images used to calculate the $R_2^*$ maps; **middle:** $R_2^*$ map of the kidneys, note the difference between the well-oxygenated renal cortex (outer blue part) and the relatively hypoxic medulla (inner green/yellow parts). The scale denotes $R_2^*$ values in $s^{-1}$, a low $R_2^*$ indicates higher oxygenation; **bottom:** automatic filter applied to exclude the renal vessels and urine collecting system.

It follows from these studies that the relationship between BOLD parameters and kidney function in kidney allografts is not fully understood. Confusingly, decreased values for $R_2^*$ are found in malfunctioning kidney allografts (which contain at least small fibrotic foci), whereas increased $R_2^*$s corresponding to blood hypoxia are found in other kidney diseases characterized by fibrosis (Neugarten and Golestaneh, 2014). For better interpretation of changes in $R_2^*$ values, it would be interesting to combine BOLD MRI with perfusion. Thus, on the one hand clinical translation of BOLD MRI remains difficult, but on the other hand it is arguable that BOLD parameters should be used if they are prognostic of allograft dysfunction, despite our lack of understanding of underlying pathophysiology.

## Arterial Spin Labeling (ASL)

Arterial Spin Labeling (ASL) is used for mapping of arterial blood flow and cortical perfusion at capillary level. In ASL, spins are labeled in the arterial phase (Ferré et al., 2013). Following a delay time to allow the labeled spins to flow in to the capillaries and diffuse into the tissue, an MRI of the tissue is acquired. The spins lose some of the magnetization due to $T_1$ decay during the delay time. Combining this with a similar image acquired without applying the label, allows for renal cortical perfusion to be assessed (Ferré et al., 2013) which results in ASL maps (**Figure 3**). In this way rate of cortical diffusion and thus degree of cortical perfusion can be assessed. In fact, ASL is an alternative to DCE-MRI, with the difference that for ASL moving blood is used as an endogenous CA, instead of a GBCA. A moderate correlation ($r = 0.66$) between the two techniques was found in a small study in which total kidney blood flow was determined in 19 healthy volunteers (Wu et al., 2011). Although substantial differences between DCE and ASL parameters are present in all studies in which the two techniques are compared, both techniques possess the ability to detect impaired kidney perfusion (Zimmer et al., 2013). ASL parameters are highly reproducible in healthy subjects, (Cutajar et al., 2012, 2014; Gillis et al., 2014; Kistner et al., 2015) with better reproducibility than DCE-MRI (Cutajar et al., 2014).

Three studies in kidney transplantation patients have demonstrated a good correlation between kidney function and cortical perfusion as assessed with ASL (**Table 3**) (Lanzman et al., 2010; Heusch et al., 2013, 2014) These studies also included patients with stable eGFR in the chronic phase (> 1 year) post-transplantation, but given its cross-sectional design yielded no information on the course of kidney perfusion in patients with stable allograft function. However, the study by Niles et al. (2016) demonstrated that after 2 years follow-up, in eight kidney allografts with stable function, cortical perfusion decreased by 34.2% ($P < 0.001$) compared to baseline. According to **Figure 1**, reduced cortical perfusion can lead to a decrease in GFR and over time to cortical hypoxia due to decreased oxygen delivery, which may initiate the "hypoxia loop." Besides, another subset of participants that was given losartan, starting 3 months post-transplantation, achieved considerably better cortical perfusion upon termination of follow-up (22.9% more in comparison to the participants without losartan, $P < 0.05$).

Preliminary results demonstrated the possibility to assess single-kidney GFR with ASL (He et al., 2014) which is an advantage over eGFR based on SCr. This might be of use in the transplantation work-up of living donors and donors after brain death to determine whether one of both kidneys would be preferred over the other for harvesting based on difference in kidney function. A comparison between cortical perfusion and histopathology has not been made in human kidney allograft recipients to date. However, the percentage of affected tubules in kidney biopsy in mice with acute kidney injury was shown to correlate ($r = 0.73$) with relative kidney perfusion as determined with ASL (Hueper et al., 2014).

## Diffusion Weighted Imaging (DWI)

Diffusion weighted imaging (DWI) measures the diffusion of water molecules in tissue. Since water motion in tissue is restricted, its diffusion constant differs from that of free water and is therefore described with the apparent diffusion coefficient (ADC). Applying a diffusion weighting (indicated by the b-value) causes loss of signal which is proportional to the ADC and can be modeled using a mono-exponential function. Seven studies investigated mono-exponential DWI in kidney transplantation patients (**Table 4**) (Thoeny et al., 2006; Blondin et al., 2011;

**TABLE 2 | Blood Oxygen Level Dependent (BOLD) MRI.**

| Study | Control subjects | Patients | Distinction between AR and ATN? | Field strength (T) | $MR_2^*$ | $CR_2^*$ |
|---|---|---|---|---|---|---|
| Sadowski et al., 2005 | NG | AR | $P < 0.01$ | 1.5 | ↓ | NS |
| | | ATN | | | NS | ↑ |
| Djamali et al., 2006 | NG | AR | $P < 0.05$ | 1.5 | ↓ | NS |
| | | ATN | | | ↓ | NS |
| Thoeny et al., 2006 | HV | NG | N/A | 1.5 | ↓ | NS |
| Djamali et al., 2007 | HV | CAN | N/A | 1.5 | ↓ | ↓ |
| Han et al., 2008 | NG | AR | $P < 0.01$ | 1.5 | ↓ | ↓ |
| | | ATN | | | ↑ | ↑ |
| Sadowski et al., 2010 | NG | AR | $P < 0.05$ | 1.5 | ↓ | NS |
| | | ATN | | | NS | NS |
| Park et al., 2012 | HV | AR | N/A | 3.0 | ↓ | NS |
| | | NG | | | = | = |
| Xiao et al., 2012 | HV | AR | N/A | 1.5 | ↓ | ↓ |
| | | NG | | | = | = |
| Liu et al., 2014 | NG | AR | $P < 0.01$ | 3.0 | ↓ | NS |
| | | ATN | | | NS | NS |
| Park et al., 2014 | NG | AR | NS | 3.0 | ↓ | ↓ |
| | | ATN | | | ↓ | ↓ |

*Medullary ($MR_2^*$) and cortical ($CR_2^*$) $R_2^*$ values were determined in malfunctioning kidney allografts. Values were compared to control subjects: either transplant patients with normal graft function (NG), or healthy volunteers (HV). AR denotes acute rejection, ATN acute tubular necrosis, CAN chronic allograft nephropathy, NS no significant difference and N/A not applicable.*

Hueper et al., 2011, 2016; Lanzman et al., 2013; Park et al., 2014; Fan et al., 2016) Next to the microscopic diffusion of water the signal measured in DWI is also sensitive to the microcirculation. As such, the measured ADC using low b-values reflects both diffusion and perfusion and the signal can be better described using a bi-exponential model that accounts for contribution of both compartments, which is also known as Intravoxel incoherent motion (IVIM) imaging. Vermathen et al. investigated the variability in eight transplantation patients with stable kidney function using the bi-exponential model (Vermathen et al., 2012). After two sessions of DWI ($7 \pm 3$ months and $32 \pm 2$ months after transplantation) coefficients of variation within and between individuals were low: <3.5 and <5.9%, respectively (Vermathen et al., 2012). A second and more important argument in favor of the use of the bi-exponential model is that contributions of pseudodiffusion and structural diffusion to total ADC can be assessed separately, and thus IVIM parameters may reveal structural tubular damage (Notohamiprodjo et al., 2015).

Another way of describing the signal measured with DWI is the tensor model, also known as Diffusion tensor imaging (DTI). Diffusion of water within a compartment such as a blood vessel or tubule is restricted to a specific direction by boundaries of the compartment. This phenomenon is known as anisotropy. If DWI is performed in at least six unique directions it becomes possible to describe the anisotropic diffusion using the diffusion tensor from which a quantitative measure of anisotropy can be derived, e.g., the fractional anisotropy (FA). Data can be displayed more sophisticatedly by showing intervoxal connectivity, which is called tractography. In tractography in each voxel the primary diffusion direction is identified and described by a vector (more precisely the direction of its primary eigenvalue, i.e., one of three eigenvalues that are determined in the calculation of the diffusion tensor) (Mukherjee et al., 2008). Interpolation of this vector field visualizes the diffusion direction as fiber tracts (Mukherjee et al., 2008). In this way, DTI might enable the assessment of tubular and vascular membrane integrity (McRobbie et al., 2006).

Fan et al. used DTI to study kidney allograft function early after transplantation and found significant differences between medullary and cortical FA in all subjects: healthy volunteers, and allograft recipients with good, moderate, and severely impaired function (Fan et al., 2016). Medullary FA was larger than cortical FA, probably reflecting the highly organized radial structure of the tubular system, clearly visible in **Figure 4**, in contrast to the mesh of small vessels and glomeruli found in the cortex (Fan et al., 2016). This element in particular relates to the clinical use of DTI, since only medullary FA correlates with eGFR (Hueper et al., 2011, 2016; Lanzman et al., 2013). Similar to other

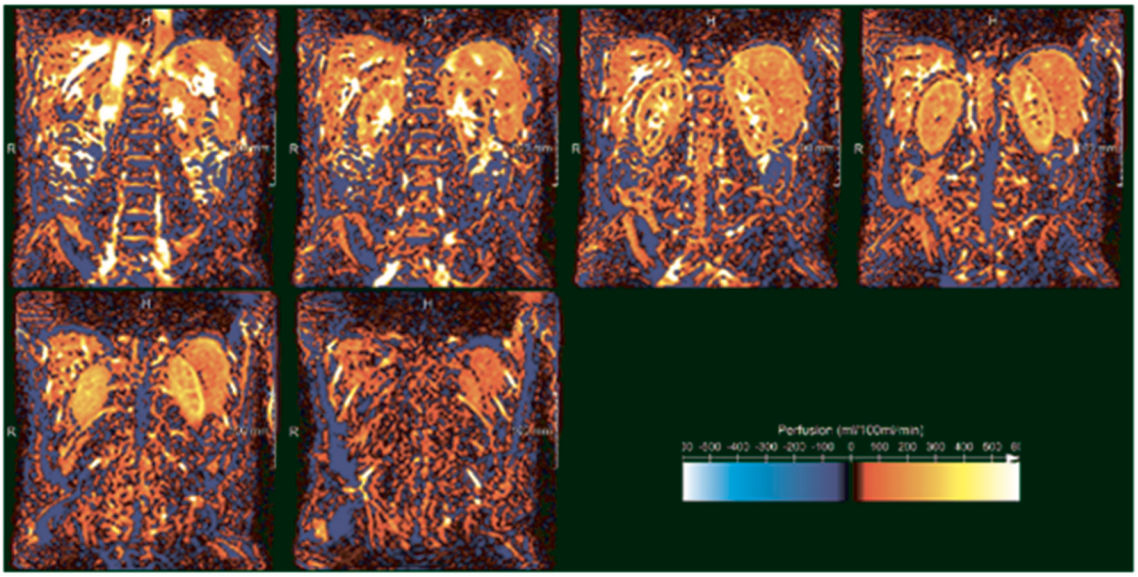


**FIGURE 3 | ASL perfusion images of the kidney in a healthy volunteer acquired at our center (unpublished data).** White and yellow denote high perfusion, while orange and red denote low perfusion. The difference between the highly-perfused cortex and less highly perfused medulla is clearly visible. In the three upper panels, starting on the left, the high signal intensity regions in the kidney centers reflect the pyelocalceal system.

studies mentioned above, lower cortical and medullary ADCs were found in patients with impaired graft function (Hueper et al., 2011; Lanzman et al., 2013; Fan et al., 2016). In addition, Cheung et al. related a decline in medullary FA and ADC to histologic injury (medullary cast formation and cell necrosis) seen in ischemic reperfusion injured kidneys of mice (Cheung et al., 2010). Hueper et al. also reported correlations between diffusion parameters and injury ($r = -0.63$ in FA and $r = -0.65$ in $ADC_{mono}$) (Hueper et al., 2016). Although ADC coefficients show correlation with eGFR and are discriminative between normal and impaired allograft function in the acute phase, chronically malfunctioning allografts have only been studied using DWI in a small number of subjects. Therefore, whether DWI is applicable for long-term follow-up is as yet unknown.

## $T_1$ in the Rotating Frame ($T_{1\rho}$)

A relatively new technique in kidney imaging is $T_1$ in the rotating frame ($T_{1\rho}$) (He et al., 2011). This modality is highly sensitive to interactions of large macromolecules including collagen (fibrosis) with water molecules. $T_{1\rho}$ is a well-established imaging technique in orthopedic radiology, originally being designed for measuring cartilage in skeletal joints (Li et al., 2011). A recent study applied this modality to the kidney (Rapacchi et al., 2015). In this study, that also investigated ASL, BOLD MRI, and DWI, a receiver operating characteristic analysis was conducted for medullary $T_{1\rho}$ relaxation time which yielded an area under the curve of 94% (95% CI: 82–100%) for prediction of lupus nephritis (Rapacchi et al., 2015). Since fibrosis is abundantly present in kidney allografts with impaired function, and, given these initial results that $T_{1\rho}$ appears to allow accurate visualization of fibrosis in kidney tissue, this technique is worth investigation in kidney allografts.

## Ultrasmall Superparamagnetic Particles of Iron Oxide (USPIO) Enhanced Imaging

Labeling of macrophages is possible with infusion of ultrasmall superparamagnetic particles of iron oxide (USPIO), since these particles diffuse into extravascular space quickly after infusion and are then taken up by macrophages (Gellissen et al., 1999). Similar to deoxyHb in BOLD MRI, these particles influence the main magnetic field. Therefore, the discrepancy on $T_2^*$ weighted images before and after infusion of ferumoxytol (i.e., USPIO) relates to regional macrophage infiltration, e.g., in glomeruli. The uptake of USPIO by macrophages in a rat model of acutely rejected kidney allografts was demonstrated more than a decade ago (Zhang et al., 2000; Ye et al., 2002) but Beckmann et al. were the first to show macrophage infiltration in rats with chronic allograft inflammation by USPIO enhanced imaging (Beckmann et al., 2003).

The clinical relevance of glomerular macrophage count (GMC) in kidney biopsies was demonstrated by Sentís et al., who found that the GMC is predictive of death-censored graft failure up to 500 days after biopsy (Sentís et al., 2015). The average time between transplantation and performance of kidney biopsy was 18 days, and therefore no conclusions could be drawn on the relevance of macrophages in chronic inflammation (Sentís et al., 2015). However, it suggests that the GMC may render valuable information in the chronic phase as macrophages play an important role in chronic inflammation leading to interstitial fibrosis and tubular atrophy (Dang et al., 2012). In a small study

**TABLE 3 | Arterial Spin Labeling (ASL).**

| Study | Control subjects | Patients | Field strength (T) | Cortical perfusion |
|---|---|---|---|---|
| Lanzman et al., 2010 | NG, HV | IG (>20% increase in SCr) | 1.5 | $\downarrow P < 0.001$ |
| Heusch et al., 2013 | N/A | Kidney allograft recipients with range of eGFRs | 1.5 | $\downarrow P < 0.05$ |
| Heusch et al., 2014 | NG | IG (eGFR $\leq$ 30 mL/min/1.73 $m^2$) | 1.5 and 3.0 | $\downarrow P < 0.0001$ |

*Arterial Spin Labeling (ASL) in kidney allografts. Impaired graft function (IG) was defined differently in all three studies, and patients were compared to transplant patients with normal graft function (NG), or healthy volunteers (HV). In the study by Heusch et al. (2013) a set of ASL maps was correlated to the corresponding values for eGFR ($r = 0.63$). N/A denotes not applicable.*

**TABLE 4 | Diffusion Weighted Imaging (DWI).**

| Study | Control subjects | Patients | Field strength (T) | Cortical ADC | Medullary ADC |
|---|---|---|---|---|---|
| Thoeny et al., 2006 | HV | NG | 1.5 | $\downarrow^{*}$ | $\downarrow^{*}$ |
| Blondin et al., 2011 | NG | IG | 1.5 | $\downarrow^{*}$ | N/A |
| Hueper et al., 2011 | HV | IG | 1.5 | $\downarrow^{*}$ | $\downarrow^{*}$ |
| Lanzman et al., 2013 | G-MG | IG | 3.0 | $\downarrow^{*}$ | $\downarrow^{\ddagger}$ |
| Park et al., 2014 | NG | IG | 3.0 | $\downarrow^{*}$ | $\downarrow^{\dagger}$ |
| Fan et al., 2016 | HV | NG | 3.0 | NS | $\uparrow^{*}$ |
| | | IG | | $\downarrow^{\circ}$ | $\downarrow^{\circ}$ |
| Hueper et al., 2016 | NG | DG | 1.5 | $\downarrow^{*}$ | $\downarrow^{*}$ |

*Several studies found decreased ADC values in patients with impaired allograft function (IG) as compared to patients with normal allograft function (NG), good to moderate allograft function (G-MG), and healthy volunteers (HV). N/A denotes not applicable, NS not significant. $^{*}P < 0.01$, $^{\dagger}P < 0.016$, $^{\ddagger}P = 0.01$, $^{\circ}$No P-values were given for IG as compared to HV in this study.*

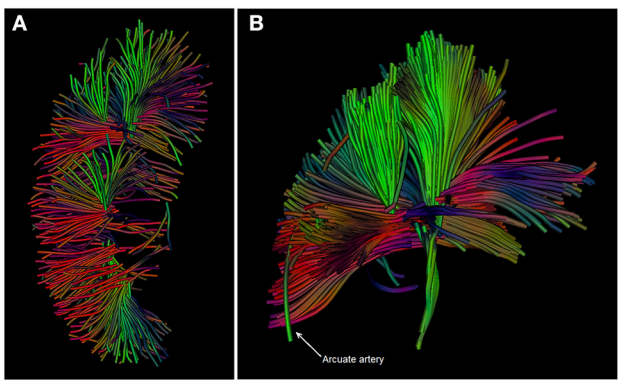


**FIGURE 4 | (A,B):** DTI images of the kidney in a healthy volunteer acquired at our center. Diffusion tracts running from the cortex through the medullary pyramids are depicted. The different colors indicate the net direction of diffusion. Source data for these images were retrieved from an existing dataset in our center (van Baalen et al., 2016).

conducted in 12 patients, including five kidney transplantation patients, signal variation on $T_2^*$ images correlated ($r = -0.7$, $P = 0.011$) to cortical macrophage infiltration (Hauger et al., 2007). A drop in medullar signal intensity could also be seen in three patients with acute tubular necrosis, which typically manifests in the renal medulla and is therefore not accompanied by cortical macrophage infiltration (Hauger et al., 2007). Apart from its potential as indicator of macrophage infiltration in functional imaging, USPIO have been suggested as a safer alternative to gadolinium in patients with severely impaired kidney function (Bashir et al., 2015; Mukundan et al., 2016). Still, it is of note that ferumoxytol, which in daily practice is mostly used for the management of iron-deficiency anemia in chronic kidney disease patients, is sporadically associated with hypersensitivity which could ultimately result in anaphylaxis. An incidence rate of 34.1 (95% CI: 23.1–50.0) per 100,000 new users for anaphylaxis was reported (Wang et al., 2015) but it must be pointed out that this study reported lower rates of anaphylaxis than clinical trials, possibly because cases of minor hypersensitivity reactions are not routinely registered if not in the setting of a clinical trial (Wang et al., 2016). It is also still unknown if rapid ferumoxytol infusion leads to increased incidence of anaphylaxis compared to slow infusion (Wang et al., 2015) but if used as a marker of macrophage infiltration slow infusion of ferumoxytol would suffice. In conclusion, experience with USPIO is limited to small studies. Large clinical trials are needed to prove safety of USPIO enhanced imaging (Finn et al., 2016).

## Magnetic Resonance Elastography (MRE)

Research in healthy volunteers has shown that magnetic resonance elastography (MRE) is feasible and reliable for the assessment of kidney stiffness (Rouvière et al., 2011; Low et al., 2015). In an animal model of renal artery stenosis MRE could detect medullary stiffness, which reflected medullary fibrosis (Korsmo et al., 2013). The potential to acquire 3D images with MRE is a great advantage over ultrasound (US), which only yields 2D images, although spatial resolution of MR imaging is inferior to US (Grenier et al., 2013). Human research in the field of MRE is limited, because US is far more practical, less expensive and less labor intensive in the clinical setting than MRE.

# SUMMARIZING DISCUSSION AND CONCLUSION

Novel imaging modalities have to pass the standard threshold of development before they are clinically implemented (Sado et al., 2011). Some of the MRI techniques discussed here are now at the stage where their disease-predictive nature has been demonstrated. All the above techniques correlate with functional parameters, mostly eGFR, and sometimes also with histopathology. However, these correlations are relatively modest, due to limitations in current interpretation software-tools, but also to the inherent insensitivity of eGFR to limited nephron loss (Pascual et al., 2012).

Most functional imaging techniques are not routinely used in clinical practice. However, chances are high that eventually imaging techniques, alone or in combination, will yield data precise enough to accurately diagnose (sub)clinical kidney disease. In the future MRI could become feasible as a screening tool in long-term follow-up of kidney allografts. Longitudinal information on active inflammation and existing fibrosis, a combination that was identified as a strong predictor for allograft loss (Haas, 2014) could be gained, and in this way MRI could contribute to clinical decision making. For instance, MRI findings suggestive for subclinical damage could support the decision to proceed to kidney biopsy in the absence of clinical symptoms. Lastly, the whole kidney fibrosis percentage can be estimated, which will allow better appreciation of the extent of fibrosis than with a biopsy.

Admittedly, progress made in the past decade toward clinical implementation is not satisfying. This may be partially explained by the fear of nephrogenic systemic fibrosis due to GBCAs. It should therefore be stressed that with current technology administration of GBCAs has become unnecessary in many cases. Awareness of the potential of functional MRI in long-term follow-up of kidney transplantation patients among nephrologists is warranted (Zhang et al., 2014a). This review illustrates that functional MRI has the potential to probe several pathophysiological mechanisms involved in kidney allograft dysfunction, and is a promising tool in long-term follow-up of kidney transplantation patients.

## AUTHOR CONTRIBUTIONS

MvE participated in the initial literature search, data analysis, and interpretation, drafting of the manuscript, study group discussions, and approved the final version of the article; AvZ participated in the literature search, data analysis and interpretation, drafting of the manuscript, study group discussions, and approved the final version of the article; AdB and MF participated in data analysis and interpretation, drafting of the article, study group discussions, and approved the final version of the article; TN participated in the literature search, data analysis and interpretation, drafting of the manuscript, study group discussions, and approved the final version of the article; JJ participated in data analysis and interpretation, drafting of the article, and approved the final version of the article; TL participated in data analysis and interpretation, drafting of the article, attending study group discussions, study supervision and approved the final version of the article; MV participated in drafting of the article, study group discussions, study supervision and approved the final version of the article.

## FUNDING

This work was supported by the Dutch Kidney Foundation (Nierstichting Nederland) [grant number 150KK119]. The Dutch Kidney Foundation had no role in deciding on the study design, or in the collection, analysis, and interpretation of data; neither has this funder contributed to writing the article nor to making the decision to submit the article for publication.

## ACKNOWLEDGMENTS

MvE was awarded a Kolff Student Researcher Grant by the Dutch Kidney Foundation; grant number 150KK119. MvE is a medical student participating in the Honours Program of the Faculty of Medicine, University Medical Center Utrecht, Utrecht, The Netherlands.

## REFERENCES

Atthe, B., Babsky, A., Hopewell, P., Phillips, C., Molitoris, B., and Bansal, N. (2009). Early monitoring of acute tubular necrosis in the rat kidney by $^{23}$Na-MRI. *Am. J. Physiol. Renal Physiol.* 297, F1288–F1298. doi: 10.1152/ajprenal.00388.2009

Bashir, M. R., Bhatti, L., Marin, D., and Nelson, R. C. (2015). Emerging applications for ferumoxytol as a contrast agent in MRI. *J. Magn. Reson. Imaging* 41, 884–898. doi: 10.1002/jmri.24691

Beckmann, N., Cannet, C., Fringeli-Tanner, M., Baumann, D., Pally, C., Bruns, C., et al. (2003). Macrophage labeling by SPIO as an early marker of allograft chronic rejection in a rat model of kidney transplantation. *Magn. Reson. Med.* 49, 459–467. doi: 10.1002/mrm.10387

Blondin, D., Lanzman, R. S., Klasen, J., Scherer, A., Miese, F., Kröpil, P., et al. (2011). Diffusion-attenuated MRI signal of renal allografts: comparison of two different statistical models. *AJR Am. J. Roentgenol.* 196, W701–W705. doi: 10.2214/AJR.10.5775

Brezis, M., Heyman, S., and Epstein, F. (1994). Determinants of intrarenal oxygenation. II. Hemodynamic effects. *Am. J. Physiol.* 267(6 Pt 2), F1063–F1068.

Brezis, M., Rosen, S., Silva, P., and Epstein, F. (1984). Renal ischemia: a new perspective. *Kidney Int.* 26, 375–383.

Chandarana, H., and Lee, V. S. (2009). Renal functional MRI: are we ready for clinical application? *AJR Am. J. Roentgenol.* 192, 1550–1557. doi: 10.2214/AJR.09.2390

Cheung, J. S., Juan, S., Chow, A. M., Zhang, J., Man, K., and Wu, E. X. (2010). Diffusion tensor imaging of renal ischemia reperfusion injury in an experimental model. *NMR Biomed.* 23, 496–502. doi: 10.1002/nbm.1486

Chung, S., Koh, E. S., Kim, S. J., Yoon, H. E., Park, C. W., Chang, Y. S., et al. (2014). Safety and tissue yield for percutaneous native kidney biopsy according to practitioner and ultrasound technique. *BMC Nephrol.* 15:96. doi: 10.1186/1471-2369-15-96

Corapi, K. M., Chen, J. L., Balk, E. M., and Gordon, C. E. (2012). Bleeding complications of native kidney biopsy: a systematic review and meta-analysis. *Am. J. Kidney Dis.* 60, 62–73. doi: 10.1053/j.ajkd.2012.02.330

Cosio, F. G., Gloor, J. M., Sethi, S., and Stegall, M. D. (2008). Transplant glomerulopathy. *Am. J. Transplant.* 8, 492–496. doi: 10.1111/j.1600-6143.2007.02104.x

Currie, S., Hoggard, N., Craven, I. J., Hadjivassiliou, M., and Wilkinson, I. D. (2013). Understanding MRI: basic MR physics for physicians. *Postgrad. Med. J.* 89, 209–223. doi: 10.1136/postgradmedj-2012-131342

Cutajar, M., Thomas, D. L., Banks, T., Clark, C. A., Golay, X., and Gordon, I. (2012). Repeatability of renal arterial spin labelling MRI in healthy subjects. *Magn. Reson. Mater. Phys. Biol. Med.* 25, 145–153. doi: 10.1007/s10334-011-0300-9

Cutajar, M., Thomas, D. L., Hales, P. W., Banks, T., Clark, C. A., and Gordon, I. (2014). Comparison of ASL and DCE MRI for the non-invasive measurement of renal blood flow: quantification and reproducibility. *Eur. Radiol.* 24, 1300–1308. doi: 10.1007/s00330-014-3130-0

Dang, Z., Mackinnon, A., Marson, L. P., and Sethi, T. (2012). Tubular atrophy and interstitial fibrosis after renal transplantation is dependent on galectin-3. *Transplantation* 93, 477–484. doi: 10.1097/TP.0b013e318242f40a

Djamali, A., Sadowski, E. A., Muehrer, R. J., Reese, S., Smavatkul, C., Vidyasagar, A., et al. (2007). BOLD-MRI assessment of intrarenal oxygenation and oxidative stress in patients with chronic kidney allograft dysfunction. *Am. J. Physiol. Renal Physiol.* 292, F513–F522. doi: 10.1152/ajprenal.00222.2006

Djamali, A., Sadowski, E. A., Samaniego-Picota, M., Fain, S. B., Muehrer, R. J., Alford, S. K., et al. (2006). Noninvasive assessment of early kidney allograft dysfunction by blood oxygen level-dependent magnetic resonance imaging. *Transplantation* 82, 621–628. doi: 10.1097/01.tp.0000234815.23630.4a

dos Santos, E. A., Li, L., Ji, L., and Prasad, P. V. (2007). Early changes with diabetes in renal medullary hemodynamics as evaluated by fiberoptic probes and BOLD magnetic resonance imaging. *Invest. Radiol.* 42, 157–162. doi: 10.1097/01.rli.0000252492.96709.36

Ebrahimi, B., Textor, S. C., and Lerman, L. O. (2014). Renal relevant radiology: renal functional magnetic resonance imaging. *Clin. J. Am. Soc. Nephrol.* 9, 395–405. doi: 10.2215/CJN.02900313

Eikefjord, E., Andersen, E., Hodneland, E., Zöllner, F., Lundervold, A., Svarstad, E., et al. (2015). Use of 3D DCE-MRI for the estimation of renal perfusion and glomerular filtration rate: an intrasubject comparison of FLASH and KWIC with a comprehensive framework for evaluation. *Genitourin Imaging* 204, W273–W281. doi: 10.2214/AJR.14.13226

Evans, R. G., Ince, C., Joles, J. A., Smith, D. W., May, C. N., O'Connor, P. M., et al. (2013). Haemodynamic influences on kidney oxygenation: clinical implications of integrative physiology. *Clin. Exp. Pharmacol. Physiol.* 40, 106–122. doi: 10.1111/1440-1681.12031

Evans, R. G., Ow, C. P. C., and Bie, P. (2015). The chronic hypoxia hypothesis: the search for the smoking gun goes on. *Am. J. Physiol. Renal Physiol.* 308, F101–F102. doi: 10.1152/ajprenal.00587.2014

Fan, W., Ren, T., Li, Q., Zuo, P. L., Long, M. M., Mo, C. B., et al. (2016). Assessment of renal allograft function early after transplantation with isotropic resolution diffusion tensor imaging. *Eur. Radiol.* 26, 567–575. doi: 10.1007/s00330-015-3841-x

Ferré J., Bannier, E., Raoult, H., Mineur, G., Carsin-Nicol, B., and Gauvrit, J.-Y. (2013). Arterial spin labeling (ASL) perfusion: techniques and clinical use. *Diagn. Interv. Imaging* 94, 1211–1223. doi: 10.1016/j.diii.2013.06.010

Fine, L. G., and Norman, J. T. (2008). Chronic hypoxia as a mechanism of progression of chronic kidney diseases: from hypothesis to novel therapeutics. *Kidney Int.* 74, 867–872. doi: 10.1038/ki.2008.350

Fine, L. G., Bandyopadhay, D., and Norman, J. T. (2000). Is there a common mechanism for the progression of different types of renal diseases other than proteinuria? Towards the unifying theme of chronic hypoxia. *Kidney Int. Suppl.*75, S22–S26. doi: 10.1046/j.1523-1755.2000.07512.x

Fine, L. G., Orphanides, C., and Norman, J. T. (1998). Progressive renal disease: the chronic hypoxia hypothesis. *Kidney Int. Suppl.* 53(Suppl. 6), S74–S78.

Finn, J. P., Nguyen, K.-L., Han, F., Zhou, Z., Salusky, I., Ayad, I., et al. (2016). Cardiovascular MRI with ferumoxytol. *Clin. Radiol.* 71, 796–806. doi: 10.1016/j.crad.2016.03.020

Gellissen, J., Axmann, C., Prescher, A., Bohndorf, K., and Lodemann, K. (1999). Extra- and intarcellular accumulation of ultrasmall superparamagnetic iron oxides (USPIO) in experimentally induced abscesses of the peripheral soft tissues and their effects on magnetic resonance imaging. *Magn. Reson. Imaging* 17, 557–567.

Gillis, K. A., McComb, C., Foster, J. E., Taylor, A. H., Patel, R. K., Morris, S. T., et al. (2014). Inter-study reproducibility of arterial spin labelling magnetic resonance imaging for measurement of renal perfusion in healthy volunteers at 3 Tesla. *BMC Nephrol.* 15:23. doi: 10.1186/1471-2369-15-23

Grenier, N., Gennisson, J.-L., Cornelis, F., Le Bras, Y., and Couzi, L. (2013). Renal ultrasound elastography. *Diagn. Interv. Imaging* 94, 545–550. doi: 10.1016/j.diii.2013.02.003

Grenier, N., Merville, P., and Combe, C. (2016). Radiologic imaging of the renal parenchyma structure and function. *Nat. Rev. Nephrol.* 12, 348–359. doi: 10.1038/nrneph.2016.44

Haas, M. (2014). Chronic allograft nephropathy or interstitial fibrosis and tubular atrophy: what is in a name? *Curr. Opin. Nephrol. Hypertens.* 23, 245–250. doi: 10.1097/01.mnh.0000444811.26884.2d

Han, F., Xiao, W., Xu, Y., Wu, J., Wang, Q., Wang, H., et al. (2008). The significance of BOLD MRI in differentiation between renal transplant rejection and acute tubular necrosis. *Nephrol. Dial. Transplant.* 23, 2666–2672. doi: 10.1093/ndt/gfn064

Haneder, S., Kettnaker, P., Konstandin, S., Morelli, J. N., Schad, L. R., Schoenberg, S. O., et al. (2013). Quantitative *in vivo* $^{23}$Na MR imaging of the healthy human kidney: determination of physiological ranges at 3.0T with comparison to DWI and BOLD. *Magn. Reson. Mater. Phys* 26, 501–509. doi: 10.1007/s10334-013-0369-4

Hauger, O., Grenier, N., Deminère, C., Lasseur, C., Delmas, Y., Merville, P., et al. (2007). USPIO-enhanced MR imaging of macrophage infiltration in native and transplanted kidneys: initial results in humans. *Eur. Radiol.* 17, 2898–2907. doi: 10.1007/s00330-007-0660-8

He, X., Aghayev, A., Gumus, S., and Ty Bae, K. (2014). Estimation of single-kidney glomerular filtration rate without exogenous contrast agent. *Magn. Reson. Med.* 71, 257–266. doi: 10.1002/mrm.24668

He, X., Moon, C.-H., Kim, J.-H., and Bae, K. T. (2011). "In vivo T1ρ study on human kidney. Proc. Intl. Soc. Mag. Reson. Med. 19, 824," in *ISMRM 2011: Proceedings of the 19th Annual Meeting and Exhibition* (Montréal, QC). Available online at: http://cds.ismrm.org/protected/11MProceedings/files/824.pdf (accessed 4 May, 2017).

Heusch, P., Wittsack, H. J., Blondin, D., Ljimani, A., Nguyen-Quang, M., Martirosian, P., et al. (2014). Functional evaluation of transplanted kidneys using arterial spin labeling MRI. *J. Magn. Reson. Imaging* 40, 84–89. doi: 10.1002/jmri.24336

Heusch, P., Wittsack, H.-J., Heusner, T., Buchbender, C., Quang, M. N., Martirosian, P., et al. (2013). Correlation of biexponential diffusion parameters with arterial spin-labeling perfusion MRI: results in transplanted kidneys. *Invest. Radiol.* 48, 140–144. doi: 10.1097/RLI.0b013e318277bfe3

Heyman, S. N., Khamaisi, M., Rosen, S., and Rosenberger, C. (2008). Renal parenchymal hypoxia, hypoxia response and the progression of chronic kidney disease. *Am. J. Nephrol.* 28, 998–1006. doi: 10.1159/000146075

Huang, Y., Sadowski, E. A., Artz, N. S., Seo, S., Djamali, A., Grist, T. M., et al. (2011). Measurement and comparison of T1 relaxation times in native and transplanted kidney cortex and medulla. *J. Magn. Reson. Imaging* 33, 1241–1247. doi: 10.1002/jmri.22543

Hueper, K., Gutberlet, M., Rodt, T., Gwinner, W., Lehner, F., Wacker, F., et al. (2011). Diffusion tensor imaging and tractography for assessment of renal allograft dysfunction — initial results. *Eur. Radiol.* 21, 2427–2433. doi: 10.1007/s00330-011-2189-0

Hueper, K., Gutberlet, M., Rong, S., Hartung, D., Mengel, M., Lu, X., et al. (2014). Acute kidney injury: arterial spin labeling to monitor renal perfusion impairment in mice-comparison with histopathologic results and renal function. *Radiology* 270, 117–124. doi: 10.1148/radiol.13130367

Hueper, K., Khalifa, A. A., Bräsen, J. H., Vo Chieu, V. D., Gutberlet, M., Wintterle, S., et al. (2016). Diffusion-weighted imaging and diffusion tensor imaging detect delayed graft function and correlate with allograft fibrosis in patients early after kidney transplantation. *J. Magn. Reson. Imaging* 44, 112–121. doi: 10.1002/jmri.25158

Kalb, B., Martin, D. R., Salman, K., Sharma, P., Votaw, J., and Larsen, C. (2008). Kidney transplantation: structural and functional evaluation using MR nephrourography. *J. Magn. Reson. Imaging* 28, 805–822. doi: 10.1002/jmri.21562

Khalifa, F., El-ghar, M. A., Abdollahi, B., Frieboes, H. B., El-diasty, T., and El-baz, A. (2013). A comprehensive non-invasive framework for automated evaluation of acute renal transplant rejection using DCE-MRI. *NMR Biomed.* 26, 1460–1470. doi: 10.1002/nbm.2977

Kistner, I., Ott, C., Jumar, A., Friedrich, S., Grosso, R., Siegl, C., et al. (2015). Applicability of measurement of renal perfusion using 1.5 Tesla MRI Arterial Spin Labelling. *J. Hypertens.* 33(Suppl. 1), e17. doi: 10.1097/01.hjh.0000467395.74215.e2

Korsmo, M. J., Ebrahimi, B., Eirin, A., Woollard, J. R., Krier, J. D., Crane, J. A., et al. (2013). Magnetic resonance elastography noninvasively detects *in vivo* renal medullary fibrosis secondary to swine renal artery stenosis. *Invest. Radiol.* 48, 61–68. doi: 10.1097/RLI.0b013e31827a4990

Lanzman, R. S., Wittsack, H., Martirosian, P., Zgoura, P., Bilk, P., Kröpil, P., et al. (2010). Quantification of renal allograft perfusion using arterial spin labeling MRI: initial results. *Eur. Radiol.* 20, 1485–1491. doi: 10.1007/s00330-009-1675-0

Lanzman, R., Ljimani, A., Pentang, G., Zgoura, P., Zenginli, H., Kröpil, P., et al. (2013). Kidney Transplant: functional assessment with diffusion-tensor MR imaging at 3T. *Radiology* 266, 218–225. doi: 10.1148/radiol.12112522

Leong, C.-L., Anderson, W. P., O'Connor, P. M., and Evans, R. G. (2007). Evidence that renal arterial-venous oxygen shunting contributes to dynamic regulation of renal oxygenation. *Am. J. Physiol. Renal Physiol.* 292, F1726–F1733. doi: 10.1152/ajprenal.00436.2006

Li, X., Cheng, J., Lin, K., Saadat, E., Bolbos, R. I., Jobke, B., et al. (2011). Quantitative MRI using T1ρ and T2 in human osteoarthritic cartilage specimens: correlation with biochemical measurements and histology. *Magn. Reson. Imaging* 29, 324–334. doi: 10.1016/j.mri.2010.09.004

Liu, G., Han, F., Xiao, W., Wang, Q., Xu, Y., and Chen, J. (2014). Detection of renal allograft rejection using blood oxygen level-dependent and diffusion weighted magnetic resonance imaging: a retrospective study. *BMC Nephrol.* 15:158. doi: 10.1186/1471-2369-15-158

Low, G., Owen, N. E., Joubert, I., Patterson, A. J., Graves, M. J., Glaser, K. J., et al. (2015). Reliability of magnetic resonance elastography using multislice two-dimensional spin-echo echo-planar imaging (SE-EPI) and three-dimensional inversion reconstruction for assessing renal stiffness. *J. Magn. Reson. Imaging* 42, 844–850. doi: 10.1002/jmri.24826

Madaio, M. (1990). Renal biopsy. *Kidney Int.* 38, 529–543.

Manotham, K., Tanaka, T., Matsumoto, M., Ohse, T., Miyata, T., Inagi, R., et al. (2004). Evidence of tubular hypoxia in the early phase in the remnant kidney model. *J. Am. Soc. Nephrol.* 15, 1277–1288. doi: 10.1097/01.ASN.0000125614.35046.10

Maril, N., Margalit, R., Rosen, S., Heyman, S., and Degani, H. (2006). Detection of evolving acute tubular necrosis with renal $^{23}$Na MRI: studies in rats. *Kidney Int.* 69, 765–768. doi: 10.1038/sj.ki.5000152

McRobbie, D. W., Moore, E. A., Graves, M. J., and Prince, M. R. (2006). "To BOLDly go: new frontiers," in *MRI From Picture to Proton*, *Vol. 2nd Edn.,* eds D. W. McRobbie, E. A. Moore, M. J. Graves, and M. R. Prince (New York, NY: Cambridge University Press), 333.

Michaely, H. J., Herrmann, K. A., Nael, K., Oesingmann, N., Reiser, M. F., and Schoenberg, S. O. (2007). Functional renal imaging: nonvascular renal disease. *Abdom. Imaging* 32, 1–16. doi: 10.1007/s00261-005-8004-0

Milman, Z., Axelrod, J., Heyman, S., Nachmansson, N., and Abramovitch, R. (2014). Assessment with unenhanced MRI techniques of renal morphology and hemodynamic changes during acute kidney injury and chronic kidney disease in mice. *Am. J. Nephrol.* 39, 268–278. doi: 10.1159/000360093

Milman, Z., Heyman, S., Corchia, N., Edrei, Y., Axelrod, J. H., Rosenberger, C., et al. (2013). Hemodynamic response magnetic resonance imaging: application for renal hemodynamic characterization. *Nephrol. Dial. Transpl.* 28, 1150–1156. doi: 10.1093/ndt/gfs541

Moon, C. H., Furlan, A., Kim, J., Zhao, T., Shapiro, R., and Bae, K. T. (2014). Quantitative sodium MR imaging of native versus transplanted kidneys using a dual-tuned proton/sodium (1H/$^{23}$Na) coil: initial experience. *Eur. Radiol.* 24, 1320–1326. doi: 10.1007/s00330-014-3138-5

Morgan, T. A., Chandran, S., Burger, I., and Goldstein, R. (2016). Complications of ultrasound guided renal transplant biopsies. *Am. J. Transplant.* 16, 1298–1305. doi: 10.1111/ajt.13622

Morozumi, K., Takeda, A., Otsuka, Y., Horike, K., Gotoh, N., and Watarai, Y. (2014). Recurrent glomerular disease after kidney transplantation: an update of selected areas and the impact of protocol biopsy. *Nephrology* 19(Suppl. 3), 6–10. doi: 10.1111/nep.12255

Mukherjee, P., Berman, J., Chung, S., Hess, C., and Henry, R. (2008). Diffusion tensor MR imaging and fiber tractography: theoretic underpinnings. *AJNR Am. J. Neuroradiol.* 29, 632–641. doi: 10.3174/ajnr.A1051

Mukundan, S., Steigner, M. L., Hsiao, L., Malek, S. K., Tullius, S. G., Chin, M. S., et al. (2016). Ferumoxytol-enhanced magnetic resonance imaging in late-stage CKD. *Am. J. Kidney Dis.* 67, 984–988. doi: 10.1053/j.ajkd.2015.12.017

Neugarten, J., and Golestaneh, L. (2014). Blood oxygenation level-dependent MRI for assessment of renal oxygenation. *Int. J. Nephrol. Renovasc. Dis.* 7, 421–435. doi: 10.3389/fphys.2016.00667

Niles, D., Artz, N., Djamali, A., Sadowski, E., Grist, T., and Fain, S. (2016). Longitudinal assessment of renal perfusion and oxygenation in transplant donor-recipient pairs using arterial spin labeling and blood oxygen level-dependent magnetic resonance imaging. *Invest. Radiol.* 51, 113–120. doi: 10.1097/RLI.0000000000000210

Notohamiprodjo, M., Chandarana, H., Mikheev, A., Rusinek, H., Grinstead, J., Feiweier, T., et al. (2015). Combined intravoxel incoherent motion and diffusion tensor imaging of renal diffusion and flow anisotropy. *Magn. Reson. Med.* 73, 1526–1532. doi: 10.1002/mrm.25245

O'Connor, P. M., Kett, M. M., Anderson, W. P., and Evans, R. G. (2006). Renal medullary tissue oxygenation is dependent on both cortical and medullary blood flow. *Am. J. Physiol. Renal Physiol.* 290, F688–F694. doi: 10.1152/ajprenal.00275.2005

Papazova, D. A., Friederich-Persson, M., Joles, J. A., and Verhaar, M. C. (2015). Renal transplantation induces mitochondrial uncoupling, increased kidney oxygen consumption, and decreased kidney oxygen tension. *Am. J. Physiol. Renal Physiol.* 308, F22–F28. doi: 10.1152/ajprenal.00278.2014

Park, S. Y., Kim, C. K., Park, B. K., Huh, W., Kim, S. J., and Kim, B. (2012). Evaluation of transplanted kidneys using blood oxygenation level-dependent MRI at 3 T: a preliminary study. *AJR Am. J. Roentgenol.* 198, 1108–1114. doi: 10.2214/AJR.11.7253

Park, S. Y., Kim, C. K., Park, B. K., Kim, S. J., Lee, S., and Huh, W. (2014). Assessment of early renal allograft dysfunction with blood oxygenation level-dependent MRI and diffusion-weighted imaging. *Eur. J. Radiol.* 83, 2114–2121. doi: 10.1016/j.ejrad.2014.09.017

Pascual, J., Pérez-Sáez, M. J., Mir, M., and Crespo, M. (2012). Chronic renal allograft injury: early detection, accurate diagnosis and management. *Transplant. Rev.* 26, 280–290. doi: 10.1016/j.trre.2012.07.002

Pascual, M., Theruvath, T., Kawai, T., Tolkoff-Rubin, N., and Cosimi, A. (2002). Strategies to improve long-term outcomes after renal transplantation. *N. Engl. J. Med.* 346, 580–590. doi: 10.1056/NEJMra011295

Prasad, P. V. (2006). Evaluation of intra-renal oxygenation by BOLD MRI. *Nephron Clin. Pract.* 103, c58–c65. doi: 10.1159/000090610

Pruijm, M., Milani, B., and Burnier, M. (2016). Blood oxygenation level-dependent MRI to assess renal oxygenation in renal diseases: progresses and challenges. *Front. Physiol.*7:667. doi: 10.3389/fphys.2016.00667

Racusen, L. C. (2006). Protocol transplant biopsies in kidney allografts: why and when are they indicated? *Clin. J. Am. Soc. Nephrol.* 1, 144–147. doi: 10.2215/CJN.01010905

Rapacchi, S., Smith, R. X., Wang, Y., Yan, L., Sigalov, V., Krasileva, K. E., et al. (2015). Towards the identification of multi-parametric quantitative MRI biomarkers in lupus nephritis. *Magn. Reson. Imaging* 33, 1066–1074. doi: 10.1016/j.mri.2015.06.019

Rosenberger, C., Pratschke, J., Rudolph, B., Heyman, S. N., Schindler, R., Babel, N., et al. (2007). Immunohistochemical detection of hypoxia-inducible factor-1alpha in human renal allograft biopsies. *J. Am. Soc. Nephrol.* 18, 343–351. doi: 10.1681/ASN.2006070792

Rouvière, O., Souchon, R., Pagnoux, G., Ménager, J. M., and Chapelon, J. Y. (2011). Magnetic resonance elastography of the kidneys: feasibility and reproducibility in young healthy adults. *J. Magn. Reson. Imaging* 34, 880–886. doi: 10.1002/jmri.22670

Sado, D., Flett, A., and Moon, J. (2011). Novel imaging techniques for diffuse myocardial fibrosis. *Future Cardiol.* 7, 643–650. doi: 10.2217/fca.11.45

Sadowski, E. A., Djamali, A., Wentland, A. L., Muehrer, R., Becker, B. N., Grist, T. M., et al. (2010). Blood oxygen level-dependent and perfusion magnetic resonance imaging: detecting differences in oxygen bioavailability and blood flow in transplanted kidneys. *Magn. Reson. Imaging* 28, 56–64. doi: 10.1016/j.mri.2009.05.044

Sadowski, E. A., Fain, S. B., Alford, S. K., Korosec, F. R., Fine, J., Muehrer, R., et al. (2005). Assessment of acute renal transplant rejection with blood oxygen level-dependent MR imaging: initial experience. *Radiology* 236, 911–919. doi: 10.1148/radiol.2363041080

Seehafer, J. U., Kalthoff, D., Farr, T. D., Wiedermann, D., and Hoehn, M. (2010). No increase of the blood oxygenation level-dependent functional magnetic resonance imaging signal with higher field strength: implications for brain activation studies. *J. Neurosci.* 30, 5234–5241. doi: 10.1523/JNEUROSCI.0844-10.2010

Sentís, A., Kers, J., Yapici, U., Claessen, N., Roelofs, J. J., Bemelman, F. J., et al. (2015). The prognostic signi fi cance of glomerular in fi ltrating leukocytes during acute renal allograft rejection. *Transpl. Immunol.* 33, 168–175. doi: 10.1016/j.trim.2015.10.004

Tanabe, T. (2014). The value of long-term protocol biopsies after kidney transplantation. *Nephrology* 19(Suppl. 3), 2–5. doi: 10.1111/nep.12253

Thoeny, H. C., Zumstein, D., Simon-Zoula, S., Eisenberger, U., De Keyzer, F., Hofmann, L., et al. (2006). Functional evaluation of transplanted kidneys with diffusion-weighted and BOLD MR imaging: initial experience. *Radiology* 241, 812–821. doi: 10.1148/radiol.2413060103

van Baalen, S., Leemans, A., Dik, P., Lilien, M., Ten Haken, B., and Froeling, M. (2016). Intravoxel incoherent motion modeling in the kidneys: comparison of mono-, bi-, and triexponential fit. *J. Magn. Reson. Imaging.* doi: 10.1002/jmri.25519. [Epub ahead of print].

Vermathen, P., Binser, T., Boesch, C., Eisenberger, U., and Thoeny, H. C. (2012). Three-year follow-up of human transplanted kidneys by diffusion-weighted MRI and blood oxygenation level-dependent imaging. *J. Magn. Reson. Imaging* 35, 1133–1138. doi: 10.1002/jmri.23537

Wang, C., Graham, D. J., Kane, R. C., Xie, D., Wernecke, M., Levenson, M., et al. (2015). Comparative risk of anaphylactic reactions associated with intravenous iron products. *JAMA* 314, 2062–2068. doi: 10.1001/jama.2015.15572

Wang, C., Wong, S., and Graham, D. (2016). Risk of anaphylaxis with intravenous iron products. *JAMA* 315, 2232–2233. doi: 10.1001/jama.2016.0962

Wu, W. C., Su, M.-Y., Chang, C. C., Tseng, W.-Y. I., and Liu, K.-L. (2011). Renal perfusion 3-T MR imaging: a comparative study of arterial spin labeling and dynamic contrast-enhanced techniques. *Radiology* 261, 845–853. doi: 10.1148/radiol.11110668

Xiao, W., Xu, J., Wang, Q., Xu, Y., and Zhang, M. (2012). Functional evaluation of transplanted kidneys in normal function and acute rejection using BOLD MR imaging. *Eur. J. Radiol.* 81, 838–845. doi: 10.1016/j.ejrad.2011.02.041

Ye, Q., Yang, D., Williams, M., Williams, D. S., Pluempitiwiriyawej, C., Moura, J. M., et al. (2002). *In vivo* detection of acute rat renal allograft rejection by MRI with USPIO particles. *Kidney Int.* 61, 1124–1135. doi: 10.1046/j.1523-1755.2002.00195.x

Zeng, M., Cheng, Y., and Zhao, B. (2015). Measurement of single-kidney glomerular filtration function from magnetic resonance perfusion renography. *Eur. J. Radiol.* 84, 1419–1423. doi: 10.1016/j.ejrad.2015.05.009

Zhang, J. L., Morrell, G., Rusinek, H., Sigmund, E. E., Chandarana, H., Lerman, L. O., et al. (2014a). New magnetic resonance imaging methods in nephrology. *Kidney Int.* 85, 768–778. doi: 10.1038/ki.2013.361

Zhang, J. L., Morrell, G., Rusinek, H., Warner, L., Vivier, P. H., Cheung, A. K., et al. (2014b). Measurement of renal tissue oxygenation with blood oxygen level-dependent MRI and oxygen transit modeling. *Am J Physiol Ren Physiol.* 306, F579–F587. doi: 10.1152/ajprenal.00575.2013

Zhang, Y., Dodd, S. J., Hendrich, K. S., Williams, M., and Ho, C. (2000). Magnetic resonance imaging detection of rat renal transplant rejection by monitoring macrophage infiltration. *Kidney Int.* 58, 1300–1310. doi: 10.1046/j.1523-1755.2000.00286.x

Zimmer, F., Zöllner, F. G., Hoeger, S., Klotz, S., Tsagogiorgas, C., Krämer, B. K., et al. (2013). Quantitative renal perfusion measurements in a rat model of acute kidney injury at 3T: testing inter- and intramethodical significance of ASL and DCE-MRI. *PLoS ONE* 8:e53849. doi: 10.1371/journal.pone.0053849

**Conflict of Interest Statement:** The authors declare that the research was conducted in the absence of any commercial or financial relationships that could be construed as a potential conflict of interest.

frontiers in Physiology

REVIEW
published: 11 April 2017
doi: 10.3389/fphys.2017.00211

# Mitochondrial Reactive Oxygen Species and Kidney Hypoxia in the Development of Diabetic Nephropathy

*Tomas A. Schiffer*[1,2] *and Malou Friederich-Persson*[1]*

[1] *Department of Medical Cell Biology, Uppsala University, Uppsala, Sweden,* [2] *Department of Medical and Health Sciences, Linköping University, Linköping, Sweden*

OPEN ACCESS

**Edited by:**
*Maarten Koeners, University of Bristol, UK*

**Reviewed by:**
*Samuel Heyman, Hadassah Medical Center, Israel*
*Roger Evans, Monash University, Australia*
*Pamela K. Carmines, University of Nebraska Medical Center, USA*

***Correspondence:**
*Malou Friederich-Persson*
*malou.friederich@mcb.uu.se*

**Specialty section:**
*This article was submitted to Renal and Epithelial Physiology, a section of the journal Frontiers in Physiology*

**Received:** *02 December 2016*
**Accepted:** *23 March 2017*
**Published:** *11 April 2017*

**Citation:**
*Schiffer TA and Friederich-Persson M (2017) Mitochondrial Reactive Oxygen Species and Kidney Hypoxia in the Development of Diabetic Nephropathy. Front. Physiol. 8:211. doi: 10.3389/fphys.2017.00211*

The underlying mechanisms in the development of diabetic nephropathy are currently unclear and likely consist of a series of dynamic events from the early to late stages of the disease. Diabetic nephropathy is currently without curative treatments and it is acknowledged that even the earliest clinical manifestation of nephropathy is preceded by an established morphological renal injury that is in turn preceded by functional and metabolic alterations. An early manifestation of the diabetic kidney is the development of kidney hypoxia that has been acknowledged as a common pathway to nephropathy. There have been reports of altered mitochondrial function in the diabetic kidney such as altered mitophagy, mitochondrial dynamics, uncoupling, and cellular signaling through hypoxia inducible factors and AMP-kinase. These factors are also likely to be intertwined in a complex manner. In this review, we discuss how these pathways are connected to mitochondrial production of reactive oxygen species (ROS) and how they may relate to the development of kidney hypoxia in diabetic nephropathy. From available literature, it is evident that early correction and/or prevention of mitochondrial dysfunction may be pivotal in the prevention and treatment of diabetic nephropathy.

**Keywords: diabetic nephropathy, kidney hypoxia, mitochondrial function, superoxide production, mitochondrial uncoupling, mitochondrial ROS, hypoxia inducible factors**

## DIABETIC NEPHROPATHY

Diabetic nephropathy accounts for ∼45% of cases with end-stage renal disease (McCullough et al., 2007) and afflict about 30% of patients with diabetes mellitus (Hasslacher et al., 1989). Early diabetic nephropathy is evident as microalbuminuria (30–300 mg/day) and disease progression is characterized by progressively worsening albuminuria, loss of glomerular filtration rate, and structural changes such as thickening of glomerular basement membranes, extracellular matrix accumulation, and tubulointerstitial damage (Mauer et al., 1984; Brito et al., 1998; Katz et al., 2002; Mauer and Drummond, 2002). Currently, there are no curative treatments and disease progression

ultimately results in requirement for renal replacement therapy i.e., dialysis or renal transplantation.

## HYPOXIA IS AN ACKNOWLEDGED PATHWAY TO NEPHROPATHY

The oxygen levels in the kidney with oxygen tension in cortex around 50–60 mmHg and as low as 10–20 mmHg in medulla (Epstein et al., 1994) makes the kidney susceptible to diverse renal pathologies. The distribution of glycolytic enzymes has a heterogeneous pattern and are scarcely found from glomerulus until the loop of Henle with a multifold increase in thick ascending limb and along the rest of the nephron to the collecting duct (Guder and Ross, 1984). The proximal tubules therefore mainly rely on mitochondrial ATP production. However, the glycolytic enzymes in proximal tubules can be induced in hypoxia (Gullans et al., 1982; Dickman and Mandel, 1990). The theory of renal hypoxia has emerged as a pathway to nephropathy. It was suggested by Fine et al. that an initial glomerular injury would decrease blood flow through peritubular capillaries and decrease oxygenation, promoting tubulointerstitial fibrosis and damage progression, ultimately resulting in nephropathy (Fine et al., 1998). This theory is proposed to be a joint pathway for development of nephropathy in a number of conditions and not restricted to diabetic nephropathy alone. The chronic hypoxia theory has gained support in experimental animal studies (Palm et al., 2003; Ries et al., 2003; Rosenberger et al., 2008; Edlund et al., 2009; Haidara et al., 2009) as well as in human studies (Sayarlioglu et al., 2005; Hochman et al., 2007; Inoue et al., 2011). Navajo Indians living at high altitude have increased incidence of ESRD (non-diabetes-related; Hochman et al., 2007) and in patients suffering from sleep apnea the degree of nocturnal hypoxemia correlates with worsening kidney function (Sakaguchi et al., 2013). Also, patients with type 2 diabetes living at high altitude had increased incidence of diabetic nephropathy when compared to a similar patient group living at sea level. Importantly, glycaemia, hypertension, and lipidemia status were similar between the groups (Sayarlioglu et al., 2005). Expertly reviewed elsewhere, the support for kidney hypoxia as a common pathway to nephropathy is quite compelling (Nangaku, 2006; Singh et al., 2008; Mimura and Nangaku, 2010; Palm and Nordquist, 2011).

This review will not focus on the mechanisms of hypoxia resulting in nephropathy but rather the mechanisms that may influence the development of hypoxia, namely mitochondrial function and reactive oxygen species (ROS) production.

**Abbreviations:** AICAR, 5-Aminoimidazole-4-carboxamide ribonucleotide; AMPK, AMP-kinase; DHE, dihydroethidium; DNA, deoxyribonucleic acid; DRP, dynamin related protein; DLP, dynamin like protein; ETS, electron transport system; FIS, mitochondrial fission protein; HIF, hypoxia inducible factor; LC3-II, LC3-phosphatidylethanolamine conjugate; NF-κB, nuclear factor kappa-light-chain-enhancer of activated B cells; mnSOD, manganese superoxide dismutase; MnTBAP, manganese (III) tetrakis (4-benzoic acid) porphyrin chloride; P62/SQSTM1 sequestosome 1; PARP, poly adenosine diphosphate ribose polymerase; PGC-1α, peroxisome proliferator-activated receptor gamma coactivator 1α; ROS, reactive oxygen species; Si, small interference; TCA, tricarboxylic acid; UCP, uncoupling protein.

## MITOCHONDRIAL PRODUCTION OF REACTIVE OXYGEN SPECIES IN THE DIABETIC KIDNEY

Production of ATP occurs in the mitochondrial inner membrane. In the electron transport system (ETS), the transferring of electrons from complex I to IV is coupled to translocation of protons to the intermembrane space, creating a membrane potential that is utilized by the ATP-synthase to produce ATP. Under normal conditions, ∼0.1–0.2% of mitochondrial oxygen consumption is due to production of ROS (Kushnareva et al., 2002; St-Pierre et al., 2002). ROS production varies between different segments of the nephron where the medullary thick ascending limb of Henle (mTAL) is the predominant site of superoxide production in the kidney (Zou et al., 2001; Li et al., 2002). NADPH oxidase seems to be the main source of superoxide production in mTAL (Li et al., 2002) and tubular flow and luminal $Na^+$ positively correlates with ROS production in this segment (Garvin and Hong, 2008; Cowley et al., 2015). Hall and colleagues demonstrated a higher total ROS production in proximal tubules compared to distal tubules (Hall et al., 2009). Inhibition of NADPH oxidase with apocynin revealed that the difference was attributed to higher NADPH oxidase activity in proximal tubules. The higher ratio of mitochondrial to nuclear volume in proximal tubules due to the larger cell size, indicate that the basal ROS production *per mitochondrion* is likely lower in proximal tubules. This fits with the lower membrane potential ($\Delta\psi_m$) and reduction grade of the electron transport chain in proximal tubules (Hall et al., 2009).

In the diabetic kidney, a large body of evidence supports the role ROS-induced damage (reviewed in Forbes et al., 2008) and oxidative markers such as 2-isoprostane, 8-hydroxy-2-deoxyguanosine, nitrotyrosine, and thiobarbituric acid reactive substances have been shown to increase in numerous studies with experimental models of diabetes and in diabetic patients (Broedbaek et al., 2011). In 2000, Nishikawa et al. put forward the view that mitochondrial superoxide was the source of oxidative stress in diabetes (Nishikawa et al., 2000). The reasoning was that cellular hyperglycemia would promote excessive pyruvate uptake into the mitochondria and therefore substrates feeding electrons to the ETS, ultimately resulting in hyperpolarization of the mitochondrial membrane and increased superoxide production. They demonstrated that hyperglycemia increased mitochondrial superoxide production that could be normalized by inhibiting complex II, uncoupling mitochondrial membrane potential by carbonyl cyanide m-chlorophenyl hydrazone or overexpression of uncoupling protein 1 (UCP-1) and by the addition of manganese superoxide dismutase (mnSOD). Importantly, the normalization of mitochondrial superoxide production prevented glucose-induced activation of known pathways to diabetes-induced damage: protein kinase C activation, nuclear factor kappa-light-chain-enhancer of activated B cells (NF-κB) activation, sorbitol accumulation, and the formation of advanced glycation end-products (Nishikawa et al., 2000).

Mitochondrial superoxide production is strongly regulated by mitochondrial membrane potential (Korshunov et al., 1997; Starkov and Fiskum, 2003; Lambert and Brand, 2004) and many reports show that mitochondria isolated from diabetic animals and cells cultured under hyperglycemic conditions display increased ROS production (Raza et al., 2004; Rosca et al., 2005; Yu et al., 2006; Quijano et al., 2007; Coughlan et al., 2009; Munusamy and MacMillan-Crow, 2009; Chacko et al., 2010; Sourris et al., 2012). Kidney cortex mitochondria isolated from type 2 diabetic db/db-mice show increased superoxide and hydrogen production that could be reduced by a mitochondrial antioxidant (Sourris et al., 2012). In kidney cortex of streptozotocin-induced diabetic rats, glycation of mitochondrial proteins was associated with decreased complex III-activity and increased superoxide production (Rosca et al., 2005). Coughlan et al. connected glucose-derived NADH (complex I substrate) to increased mitochondrial superoxide production in mesangial cells from diabetic rats (Coughlan et al., 2009). In bovine aortic endothelial cells, hyperglycemic culture conditions resulted in increased glucose metabolism, increased mitochondrial membrane potential, and increased formation of superoxide and hydrogen peroxide. Reducing mitochondrial membrane potential or inhibiting electron transport lowered mitochondrial ROS production whereas cells lacking mitochondria did not respond with increased ROS formation to hyperglycemic conditions (Quijano et al., 2007). Mitochondrial ROS production is also dependent on mitochondrial dynamics (Yu et al., 2006). Yu et al. showed in rat liver cells that upon high glucose exposure, mitochondria underwent rapid fragmentation and concomitantly increased ROS production. Inhibiting mitochondrial fragmentation prevented the glucose induced ROS production in several cell types (Yu et al., 2006, 2008).

Not all studies show increased mitochondrial ROS in diabetes. Real-time imaging and systemic administration of dihydroethidium (DHE) by Dugan et al. observed decreased superoxide production in intact kidneys of type 1 diabetic mice compared to control mice, also supported by electron paramagnetic resonance data in whole kidney homogenates. The reduced superoxide production was accompanied by hyper-phosphorylation of pyruvate dehydrogenase that contributes to deactivation of the enzyme. This leads to reduced conversion of pyruvate to acetyl coenzyme A and therefore reduced equivalents to the ETS that can reduce oxygen. The AMP-kinase (AMPK) activator 5-Aminoimidazole-4-carboxamide ribonucleotide (AICAR) restored the observed effects and the authors proposed a feed-forward cycle in which decreased AMPK activity would decrease mitochondrial biogenesis via peroxisome proliferator-activated receptor gamma coactivator 1-alpha (PGC-1α), a cycle that would be initiated and maintained through decreased mitochondrial ROS production (Dugan et al., 2013). However, DHE is prone to spontaneous oxidation and is affected by the general oxygen metabolism and technical aspects of its use are therefore important. Superoxide-specific DHE-metabolites can be separated by high performance liquid chromatography but not by its general fluorescence (Halliwell and Whiteman, 2004). Also, cortical tubular cells in diabetic animals have increased oxygen metabolism (Korner et al., 1994) with concomitantly decreased kidney oxygen tension (Palm et al., 2003) which will also affect general DHE-fluorescence even if the superoxide-specific products are still present. In the study by Dugan et al. measurements of ROS production were done in whole homogenate of kidneys (Dugan et al., 2013). Structural changes in diabetic nephropathy primarily affects the glomeruli and tubules, sites were diabetes-induced mitochondrial ROS-production has been reported. It may be postulated that measuring whole kidney ROS-production is not representative of alterations at the actual site of damage.

It has been proposed that the data in Dugan et al. (2013) can also be explained by glucose-induced increase in mitochondrial ROS production causing deoxyribonucleic acid (DNA) breaks in the nucleus, activating the repair enzyme poly adenosine diphosphate ribose polymerase (PARP). As $NAD^+$ is a substrate for PARP its activation concomitantly reduces the $NAD^+$ pool, reducing its availability for sirtuin 1, a known AMPK activator (Nishikawa et al., 2015). Therefore, PARP-activation could result in reduced AMPK activation creating a feed-forward loop of reduced AMPK and decreased mitochondrial biogenesis that is initiated by high mitochondrial ROS (Nishikawa et al., 2015). In contrast, Al-Kafaji et al. observed increased mitochondrial ROS with concomitant increased mitochondrial copy number in human mesangial cells as a result of high glucose exposure. These effects were abolished by addition of the MnSOD mimetic manganese (III) tetrakis (4-benzoic acid) porphyrin chloride (MnTBAP; Al-Kafaji and Golbahar, 2013).

It is important to remember that the inconclusive reports showing both higher and lower ROS production in the kidney in diabetes may represent a temporal effect in which the development of diabetic nephropathy may be a series of dynamic events where hyperglycemia may initially increase mitochondrial superoxide production but not able to maintain it as the disease progresses. Mitochondrial superoxide production may damage mitochondrial DNA and ETS itself, eventually resulting in reduced superoxide production (Xie et al., 2008; Tewari et al., 2012). Also, mitochondrial uncoupling, covered in the next section, may be an important mechanism to prevent excessive mitochondrial superoxide production.

## MITOCHONDRIAL UNCOUPLING—A POTENTIALLY DETRIMENTAL CONSEQUENCE OF INCREASED ROS

Mitochondrial uncoupling is a process in which protons are released over the mitochondrial inner membrane independently of ATP-synthesis. This process results in the reduction of the mitochondrial membrane potential and therefore also decreased mitochondrial superoxide production (Nishikawa et al., 2000; Duval et al., 2002; Miwa and Brand, 2003; Starkov and Fiskum, 2003). However, in order to sustain ATP-production more electrons are transferred through the ETS and oxygen consumption is therefore increased. As the increased respiration is independent of ATP-production it is defined as leak-respiration and can be observed in isolated mitochondria under state 2 or 4

respirations or when the ATP-synthase is blocked by oligomycin. Physiologically, mitochondrial uncoupling is mediated by UCPs (Nicholls, 1976) that are sensitive to inhibition by purine nucleotides (Jaburek et al., 1999; Echtay et al., 2001) but can also be mediated by the adenine nucleotide transporter that is sensitive to carboxyatractyloside (Shabalina et al., 2006). UCP-2 is expressed in human kidney mitochondria (Fleury et al., 1997) as well as in rats and mice (Jezek et al., 1999; Friederich et al., 2009). In kidney cortex from type 1 diabetic rats UCP-2 expression was increased, resulting in increased mitochondrial leak-respiration that was sensitive to purine nucleotides (Friederich et al., 2008).

UCPs are proposed as the mitochondrial internal defense system against increased ROS production and several reports show that UCPs can be activated by superoxide (Echtay et al., 2002; Krauss et al., 2003) as well as by lipid peroxidation products (Echtay et al., 2003). In support, kidney cortex mitochondria of type 2 diabetic db/db-mice displayed increased mitochondrial leak respiration that was corrected after treatment with the antioxidant Q10 (Persson et al., 2012). The role of UCP-2 in regulating mitochondrial membrane potential and therefore ROS production has been reported in several studies. In murine endothelial cells, small interfering (si)-RNA toward UCP-2 resulted in increased mitochondrial membrane potential and ROS production (Duval et al., 2002). Macrophages from UCP-2 knockout mice display increased ROS production (Arsenijevic et al., 2000) and these mice display increased survival and clearance rates following infections (Arsenijevic et al., 2000; Rousset et al., 2006). In mice, the overexpression of UCP-2 in the brain is reported to decrease lesions and enhance neurological functions after ischemic insults (Mattiasson et al., 2003). Interestingly, after siRNA-mediated silencing of UCP-2 in diabetic rats it was observed that the adenine nucleotide transporter compensated with a further increased mitochondrial uncoupling in kidney cortex mitochondria (Friederich-Persson et al., 2012), indicating mitochondrial uncoupling as a mechanism of importance in the diabetic kidney.

While some report increased mitochondrial membrane potential with diabetes or hyperglycemic culture conditions (Nishikawa et al., 2000; Raza et al., 2004; Rosca et al., 2005; Yu et al., 2006; Quijano et al., 2007; Coughlan et al., 2009; Munusamy and MacMillan-Crow, 2009; Chacko et al., 2010; Sourris et al., 2012) not all studies do (Friederich-Persson et al., 2012; Persson et al., 2012). Studies that did not observe hyperpolarized mitochondria in diabetic kidneys also show the presence of mitochondrial uncoupling and increased mitochondrial membrane potential was only observed when mitochondrial uncoupling was blocked (Friederich-Persson et al., 2012; Persson et al., 2012). Thus, mitochondrial uncoupling may be a defensive strategy in order to maintain mitochondrial membrane potential at a normal level. Temporal effects may also be important. Munusamy et al. cultured proximal tubular cells under hyperglycemic condition and saw an initial increase in mitochondrial membrane potential and increased ROS-production. Importantly, this was followed by a second phase with reduced mitochondrial membrane potential and ROS production (Munusamy and MacMillan-Crow, 2009). It may be postulated that the second phase represents the initiation of mitochondrial uncoupling but the use of purine nucleotides or carboxyatractyloside were not employed to probe for possible mechanisms of leak respiration (Munusamy and MacMillan-Crow, 2009).

While mitochondrial uncoupling can be viewed as a mechanism protective of mitochondrial function it may be detrimental for the kidney due to the resulting increased oxygen consumption. The kidney is unable to correct increased oxygen usage with increased renal blood flow since that would increase tubular load of electrolytes destined for active transport and therefore in itself increase oxygen demand. Therefore, increased mitochondrial leak respiration would cause a decrease in renal oxygen availability and it has been suggested that diabetes-induced mitochondrial uncoupling contributes to the low oxygen tension seen in diabetic kidneys (Friederich-Persson et al., 2012). Indeed, treating healthy rats with the mitochondrial uncoupler dinitrophenol for 30 days results in kidney hypoxia, albuminuria, and tubulointerstitial damage without affecting levels of glycaemia or oxidative stress (Friederich-Persson et al., 2013).

## AMPK SIGNALING IN THE DIABETIC KIDNEY

AMPK regulates anabolic processes and the AMPK activity is dependent upon the surrounding energy levels (Hardie et al., 2012). When AMP/ATP ratio is increased under conditions such as hypoxia, exercise and hypoglycemia AMPK is allosterically activated (Hardie et al., 2012). In addition, AMPK can also be activated by upstream kinases such as the liver kinase B1 (Hawley et al., 2003) and $Ca^{2+}$/calmodulin-dependent protein kinase kinases β (Emerling et al., 2009). When activated, AMPK contributes to the inhibition of anabolic energy-consuming pathways and stimulates catabolic energy-producing pathways, thus leading to increased intracellular energy levels (Hardie et al., 2003).

In the diabetic kidney, despite renal hypoxia, AMPK is downregulated (Dugan et al., 2013). One possibility is that the degree of hypoxia may not be severe enough to result in AMPK-activation. Another possibility is the role of mitochondrial ROS production. Nishikawa recently proposed a hypothesis where ROS-induced activation of PARP may reduce the levels of $NAD^+$ and thus AMPK-activity through reduced SIRT1-activity (Nishikawa et al., 2015). Also, Emerling and colleagues reported that hypoxic activation of AMPK is dependent on mitochondrial ROS production rather than AMP:ATP ratios (Emerling et al., 2009). ROS also appear to mediate calcium release from the endoplasmic reticulum which then contributes to the formation of CRAC channels. This contributes to amplification of the signal through the entry of calcium that subsequently activates $Ca^{2+}$/calmodulin-dependent protein kinase kinases β that targets AMPK (Mungai et al., 2011). On the contrary, Dugan et al. observed decreased levels of ROS in the diabetic kidney and suggested a feed-forward cycle of decreased AMPK, PGC-1α, and

mitochondrial biogenesis initiated and maintained by reduced mitochondrial ROS production (Dugan et al., 2013).

AMPK has emerged as a regulator of cellular redox state and expression of antioxidants through the class O forkhead box signaling pathway (Sanchez et al., 2012) that promotes cell survival, mitochondrial biogenesis, and longevity (Fernandez-Marcos and Auwerx, 2011; Martins et al., 2016). In response to metabolic stress, class O forkhead box 3 is activated by AMPK that subsequently leads to increased levels of endogenous antioxidants such as mnSOD as well as thioredoxin, peroxiredoxin, and catalase (Kops et al., 2002; Zrelli et al., 2011). Therefore, AMPK activation may have the potential to attenuate glucose-induced oxidative stress in diabetic nephropathy. The antidiabetic and AMPK activating drug metformin lowered ROS production, lipid peroxidation and increased the antioxidant system in kidneys in a rat model of gentamicin toxicity (Morales et al., 2010). HUVEC cells treated with AMPK activator AICAR displayed decreased hyperglycemia-induced ROS production, increased expression of PGC-1α, mnSOD, nuclear respiratory factor-1, and mitochondrial transcription factor A together with stimulated mitochondrial proliferation (Kukidome et al., 2006).

The conflicting literature regarding mitochondrial ROS production in diabetes makes the relationship between mitochondrial ROS production and AMPK activation especially difficult to interpret. However, if mitochondrial ROS production is increased with hyperglycemia, locally if not represented in the whole kidney, not only would increased mitochondrial ROS production result in mitochondrial uncoupling and contribute to hypoxia through that pathway but also result in reduced AMPK activation and thus fails to divert oxygen consumption from oxidative phosphorylation to the more oxygen-saving glycolysis. As AMPK is reported to be down-regulated in the diabetic kidney (Dugan et al., 2013), AMPK activators may have beneficial effects on kidney hypoxia. In cultured liver epithelial cells, metformin suppressed hypoxia inducible factor (HIF)-1α stabilization by decreasing cellular oxygen consumption (Minokoshi et al., 2004; Zhou et al., 2016). No studies to date have investigated whether AMPK-activators can affect kidney oxygenation *in vivo*. See **Figure 1** for summary of proposed mechanisms.

Some caution is needed regarding possible off target effects of AMPK activators. Inhibition of hypothalamic AMPK is necessary for leptin's negative effects on food intake and body weight (Minokoshi et al., 2004; Hardie, 2015) and pharmacological AMPK activation may therefore alter the hormonal and nutrient-derived signals and energy balance (Hardie, 2015). Achieving tissue specific AMPK activation would therefore be optimal in any future AMPK-dependent treatments.

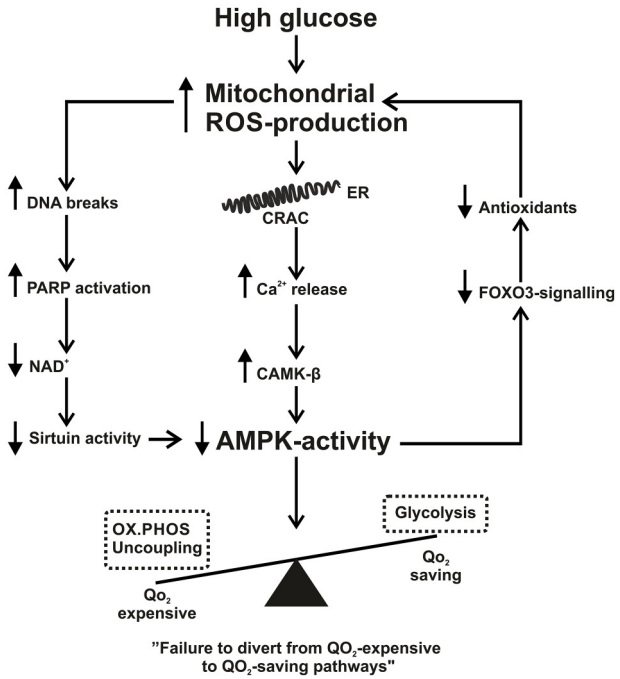


**FIGURE 1 | Summary scheme of how increased mitochondrial reactive oxygen species production (ROS) connects to decreased 5′ AMP-activated protein kinase activity.** See text for further details. AMPK, AMP-activated protein kinase; CAMK-β, $Ca^{2+}$/calmodulin-dependent protein kinase; CRAC, calcium release activated channel; ER, endoplasmic reticulum; FOXO3, Forkhead box O3; NAD, nicotinamide adenine dinucleotide; OX.PHOS, oxidative phosphorylation; PARP, poly (ADP-ribose) polymerase; ROS, reactive oxygen species; $QO_2$, oxygen consumption.

## HYPOXIA INDUCIBLE FACTORS IN THE DIABETIC KIDNEY

The oxygen dependent degradation of HIF-1α regulates the activity of HIF-1 transcription factor complex (Chen and Sang, 2016). In normoxia, prolyl 4-hydroxylases hydroxylate HIF-1α, enables the binding to the von-Hippel-Lindau complex and subsequent proteosomal degradation by an E3 ubiquitin ligase complex (Chen and Sang, 2016). The stabilization or degradation of HIF is a swiftly regulated process. Upon reoxygenation after hypoxia, degradation of the HIF-1α protein occurs with a half-life of <1 min (Yu et al., 1998). Recent studies highlight that ROS partly play a role in the stabilization of HIF-1α (Irwin et al., 2009; Niecknig et al., 2012; Zepeda et al., 2013). Mitochondrial ROS in particular (Brunelle et al., 2005) and sirtuin-dependent transactivation of HIF have emerged as a key factor (Lim et al., 2010; Zhong et al., 2010; Finley et al., 2011; Hubbi et al., 2013). HIF-target genes include pyruvate dehydrogenase kinase 1 (Loenarz et al., 2011) that inhibits pyruvate dehydrogenase, reducing the entry of acetyl-coenzyme A to the tricarboxylic acid cycle (TCA) and therefore contributes to the hypoxia-induced switch from oxidative phosphorylation to glycolysis. Sustained HIF-signaling also induces angiogenesis through vascular endothelial growth factor (Conway et al., 2001) and hematopoiesis via erythropoietin (Semenza, 1999) and fibrotic encapsulation will occur in long-term hypoxia (Tanaka, 2017).

Systemic hypoxia leads to accumulation of HIF-1α in most tubular segments with varied intensity, depending on the nature of hypoxic stimulus (Rosenberger et al., 2002). By contrast, HIF-2α is expressed in endothelial cells of a small subset of glomeruli, peritubular endothelial cells and fibroblasts (Rosenberger et al., 2002). Interestingly, inducing HIF by the

hypoxia mimetic cobalt chloride mainly contributes to HIF-1α in distal convoluted tubuli presumably related to uptake and accumulation (Nagao et al., 1999). Induced HIF-1α expression in the kidney has been demonstrated with diabetes in both rats (Rosenberger et al., 2008) and humans (Higgins et al., 2007; Shao et al., 2016) where overall HIF-signaling may contribute to renal injury. Higgins et al. showed that genetic ablation of epithelial HIF-1α in primary renal epithelial cells and in proximal tubules of kidneys subjected to unilateral ureteral obstruction inhibited the development of tubulointerstitial fibrosis, decreased inflammatory cell infiltration and reduced the number of fibroblast-specific protein-1-expressing interstitial cells (Higgins et al., 2007). Renal HIF-1α expression is also associated with tubulointerstitial injury in patients with chronic kidney disease (Higgins et al., 2007) and increased area of renal fibrosis has been observed in tubular epithelial cell specific von-Hippel-Lindau knockout mice (Kimura et al., 2008). Silencing HIF-1α with short hairpin RNA-technique significantly attenuated levels of collagen and α-smooth muscle actin and injury in kidneys from hypertensive rats (Wang et al., 2014). In addition, Nayak and colleagues observed reduced whole kidney glomerular hypertrophy, mesangial matrix expansion, extracellular matrix accumulation and urinary albumin excretion in diabetic mice upon treatment with the HIF-1 inhibitor YC-1 (Nayak et al., 2016).

In contrast, Nordquist et al. found no increase in HIF-responsive genes measured in whole kidney homogenates after 4 weeks of streptozotocin-induced diabetes where renal hypoxia was present (Nordquist et al., 2015). In this study diabetes-induced renal hypoxia, proteinuria and kidney injury were prevented by chronic HIF-activation via cobalt chloride (Nordquist et al., 2015), highlighting the importance of HIF-activation on regulating oxygen metabolism in diabetic nephropathy (further highlighted in Haase, 2015). Chronic HIF-activation has also been reported to be beneficial in an obese hypertensive model of type 2 diabetes where cobalt chloride did not affect metabolic parameters, obesity or hypertension but reduced proteinuria, improved kidney histology and decreased expression of fibrotic markers transforming growth factor β and connective tissue growth factor (Ohtomo et al., 2008).

Interestingly, kidney cortex mitochondria from diabetic animals in Nordquist et al. displayed mitochondrial uncoupling that was completely prevented by HIF-activation (Nordquist et al., 2015). In pulmonary artery smooth muscle cells, deficiency of mitochondrial UCP-2 resulted in hyperpolarized mitochondria, resistance to apoptosis, and reduced TCA cycle intermediates, changes that were replicated by hypoxia in wild type pulmonary artery smooth muscle cells. These results were substantiated in UCP-2 knockout mice when the mice displayed a pseudohypoxic state with increased pulmonary HIF-1α signaling, vascular remodeling and spontaneous development of pulmonary hypertension (Dromparis et al., 2013). It has been shown that mitochondrial ROS contributes to the stabilization of HIF (Brunelle et al., 2005), this through a ROS mediated activation of p38 mitogen-activated protein kinase (Emerling et al., 2005). However, as mitochondrial uncoupling proteins are also activated by ROS (Echtay et al., 2002) and some studies report normalized membrane potential in kidney cortex mitochondria isolated from diabetic rats and mice (Friederich-Persson et al., 2012; Persson et al., 2012) the glucose-induced mitochondrial uncoupling may act to prevent HIF-activation. Rosenberger et al. also observe this in a study where HIF-signaling could be enhanced by Tempol administration (Rosenberger et al., 2008), further suggesting an involvement of ROS. It has also been suggested that hyperglycemia directly interferes with HIF-signaling through hyperosmolarity as shown in endothelial cells and dermal fibroblasts (Catrina et al., 2004). Together, mitochondrial ROS and hyperglycemia may act to render the HIF-activation in diabetic kidneys submaximal.

Summarizing available data, a case can be made both for and against using chronic HIF-1α activation in diabetic nephropathy. Disparate results may well reflect the use of different models of diabetes but is also likely to reflect temporal aspects of HIF-activation; how long should HIF-activation be sustained and early or late in disease progression? These are just some of the issues that should be clarified in further studies.

## MITOCHONDRIAL DYNAMICS AND MITOPHAGY IN THE DIABETIC KIDNEY

In healthy tissues, mitochondria are present in tubular networks that are constantly reworked by mitochondrial fission and fusion. Fission results in mitochondrial fragmentation and production of short rods and spheres whereas fusion results in long filamentous mitochondria. It is a highly dynamic process (Liesa et al., 2009; Westermann, 2010) and controlled by a set of proteins where dynamin related protein 1 (DRP1) and mitochondrial fission 1 protein (FIS1) controls fission and mitofusin 1–2 and optic atrophy 1 is in control of fusion (Chan, 2006).

As previously mentioned, mitochondrial dynamics is important for glucose-induced increase in mitochondrial ROS production (Yu et al., 2006). Wang et al. elegantly showed the role of Rho-associated coiled coil-containing protein kinase 1 in activation and recruitment of DRP1 to mitochondria upon high glucose stimulation, promoting mitochondrial fission, fragmentation, and higher ROS production in podocytes (Wang et al., 2012). High glucose exposure, expression of DRP1 and FIS1 is induced in endothelial cells together with a loss of the mitochondrial network (Shenouda et al., 2011). Inhibiting DRP1 can also attenuate acute kidney injury and tubular cell apoptosis in mice (Brooks et al., 2009). Similarly, boosting mitochondrial fusion by overexpressing mitofusion 2 resulted in reduced proteinuria, kidney hypertrophy and albumin:creatinine ratio together with improved pathological changes in diabetic rats (Pawlikowska et al., 2007). Mitochondrial fission and concomitantly increased ROS production that contributes to the deleterious impact on kidney function is evident in diabetes. Thus, inhibiting fission and/or promoting fusion may impede the progression of DN.

Selective degradation of mitochondria by the autophagic machinery is termed mitophagy (Lemasters, 2005) and mitochondria must undergo fragmentation into spheroids

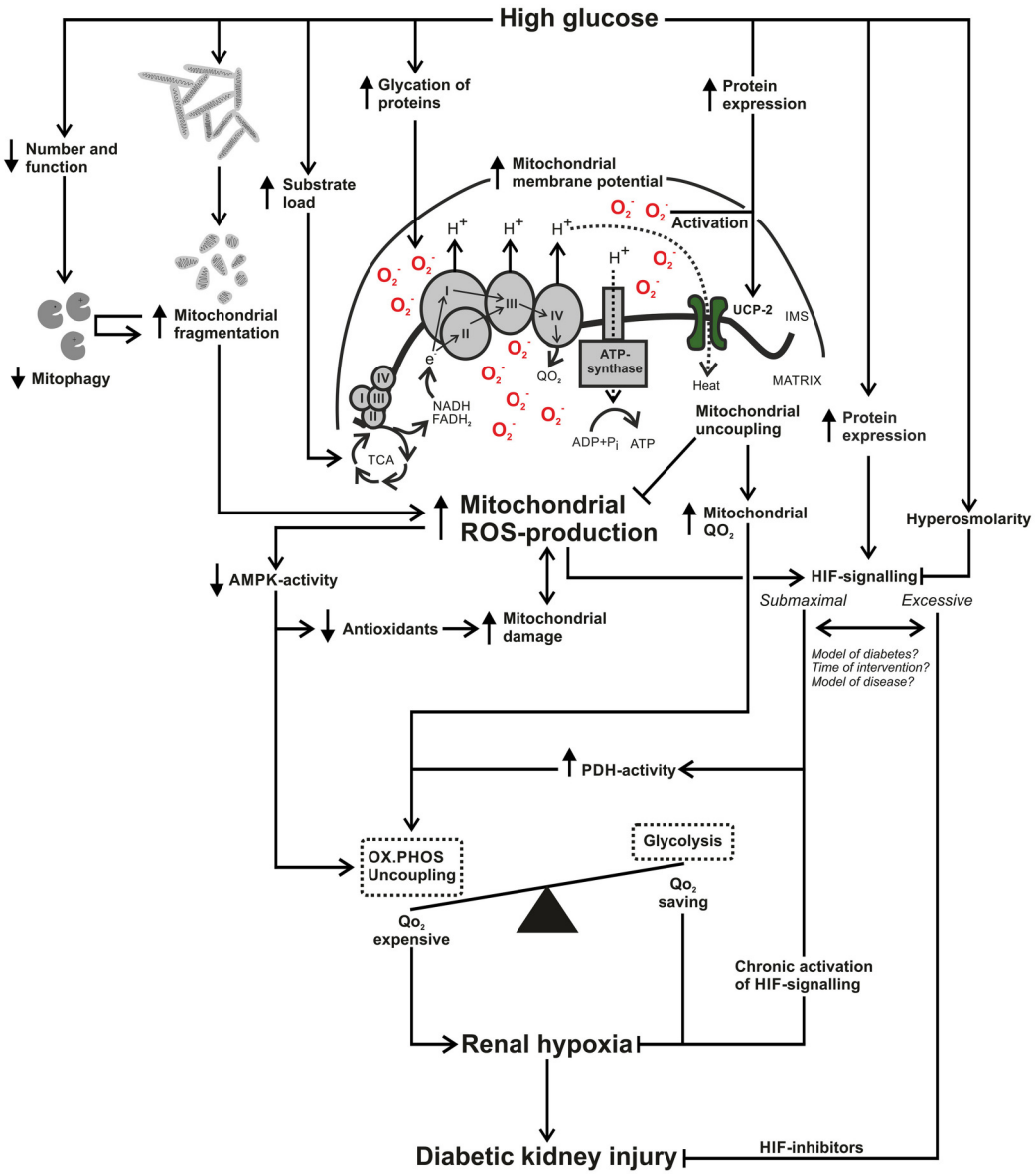


**FIGURE 2 | Schematic summary of how increased mitochondrial reactive oxygen species (ROS) production connects to renal hypoxia and diabetic kidney injury.** High glucose results in increased mitochondrial ROS-production through glycation and damage of electron transporting complexes and an increased load of electron donating substrates, resulting in an increased mitochondrial membrane potential. High glucose results in mitochondrial fragmentation and due to glucose-induced alterations in mitophagy there may be an accumulation of damaged and fragmented kidney mitochondria in diabetes. Mitochondrial ROS-production can reduce activation of 5′ AMP-activated protein kinase (AMPK), resulting in decreased antioxidant systems, creating a circle that contributes to mitochondrial damage and perhaps further enhanced ROS-production. Decreased AMPK-activity will also fail to divert oxygen consumption ($QO_2$)-expensive pathways such as oxidative phosphorylation to $QO_2$-saving pathways such as glycolysis. High glucose and increased mitochondrial ROS production will increase expression and activation of uncoupling protein-2. The process of mitochondrial uncoupling will reduce mitochondrial membrane potential and ROS production but will concomitantly increase mitochondrial $QO_2$. High glucose can increase hypoxia inducible factor (HIF)-1α expression and mitochondrial ROS-production contributes to HIF activation. Hyperosmolarity can interfere with HIF signaling and chronic activation of HIF can prevent renal hypoxia. On the other hand, various inhibitors of HIF attenuates renal injury, raising the issue whether kidney HIF signaling is submaximal or excessive in diabetes. Differences in study results may involve methodological setup in terms of model of diabetes or other kidney disease but also the time point of intervention. In summary, increased mitochondrial ROS-production affects pathways in manners that can contribute to increased kidney $QO_2$ and may therefore be an important mechanism in the development of kidney hypoxia and diabetic kidney injury. AMPK, AMP-activated protein kinase; FAD, flavin adenine dinucleotide; $H^+$, proton; HIF, hypoxia inducible factor; IMS, intermembrane space; NAD, nicotinamide adenine dinucleotide; $O_2^{\cdot-}$, superoxide ion; OX.PHOS, oxidative phosphorylation; PDH, pyruvate dehydrogenase; TCA, tricarboxylic acid cycle; ROS, reactive oxygen species; UCP, uncoupling protein; $QO_2$, oxygen consumption.

before being encapsulated within autophagic vesicles (Twig et al., 2008). Dysfunctional mitochondria that have lost their membrane potential are tagged for mitophagy clearance via the PTEN-induced putative kinase (Matsuda et al., 2010; Vives-Bauza et al., 2010), a serine/threonine-protein kinase located on the mitochondrial outer membrane. PTEN-induced putative kinase is a docking protein for parkin, a key protein to direct damaged mitochondria for engulfment by autophagosomes (Matsuda et al., 2010; Narendra et al., 2010; Vives-Bauza et al., 2010; Lazarou et al., 2013).

The observed accumulation of damaged mitochondria in the kidney in diabetes indicates impairment in the mitophagy system (Kimura et al., 2011; Liu et al., 2012; Takahashi et al., 2012) and autophagy has previously been linked to the pathogenesis of diabetic nephropathy, acute kidney injury and polycystic kidney disease (Huber et al., 2012). Sequestosome 1 (P62/SQSTM1) is an autophagy marker that correlates inversely to autophagic flux (Vallon et al., 2013). In a rat type 2 diabetes model, p62/SQSTM1 was increased (Kitada et al., 2011) and reduced levels of autophagy markers were observed in mouse glomerular lysates 28 days after streptozotocin injection (Fang et al., 2013). Decreased staining of the autophagy marker, LC3-phosphatidylethanolamine conjugate (LC3-II) was also observed in podocytes from human biopsies obtained from patients with diabetes (Fang et al., 2013). Thioredoxin interacting protein, another mitophagy regulator, is upregulated and results in increased ROS production, inflammation and fibrosis in the diabetic kidney (Devi et al., 2012; Mahmood et al., 2013).

Cellular homeostasis is dependent on a dynamic balance between fission and fusion and it is clear that in mitochondrial dynamics and mitophagy is affected in the diabetic kidneys. Many reports relate this to mitochondrial ROS production that will in turn affect pathways related to kidney hypoxia such as AMPK-signaling, HIF-activity and mitochondrial uncoupling. Interestingly, Galloway and colleagues showed that inhibiting mitochondrial fission in hepatocytes overexpressing dynamin like protein (DLP-1) caused increased proton leak with a functionally intact electron transport chain (Galloway et al., 2012). Whether pharmacological blockade of mitochondrial fission is beneficial in diabetic nephropathy is currently unclear and it should be cautioned that chronic disruption of fission might eventually induce mitochondrial dysfunction via uncoupling, accumulation of damaged mitochondria, and cell injury.

## SUMMARY AND CONCLUSIONS

The development of diabetic nephropathy is likely to represent a series of dynamic events. Many studies report altered mitochondrial function in the diabetic kidney. These alterations include altered mitophagy, mitochondrial dynamics, mitochondrial uncoupling, and signaling through AMPK and HIF. Herein, we have discussed how these pathways may relate to mitochondrial ROS production in the diabetic kidney. In experimental models, correcting mitochondrial ROS production reduces albuminuria in diabetic mice (Sourris et al., 2012) and preventing ROS induced mitochondrial leak-respiration improves kidney function (Persson et al., 2012). However, a recent phase 3 study where the nuclear respiratory factor 2-inducer bardoxolone methyl was used for targeting diabetic nephropathy failed to improve the outcome of end-stage renal disease or cardiovascular mortality. Instead, increased albuminuria, heart-failure, and hypertension in patients with advanced diabetic nephropathy contributed to early termination of the study (de Zeeuw et al., 2013).

Many of the discussed factors are intertwined in a complex manner, making it very difficult to highlight a specific mechanism in the diabetic kidney. Partly underlying the difficulty of highlighting a specific mechanism is the functional heterogeneity of the kidney. Different segments have different function and surrounding oxygen levels, different levels of the discussed cellular pathways and different sources and levels of ROS production. However, from available literature it seems clear that mitochondrial ROS production may be a joint mechanism. The resulting effects on mitochondrial and cellular pathways affecting oxygen metabolism may play an important role in the development of diabetic nephropathy. For a schematic summary, see **Figure 2**. The correction and/or prevention of mitochondrial dysfunction may be pivotal in the prevention and treatment of diabetic nephropathy.

## AUTHOR CONTRIBUTIONS

TS and MFP both wrote manuscript, viewed the content critically and approved the final submitted version.

## FUNDING

MFP is supported by the Wenner-Gren Foundations.

## REFERENCES

Al-Kafaji, G., and Golbahar, J. (2013). High glucose-induced oxidative stress increases the copy number of mitochondrial DNA in human mesangial cells. *Biomed Res. Int.* 2013:754946. doi: 10.1155/2013/754946

Arsenijevic, D., Onuma, H., Pecqueur, C., Raimbault, S., Manning, B. S., Miroux, B., et al. (2000). Disruption of the uncoupling protein-2 gene in mice reveals a role in immunity and reactive oxygen species production. *Nat. Genet.* 26, 435–439. doi: 10.1038/82565

Brito, P. L., Fioretto, P., Drummond, K., Kim, Y., Steffes, M. W., Basgen, J. M., et al. (1998). Proximal tubular basement membrane width in insulin-dependent diabetes mellitus. *Kidney Int.* 53, 754–761. doi: 10.1046/j.1523-1755.1998.00809.x

Broedbaek, K., Weimann, A., Stovgaard, E. S., and Poulsen, H. E. (2011). Urinary 8-oxo-7,8-dihydro-2′-deoxyguanosine as a biomarker in type 2 diabetes. *Free Radic. Biol. Med.* 51, 1473–1479. doi: 10.1016/j.freeradbiomed.2011.07.007

Brooks, C., Wei, Q., Cho, S. G., and Dong, Z. (2009). Regulation of mitochondrial dynamics in acute kidney injury in cell culture and rodent models. *J. Clin. Invest.* 119, 1275–1285. doi: 10.1172/JCI37829

Brunelle, J. K., Bell, E. L., Quesada, N. M., Vercauteren, K., Tiranti, V., Zeviani, M., et al. (2005). Oxygen sensing requires mitochondrial ROS but not oxidative phosphorylation. *Cell Metab.* 1, 409–414. doi: 10.1016/j.cmet.2005.05.002

Catrina, S. B., Okamoto, K., Pereira, T., Brismar, K., and Poellinger, L. (2004). Hyperglycemia regulates hypoxia-inducible factor-1α protein stability and function. *Diabetes* 53, 3226–3232. doi: 10.2337/diabetes.53.12.3226

Chacko, B. K., Reily, C., Srivastava, A., Johnson, M. S., Ye, Y., Ulasova, E., et al. (2010). Prevention of diabetic nephropathy in $Ins2^{+/-AkitaJ}$ mice by the mitochondria-targeted therapy MitoQ. *Biochem. J.* 432, 9–19. doi: 10.1042/BJ20100308

Chan, D. C. (2006). Mitochondrial fusion and fission in mammals. *Annu. Rev. Cell Dev. Biol.* 22, 79–99. doi: 10.1146/annurev.cellbio.22.010305.104638

Chen, S., and Sang, N. (2016). Hypoxia-inducible factor-1: a critical player in the survival strategy of stressed cells. *J. Cell. Biochem.* 117, 267–278. doi: 10.1002/jcb.25283

Conway, E. M., Collen, D., and Carmeliet, P. (2001). Molecular mechanisms of blood vessel growth. *Cardiovasc. Res.* 49, 507–521. doi: 10.1016/S0008-6363(00)00281-9

Coughlan, M. T., Thorburn, D. R., Penfold, S. A., Laskowski, A., Harcourt, B. E., Sourris, K. C., et al. (2009). RAGE-induced cytosolic ROS promote mitochondrial superoxide generation in diabetes. *J. Am. Soc. Nephrol.* 20, 742–752. doi: 10.1681/ASN.2008050514

Cowley, A. W. Jr., Abe, M., Mori, T., O'Connor, P. M., Ohsaki, Y., and Zheleznova, N. N. (2015). Reactive oxygen species as important determinants of medullary flow, sodium excretion, and hypertension. *Am. J. Physiol. Renal Physiol.* 308, F179–F197. doi: 10.1152/ajprenal.00455.2014

de Zeeuw, D., Akizawa, T., Audhya, P., Bakris, G. L., Chin, M., Christ-Schmidt, H., et al. (2013). Bardoxolone methyl in type 2 diabetes and stage 4 chronic kidney disease. *N.Engl. J. Med.* 369, 2492–2503. doi: 10.1056/NEJMoa1306033

Devi, T. S., Lee, I., Hüttemann, M., Kumar, A., Nantwi, K. D., and Singh, L. P. (2012). TXNIP links innate host defense mechanisms to oxidative stress and inflammation in retinal Muller glia under chronic hyperglycemia: implications for diabetic retinopathy. *Exp. Diabetes Res.* 2012:438238. doi: 10.1155/2012/438238

Dickman, K. G., and Mandel, L. J. (1990). Differential effects of respiratory inhibitors on glycolysis in proximal tubules. *Am. J. Physiol.* 258(6 Pt 2), F1608–F1615.

Dromparis, P., Paulin, R., Sutendra, G., Qi, A. C., Bonnet, S., and Michelakis, E. D. (2013). Uncoupling protein 2 deficiency mimics the effects of hypoxia and endoplasmic reticulum stress on mitochondria and triggers pseudohypoxic pulmonary vascular remodeling and pulmonary hypertension. *Circ. Res.* 113, 126–136. doi: 10.1161/CIRCRESAHA.112.300699

Dugan, L. L., You, Y. H., Ali, S. S., Diamond-Stanic, M., Miyamoto, S., DeCleves, A. E., et al. (2013). AMPK dysregulation promotes diabetes-related reduction of superoxide and mitochondrial function. *J. Clin. Invest.* 123, 4888–4899. doi: 10.1172/JCI66218

Duval, C., Nègre-Salvayre, A., Dogilo, A., Salvayre, R., Pénicaud, L., and Casteilla, L. (2002). Increased reactive oxygen species production with antisense oligonucleotides directed against uncoupling protein 2 in murine endothelial cells. *Biochem. Cell Biol.* 80, 757–764. doi: 10.1139/o02-158

Echtay, K. S., Esteves, T. C., Pakay, J. L., Jekabsons, M. B., Lambert, A. J., Portero-Otín, M., et al. (2003). A signalling role for 4-hydroxy-2-nonenal in regulation of mitochondrial uncoupling. *EMBO J.* 22, 4103–4110. doi: 10.1093/emboj/cdg412

Echtay, K. S., Roussel, D., St-Pierre, J., Jekabsons, M. B., Cadenas, S., Stuart, J. A., et al. (2002). Superoxide activates mitochondrial uncoupling proteins. *Nature* 415, 96–99. doi: 10.1038/415096a

Echtay, K. S., Winkler, E., Frischmuth, K., and Klingenberg, M. (2001). Uncoupling proteins 2 and 3 are highly active $H^+$ transporters and highly nucleotide sensitive when activated by coenzyme Q (ubiquinone). *Proc. Natl. Acad. Sci. U.S.A.* 98, 1416–1421. doi: 10.1073/pnas.98.4.1416

Edlund, J., Hansell, P., Fasching, A., Liss, P., Weis, J., Glickson, J. D., et al. (2009). Reduced oxygenation in diabetic rat kidneys measured by T2∗ weighted magnetic resonance micro-imaging. *Adv. Exp. Med. Biol.* 645, 199–204. doi: 10.1007/978-0-387-85998-9_31

Emerling, B. M., Platanias, L. C., Black, E., Nebreda, A. R., Davis, R. J., and Chandel, N. S. (2005). Mitochondrial reactive oxygen species activation of p38 mitogen-activated protein kinase is required for hypoxia signaling. *Mol. Cell. Biol.* 25, 4853–4862. doi: 10.1128/MCB.25.12.4853-4862.2005

Emerling, B. M., Weinberg, F., Snyder, C., Burgess, Z., Mutlu, G. M., Viollet, B., et al. (2009). Hypoxic activation of AMPK is dependent on mitochondrial ROS but independent of an increase in AMP/ATP ratio. *Free Radic. Biol. Med.* 46, 1386–1391. doi: 10.1016/j.freeradbiomed.2009.02.019

Epstein, F. H., Agmon, Y., and Brezis, M. (1994). Physiology of renal hypoxia. *Ann. N.Y Acad. Sci.* 718, 72–81. discussion 81–72.

Fang, L., Zhou, Y., Cao, H., Wen, P., Jiang, L., He, W., et al. (2013). Autophagy attenuates diabetic glomerular damage through protection of hyperglycemia-induced podocyte injury. *PLoS ONE* 8:e60546. doi: 10.1371/journal.pone.0060546

Fernandez-Marcos, P. J., and Auwerx, J. (2011). Regulation of PGC-1α, a nodal regulator of mitochondrial biogenesis. *Am. J. Clin. Nutr.* 93, 884S–890S. doi: 10.3945/ajcn.110.001917

Fine, L. G., Orphanides, C., and Norman, J. T. (1998). Progressive renal disease: the chronic hypoxia hypothesis. *Kidney Int. Suppl.* 65, S74–S78.

Finley, L. W., Carracedo, A., Lee, J., Souza, A., Egia, A., Zhang, J., et al. (2011). SIRT3 opposes reprogramming of cancer cell metabolism through HIF1α destabilization. *Cancer Cell* 19, 416–428. doi: 10.1016/j.ccr.2011.02.014

Fleury, C., Neverova, M., Collins, S., Raimbault, S., Champigny, O., Levi-Meyrueis, C., et al. (1997). Uncoupling protein-2: a novel gene linked to obesity and hyperinsulinemia. *Nat. Genet.* 15, 269–272. doi: 10.1038/ng0397-269

Forbes, J. M., Coughlan, M. T., and Cooper, M. E. (2008). Oxidative stress as a major culprit in kidney disease in diabetes. *Diabetes* 57, 1446–1454. doi: 10.2337/db08-0057

Friederich, M., Fasching, A., Hansell, P., Nordquist, L., and Palm, F. (2008). Diabetes-induced up-regulation of uncoupling protein-2 results in increased mitochondrial uncoupling in kidney proximal tubular cells. *Biochim. Biophys. Acta* 1777, 935–940. doi: 10.1016/j.bbabio.2008.03.030

Friederich, M., Nordquist, L., Olerud, J., Johansson, M., Hansell, P., and Palm, F. (2009). Identification and distribution of uncoupling protein isoforms in the normal and diabetic rat kidney. *Adv. Exp. Med. Biol.* 645, 205–212. doi: 10.1007/978-0-387-85998-9_32

Friederich-Persson, M., Aslam, S., Nordquist, L., Welch, W. J., Wilcox, C. S., and Palm, F. (2012). Acute knockdown of uncoupling protein-2 increases uncoupling via the adenine nucleotide transporter and decreases oxidative stress in diabetic kidneys. *PLoS ONE* 7:e39635. doi: 10.1371/journal.pone.0039635

Friederich-Persson, M., Thörn, E., Hansell, P., Nangaku, M., Levin, M., and Palm, F. (2013). Kidney hypoxia, attributable to increased oxygen consumption, induces nephropathy independently of hyperglycemia and oxidative stress. *Hypertension* 62, 914–919. doi: 10.1161/HYPERTENSIONAHA.113.01425

Galloway, C. A., Lee, H., Nejjar, S., Jhun, B. S., Yu, T., Hsu, W., et al. (2012). Transgenic control of mitochondrial fission induces mitochondrial uncoupling and relieves diabetic oxidative stress. *Diabetes* 61, 2093–2104. doi: 10.2337/db11-1640

Garvin, J. L., and Hong, N. J. (2008). Cellular stretch increases superoxide production in the thick ascending limb. *Hypertension* 51, 488–493. doi: 10.1161/HYPERTENSIONAHA.107.102228

Guder, W. G., and Ross, B. D. (1984). Enzyme distribution along the nephron. *Kidney Int.* 26, 101–111. doi: 10.1038/ki.1984.143

Gullans, S. R., Brazy, P. C., Soltoff, S. P., Dennis, V. W., and Mandel, L. J. (1982). Metabolic inhibitors: effects on metabolism and transport in the proximal tubule. *Am. J. Physiol.* 243, F133–F140.

Haase, V. H. (2015). A breath of fresh air for diabetic nephropathy. *J. Am. Soc. Nephrol.* 26, 239–241. doi: 10.1681/ASN.2014080754

Haidara, M. A., Mikhailidis, D. P., Rateb, M. A., Ahmed, Z. A., Yassin, H. Z., Ibrahim, I. M., et al. (2009). Evaluation of the effect of oxidative stress and vitamin E supplementation on renal function in rats with streptozotocin-induced Type 1 diabetes. *J. Diabetes Complicat.* 23, 130–136. doi: 10.1016/j.jdiacomp.2008.02.011

Hall, A. M., Unwin, R. J., Parker, N., and Duchen, M. R. (2009). Multiphoton imaging reveals differences in mitochondrial function between nephron segments. *J. Am. Soc. Nephrol.* 20, 1293–1302. doi: 10.1681/ASN.2008070759

Halliwell, B., and Whiteman, M. (2004). Measuring reactive species and oxidative damage *in vivo* and in cell culture: how should you do it and what do the results mean? *Br. J. Pharmacol.* 142, 231–255. doi: 10.1038/sj.bjp.0705776

Hardie, D. G. (2015). AMPK: positive and negative regulation, and its role in whole-body energy homeostasis. *Curr. Opin. Cell Biol.* 33, 1–7. doi: 10.1016/j.ceb.2014.09.004

Hardie, D. G., Ross, F. A., and Hawley, S. A. (2012). AMPK: a nutrient and energy sensor that maintains energy homeostasis. *Nat. Rev. Mol. Cell Biol.* 13, 251–262. doi: 10.1038/nrm3311

Hardie, D. G., Scott, J. W., Pan, D. A., and Hudson, E. R. (2003). Management of cellular energy by the AMP-activated protein kinase system. *FEBS Lett.* 546, 113–120. doi: 10.1016/S0014-5793(03)00560-X

Hasslacher, C., Ritz, E., Wahl, P., and Michael, C. (1989). Similar risks of nephropathy in patients with type I or type II diabetes mellitus. *Nephrol. Dial. Transplant* 4, 859–863. doi: 10.1093/ndt/4.10.859

Hawley, S. A., Boudeau, J., Reid, J. L., Mustard, K. J., Udd, L., Makela, T. P., et al. (2003). Complexes between the LKB1 tumor suppressor, STRAD α/β and MO25 α/β are upstream kinases in the AMP-activated protein kinase cascade. *J. Biol.* 2:28. doi: 10.1186/1475-4924-2-28

Higgins, D. F., Kimura, K., Bernhardt, W. M., Shrimanker, N., Akai, Y., Hohenstein, B., et al. (2007). Hypoxia promotes fibrogenesis *in vivo* via HIF-1 stimulation of epithelial-to-mesenchymal transition. *J. Clin. Invest.* 117, 3810–3820. doi: 10.1172/jci30487

Hochman, M. E., Watt, J. P., Reid, R., and O'Brien, K. L. (2007). The prevalence and incidence of end-stage renal disease in Native American adults on the Navajo reservation. *Kidney Int.* 71, 931–937. doi: 10.1038/sj.ki.5002100

Hubbi, M. E., Hu, H., Kshitiz, Gilkes, D. M., and Semenza, G. L. (2013). Sirtuin-7 inhibits the activity of hypoxia-inducible factors. *J. Biol. Chem.* 288, 20768–20775. doi: 10.1074/jbc.M113.476903

Huber, T. B., Edelstein, C. L., Hartleben, B., Inoki, K., Jiang, M., Koya, D., et al. (2012). Emerging role of autophagy in kidney function, diseases and aging. *Autophagy* 8, 1009–1031. doi: 10.4161/auto.19821

Inoue, T., Kozawa, E., Okada, H., Inukai, K., Watanabe, S., Kikuta, T., et al. (2011). Noninvasive evaluation of kidney hypoxia and fibrosis using magnetic resonance imaging. *J. Am. Soc. Nephrol.* 22, 1429–1434. doi: 10.1681/ASN.2010111143

Irwin, D. C., McCord, J. M., Nozik-Grayck, E., Beckly, G., Foreman, B., Sullivan, T., et al. (2009). A potential role for reactive oxygen species and the HIF-1α-VEGF pathway in hypoxia-induced pulmonary vascular leak. *Free Radic. Biol. Med.* 47, 55–61. doi: 10.1016/j.freeradbiomed.2009.03.027

Jaburek, M., Varecha, M., Gimeno, R. E., Dembski, M., Jezek, P., Zhang, M., et al. (1999). Transport function and regulation of mitochondrial uncoupling proteins 2 and 3. *J. Biol. Chem.* 274, 26003–26007. doi: 10.1074/jbc.274.37.26003

Jezek, P., Zackova, M., Rehakova, Z., Ruzicka, M., Borecky, J., Skobisova, E., et al. (1999). Existence of uncoupling protein-2 antigen in isolated mitochondria from various tissues. *FEBS Lett.* 455, 79–82. doi: 10.1016/S0014-5793(99)00853-4

Katz, A., Caramori, M. L., Sisson-Ross, S., Groppoli, T., Basgen, J. M., and Mauer, M. (2002). An increase in the cell component of the cortical interstitium antedates interstitial fibrosis in type 1 diabetic patients. *Kidney Int.* 61, 2058–2066. doi: 10.1046/j.1523-1755.2002.00370.x

Kimura, K., Iwano, M., Higgins, D. F., Yamaguchi, Y., Nakatani, K., Harada, K., et al. (2008). Stable expression of HIF-1α in tubular epithelial cells promotes interstitial fibrosis. *Am. J. Physiol. Renal Physiol.* 295, F1023–F1029. doi: 10.1152/ajprenal.90209.2008

Kimura, T., Takabatake, Y., Takahashi, A., Kaimori, J. Y., Matsui, I., Namba, T., et al. (2011). Autophagy protects the proximal tubule from degeneration and acute ischemic injury. *J. Am. Soc. Nephrol.* 22, 902–913. doi: 10.1681/ASN.2010070705

Kitada, M., Takeda, A., Nagai, T., Ito, H., Kanasaki, K., and Koya, D. (2011). Dietary restriction ameliorates diabetic nephropathy through anti-inflammatory effects and regulation of the autophagy via restoration of Sirt1 in diabetic Wistar fatty (fa/fa) rats: a model of type 2 diabetes. *Exp. Diabetes Res.* 2011:908185. doi: 10.1155/2011/908185

Kops, G. J., Dansen, T. B., Polderman, P. E., Saarloos, I., Wirtz, K. W., Coffer, P. J., et al. (2002). Forkhead transcription factor FOXO3a protects quiescent cells from oxidative stress. *Nature* 419, 316–321. doi: 10.1038/nature01036

Korner, A., Eklof, A. C., Celsi, G., and Aperia, A. (1994). Increased renal metabolism in diabetes. Mechanism and functional implications. *Diabetes* 43, 629–633.

Korshunov, S. S., Skulachev, V. P., and Starkov, A. A. (1997). High protonic potential actuates a mechanism of production of reactive oxygen species in mitochondria. *FEBS Lett.* 416, 15–18. doi: 10.1016/S0014-5793(97)01159-9

Krauss, S., Zhang, C. Y., Scorrano, L., Dalgaard, L. T., St-Pierre, J., Grey, S. T., et al. (2003). Superoxide-mediated activation of uncoupling protein 2 causes pancreatic β cell dysfunction. *J. Clin. Invest.* 112, 1831–1842. doi: 10.1172/JCI200319774

Kukidome, D., Nishikawa, T., Sonoda, K., Imoto, K., Fujisawa, K., Yano, M., et al. (2006). Activation of AMP-activated protein kinase reduces hyperglycemia-induced mitochondrial reactive oxygen species production and promotes mitochondrial biogenesis in human umbilical vein endothelial cells. *Diabetes* 55, 120–127. doi: 10.2337/diabetes.55.01.06.db05-0943

Kushnareva, Y., Murphy, A. N., and Andreyev, A. (2002). Complex I-mediated reactive oxygen species generation: modulation by cytochrome c and $NAD^{P+}$ oxidation-reduction state. *Biochem. J.* 368(Pt 2), 545–553. doi: 10.1042/bj20021121

Lambert, A. J., and Brand, M. D. (2004). Superoxide production by NADH:ubiquinone oxidoreductase (complex I) depends on the pH gradient across the mitochondrial inner membrane. *Biochem J.* 382(Pt 2), 511–517. doi: 10.1042/BJ20040485

Lazarou, M., Narendra, D. P., Jin, S. M., Tekle, E., Banerjee, S., and Youle, R. J. (2013). PINK1 drives Parkin self-association and HECT-like E3 activity upstream of mitochondrial binding. *J. Cell Biol.* 200, 163–172. doi: 10.1083/jcb.201210111

Lemasters, J. J. (2005). Selective mitochondrial autophagy, or mitophagy, as a targeted defense against oxidative stress, mitochondrial dysfunction, and aging. *Rejuvenation Res.* 8, 3–5. doi: 10.1089/rej.2005.8.3

Li, N., Yi, F. X., Spurrier, J. L., Bobrowitz, C. A., and Zou, A. P. (2002). Production of superoxide through NADH oxidase in thick ascending limb of Henle's loop in rat kidney. *Am. J. Physiol. Renal Physiol.* 282, F1111–F1119. doi: 10.1152/ajprenal.00218.2001

Liesa, M., Palacin, M., and Zorzano, A. (2009). Mitochondrial dynamics in mammalian health and disease. *Physiol. Rev.* 89, 799–845. doi: 10.1152/physrev.00030.2008

Lim, J. H., Lee, Y. M., Chun, Y. S., Chen, J., Kim, J. E., and Park, J. W. (2010). Sirtuin 1 modulates cellular responses to hypoxia by deacetylating hypoxia-inducible factor 1α. *Mol. Cell* 38, 864–878. doi: 10.1016/j.molcel.2010.05.023

Liu, S., Hartleben, B., Kretz, O., Wiech, T., Igarashi, P., Mizushima, N., et al. (2012). Autophagy plays a critical role in kidney tubule maintenance, aging and ischemia-reperfusion injury. *Autophagy* 8, 826–837. doi: 10.4161/auto.19419

Loenarz, C., Coleman, M. L., Boleininger, A., Schierwater, B., Holland, P. W., Ratcliffe, P. J., et al. (2011). The hypoxia-inducible transcription factor pathway regulates oxygen sensing in the simplest animal, Trichoplax adhaerens. *EMBO Rep.* 12, 63–70. doi: 10.1038/embor.2010.170

Mahmood, D. F., Abderrazak, A., El Hadri, K., Simmet, T., and Rouis, M. (2013). The thioredoxin system as a therapeutic target in human health and disease. *Antioxid. Redox Signal.* 19, 1266–1303. doi: 10.1089/ars.2012.4757

Martins, R., Lithgow, G. J., and Link, W. (2016). Long live FOXO: unraveling the role of FOXO proteins in aging and longevity. *Aging Cell* 15, 196–207. doi: 10.1111/acel.12427

Matsuda, N., Sato, S., Shiba, K., Okatsu, K., Saisho, K., Gautier, C. A., et al. (2010). PINK1 stabilized by mitochondrial depolarization recruits Parkin to damaged mitochondria and activates latent Parkin for mitophagy. *J. Cell Biol.* 189, 211–221. doi: 10.1083/jcb.200910140

Mattiasson, G., Shamloo, M., Gido, G., Mathi, K., Tomasevic, G., Yi, S., et al. (2003). Uncoupling protein-2 prevents neuronal death and diminishes brain dysfunction after stroke and brain trauma. *Nat. Med.* 9, 1062–1068. doi: 10.1038/nm903

Mauer, M., and Drummond, K. (2002). The early natural history of nephropathy in type 1 diabetes: I. study design and baseline characteristics of the study participants. *Diabetes* 51, 1572–1579. doi: 10.2337/diabetes.51.5.1572

Mauer, S. M., Steffes, M. W., Ellis, E. N., Sutherland, D. E., Brown, D. M., and Goetz, F. C. (1984). Structural-functional relationships in diabetic nephropathy. *J. Clin. Invest.* 74, 1143–1155. doi: 10.1172/JCI111523

McCullough, P. A., Jurkovitz, C. T., Pergola, P. E., McGill, J. B., Brown, W. W., Collins, A. J., et al. (2007). Independent components of chronic kidney disease as a cardiovascular risk state: results from the Kidney Early Evaluation Program (KEEP). *Arch. Intern. Med.* 167, 1122–1129. doi: 10.1001/archinte.167.11.1122

Mimura, I., and Nangaku, M. (2010). The suffocating kidney: tubulointerstitial hypoxia in end-stage renal disease. *Nat. Rev. Nephrol.* 6, 667–678. doi: 10.1038/nrneph.2010.124

Minokoshi, Y., Alquier, T., Furukawa, N., Kim, Y. B., Lee, A., Xue, B., et al. (2004). AMP-kinase regulates food intake by responding to hormonal and nutrient signals in the hypothalamus. *Nature* 428, 569–574. doi: 10.1038/nature02440

Miwa, S., and Brand, M. D. (2003). Mitochondrial matrix reactive oxygen species production is very sensitive to mild uncoupling. *Biochem. Soc. Trans.* 31(Pt 6), 1300–1301. doi: 10.1042/bst0311300

Morales, A. I., Detaille, D., Prieto, M., Puente, A., Briones, E., Arevalo, M., et al. (2010). Metformin prevents experimental gentamicin-induced nephropathy by a mitochondria-dependent pathway. *Kidney Int.* 77, 861–869. doi: 10.1038/ki.2010.11

Mungai, P. T., Waypa, G. B., Jairaman, A., Prakriya, M., Dokic, D., Ball, M. K., et al. (2011). Hypoxia triggers AMPK activation through reactive oxygen species-mediated activation of calcium release-activated calcium channels. *Mol. Cell. Biol.* 31, 3531–3545. doi: 10.1128/MCB.05124-11

Munusamy, S., and MacMillan-Crow, L. A. (2009). Mitochondrial superoxide plays a crucial role in the development of mitochondrial dysfunction during high glucose exposure in rat renal proximal tubular cells. *Free Radic. Biol. Med.* 46, 1149–1157. doi: 10.1016/j.freeradbiomed.2009.01.022

Nagao, M., Sugaru, E., Kambe, T., and Sasaki, R. (1999). Unidirectional transport from apical to basolateral compartment of cobalt ion in polarized Madin-Darby canine kidney cells. *Biochem. Biophys. Res. Commun.* 257, 289–294. doi: 10.1006/bbrc.1999.0446

Nangaku, M. (2006). Chronic hypoxia and tubulointerstitial injury: a final common pathway to end-stage renal failure. *J. Am. Soc. Nephrol.* 17, 17–25. doi: 10.1681/ASN.2005070757

Narendra, D. P., Jin, S. M., Tanaka, A., Suen, D. F., Gautier, C. A., Shen, J., et al. (2010). PINK1 is selectively stabilized on impaired mitochondria to activate Parkin. *PLoS Biol.* 8:e1000298. doi: 10.1371/journal.pbio.1000298

Nayak, B. K., Shanmugasundaram, K., Friedrichs, W. E., Cavaglierii, R. C., Patel, M., Barnes, J., et al. (2016). HIF-1 mediates renal fibrosis in OVE26 type 1 diabetic mice. *Diabetes* 65, 1387–1397. doi: 10.2337/db15-0519

Nicholls, D. G. (1976). Hamster brown-adipose-tissue mitochondria. Purine nucleotide control of the ion conductance of the inner membrane, the nature of the nucleotide binding site. *Eur. J. Biochem.* 62, 223–228.

Niecknig, H., Tug, S., Reyes, B. D., Kirsch, M., Fandrey, J., and Berchner-Pfannschmidt, U. (2012). Role of reactive oxygen species in the regulation of HIF-1 by prolyl hydroxylase 2 under mild hypoxia. *Free Radic. Res.* 46, 705–717. doi: 10.3109/10715762.2012.669041

Nishikawa, T., Brownlee, M., and Araki, E. (2015). Mitochondrial reactive oxygen species in the pathogenesis of early diabetic nephropathy. *J. Diabetes Investig.* 6, 137–139. doi: 10.1111/jdi.12258

Nishikawa, T., Edelstein, D., Du, X. L., Yamagishi, S., Matsumura, T., Kaneda, Y., et al. (2000). Normalizing mitochondrial superoxide production blocks three pathways of hyperglycaemic damage. *Nature* 404, 787–790. doi: 10.1038/35008121

Nordquist, L., Friederich-Persson, M., Fasching, A., Liss, P., Shoji, K., Nangaku, M., et al. (2015). Activation of hypoxia-inducible factors prevents diabetic nephropathy. *J. Am. Soc. Nephrol.* 26, 328–338. doi: 10.1681/ASN.2013090990

Ohtomo, S., Nangaku, M., Izuhara, Y., Takizawa, S., Strihou, C. Y., and Miyata, T. (2008). Cobalt ameliorates renal injury in an obese, hypertensive type 2 diabetes rat model. *Nephrol. Dial. Transplant.* 23, 1166–1172. doi: 10.1093/ndt/gfm715

Palm, F., and Nordquist, L. (2011). Renal tubulointerstitial hypoxia: cause and consequence of kidney dysfunction. *Clin. Exp. Pharmacol. Physiol.* 38, 474–480. doi: 10.1111/j.1440-1681.2011.05532.x

Palm, F., Cederberg, J., Hansell, P., Liss, P., and Carlsson, P. O. (2003). Reactive oxygen species cause diabetes-induced decrease in renal oxygen tension. *Diabetologia* 46, 1153–1160. doi: 10.1007/s00125-003-1155-z

Pawlikowska, P., Gajkowska, B., and Orzechowski, A. (2007). Mitofusin 2 (Mfn2): a key player in insulin-dependent myogenesis *in vitro*. *Cell Tissue Res.* 327, 571–581. doi: 10.1007/s00441-006-0320-3

Persson, M. F., Franzen, S., Catrina, S. B., Dallner, G., Hansell, P., Brismar, K., et al. (2012). Coenzyme Q10 prevents GDP-sensitive mitochondrial uncoupling, glomerular hyperfiltration and proteinuria in kidneys from db/db mice as a model of type 2 diabetes. *Diabetologia* 55, 1535–1543. doi: 10.1007/s00125-012-2469-5

Quijano, C., Castro, L., Peluffo, G., Valez, V., and Radi, R. (2007). Enhanced mitochondrial superoxide in hyperglycemic endothelial cells: direct measurements and formation of hydrogen peroxide and peroxynitrite. *Am. J. Physiol. Heart Circ. Physiol.* 293, H3404–H3414. doi: 10.1152/ajpheart.00761.2007

Raza, H., Prabu, S. K., Robin, M. A., and Avadhani, N. G. (2004). Elevated mitochondrial cytochrome P450 2E1 and glutathione S-transferase A4-4 in streptozotocin-induced diabetic rats: tissue-specific variations and roles in oxidative stress. *Diabetes* 53, 185–194. doi: 10.2337/diabetes.53.1.185

Ries, M., Basseau, F., Tyndal, B., Jones, R., Deminiere, C., Catargi, B., et al. (2003). Renal diffusion and BOLD MRI in experimental diabetic nephropathy. Blood oxygen level-dependent. *J. Magn. Reson. Imaging* 17, 104–113. doi: 10.1002/jmri.10224

Rosca, M. G., Mustata, T. G., Kinter, M. T., Ozdemir, A. M., Kern, T. S., Szweda, L. I., et al. (2005). Glycation of mitochondrial proteins from diabetic rat kidney is associated with excess superoxide formation. *Am. J. Physiol. Renal Physiol.* 289, F420–F430. doi: 10.1152/ajprenal.00415.2004

Rosenberger, C., Khamaisi, M., Abassi, Z., Shilo, V., Weksler-Zangen, S., Goldfarb, M., et al. (2008). Adaptation to hypoxia in the diabetic rat kidney. *Kidney Int.* 73, 34–42. doi: 10.1038/sj.ki.5002567

Rosenberger, C., Mandriota, S., Jurgensen, J. S., Wiesener, M. S., Horstrup, J. H., Frei, U., et al. (2002). Expression of hypoxia-inducible factor-1α and -2α in hypoxic and ischemic rat kidneys. *J. Am. Soc. Nephrol.* 13, 1721–1732. doi: 10.1097/01.ASN.0000017223.49823.2A

Rousset, S., Emre, Y., Join-Lambert, O., Hurtaud, C., Ricquier, D., and Cassard-Doulcier, A. M. (2006). The uncoupling protein 2 modulates the cytokine balance in innate immunity. *Cytokine* 35, 135–142. doi: 10.1016/j.cyto.2006.07.012

Sakaguchi, Y., Hatta, T., Hayashi, T., Shoji, T., Suzuki, A., Tomida, K., et al. (2013). Association of nocturnal hypoxemia with progression of CKD. *Clin. J. Am. Soc. Nephrol.* 8, 1502–1507. doi: 10.2215/CJN.11931112

Sanchez, A. M., Csibi, A., Raibon, A., Cornille, K., Gay, S., Bernardi, H., et al. (2012). AMPK promotes skeletal muscle autophagy through activation of forkhead FoxO3a and interaction with Ulk1. *J. Cell. Biochem.* 113, 695–710. doi: 10.1002/jcb.23399

Sayarlioglu, H., Erkoc, R., Dogan, E., Topal, C., Algun, E., Erem, C., et al. (2005). Nephropathy and retinopathy in type 2 diabetic patients living at moderately high altitude and sea level. *Ren. Fail.* 27, 67–71. doi: 10.1081/JDI-42794

Semenza, G. L. (1999). Regulation of mammalian O2 homeostasis by hypoxia-inducible factor 1. *Annu. Rev. Cell Dev. Biol.* 15, 551–578. doi: 10.1146/annurev.cellbio.15.1.551

Shabalina, I. G., Kramarova, T. V., Nedergaard, J., and Cannon, B. (2006). Carboxyatractyloside effects on brown-fat mitochondria imply that the adenine nucleotide translocator isoforms ANT1 and ANT2 may be responsible for basal and fatty-acid-induced uncoupling respectively. *Biochem. J.* 399, 405–414. doi: 10.1042/BJ20060706

Shao, Y., Lv, C., Yuan, Q., and Wang, Q. (2016). Levels of serum 25(OH)VD3, HIF-1α, VEGF, vWf, and IGF-1 and their correlation in type 2 diabetes patients with different urine albumin creatinine ratio. *J. Diabetes Res.* 2016:1925424. doi: 10.1155/2016/1925424

Shenouda, S. M., Widlansky, M. E., Chen, K., Xu, G., Holbrook, M., Tabit, C. E., et al. (2011). Altered mitochondrial dynamics contributes to endothelial dysfunction in diabetes mellitus. *Circulation* 124, 444–453. doi: 10.1161/CIRCULATIONAHA.110.014506

Singh, D. K., Winocour, P., and Farrington, K. (2008). Mechanisms of disease: the hypoxic tubular hypothesis of diabetic nephropathy. *Nat. Clin. Pract. Nephrol.* 4, 216–226. doi: 10.1038/ncpneph0757

Sourris, K. C., Harcourt, B. E., Tang, P. H., Morley, A. L., Huynh, K., Penfold, S. A., et al. (2012). Ubiquinone (coenzyme Q10) prevents renal mitochondrial dysfunction in an experimental model of type 2 diabetes. *Free Radic. Biol. Med.* 52, 716–723. doi: 10.1016/j.freeradbiomed.2011.11.017

Starkov, A. A., and Fiskum, G. (2003). Regulation of brain mitochondrial H2O2 production by membrane potential and NAD(P)H redox state. *J. Neurochem.* 86, 1101–1107. doi: 10.1046/j.1471-4159.2003.01908.x

St-Pierre, J., Buckingham, J. A., Roebuck, S. J., and Brand, M. D. (2002). Topology of superoxide production from different sites in the mitochondrial electron transport chain. *J. Biol. Chem.* 277, 44784–44790. doi: 10.1074/jbc.M207217200

Takahashi, A., Kimura, T., Takabatake, Y., Namba, T., Kaimori, J., Kitamura, H., et al. (2012). Autophagy guards against cisplatin-induced acute kidney injury. *Am. J. Pathol.* 180, 517–525. doi: 10.1016/j.ajpath.2011.11.001

Tanaka, T. (2017). A mechanistic link between renal ischemia and fibrosis. *Med. Mol. Morphol.* 50, 1–8. doi: 10.1007/s00795-016-0146-3

Tewari, S., Santos, J. M., and Kowluru, R. A. (2012). Damaged mitochondrial DNA replication system and the development of diabetic retinopathy. *Antioxid. Redox Signal.* 17, 492–504. doi: 10.1089/ars.2011.4333

Twig, G., Elorza, A., Molina, A. J., Mohamed, H., Wikstrom, J. D., Walzer, G., et al. (2008). Fission and selective fusion govern mitochondrial segregation and elimination by autophagy. *EMBO J.* 27, 433–446. doi: 10.1038/sj.emboj.7601963

Vallon, V., Rose, M., Gerasimova, M., Satriano, J., Platt, K. A., Koepsell, H., et al. (2013). Knockout of Na-glucose transporter SGLT2 attenuates hyperglycemia and glomerular hyperfiltration but not kidney growth or injury in diabetes mellitus. *Am. J. Physiol. Renal Physiol.* 304, F156–F167. doi: 10.1152/ajprenal.00409.2012

Vives-Bauza, C., Zhou, C., Huang, Y., Cui, M., de Vries, R. L., Kim, J., et al. (2010). PINK1-dependent recruitment of Parkin to mitochondria in mitophagy. *Proc. Natl. Acad. Sci. U.S.A.* 107, 378–383. doi: 10.1073/pnas.0911187107

Wang, W., Wang, Y., Long, J., Wang, J., Haudek, S. B., Overbeek, P., et al. (2012). Mitochondrial fission triggered by hyperglycemia is mediated by ROCK1 activation in podocytes and endothelial cells. *Cell Metab.* 15, 186–200. doi: 10.1016/j.cmet.2012.01.009

Wang, Z., Zhu, Q., Li, P. L., Dhaduk, R., Zhang, F., Gehr, T. W., et al. (2014). Silencing of hypoxia-inducible factor-1α gene attenuates chronic ischemic renal injury in two-kidney, one-clip rats. *Am. J. Physiol. Renal Physiol.* 306, F1236–F1242. doi: 10.1152/ajprenal.00673.2013

Westermann, B. (2010). Mitochondrial fusion and fission in cell life and death. *Nat. Rev. Mol. Cell Biol.* 11, 872–884. doi: 10.1038/nrm3013

Xie, L., Zhu, X., Hu, Y., Li, T., Gao, Y., Shi, Y., et al. (2008). Mitochondrial DNA oxidative damage triggering mitochondrial dysfunction and apoptosis in high glucose-induced HRECs. *Invest. Ophthalmol. Vis. Sci.* 49, 4203–4209. doi: 10.1167/iovs.07-1364

Yu, A. Y., Frid, M. G., Shimoda, L. A., Wiener, C. M., Stenmark, K., and Semenza, G. L. (1998). Temporal, spatial, and oxygen-regulated expression of hypoxia-inducible factor-1 in the lung. *Am. J. Physiol.* 275(4 Pt 1), L818–L826.

Yu, T., Robotham, J. L., and Yoon, Y. (2006). Increased production of reactive oxygen species in hyperglycemic conditions requires dynamic change of mitochondrial morphology. *Proc. Natl. Acad. Sci. U.S.A.* 103, 2653–2658. doi: 10.1073/pnas.0511154103

Yu, T., Sheu, S. S., Robotham, J. L., and Yoon, Y. (2008). Mitochondrial fission mediates high glucose-induced cell death through elevated production of reactive oxygen species. *Cardiovasc. Res.* 79, 341–351. doi: 10.1093/cvr/cvn104

Zepeda, A. B., Pessoa, A. Jr., Castillo, R. L., Figueroa, C. A., Pulgar, V. M., and Farias, J. G. (2013). Cellular and molecular mechanisms in the hypoxic tissue: role of HIF-1 and ROS. *Cell Biochem. Funct.* 31, 451–459. doi: 10.1002/cbf.2985

Zhong, L., D'Urso, A., Toiber, D., Sebastian, C., Henry, R. E., Vadysirisack, D. D., et al. (2010). The histone deacetylase Sirt6 regulates glucose homeostasis via Hif1α. *Cell* 140, 280–293. doi: 10.1016/j.cell.2009.12.041

Zhou, X., Chen, J., Yi, G., Deng, M., Liu, H., Liang, M., et al. (2016). Metformin suppresses hypoxia-induced stabilization of HIF-1α through reprogramming of oxygen metabolism in hepatocellular carcinoma. *Oncotarget* 7, 873–884. doi: 10.18632/oncotarget.6418

Zou, A. P., Li, N., and Cowley, A. W. Jr. (2001). Production and actions of superoxide in the renal medulla. *Hypertension* 37(2 Pt 2), 547–553. doi: 10.1161/01.HYP.37.2.547

Zrelli, H., Matsuoka, M., Kitazaki, S., Zarrouk, M., and Miyazaki, H. (2011). Hydroxytyrosol reduces intracellular reactive oxygen species levels in vascular endothelial cells by upregulating catalase expression through the AMPK-FOXO3a pathway. *Eur. J. Pharmacol.* 660, 275–282. doi: 10.1016/j.ejphar.2011.03.045

**Conflict of Interest Statement:** The authors declare that the research was conducted in the absence of any commercial or financial relationships that could be construed as a potential conflict of interest.

frontiers in Physiology

ORIGINAL RESEARCH
published: 06 April 2017
doi: 10.3389/fphys.2017.00205

# Circadian Rhythm in Kidney Tissue Oxygenation in the Rat

*Tonja W. Emans[1,2], Ben J. Janssen[3], Jaap A. Joles[2] and C. T. Paul Krediet[1]**

[1] Department of Internal Medicine, Academic Medical Center at the University of Amsterdam, Amsterdam, Netherlands, [2] Department of Nephrology and Hypertension, University Medical Center Utrecht, Utrecht, Netherlands, [3] Department of Pharmacology and Toxicology, Maastricht University, Maastricht, Netherlands

Blood pressure, renal hemodynamics, electrolyte, and water excretion all display diurnal oscillation. Disturbance of these patterns is associated with hypertension and chronic kidney disease. Kidney oxygenation is dependent on oxygen delivery and consumption that in turn are determined by renal hemodynamics and metabolism. We hypothesized that kidney oxygenation also demonstrates 24-h periodicity. Telemetric oxygen-sensitive carbon paste electrodes were implanted in Sprague-Dawley rats (250–300 g), either in renal medulla ($n = 9$) or cortex ($n = 7$). Arterial pressure (MAP) and heart rate (HR) were monitored by telemetry in a separate group ($n = 8$). Data from 5 consecutive days were analyzed for rhythmicity by cosinor analysis. Diurnal electrolyte excretion was assessed by metabolic cages. During lights-off, oxygen levels increased to 105.3 ± 2.1% in cortex and 105.2 ± 3.8% in medulla. MAP was 97.3 ± 1.5 mmHg and HR was 394.0 ± 7.9 bpm during lights-off phase and 93.5 ± 1.3 mmHg and 327.8 ± 8.9 bpm during lights-on. During lights-on, oxygen levels decreased to 94.6 ± 1.4% in cortex and 94.2 ± 8.5% in medulla. There was significant 24-h periodicity in cortex and medulla oxygenation. Potassium excretion (1,737 ± 779 vs. 895 ± 132 μmol/12 h, $P = 0.005$) and the distal $Na^+/K^+$ exchange (0.72 ± 0.02 vs. 0.59 ± 0.02 $P < 0.001$) were highest in the lights-off phase, this phase difference was not found for sodium excretion ($P = 0.4$). It seems that oxygen levels in the kidneys follow the pattern of oxygen delivery, which is known to be determined by renal blood flow and peaks in the active phase (lights-off).

**Keywords: kidney oxygenation, circadian rhythm, renal cortex, renal medulla, hypertension, hypoxia**

OPEN ACCESS

***Edited by:***
*Michelle L. Gumz, University of Florida, USA*

***Reviewed by:***
*Gad Asher, Weizmann Institute of Science, Israel*
*Jennifer M. Sasser, University of Mississippi Medical Center School of Dentistry, USA*

****Correspondence:***
*C. T. Paul Krediet*
*c.t.krediet@amc.nl*

***Specialty section:***
*This article was submitted to Renal and Epithelial Physiology, a section of the journal Frontiers in Physiology*

***Received:*** *07 November 2016*
***Accepted:*** *20 March 2017*
***Published:*** *06 April 2017*

***Citation:***
*Emans TW, Janssen BJ, Joles JA and Krediet CTP (2017) Circadian Rhythm in Kidney Tissue Oxygenation in the Rat. Front. Physiol. 8:205. doi: 10.3389/fphys.2017.00205*

## INTRODUCTION

Endogenous timing mechanisms have evolved to adapt to environmental changes imposed by alternating periods of light and darkness. Twenty-four hours patterns in sleep, activity, food intake, and excretion are well-known representatives of such physiological homeostatic adaptations. Via the kidneys, these homeostatic mechanisms maintain constancy of the bodies' extracellular fluid compartment throughout the 24-h cycle.

In mammals, diurnal variations in urinary volume and electrolyte excretion are the best studied features of 24-h renal rhythm. Urinary excretion of water, sodium, and potassium peak during the

**Abbreviations:** CKD, chronic kidney disease; GFR, glomerular filtration rate; HR, heart rate; MAP, mean arterial pressure; MESOR, circadian rhythm adjusted mean; $pO_2$, tissue oxygen concentration; RAAS, renin-angiotensin-aldosterone system; RBF, renal blood flow.

active period of the day when intake is also highest (Cohn et al., 1970; Hilfenhaus, 1976; Pons et al., 1996; Zhang et al., 2015). Concomitantly, the activity of the renin-angiotensin-aldosterone system (RAAS), which is a major regulator of blood pressure, appears in a circadian fashion in rodents (Hilfenhaus, 1976), and humans (Armbruster et al., 1975; Mahler et al., 2015). Herein, plasma aldosterone levels peak just before the activity phase and are inverted by reversal of the light-dark cycle (Hilfenhaus, 1976).

Disturbance of the circadian blood pressure pattern, exposed as a non-dipping profile at night, is associated with hypertension and nephropathy (Fukuda et al., 2006; Sachdeva and Weder, 2006). Sleep problems have been reported in almost 80% of end-stage renal disease patients (Koch et al., 2009), and a disturbed blood pressure pattern is associated with higher risk for chronic kidney disease (CKD) (Portaluppi et al., 1991). Not surprisingly, restoration of the dipping profile during the inactive phase has been a target of interest for anti-hypertensive chronotherapy (Simko and Pechanova, 2009). Timed-inhibition of the renin angiotensin system can be used to suppress the rise in blood pressure upon awakening (Oosting et al., 1999). Disturbed renal sodium transport seems to be linked to abnormal circadian blood pressure profiles (Fujii et al., 1999).

Troughs in the excretion patterns of electrolytes typically occur during the resting or sleeping phase of the 24-h cycle. Assuming that the kidneys consume most energy and oxygen on sodium transport (Brezis et al., 1994), one could hypothesize that tissue oxygen concentration ($pO_2$) in renal tissue is lowest when sodium reabsorption activity is highest. On the other hand, the increased oxygen use in the kidney may be fully matched by increased oxygen delivery because 24-h variations in blood pressure and renal blood flow coincide with periods of highest excretion (Pons et al., 1996). Normal kidney oxygenation is crucial as disturbed $pO_2$ within the kidneys has been linked to the progression of CKD (Evans et al., 2013). Data on 24-h variations in oxygenation are lacking because, until recently, it was not possible to measure kidney oxygenation continuously. To answer the question whether 24-h variations in renal function are associated with synchronous variations in renal oxygenation, $pO_2$ levels in the kidney were continuously monitored in healthy rats by a telemetry based technique for 5 consecutive days. Additionally, 24-h variations in tissue oxygenation were compared for renal cortical and medullary tissue and linked to the magnitude of day/night differences in water and food intake, and urinary water and electrolyte excretion. Very recently, Adamovich et al. described that oxygen levels may adjust the timing of the internal circadian clock (Adamovich et al., 2017). They showed that in the rat kidney (cortex) a circadian rhythm in $pO_2$ levels can be detected. In this study we further substantiate these finding and expand this to both the medullary and cortical region in the kidney.

# METHODS

## Animals

Experiments were conducted in male Sprague Dawley rats (250–300 grams, supplier: Charles River). All procedures were approved by the Animal Ethics Committee of University of Utrecht (DEC 2014.II.03.015) and were in accordance with the Dutch Codes of Practice for the Care and Use of Animals for Scientific Purposes. All animals were kept on a 12 h light/dark cycle with lights-on at 6 a.m. (ZT 0), and lights-off at 6 p.m. (ZT 12). Rats had access to water and standard rat chow (contains 0.3% $Na^+$ and 0.69% $K^+$) *ad libitum*. To promote animal welfare and normal physiological activity around the clock, the rats were cohoused. Only during urine collection for electrolyte analysis were the rats housed individually for 24 h.

## System Overview

The telemetry based technique to measure oxygenation in the kidney has been described in detail (Emans et al., 2016; Koeners et al., 2016). In summary, oxygen sensitive carbon paste electrodes were implanted in the right kidney, either in the cortex ($n = 7$) or medulla ($n = 9$). The kidney was exposed via laparotomy. The telemeter (TR57Y, Millar, Houston, US) was placed in the rat abdomen. After 2 weeks of complete recovery and stabilization of oxygen signal, 24-h oscillations in $pO_2$ were recorded continuously. In a third group, blood pressure telemeters (TRM54P, Millar, Houston, US) were implanted in the abdominal aorta ($n = 8$).

## Analysis

After subtraction of the off-set value, original $pO_2$ data were filtered with a 25 Hz low-pass digital filter. Artifacts were removed when the 1st order derivative exceeded a threshold of 5 nA/s, as described previously (Emans et al., 2016). To describe the 24-h rhythm, 1 h average $pO_2$-values were calculated. These hourly averages were used to determine the mean $pO_2$ level over the 5 consecutive days and were then re-expressed relatively to this 5-day mean value (MESOR). The Cosinor method was applied to determine the amplitude and phase of the oscillation in the $pO_2$ signal (Refinetti et al., 2007). Twenty-four hours rhythmicity was determined when the amplitude of the fitted curve was significantly $>0$. For blood pressure and heart rate, absolute values were used.

## Electrolyte Excretion

Rats were individually housed in metabolic cages for 24 h ($n = 13$) to determine water and food intake and to collect urine. Urine was sampled in epochs of 12 h starting at 6 p.m. (lights-off/active phase) and continued at 6 a.m. (lights-on/resting phase). In these 12-h urine samples sodium and potassium concentrations were determined by flame photometry (Model 420, Sherwood, UK). Urinary creatinine was determined by DiaSys Kit (DiaSys Diagnostic Systems, Holzheim, Germany). Distal sodium/potassium exchange was quantified as kaliuresis/(natriuresis + kaliuresis; Hene et al., 1984).

## Statistics

Data are expressed as mean ± SEM. The data collected during active respectively resting phase were compared by paired Student's *t*-test. Differences were considered significant when $p < 0.05$.

## RESULTS

An original tracing of 3.5-day consecutive recording of cortical $pO_2$ levels is depicted in **Figure 1A**. An example of a tracing obtained with the probe in the medulla is presented in **Figure 1B**. On visual inspection of the raw telemetric data, oxygen levels in both the cortex and medulla peaked during the lights-off period in these nocturnally active rats, while trough values were usually found during the lights-on or resting period of the day. The 5-day mean was set at 100% $pO_2$. Quantification of these observations by the Cosinor analyses revealed that during the lights-off phase, oxygen levels increased to 105.3 ± 2.1 and 105.2 ± 3.8% in renal cortex and medulla, respectively. During the lights-on phase, oxygen levels decreased to 94.6 ± 1.4% in cortex and 94.2 ± 8.5% in medulla, relatively to the 5-day mean (**Table 1**). The mean amplitude of the fitted curve for $pO_2$ rhythmicity tended to be larger in cortex than in medulla (5.8 vs. 4.9%), although this difference was not significant (**Figure 2**). Ninety-five percentage Confidence intervals (95% CI) of both cortex and medulla oxygenation did not exceed the MESOR. Twenty-four hours blood pressure and heart rate rhythms were in phase with those occurring in $pO_2$.

Water and food intake were significantly higher during the lights-off phase than during the lights-on phase (28 ± 2 vs. 4 ± 1 ml and 20 ± 1 vs. 3 ± 1 g, $P < 0.001$, **Figures 3A,B**). Urine volume did not differ much between lights-off and lights on (**Figure 3C**). Creatinine excretion tended to increase during the lights-off vs. lights-on phase ($P = 0.052$, **Figure 3D**). There was no phase difference for urinary sodium excretion or $Na^+$/creatinine (**Figures 3E,H**), but urinary potassium excretion and $K^+$/creatinine were increased during the 12 h lights-off vs. the lights on period ($P < 0.01$, **Figures 3F,I**). Distal $Na^+/K^+$ exchange (kaliuresis/natriuresis + kaliuresis) was increased in the lights-off period ($P < 0.001$, **Figure 3G**).

## DISCUSSION

Normotensive rats display a significant diurnal rhythmicity in renal oxygenation (Adamovich et al., 2017). In this study we

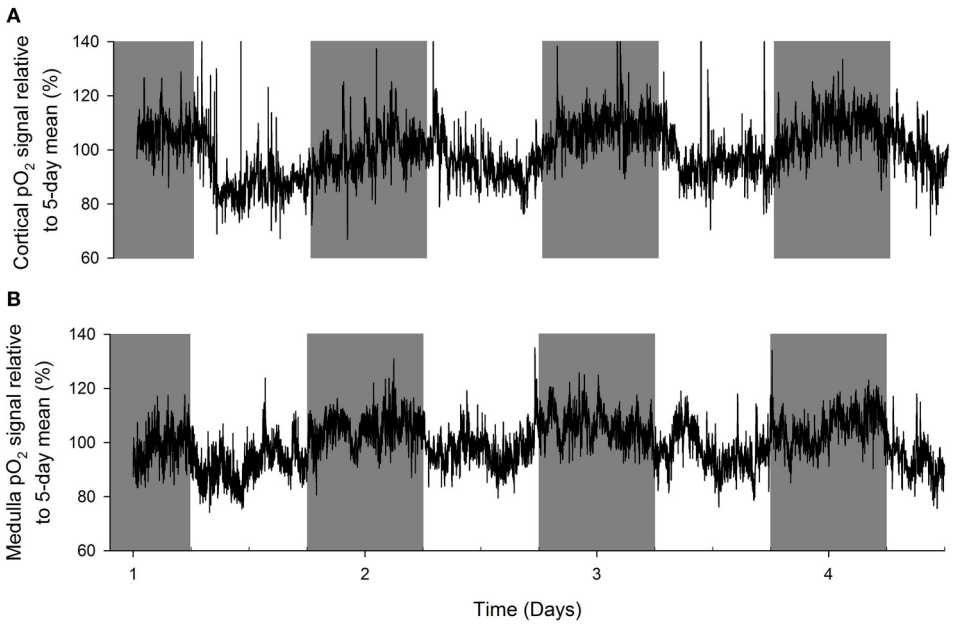


**FIGURE 1 | Representative examples of original recordings (A)** in a rat with an oxygen sensor placed in the cortex of the kidney and **(B)** in another rat with the probe in the renal medulla. Data are 10 second averages during consecutive days. Note that in both cortex and medulla, tissue oxygenation peaks during the lights-off (active) period of the day (marked in gray). Troughs in tissue $pO_2$ are visible in the lights-on (resting) period.

**TABLE 1 | Circadian parameters in oxygenation, blood pressure, and heart rate.**

| | MESOR | Amplitude | Lights-off peak (active) | Lights-on peak (rest) | Acrophase (ZT h) | Robustness (%) |
|---|---|---|---|---|---|---|
| Oxygenation cortex (%) | 100.0 (99.3–100.7) | 5.8 (4.7–6.8)* | 105.3 ± 2.1 | 94.6 ± 1.4 | 16.9 (16.3–17.4) | 93.3 |
| Oxygenation medulla (%) | 100.0 (98.8–101.2) | 4.9 (3.6–6.3)* | 105.2 ± 3.8 | 94.2 ± 8.5 | 16.9 (16.0–17.7) | 86.2 |
| Blood pressure (mmHg) | 95.5 (94.6–95.8) | 1.6 (0.8–2.4)* | 97.3 ± 1.5 | 93.5 ± 1.3 | 18.9 (17.6–20.2) | 69.9 |
| Heart rate (bpm) | 361 (356–365) | 33 (28–38)* | 394 ± 8 | 328 ± 9 | 16.9 (16.2–17.6) | 87.4 |

*Data were analyzed by cosinor analysis (period = 24 h), lighting schedule; lights-on at 6 a.m. (ZT0), and lights-off at 6 p.m. (ZT12). Circadian rhythm-adjusted mean, MESOR. Peak time of cosine function, Acrophase. Percentage of variance accounted for by the computed rhythm, Robustness. (95% CI except for peak values mean ± SEM), *P < 0.01 vs. zero amplitude = no rhythm.*

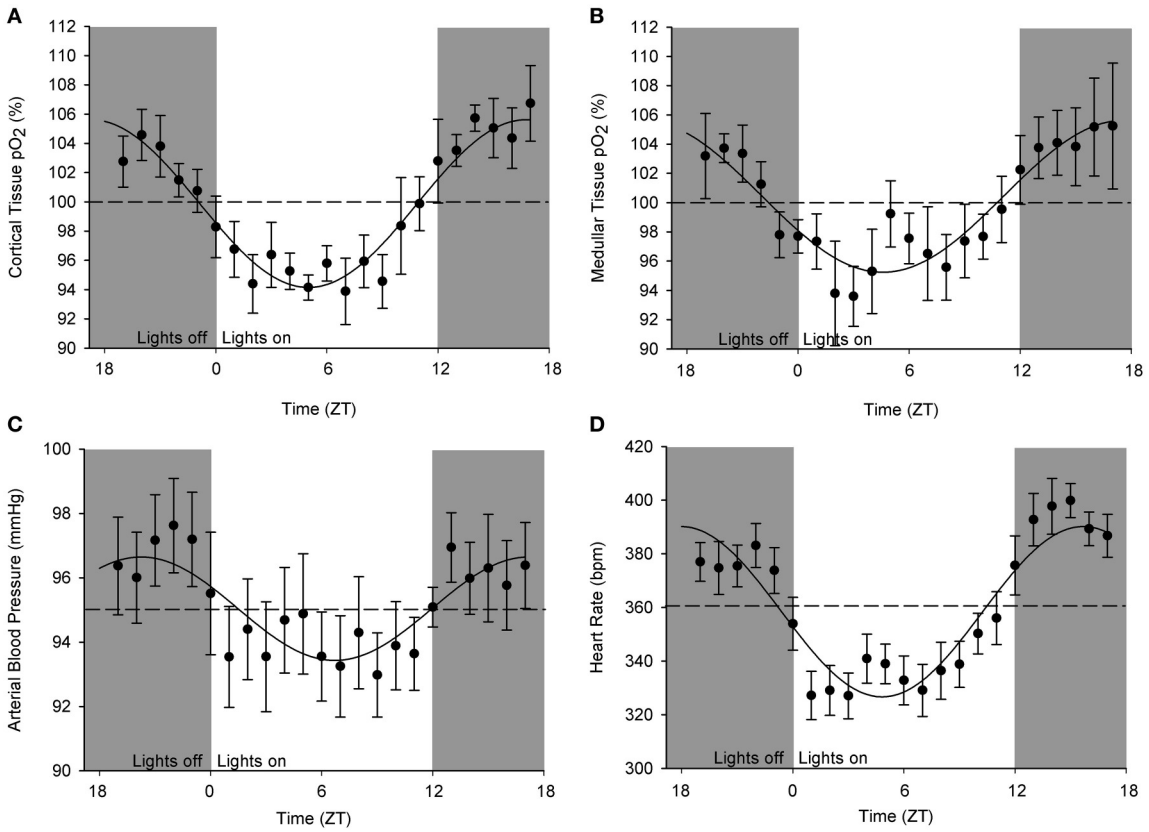


**FIGURE 2 | Cosinor analysis of the averaged circadian rhythms in kidney oxygenation, blood pressure, and heart rate.** Data are plotted as hourly mean values ± SEM as recorded over 5 days in each rat relatively to the overall mean value (=MESOR, indicated by the dotted line). Note that different rats were used for obtaining oxygenation in **(A)** cortical and **(B)** medullary $pO_2$ as well as for the **(C)** blood pressure. **(D)** Heart rate values were derived from blood pressure measurements. A significant circadian rhythm was assessed when the amplitude of the fitted curve was statistically >0, see **Table 1**.

dissected the rhythmicity of cortical and medullary oxygenation, that both follow a diurnal pattern. Using telemetric techniques, peak values in tissue oxygenation were found during the lights-off period when renal excretion of electrolytes was highest. Trough values in renal $pO_2$-values were observed during the lights-on period when excretion patterns are minimal. These data suggest that the circadian rhythm in (both cortical and medullar) $pO_2$ is mainly the result of a 24 variation in oxygen delivery to the kidneys.

In rats, cardiac output and blood pressure are highest during the lights-off period (Oosting et al., 1997), when rats display highest locomotor activity and eat and drink the most. Assuming that during normal activity renal blood flow is stable at approximately 20% of cardiac output, oxygen delivery is highest to this organ during the active phase. While direct renal blood flow measurements are not available over 24 h, previous studies in rats using inulin and p-aminohippuric acid clearance have repeatedly (Pons et al., 1996) shown that GFR and RBF indeed peak during the lights-off period. This corroborates the hypothesis that oxygen delivery is the most important determinant of this circadian pattern in oxygenation. Recently, 24-h oxygen recordings in the kidneys have been obtained in sheep (Calzavacca et al., 2015). In that study, a clear 24-h pattern in tissue oxygenation of the kidneys was absent. RBF and tissue perfusion did not show a circadian fluctuation either. Presumably, there was a suppression of normal locomotor activity in these sheep because they were housed in metabolic cages. In the current study, we co-housed the rats to facilitate normal social behavior and thereby normal locomotor activity. An alternative explanation for the discrepancy between our observations and those in sheep may be that ruminants have a less pronounced fasting phase than omnivorous species such as rats and that that the delivery of nutrients is more constant than in diurnal active species such as rats. While studying mechanisms of 24-h variation in potassium excretion, Steel et al. found that the bulk of potassium excretion was determined by food intake (delivery) rather than the flow (Steele et al., 1994). This suggests that peak oxygen levels in the kidneys may also occur in parallel with delivery patterns of certain nutrients, waste products, or electrolytes. Future studies are needed to sort out cause and consequence of such associations. Very recently, a similar daily pattern in $pO_2$ in the kidney was briefly described in rodents. Peak values were found during lights-off, when oxygen consumption rate was highest as well (Adamovich et al., 2017).

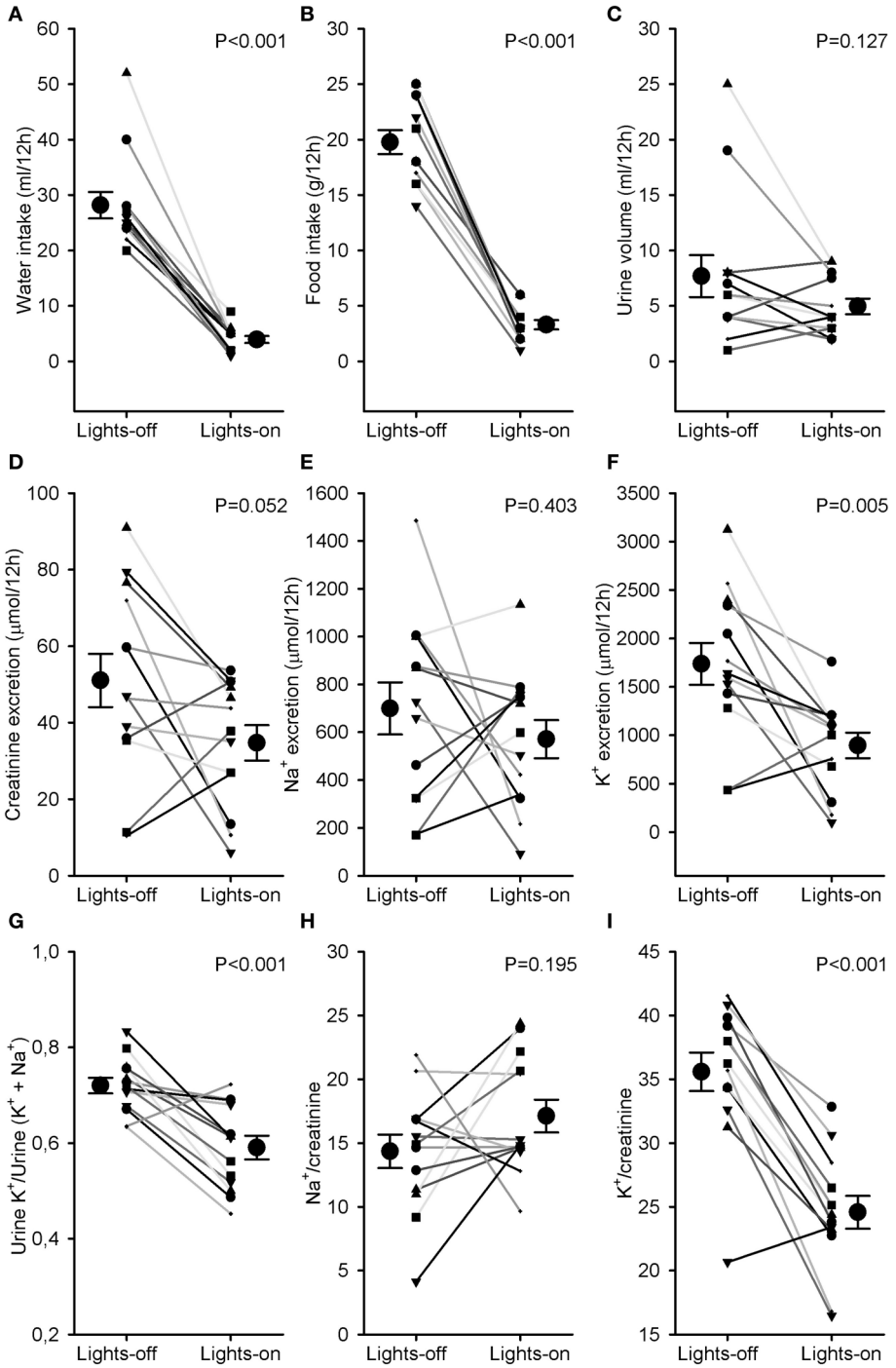


**FIGURE 3 | Water and food intake and urine analysis.** Rats were individually housed in metabolic cages for 24 h. Urine was collected in 2 samples, one during the lights-off (active) and one during the lights-on (resting) period. Individual data and mean ± SEM are indicated for **(A)** water intake, **(B)** food intake, **(C)** urine volume, **(D)** creatinine excretion, **(E)** $Na^+$ excretion, **(F)** $K^+$ excretion, **(G)** Urine $K^+$/Urine ($K^+ + Na^+$) as an estimate of distal $Na^+/K^+$ exchange, **(H)** $Na^+$/creatinine, and **(I)** $K^+$/creatinine. Lights-on/off differences were compared with paired Student's *t*-tests.

In rats ANGII and Aldosterone peak during the lights-on period, when electrolyte excretion is lowest (Hilfenhaus, 1976; Lemmer et al., 2000; Naito et al., 2009). These hormones stimulate tubular sodium re-absorption during the lights-on period and thereby determine oxygen use. Presumably, this is an evolutionary mechanism to retain fluids when water intake is low. RBF and GFR also exhibit 24 h periodicity, peaks during lights-off and troughs during lights-on (Pons et al., 1996). Important genes

related to renal sodium and water transport, like NHE, aquaporin 2 and 4, have been linked to circadian expression (Saifur Rohman et al., 2005). A lower kaliuresis and distal $Na^+/K^+$ exchange at the time of a decline in tissue oxygenation at rest suggest that oxygen consumption *per se* is not contributing to the pattern of renal oxygen content in our study.

The variations in arterial blood pressure and heart rate throughout the day have been studied in detail in healthy, chronically instrumented rats (Henry et al., 1990; Janssen et al., 1992; Teerlink and Clozel, 1993; van den Buuse, 1994). The variation between the nightly peaks and daily troughs are less pronounced in our study than reported by some others. This is probably caused by the fact that the light dark cycle in the animal room corresponded with real day and night making it possible that researcher or care taker-induced minor disturbances may have occurred in the recordings during the daily resting phase of the animals thereby underestimating the current 24-h amplitude in blood pressure oscillation. Reversing the experimental light/dark cycle would probably not have diminished the current 24-h amplitudes but actually magnified them. This may also apply for $pO_2$-values. We decided to set the 5-day mean at 100% $pO_2$ for each animal to allow inter-animal comparison (Emans et al., 2016). The between animal comparison would decrease the sensitivity by introducing a large SD between animals and obscuring day/night variation within one animal. Another technical limitation (inherent to studying small rodents) was that we were not able to record RBF variations. However, our setting does not interfere with natural behavior and physiological processes of the nocturnal animals. The rats were unrestrained and cohoused, which allows them full activity at night, accompanied by higher heart rates and probably a higher RBF as well.

Oxygen and arterial pressure assessment could not be performed in the same animal. Cortex and medulla recordings were also performed in separate animals. However, the rhythms were consistent within each of the three groups, suggesting that extrapolation of the results to the full set is acceptable. The animals were fully acclimatized toward the 12:12 light dark cycle in our facility. Our assessment of natriuresis may have been affected by our chosen 12-h sampling period, because sodium excretion can peak just before the light phase (Roelfsema et al., 1980; Pons et al., 1996). Due to ethical and technical issues, we decided not to acclimatize our rats to metabolic cage housing. This may have interfered with the excretion values calculated from collected urine. Other researchers, who applied an equilibration period in metabolic cages for 2–3 days (Nikolaeva et al., 2012; Johnston et al., 2016) did find significant differences in urine sodium excretion in rodents. However, since diurnal effects were prominent for fluid and food intake, urine flow, kaliuresis, and distal Na/K exchange, this suggests that, if anything, these diurnal differences would have been even more marked in acclimatized rats.

The kidney has more clock regulated genes than most other organs (Gumz, 2016). It has also been suggested that every cell type in the kidney follows its own circadian clock (Tokonami et al., 2014). Probably cortex and medulla follow their own circadian pattern as well. However, we did not find a different pattern in oxygenation between cortex and medulla. Our data suggest that the kidney may be more vulnerable to hypoxia during sleep. Actions that make the kidneys hypoxic in general could lead to damage during the resting phase, when the oxygen concentrations are already somewhat lower. This could be relevant in the pathogenesis of diseases that are associated with low oxygenation at night, such as obstructive sleep apnea and the associated progression of renal disease. One could argue that diseases associating with kidney hypoxia, for instance CKD (Evans et al., 2013) and diabetes (Franzen et al., 2016), could be more progressive during the resting phase. On the other hand, our data may also provide a new look at the association of neglecting to align with the inner circadian clock (e.g., in shift workers) with the development of hypertension and CKD (Lieu et al., 2012). Furthermore, low oxygen levels at rest could contribute to the non-dipping profile and hypertension, because low levels of oxygen in the kidneys may not allow a normal decline in MAP and RBF during rest.

In conclusion, the circadian rhythm of regional kidney oxygenation that we describe, is a new phenomenon that provides further research opportunities for the onset and progression of hypertension and CKD.

## AUTHOR CONTRIBUTIONS

TE, BJ, JJ, CK concept and design of research; TE performed experiments; TE, BJ, JJ, CK analyzed data; TE, BJ, JJ, CK interpreted results of experiments; TE prepared figures; TE, BJ drafted manuscript; TE, BJ, JJ, CK edited and revised manuscript; TE, BJ, JJ, CK approved final version of manuscript; TE, BJ, JJ, CK ensure integrity.

## FUNDING

CK is supported by the Netherlands Organization for Health Research (ZonMw, Clinical Fellowship 40007039712461) and by the Dutch Kidney Foundation (Project KJPB 12.029). BJ is supported by the Dutch Kidney Foundation (Grant 16OI21). This support is gratefully acknowledged.

## ACKNOWLEDGMENTS

We thank Paula Martens for technical expert assistance and Adele Dijk for excellent laboratory assistance.

## REFERENCES

Adamovich, Y., Ladeuix, B., Golik, M., Koeners, M. P., and Asher, G. (2017). Rhythmic oxygen levels reset circadian clocks through HIF1α. *Cell Metab.* 25, 93–101. doi: 10.1016/j.cmet.2016.09.014

Armbruster, H., Vetter, W., Uhlschmid, G., Zaruba, K., Beckerhoff, B., Nussberger, J., et al. (1975). Circadian rhythm of plasma renin activity and plasma

aldosterone in normal man and in renal allograft recipients. *Proc. Eur. Dial. Transplant. Assoc.* 11, 268–276.

Brezis, M., Agmon, Y., and Epstein, F. H. (1994). Determinants of intrarenal oxygenation. I. Effects of diuretics. *Am. J. Physiol.* 267, F1059–F1062.

Calzavacca, P., Evans, R. G., Bailey, M., Lankadeva, Y. R., Bellomo, R., and May, C. N. (2015). Long-term measurement of renal cortical and medullary tissue oxygenation and perfusion in unanesthetized sheep. *Am. J. Physiol. Regul. Integr. Comp. Physiol.* 308, R832–R839. doi: 10.1152/ajpregu.00515.2014

Cohn, C., Webb, L., and Joseph, D. (1970). Diurnal rhythms in urinary electrolyte excretions by the rat: influence of feeding habits. *Life Sci.* 9, 803–809. doi: 10.1016/0024-3205(70)90336-X

Emans, T. W., Janssen, B. J., Pinkham, M. I., Ow, C. P., Evans, R. G., Joles, J. A., et al. (2016). Exogenous and endogenous angiotensin-II decrease renal cortical oxygen tension in conscious rats by limiting renal blood flow. *J. Physiol.* 594, 6287–6300. doi: 10.1113/JP270731

Evans, R. G., Ince, C., Joles, J. A., Smith, D. W., May, C. N., O'Connor, P. M., et al. (2013). Haemodynamic influences on kidney oxygenation: clinical implications of integrative physiology. *Clin. Exp. Pharmacol. Physiol.* 40, 106–122. doi: 10.1111/1440-1681.12031

Franzen, S., Pihl, L., Khan, N., Gustafsson, H., and Palm, F. (2016). Pronounced kidney hypoxia precedes albuminuria in type 1 diabetic mice. *Am. J. Physiol. Ren. Physiol.* 310, F807–F809. doi: 10.1152/ajprenal.00049.2016

Fujii, T., Uzu, T., Nishimura, M., Takeji, M., Kuroda, S., Nakamura, S., et al. (1999). Circadian rhythm of natriuresis is disturbed in nondipper type of essential hypertension. *Am. J. Kidney Dis.* 33, 29–35. doi: 10.1016/S0272-6386(99)70254-4

Fukuda, M., Goto, N., and Kimura, G. (2006). Hypothesis on renal mechanism of non-dipper pattern of circadian blood pressure rhythm. *Med. Hypotheses* 67, 802–806. doi: 10.1016/j.mehy.2006.04.024

Gumz, M. L. (2016). Molecular basis of circadian rhythmicity in renal physiology and pathophysiology. *Exp. Physiol.* 101, 1025–1029. doi: 10.1113/EP085781

Hene, R. J., Koomans, H. A., Boer, P., Roos, J. C., and Dorhout Mees, E. J. (1984). Relation between plasma aldosterone concentration and renal handling of sodium and potassium, in particular in patients with chronic renal failure. *Nephron* 37, 94–99.

Henry, R., Casto, R., and Printz, M. P. (1990). Diurnal cardiovascular patterns in spontaneously hypertensive and Wistar-Kyoto rats. *Hypertension* 16, 422–428. doi: 10.1161/01.HYP.16.4.422

Hilfenhaus, M. (1976). Circadian rhythm of the renin-angiotensin-aldosterone system in the rat. *Arch. Toxicol.* 36, 305–316. doi: 10.1007/BF00340536

Janssen, B. J., Tyssen, C. M., Struijker Boudier, H. A., and Hutchins, P. M. (1992). 24-hour homeodynamic states of arterial blood pressure and pulse interval in conscious rats. *J. Appl. Physiol.* 73, 754–761.

Johnston, J. G., Speed, J. S., Jin, C., and Pollock, D. M. (2016). Loss of endothelin B receptor function impairs sodium excretion in a time- and sex-dependent manner. *Am. J. Physiol. Ren. Physiol.* 311, F991–F998. doi: 10.1152/ajprenal.00103.2016

Koch, B. C., Nagtegaal, J. E., Kerkhof, G. A., and ter Wee, P. M. (2009). Circadian sleep-wake rhythm disturbances in end-stage renal disease. *Nat. Rev. Nephrol.* 5, 407–416. doi: 10.1038/nrneph.2009.88

Koeners, M. P., Ow, C. P., Russell, D. M., Evans, R. G., and Malpas, S. C. (2016). Prolonged and continuous measurement of kidney oxygenation in conscious rats. *Methods Mol. Biol.* 1397, 93–111. doi: 10.1007/978-1-4939-3353-2_9

Lemmer, B., Witte, K., Schanzer, A., and Findeisen, A. (2000). Circadian rhythms in the renin-angiotensin system and adrenal steroids may contribute to the inverse blood pressure rhythm in hypertensive TGR(mREN-2)27 rats. *Chronobiol. Int.* 17, 645–658. doi: 10.1081/CBI-100101071

Lieu, S. J., Curhan, G. C., Schernhammer, E. S., and Forman, J. P. (2012). Rotating night shift work and disparate hypertension risk in African-Americans. *J. Hypertens.* 30, 61–66. doi: 10.1097/HJH.0b013e32834e1ea3

Mahler, B., Kamperis, K., Ankarberg-Lindgren, C., Djurhuus, J. C., and Rittig, S. (2015). The effect of puberty on diurnal sodium regulation. *Am. J. Physiol. Ren. Physiol.* 309, F873–F879. doi: 10.1152/ajprenal.00319.2014

Naito, Y., Tsujino, T., Matsumoto, M., Okuda, S., Sakoda, T., Ohyanagi, M., et al. (2009). The mechanism of distinct diurnal variations of renin-angiotensin system in aorta and heart of spontaneously hypertensive rats. *Clin. Exp. Hypertens.* 31, 625–638. doi: 10.3109/10641960903406993

Nikolaeva, S., Pradervand, S., Centeno, G., Zavadova, V., Tokonami, N., Maillard, M., et al. (2012). The circadian clock modulates renal sodium handling. *J. Am. Soc. Nephrol.* 23, 1019–1026. doi: 10.1681/ASN.2011080842

Oosting, J., Struijker-Boudier, H. A., and Janssen, B. J. (1997). Circadian and ultradian control of cardiac output in spontaneous hypertension in rats. *Am. J. Physiol.* 273, H66–H75.

Oosting, J., Struijker-Boudier, H. A., and Janssen, B. J. (1999). Timed inhibition of the renin-angiotensin system suppresses the rise in blood pressure upon awakening in spontaneously hypertensive rats. *Am. J. Hypertens.* 12, 1109–1118. doi: 10.1016/S0895-7061(99)00120-X

Pons, M., Cambar, J., and Waterhouse, J. M. (1996). Renal hemodynamic mechanisms of blood pressure rhythms. *Ann. N.Y. Acad. Sci.* 783, 95–112. doi: 10.1111/j.1749-6632.1996.tb26710.x

Portaluppi, F., Montanari, L., Massari, M., Di Chiara, V., and Capanna, M. (1991). Loss of nocturnal decline of blood pressure in hypertension due to chronic renal failure. *Am. J. Hypertens.* 4, 20–26. doi: 10.1093/ajh/4.1.20

Refinetti, R., Lissen, G. C., and Halberg, F. (2007). Procedures for numerical analysis of circadian rhythms. *Biol. Rhythm Res.* 38, 275–325. doi: 10.1080/09291010600903692

Roelfsema, F., van der Heide, D., and Smeenk, D. (1980). Circadian rhythms of urinary electrolyte excretion in freely moving rats. *Life Sci.* 27, 2303–2309. doi: 10.1016/0024-3205(80)90498-1

Sachdeva, A., and Weder, A. B. (2006). Nocturnal sodium excretion, blood pressure dipping, and sodium sensitivity. *Hypertension* 48, 527–533. doi: 10.1161/01.HYP.0000240268.37379.7c

Saifur Rohman, M., Emoto, N., Nonaka, H., Okura, R., Nishimura, M., Yagita, K., et al. (2005). Circadian clock genes directly regulate expression of the Na(+)/H(+) exchanger NHE3 in the kidney. *Kidney Int.* 67, 1410–1419. doi: 10.1111/j.1523-1755.2005.00218.x

Simko, F., and Pechanova, O. (2009). Potential roles of melatonin and chronotherapy among the new trends in hypertension treatment. *J. Pineal Res.* 47, 127–133. doi: 10.1111/j.1600-079X.2009.00697.x

Steele, A., deVeber, H., Quaggin, S. E., Scheich, A., Ethier, J., and Halperin, M. L. (1994). What is responsible for the diurnal variation in potassium excretion?. *Am. J. Physiol.* 267, R554–R560.

Teerlink, J. R., and Clozel, J. P. (1993). Hemodynamic variability and circadian rhythm in rats with heart failure: role of locomotor activity. *Am. J. Physiol.* 264, H2111–H2118.

Tokonami, N., Mordasini, D., Pradervand, S., Centeno, G., Jouffe, C., Maillard, M., et al. (2014). Local renal circadian clocks control fluid-electrolyte homeostasis and BP. *J. Am. Soc. Nephrol.* 25, 1430–1439. doi: 10.1681/ASN.2013060641

van den Buuse, M. (1994). Circadian rhythms of blood pressure, heart rate, and locomotor activity in spontaneously hypertensive rats as measured with radio-telemetry. *Physiol. Behav.* 55, 783–787. doi: 10.1016/0031-9384(94)90060-4

Zhang, R. Y., Mou, L. J., Li, X. M., Li, X. W., and Qin, Y. (2015). Temporally relationship between renal local clock system and circadian rhythm of the water electrolyte excretion. *Zhongguo Yi Xue Ke Xue Yuan Xue Bao* 37, 698–704. doi: 10.3881/j.issn.1000-503X.2015.06.010

**Conflict of Interest Statement:** The authors declare that the research was conducted in the absence of any commercial or financial relationships that could be construed as a potential conflict of interest.

frontiers in Physiology

ORIGINAL RESEARCH
published: 30 March 2017
doi: 10.3389/fphys.2017.00186

# Blood Pressure Increase during Oxygen Supplementation in Chronic Kidney Disease Patients Is Mediated by Vasoconstriction Independent of Baroreflex Function

*René van der Bel*[1], *Müşerref Çalişkan*[1], *Robert A. van Hulst*[2], *Johannes J. van Lieshout*[1,3], *Erik S. G. Stroes*[1] *and C. T. Paul Krediet*[1]*

[1] Department of Internal Medicine, Academic Medical Center at the University of Amsterdam, Amsterdam, Netherlands,
[2] Department of Hyperbaric Medicine, Academic Medical Center at the University of Amsterdam, Amsterdam, Netherlands,
[3] MRC-Arthritis Research UK Centre of Musculoskeletal Ageing Research, School of Life Sciences, Medical School, University of Nottingham, Queen's Medical Centre, Nottingham, UK

OPEN ACCESS

**Edited by:**
Fredrik Palm,
Uppsala University, Sweden

**Reviewed by:**
Heather Drummond,
University of Mississippi Medical Center School of Dentistry, USA
Anand R. Nair,
University of Iowa, USA
Daniela Patinha,
University of Bristol, UK

***Correspondence:**
C. T. Paul Krediet
c.t.krediet@amc.uva.nl

**Specialty section:**
This article was submitted to Renal and Epithelial Physiology, a section of the journal Frontiers in Physiology

**Received:** 29 November 2016
**Accepted:** 13 March 2017
**Published:** 30 March 2017

**Citation:**
van der Bel R, Çalişkan M, van Hulst RA, van Lieshout JJ, Stroes ESG and Krediet CTP (2017) Blood Pressure Increase during Oxygen Supplementation in Chronic Kidney Disease Patients Is Mediated by Vasoconstriction Independent of Baroreflex Function. Front. Physiol. 8:186. doi: 10.3389/fphys.2017.00186

Renal hypoxia is thought to be an important pathophysiological factor in the progression of chronic kidney disease (CKD) and the associated hypertension. In a previous study among CKD patients, supplementation with 100% oxygen reduced sympathetic nerve activity (SNA) and lowered blood pressure (BP). We aimed to assess the underlying haemodynamic modulation and hypothesized a decreased systemic vascular resistance (SVR). To that end, 19 CKD patients were studied during 15-min intervals of increasing partial oxygen pressure ($ppO_2$) from room air (0.21 ATA) to 1.0 ATA and further up to 2.4 ATA, while continuously measuring finger arterial blood pressure (Finapres). Off-line, we derived indexes of SVR, cardiac output (CO) and baroreflex sensitivity from the continuous BP recordings (Modelflow). During oxygen supplementation, systolic, and diastolic BP both increased dose-dependently from 128 ± 24 and 72 ± 19 mmHg respectively at baseline to 141 ± 23 ($p < 0.001$) and 80 ± 21 mmHg ($p < 0.001$) at 1.0 ATA oxygen. Comparing baseline and 1.0 ATA oxygen, SVR increased from 1440 ± 546 to 1745 ± 710 dyn·s/cm$^5$ ($p = 0.009$), heart rate decreased from 60 ± 8 to 58 ± 6 bpm ($p < 0.001$) and CO from 5.0 ± 1.3 to 4.6 ± 1.1 L/min ($p = 0.02$). Baroreflex sensitivity remained unchanged (13 ± 13 to 15 ± 12 ms/mmHg). These blood pressure effects were absent in a negative control group of eight young healthy subjects. We conclude that oxygen supplementation in CKD patients causes a non-baroreflex mediated increased in SVR and blood pressure.

**Keywords: chronic kidney disease, hypertension, hyperbaric oxygen supplementation, renal hypoxia, systemic vascular resistance, cardiac output**

## INTRODUCTION

Hypertension is a hallmark of chronic kidney disease (CKD). There is substantial evidence that this can be attributed to increased sympathetic nerve activity (SNA) (Converse et al., 1992; Koomans et al., 2004; Neumann et al., 2004; Herzog et al., 2008). The mechanisms underlying increased SNA in CKD are not completely understood. Several studies have reported an attenuation of SNA and

blood pressure (BP) following bilateral nephrectomy (Medina et al., 1972; Getts et al., 2006; Gawish et al., 2010). This has founded the concept that the trigger of the enhanced central sympathetic outflow in CKD patients resides in the affected kidneys themself. Deterioration of renal oxygenation by altered renal perfusion and increased metabolic demand has been postulated as a common factor in the progression of CKD (Eckardt et al., 2005; Evans et al., 2013) and nephrogenic sympathetic hyperactivity and hypertension (Converse et al., 1992; Hausberg, 2002; Siddiqi et al., 2009).

In this respect, altered renal chemo-receptor activation in CKD has been studied by various groups (Hausberg and Grassi, 2007; Hering et al., 2007; Park et al., 2008). Of special interest is a study by Hering et al. who exposed CKD patients (mean serum creatinine 5.5 ± 0.3 mg/dL) to 100% oxygen over a non-rebreathing mask for 15 min. This resulted in a 30% reduction in SNA accompanied by a lower pulse pressure (Hering et al., 2007). This response was absent in healthy controls and non-CKD patient populations (Kones, 2011; Stub et al., 2015). Therefore, the observed effects on sympathetic nerve activity and BP were attributed to CKD-specific hypoxia-mediated renal chemo-reflex deactivation. Additional support for the existence of a kidney-derived chemo-reflex, were the observations in non-CKD sympathetically hyperactive patient groups not showing such a response (Ganz et al., 1972; Thomson et al., 2002). Thus, the haemodynamic response to oxygen supplementation appears to be uniquely different in CKD patients.

Ever since, it has been assumed that the underlying mechanism of the BP effects of oxygen supplementation in CKD patients is mediated by a decrease in sympathetic outflow leading to a reduction in systemic vascular resistance (Thukkani and Bhatt, 2013). However, so far this has never been substantiated. Therefore, we set out to revisit and further explore the concept that systemic hyperoxia suppresses vasoconstrictor activity and BP in CKD patients. Our aim was to elaborate on the haemodynamic mechanisms underlying the BP changes as previously reported by others. We hypothesized: (1) that the previously observed decrease in BP is the effect of a decrease in (sympathetically mediated) systemic vascular resistance (SVR), and (2) that this effect is related to the amount of oxygen provided in a dose-dependent fashion.

# MATERIALS AND METHODS

## Participants

We studied 19 CKD patients (14 males, 5 females; age 62 ± 10 years, BMI 25.7 ± 3.7 kg/m$^2$, eGFR 23.6 ± 7.2 mL/min/1.73 m$^2$). Of all patients, values of hemoglobin and proteinuria were available from clinical routine testing within 3 months before the study. Baseline characteristics, including medication use and disease background are given in **Table 1**. To verify the known hemodynamic effects of hyperoxia and thereby the accuracy of our methods, we also included a group of eight young healthy subjects (6 males and 2 females, mean age 26 ± 3 years, BMI 23.1 ± 2.7 kg/m$^2$). The study was carried out in accordance with the Declaration of Helsinki of the World Medical Association (2013). The Medical Ethics Review Committee of the Academic Medical Center (University of Amsterdam, Amsterdam, The Netherlands) approved the study protocol. Before inclusion all participants provided written informed consent.

**TABLE 1 | Baseline characteristics of the CKD patients.**

| | | Patients |
|---|---|---|
| Age (years) | | 62 (10) |
| Gender (m/f) | | 14/5 |
| Body weight (kg) | | 77 (13) |
| BMI (kg/m2) | | 25.7 (3.7) |
| Smoking status | Yes/No | 4/15 |
| Systolic/diastolic blood pressure (mmHg) | | 128 (24)/72 (19) |
| eGFR (mL/min/1.73 m2) | | 22.5 (5–40) |
| Haemoglobin (mmol/L) | | 7.9 (1.3)* |
| Proteinuria (g/L) | | 0.53 (0.03–2.8) |
| Renal disease | Vascular | 10 |
| | Glomerulonephritis | 4 |
| | Tubulo-interstitial | 1 |
| | Polycystic disease | 3 |
| | Unknown | 1 |
| Antihypertensive medication | Alpha blockers | 4 |
| | Beta blockers | 10 |
| | ACE inhibitors | 6 |
| | ARBs | 8 |
| | Calcium antagonists | 11 |
| | Diuretics | 8 |

*Data are presented as absolute number or mean (SD) or with range in case the outcome measure is skewed. ACE, angiotensin converting enzyme. ARB, Angiotensin II receptor blocker. *Six patients used erythropoietin-analogs.*

## Normobaric Challenge

After an initial baseline measurement of 15 min room air (RA), a non-rebreathing mask was positioned over nose and mouth. Blood pressure measurement (see below) was continued while room air, partial pressure of oxygen ($ppO_2$) 0.21 ATA, was provided over the mask at 15 L/min for another 15 min. Thereafter the $ppO_2$ in the breathing gas was increased to 50% $O_2$ ($ppO_2$ 0.5 ATA) and 100% $O_2$ ($ppO_2$ 1.0 ATA) respectively again for 15 min at each dose (**Figure 1**). The oxygen dose was regulated using an air-oxygen blender (Precision Medical Inc., Northampton, USA). Patients were blinded to the dosage and were not aware when the oxygen dose was altered. Measurements were performed in a quiet room with the temperature controlled at 22°C. During all measurements, participants remained quietly in the supine position. Patients receiving angiotensin-converting-enzyme (ACE) inhibitors and/or angiotensin II receptor blockers (ARBs) had postponed the intake of these medications until after the study visit.

## Hyperbaric Challenge

In another session, subjects were exposed to hyperbaric oxygen in a hyperbaric chamber. Again, during all measurements patients

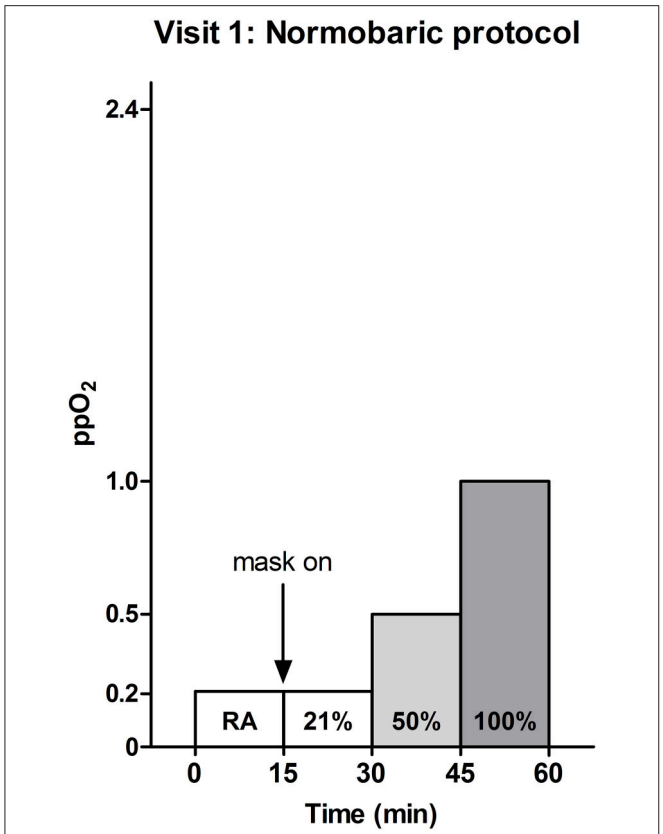


**FIGURE 1 | Normobaric oxygen supplementation protocol.** Room air (RA) and oxygen at different concentrations (21, 50, or 100%) were provided for 15 min each. Measurements were performed at atmospheric pressure, i.e., 1 atmosphere absolute (ATA). At atmospheric pressure a partial oxygen pressure ($ppO_2$) of 1.0 ATA is reached, when 100% oxygen is provided.

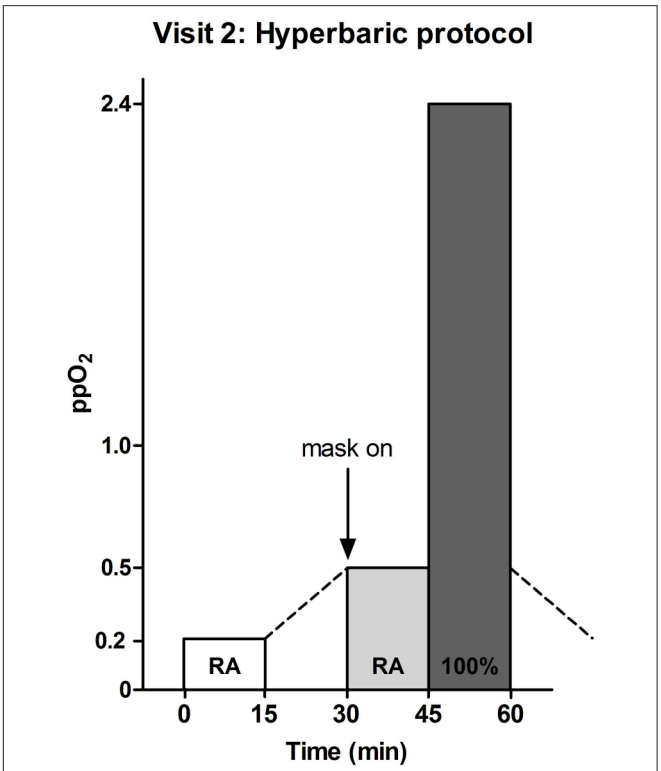


**FIGURE 2 | Hyperbaric oxygen supplementation protocol.** Normobaric and hyperbaric room air (RA) and hyperbaric oxygen (100%) were provided for 15 min each. Measurements were performed at atmospheric pressure (1 ATA) and under hyperbaric conditions (2.4 ATA). At atmospheric pressure a partial oxygen pressure ($ppO_2$) of 1.0 ATA was reached, when 100% oxygen was provided. During hyperbaric oxygen supplementation this further increased 2.4-fold, to 2.4 ATA.

assumed a supine position. Continuous blood pressure was recorded while breathing room air (RA) at atmospheric pressure ($ppO_2$ 0.21 ATA), under hyperbaric conditions at 2.4 ATA ($ppO_2$ 0.5 ATA) and at 2.4 ATA during 100% oxygen supplementation ($ppO_2$ 2.4 ATA, **Figure 2**).

## Continuous Blood Pressure Measurements and Analysis

During all sessions, continuous blood pressure was measured using finger arterial photo-plethysmography (Portapres™, Finapres Medical Systems, Amsterdam, The Netherlands). The device has been validated for use in CKD patients (Imholz et al., 1998). The appropriate size finger cuff was positioned around the mid-phalanx of the left middle finger for all recordings and passively positioned at heart level. The system had been adapted for use under hyperbaric conditions as previously reported in detail (van der Bel et al., 2016).

The finger arterial pressure signal was recorded at 100 Hz and analyzed off-line using the Modelflow algorithm (Beatscope® version 1.1a, Finapres Medical Systems, Amsterdam, The Netherlands). This algorithm provides a validated beat-to-beat estimate of left ventricular stroke volume (SV), based on a nonlinear 3-element model of the input impedance of the aorta (Jellema et al., 1999). Mean arterial pressure (MAP) was the integral over one heart beat and the heart rate (HR) was the inverse of the pulse interval. Cardiac output (CO) was SV times HR. SVR was MAP divided by CO, in $dyn{\cdot}s/cm^5$. Pulse pressure (PP) was systolic BP (SBP) minus diastolic BP (DBP). All hemodynamic parameters were derived from the last minute of the measurements at baseline and at each oxygen dose. Time domain cross-correlation baroreflex sensitivity (xBRS) was calculated from the same intervals as the other parameters, using dedicated software (WinXBRS 2, BMEye, Amsterdam, The Netherlands; Westerhof et al., 2004). The xBRS was computed using beat-to-beat SBP and R–R interval, in a sliding 10 s window. Each instance that a correlation with a significance level of $p \leq 0.01$ was found the xBRS value was recorded.

## Statistical Analysis

Normal distribution of the data was verified using Levine's test and data are presented as mean ± standard deviation, unless otherwise indicated. The within group responses to increasing $ppO_2$ were assessed using general linear modeling. $P < 0.05$ were considered significant.

# RESULTS

## Normobaric Oxygen Challenge (CKD Patients)

SBP and DBP both increased with increasing oxygen supplementation from 128 ± 24/72 ± 19 at baseline to 141 ± 23/80 ± 21 mmHg systolic/diastolic at a $ppO_2$ of 1.0 ATA, $F_{(3, 18)} = 12.6$, $p < 0.001$ for SBP and $F_{(3, 18)} = 8.8$, $p < 0.001$ for DBP (**Figures 3A,B**). The pulse pressure increased as well, from 55 ± 13 to 61 ± 11 mmHg [$F_{(3, 18)} = 5.8$, $p = 0.002$, **Figure 3D**]. HR [60 ± 8 bpm at baseline; 58 ± 6 bpm at 1.0 ATA $ppO_2$, $F_{(3, 18)} = 25.1$, $p < 0.001$] and CO [5.0 ± 1.3 L/min at baseline; 4.6 ± 1.1 L/min at 1.0 ATA $ppO_2$, $F_{(3, 18)} = 3.6$, $p = 0.02$] decreased during oxygen supplementation (**Figures 3E,G**). SVR increased from 1440 ± 546 to 1745 ± 710 dyn·s/cm$^5$, [$F_{(3, 18)} = 4.3$, $p = 0.009$, **Figure 3F**]. xBRS remained unchanged with 13 ± 13 ms/mmHg at baseline and 15 ± 12 ms/mmHg at 1.0 ATA $ppO_2$ [$F_{(3, 7)} = 0.647$; $p = 0.59$, **Figure 3H**].

## Hyperbaric Oxygen Challenge (CKD Patients)

Due to the results of oxygen supplementation under normobaric conditions, the hyperbaric experiments were suspended for ethical reasons after studying four patients (and not carried out in the control subjects). When changing from a normobaric (1 ATA) to a hyperbaric condition (2.4 ATA, **Figure 4**), SBP and DBP where 121 ± 17/70 ± 16 at baseline and 146 ± 18/84 ± 11 mmHg systolic/diastolic at a $ppO_2$ of 2.4 ATA (**Figures 4A,B**). Pulse pressure was 51 ± 9 at baseline and 62 ± 13 mmHg at 2.4 ATA $ppO_2$ (**Figure 4D**). HR was 64 ± 9 bpm at baseline and 60 ± 8 bpm at 2.4 ATA $ppO_2$ and CO was 4.2 ± 1.3 L/min at baseline and 3.6 ± 0.4 L/min at 2.4 ATA $ppO_2$ (**Figures 4E,G**). No further increase in SVR was observed during hyperbaric oxygen supplementation (**Figure 4F**). Changes in SBP did not correlate with eGFR ($R = 0.013$).

## Control Subjects

During the normobaric oxygen challenge in the control group, SVR increased significantly from 903 at baseline to 985 dyn·s/cm$^5$ at a $ppO_2$ of 1.0 ATA, $F_{(3, 7)} = 11.6$; $p < 0.001$ (**Figure 3F**). SBP [$F_{(3, 7)} = 2.60$; $p = 0.08$], DBP [$F_{(3, 7)} = 1.33$; $p = 0.29$], MAP [$F_{(3, 7)} = 1.28$; $p = 0.31$] and PP [$F_{(3, 7)} = 2.07$; $p = 0.13$], did not change (**Figures 3A–D**), HR [$F_{(3,7)} = 13.0$; $p < 0.001$] and CO [$F_{(3, 7)} = 6.73$; $p = 0.002$] decreased with oxygen supplementation (**Figures 3E,G**). xBRS remained unchanged [$F_{(3, 7)} = 0.884$; $p = 0.47$, **Figure 3H**].

# DISCUSSION

The findings of this study can be summarized as follows: (1) Oxygen supplementation causes a dose-dependent blood pressure increase among CKD patients. (2) This blood pressure increase is caused by an SVR increase. (3) The simultaneous HR decrease with unchanged baroreflex sensitivity indicates that the SVR increase is caused by a direct vascular effect of the increased plasma $ppO_2$ rather than a response of the baroreflex.

Our results seem to contradict previous findings in CKD patients (Hering et al., 2007). Hering et al. found that in a similar experiment, exposing CKD patients to 100% oxygen resulted in a 30% reduction in muscle sympathetic nerve activity (Hering et al., 2007), whereas we find an increased systemic vasoconstriction. Upon closer inspection, their SNA decrease was accompanied by a slight increase in diastolic blood pressure—similar to what we found—which was not elaborated upon further. Instead, the analysis focussed on a decreased pulse pressure. However, this rise in diastolic blood pressure may be the key to explaining the decreased SNA during oxygen supplementation in CKD patients. Therefore, we need to consider the haemodynamic effects of hyperoxia in health with regard to baroreflex function.

In healthy humans, oxygen supplementation induces hyperoxic vasoconstriction as observed in our controls and previously reported data (Waring et al., 2003; Gill and Bell, 2004). This response is due to (1) the direct vasoconstrictive effect of plasma $pO_2$ itself and (2) its ability to simultaneously hinder vasodilatation by reducing nitric oxide (NO) bioavailability (Waring et al., 2003; Gill and Bell, 2004). In contrast to sympathetically mediated vasoconstriction, hyperoxic vasoconstriction acts independent of baroreflex function (Whalen et al., 1965; Villanucci et al., 1990). CKD patients have an intact arterial baroreflex system (Eckberg and Sleight, 1992), therefore modulation of the baroreflex leads to changes in HR and sympathetic activation to occur simultaneously and in the same direction, i.e., HR increase and sympathetic vasoconstriction versus HR decrease and sympathetic decrease (leading to vasodilation). However, in our experiment vasoconstriction is observed with a simultaneous decrease in HR during oxygen supplementation. This is indicative of a deactivating signal by the baroreflex, resulting in a reduction in HR. Based on the coupling of sympathetic activity and HR, this explains the decrease in sympathetic activity while diastolic blood pressure increases due to direct oxygen driven and non-baroreflex mediated vasoconstriction (Hering et al., 2007).

To explain the blood pressure increase that we observed in CKD patients, we consider the ability of hyperoxia to decrease vasodilatory capacity by reducing NO bioavailability. Reduced NO bioavailability in CKD patients (similar to diabetic and hypertension patients; Al-Waili et al., 2006) may impede the attenuation of the hemodynamic effects of hyperoxic vasoconstriction (Endemann and Schiffrin, 2004; Martens and Edwards, 2011). Therefore, our data are most consistent with inadequate attenuation of hyperoxic vasoconstriction in patients with CKD-related endothelial dysfunction.

Thus, it appears that the hemodynamic response to hyperoxia is not uniquely affected in CKD patients. Instead, it seems that hyperoxic vasoconstriction induces an increase in blood pressure, leading to baroreflex deactivation with a reduction in systemic sympathetic tone. Our data (and in hindsight those from Hering et al.) do not support nor exclude the existence of a CKD-kidney specific hypoxic triggering of (either renal or extra-renal) chemo receptors. The overwhelming effects of oxygen on systemic vasoconstriction render the experimental set-up unsuitable to

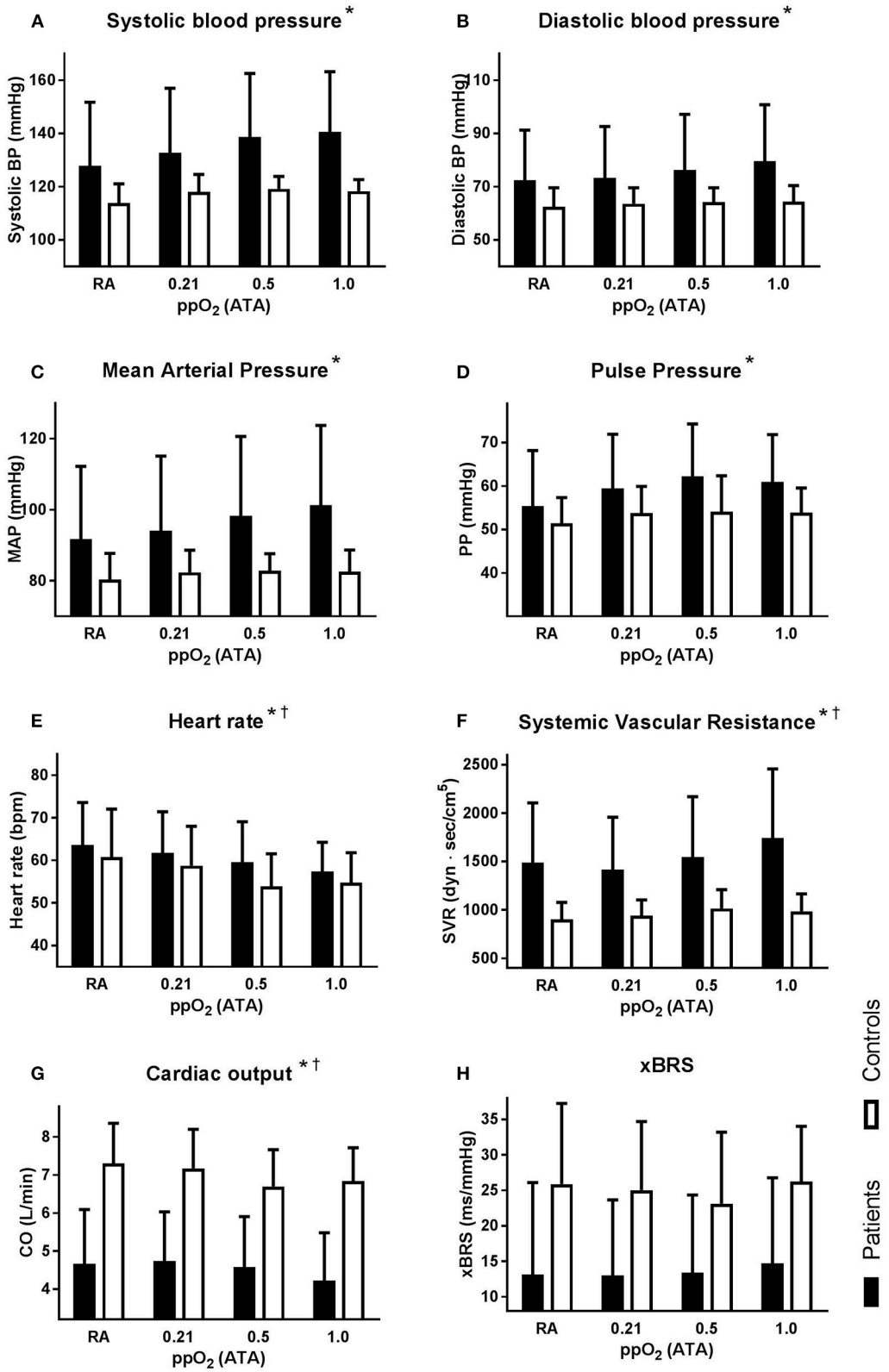


**FIGURE 3 | Hemodynamic response to normobaric oxygen supplementation, for the patient (solid bars) and the young healthy controls (open bars).** All graphs depict absolute mean ± *SD* at each condition: room air (RA), 21% oxygen over a non-rebreathing mask ($ppO_2$ 0.21 ATA), 50% oxygen ($ppO_2$ 0.5 ATA), and 100% oxygen ($ppO_2$ 1.0 ATA). Averages over the last minute of each condition for: **(A)** systolic blood pressure; **(B)** diastolic blood pressure; **(C)** mean arterial pressure (MAP); **(D)** pulse pressure (PP); **(E)** heart rate (HR); **(F)** systemic vascular resistance (SVR); **(G)** cardiac output (CO); **(H)** baroreflex sensitivity (xBRS). Designation of significant responses to oxygen supplementation in patients * and in controls†.

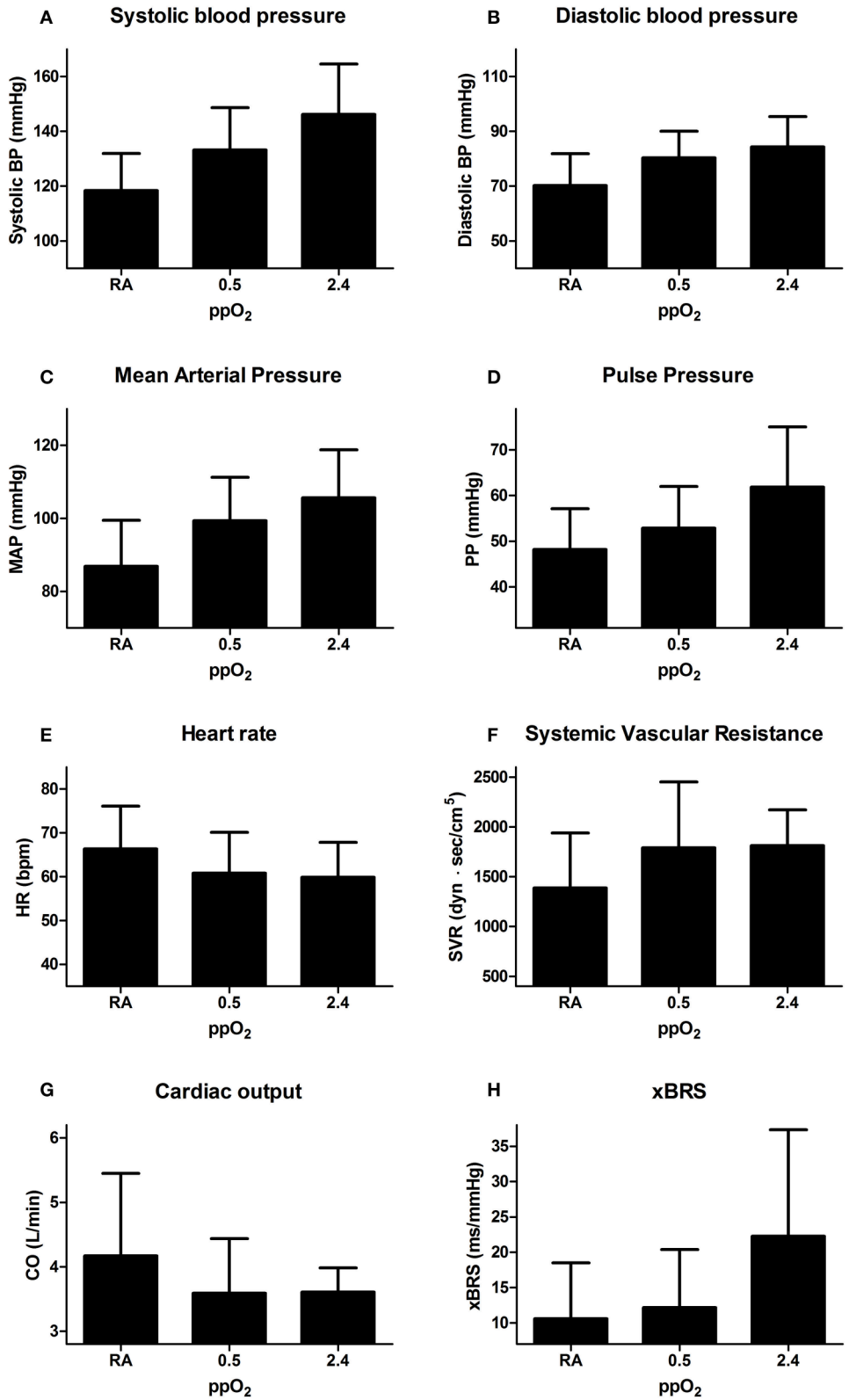


**FIGURE 4 | Hemodynamic response to hyperbaric oxygen supplementation.** All graphs depict absolute mean ± *SD* at each condition: room air (RA), hyperbaric RA ($ppO_2$ 0.5 ATA), and hyperbaric oxygen ($ppO_2$ 2.4 ATA). Averages over the last minute of blood pressure registration at each condition of: **(A)** systolic blood pressure; **(B)** diastolic blood pressure; **(C)** mean arterial pressure (MAP); **(D)** pulse pressure (PP); **(E)** heart rate (HR); **(F)** systemic vascular resistance (SVR); **(G)** cardiac output (CO); **(H)** baroreflex sensitivity (xBRS).

detect any possible subtle effects of kidney specific oxygenation on sympathetic outflow.

A possible clinical implication of these results is that oxygen supplementation might act as a cardiovascular stressor in CKD patients. Interestingly, this is in line with observations that oxygen supplementation in selected clinical patients is associated with worse outcome (Kones, 2011; Stub et al., 2015). Additionally, our study provides some more explanation on the lack of efficacy of catheter based renal denervation. The presumed decrease in SNA and blood pressure by oxygen supplementation in CKD patients was one of the founding principles of the pathophysiological rationale for renal sympathetic denervation (Schlaich et al., 2011; Davis et al., 2013). Eventually, renal sympathetic denervation showed not to have any effect on blood pressure, and specifically not in CKD patients (Bhatt et al., 2014). Our data question part of the founding rationale for renal sympathetic denervation.

Our study has several methodological limitations that merit discussion. First, patients continued the use of anti-hypertensive medication during the study. For ethical reasons these medications could not be fully withdrawn and was a compromise between taking out possible interfering factors versus patient risk. Our considerations were as follows: because of the specific effects on renal hemodynamics and oxygenation, ACE inhibitors and ARB's were stopped, as other antihypertensive drugs have a less (if any) pronounced effect on RAAS activity or intrarenal oxygen delivery. However, this may only have blunted the hemodynamic effects and thereby would not have affected our eventual conclusions, especially since patients acted as their own control. The same holds for the heterogeneous distributed baseline parameters (e.g., eGFR, smoking status, hemoglobin level) in our relatively small patient group. Secondly, we did not assess changes in $CO_2$ partial pressure during oxygen supplementation. However, this has previously been shown not to be influenced by oxygen supplementation (Whalen et al., 1965). Also, the group of young healthy controls was not selected to be age matched, because it intended to verify the accuracy of our method. Others have reported upon the effects of hyperoxia in healthy elderly subjects previously (Whalen et al., 1965; Al-Waili et al., 2006). Lastly, the observers were not blinded but this was corrected by standardizing the time frame selection for analysis.

## CONCLUSIONS

We have shown that oxygen supplementation in CKD patients increases blood pressure in a dose dependent fashion. This response is mediated by an increase in SVR, likely as the result of hyperoxic vasoconstriction independent of baroreflex function.

## AUTHOR CONTRIBUTIONS

Study conception and design by RB, RH, ES, CK; Data acquisition, analysis and/or interpretation by RB, MÇ, RH, JL, CK; Drafting of the manuscript by RB, CK; Revising by MÇ, RH, JL, ES, CK; Final approval of manuscript provided by RB, MÇ, RH, JL, ES, CK.

## FUNDING

This project was funded by the Dutch Kidney Foundation (Project KJPB 12.029 to CP). CP is supported by the Netherlands Organization for Health Research and Development (ZonMw, Clinical Fellowship 40007039712461).

## REFERENCES

Al-Waili, N. S., Butler, G. J., Beale, J., Abdullah, M. S., Finkelstein, M., Merrow, M., et al. (2006). Influences of hyperbaric oxygen on blood pressure, heart rate and blood glucose levels in patients with diabetes mellitus and hypertension. *Arch. Med. Res.* 37, 991–997. doi: 10.1016/j.arcmed.2006.05.009

Bhatt, D. L., Kandzari, D. E., O'Neill, W. W., D'Agostino, R., Flack, J. M., Katzen, B. T., et al. (2014). A controlled trial of renal denervation for resistant hypertension. *N. Engl. J. Med.* 370, 1393–1401. doi: 10.1056/NEJMoa1402670

Converse, R. L. Jr., Jacobsen, T. N., Toto, R. D., Jost, C. M., Cosentino, F., Fouad-Tarazi, F., et al. (1992). Sympathetic overactivity in patients with chronic renal failure. *N. Engl. J. Med.* 327, 1912–1918. doi: 10.1056/NEJM199212313272704

Davis, M. I., Filion, K. B., Zhang, D., Eisenberg, M. J., Afilalo, J., Schiffrin, E. L., et al. (2013). Effectiveness of renal denervation therapy for resistant hypertension: a systematic review and meta-analysis. *J. Am. Coll. Cardiol.* 62, 231–241. doi: 10.1016/j.jacc.2013.04.010

Eckardt, K. U., Bernhardt, W. M., Weidemann, A., Warnecke, C., Rosenberger, C., Wiesener, M. S., et al. (2005). Role of hypoxia in the pathogenesis of renal disease. *Kidney Int. Suppl.* 68, S46–S51. doi: 10.1111/j.1523-1755.2005.09909.x

Eckberg, D. L., and Sleight, P. (1992). *Human Baroreflexes in Health and Disease*. Oxford: Oxford University Press.

Endemann, D. H., and Schiffrin, E. L. (2004). Endothelial dysfunction. *J. Am. Soc. Nephrol.* 15, 1983–1992. doi: 10.1097/01.ASN.0000132474.50966.DA

Evans, R. G., Ince, C., Joles, J. A., Smith, D. W., May, C. N., O'Connor, P. M., et al. (2013). Haemodynamic influences on kidney oxygenation: clinical implications of integrative physiology. *Clin. Exp. Pharmacol. Physiol.* 40, 106–122. doi: 10.1111/1440-1681.12031

Ganz, W., Donoso, R., Marcus, H., and Swan, H. J. (1972). Coronary hemodynamics and myocardial oxygen metabolism during oxygen breathing in patients with and without coronary artery disease. *Circulation* 45, 763–768. doi: 10.1161/01.CIR.45.4.763

Gawish, A. E., Donia, F., Fathi, T., Al-Mousawi, M., and Samhan, M. (2010). It takes time after bilateral nephrectomy for better control of resistant hypertension in renal transplant patients. *Transplant. Proc.* 42, 1682–1684. doi: 10.1016/j.transproceed.2010.04.014

Getts, R. T., Hazlett, S. M., Sharma, S. B., McGill, R. L., Biederman, R. W., Marcus, R. J., et al. (2006). Regression of left ventricular hypertrophy after bilateral nephrectomy. *Nephrol. Dial. Transplant* 21, 1089–1091. doi: 10.1093/ndt/gfi321

Gill, A. L., and Bell, C. N. (2004). Hyperbaric oxygen: its uses, mechanisms of action and outcomes. *QJM* 97, 385–395. doi: 10.1093/qjmed/hch074

Hausberg, M. (2002). Sympathetic nerve activity in end-stage renal disease. *Circulation* 106, 1974–1979. doi: 10.1161/01.CIR.0000034043.16664.96

Hausberg, M., and Grassi, G. (2007). Mechanisms of sympathetic overactivity in patients with chronic renal failure: a role for chemoreflex activation? *J. Hypertens.* 25, 47–49. doi: 10.1097/HJH.0b013e3280119286

Hering, D., Zdrojewski, Z., Krol, E., Kara, T., Kucharska, W., Somers, V. K., et al. (2007). Tonic chemoreflex activation contributes to the elevated muscle sympathetic nerve activity in patients with chronic renal failure. *J. Hypertens.* 25, 157–161. doi: 10.1097/HJH.0b013e3280102d92

Herzog, C. A., Mangrum, J. M., and Passman, R. (2008). Sudden cardiac death and dialysis patients. *Semin. Dial.* 21, 300–307. doi: 10.1111/j.1525-139X.2008.00455.x

Imholz, B. P., Wieling, W., Van Montfrans, G. A., and Wesseling, K. H. (1998). Fifteen years experience with finger arterial pressure

monitoring: assessment of the technology. *Cardiovasc. Res.* 38, 605–616. doi: 10.1016/S0008-6363(98)00067-4

Jellema, W. T., Wesseling, K. H., Groeneveld, A. B., Stoutenbeek, C. P., Thijs, L. G., and van Lieshout, J. J. (1999). Continuous cardiac output in septic shock by simulating a model of the aortic input impedance: a comparison with bolus injection thermodilution. *Anesthesiology* 90, 1317–1328. doi: 10.1097/00000542-199905000-00016

Kones, R. (2011). Oxygen therapy for acute myocardial infarction-then and now. A century of uncertainty. *Am. J. Med.* 124, 1000–1005. doi: 10.1016/j.amjmed.2011.04.034

Koomans, H. A., Blankestijn, P. J., and Joles, J. A. (2004). Sympathetic hyperactivity in chronic renal failure: a wake-up call. *J. Am. Soc. Nephrol.* 15, 524–537. doi: 10.1097/01.ASN.0000113320.57127.B9

Martens, C. R., and Edwards, D. G. (2011). Peripheral vascular dysfunction in chronic kidney disease. *Cardiol. Res. Pract.* 2011:267257. doi: 10.4061/2011/267257

Medina, A., Bell, P. R., Briggs, J. D., Brown, J. J., Fine, A., Lever, A. F., et al. (1972). Changes of blood pressure, renin, and angiotensin after bilateral nephrectomy in patients with chronic renal failure. *Br. Med. J.* 4, 694–696. doi: 10.1136/bmj.4.5842.694

Neumann, J., Ligtenberg, G., Klein, I. I., Koomans, H. A., and Blankestijn, P. J. (2004). Sympathetic hyperactivity in chronic kidney disease: pathogenesis, clinical relevance, and treatment. *Kidney Int.* 65, 1568–1576. doi: 10.1111/j.1523-1755.2004.00552.x

Park, J., Campese, V. M., and Middlekauff, H. R. (2008). Exercise pressor reflex in humans with end-stage renal disease. *Am. J. Physiol. Regul. Integr. Comp. Physiol.* 295, R1188–R1194. doi: 10.1152/ajpregu.90473.2008

Schlaich, M. P., Krum, H., Sobotka, P. A., and Esler, M. D. (2011). Renal denervation and hypertension. *Am. J. Hypertens.* 24, 635–642. doi: 10.1038/ajh.2011.35

Siddiqi, L., Joles, J. A., Grassi, G., and Blankestijn, P. J. (2009). Is kidney ischemia the central mechanism in parallel activation of the renin and sympathetic system? *J. Hypertens.* 27, 1341–1349. doi: 10.1097/HJH.0b013e32832b521b

Stub, D., Smith, K., Bernard, S., Nehme, Z., Stephenson, M., Bray, J. E., et al. (2015). Air versus oxygen in ST-segment-elevation myocardial infarction. *Circulation* 131, 2143–2150. doi: 10.1161/CIRCULATIONAHA.114.014494

Thomson, A. J., Webb, D. J., Maxwell, S. R., and Grant, I. S. (2002). Oxygen therapy in acute medical care. *BMJ* 324, 1406–1407. doi: 10.1136/bmj.324.7351.1406

Thukkani, A. K., and Bhatt, D. L. (2013). Renal denervation therapy for hypertension. *Circulation* 128, 2251–2254. doi: 10.1161/CIRCULATIONAHA.113.004660

van der Bel, R., Sliggers, B. C., van Houwelingen, M. J., van Lieshout, J. J., Halliwill, J. R., van Hulst, R. A., et al. (2016). A modified device for continuous non-invasive blood pressure measurements in humans under hyperbaric and/or oxygen-enriched conditions. *Diving Hyperb. Med.* 46, 38–42.

Villanucci, S., Di Marzio, G. E., Scholl, M., Pivorine, C., d'Adamo, C., and Settimi, F. (1990). Cardiovascular changes induced by hyperbaric oxygen therapy. *Undersea Biomed. Res.* 17(Suppl. 1):117.

Waring, W. S., Thomson, A. J., Adwani, S. H., Rosseel, A. J., Potter, J. F., Webb, D. J., et al. (2003). Cardiovascular effects of acute oxygen administration in healthy adults. *J. Cardiovasc. Pharmacol.* 42, 245–250. doi: 10.1097/00005344-200308000-00014

Westerhof, B. E., Gisolf, J., Stok, W. J., Wesseling, K. H., and Karemaker, J. M. (2004). Time-domain cross-correlation baroreflex sensitivity: performance on the EUROBAVAR data set. *J. Hypertens.* 22, 1371–1380. doi: 10.1097/01.hjh.0000125439.28861.ed

Whalen, R. E., Saltzman, H. A., Holloway, D. H. Jr., McIntosh, H. D., Sieker, H. O., and Brown, I. W. Jr. (1965). Cardiovascular and blood gas responses to hyperbaric oxygenation. *Am. J. Cardiol.* 15, 638–646. doi: 10.1016/0002-9149(65)90350-4

**Conflict of Interest Statement:** The authors declare that the research was conducted in the absence of any commercial or financial relationships that could be construed as a potential conflict of interest.

frontiers in Physiology

REVIEW
published: 21 February 2017
doi: 10.3389/fphys.2017.00099

# Renal Hypoxia in CKD; Pathophysiology and Detecting Methods

*Yosuke Hirakawa, Tetsuhiro Tanaka and Masaomi Nangaku **

*Division of Nephrology, The University of Tokyo School of Medicine, Hongo, Japan*

Chronic kidney disease (CKD) is a major public health problem. Accumulating evidence suggests that CKD aggravates renal hypoxia, and in turn, renal hypoxia accelerates CKD progression. To eliminate this vicious cycle, hypoxia-related therapies, such as hypoxia-inducible factor (HIF) activation (prolyl hydroxylase domain inhibition) or NF-E2-related factor 2 activation, are currently under investigation. Clinical studies have revealed heterogeneity in renal oxygenation; therefore, the detection of patients with more hypoxic kidneys can be used to identify likely responders to hypoxia-oriented therapies. In this review, we provide a detailed description of current hypoxia detection methods. HIF degradation correlates with the intracellular oxygen concentration; thus, methods that can detect intracellular oxygen tension changes are desirable. The use of a microelectrode is a classical technique that is superior in quantitative performance; however, its high invasiveness and the fact that it reflects the extracellular oxygen tension are disadvantages. Pimonidazole protein adduct immunohistochemistry and HIF activation detection reflect intracellular oxygen tension, but these techniques yield qualitative data. Blood oxygen level-dependent magnetic resonance imaging has the advantage of low invasiveness, high quantitative performance, and application in clinical use, but its biggest disadvantage is that it measures only deoxyhemoglobin concentrations. Phosphorescence lifetime measurement is a relatively novel *in vivo* oxygen sensing technique that has the advantage of being quantitative; however, it has several disadvantages, such as toxicity of the phosphorescent dye and the inability to assess deeper tissues. Understanding the advantages and disadvantages of these hypoxia detection methods will help researchers precisely assess renal hypoxia and develop new therapeutics against renal hypoxia-associated CKD.

**Keywords: chronic kidney disease, hypoxia, hypoxia-inducible factor, Nrf2, microelectrode, pimonidazole, BOLD-MRI, phosphorescence**

OPEN ACCESS

***Edited by:***
*Maarten Koeners, University of Bristol, UK*

***Reviewed by:***
*Prabhleen Singh, UC San Diego, USA*
*Agnieszka Swiatecka-Urban, University of Pittsburgh, USA*
*William J. Welch, Georgetown University, USA*

***Correspondence:**
*Masaomi Nangaku*
*mnangaku-tky@umin.ac.jp*

***Specialty section:***
*This article was submitted to Renal and Epithelial Physiology, a section of the journal Frontiers in Physiology*

***Received:*** *30 November 2016*
***Accepted:*** *06 February 2017*
***Published:*** *21 February 2017*

***Citation:***
*Hirakawa Y, Tanaka T and Nangaku M (2017) Renal Hypoxia in CKD; Pathophysiology and Detecting Methods. Front. Physiol. 8:99. doi: 10.3389/fphys.2017.00099*

## INTRODUCTION

Chronic kidney disease (CKD) remains a major public health problem in both developed and developing countries despite enormous treatment efforts (Collins et al., 2015; Liyanage et al., 2015). Many clinical conditions, such as diabetes mellitus, glomerulonephritis, hypertension, and genetic disorders, are causative factors of CKD. However, once renal fibrosis, a major pathological hallmark

of CKD, reaches a certain threshold, CKD progression becomes irreversible and independent of the initial cause (Fine et al., 2000; Nangaku, 2006). Thus, the final common pathways of CKD progression have been extensively studied. Renal hypoxia (i.e., decreased oxygen tension in the kidney), particularly in the tubulointerstitium, is a candidate prognostic marker for CKD progression (Nangaku, 2006; Mimura and Nangaku, 2010). Increased hemoglobin concentrations, which ameliorate renal hypoxia, are associated with a better renal prognosis in CKD patients (Tsubakihara et al., 2012). In support of hypoxia as a marker of poor renal function, sleep apnea syndrome and chronic obstructive pulmonary disease have been identified as risk factors for CKD (Iseki et al., 2008; Hanly and Ahmed, 2014; Chen and Liao, 2016). Although these studies are observational and no intervention studies with domiciliary oxygen therapy or continuous positive air pressure ventilation have been conducted, our results raise the possibility that conditions, such as SAS and COPD result in intermittent or continuous hypoxemia and increase the risk of CKD development via renal hypoxia aggravation.

## CELLULAR RESPONSE TO HYPOXIA

Oxygen is imperative for mitochondrial oxidative phosphorylation, a process that produces sufficient ATP amounts in metazoans. Thus, cellular response against insufficient oxygen supply is precisely controlled. Transcriptional factors known as hypoxia-inducible factors (HIFs) play a central role in the anti-hypoxia defense system (Semenza, 2014). HIFs are composed of two subunits: HIF-α, an oxygen-sensitive subunit, and HIF-β, an oxygen-insensitive subunit. The cellular concentration of HIF-α is strictly tuned by the oxygen tension. Prolyl hydroxylase domain (PHD) proteins hydroxylate HIF-α using oxygen molecules as substrates. Next, hydroxylated HIF-α recruits von Hippel–Lindau tumor suppressor, which triggers ubiquitination and proteasomal degradation (**Figure 1**). In this mechanism, HIF-α hydroxylation is the rate-limiting step. Therefore, the cellular concentration of HIF-α is dependent on oxygen tension. Given that HIF-α hydroxylation occurs in the cytosol, the intracellular oxygen tension is more important than the extracellular oxygen tension, which is usually estimated by measuring the intravascular oxygen tension.

Increases in cytoplasmic HIF-α concentrations due to decreased intracellular oxygen tension or PHD pharmacological inhibition lead to the formation of a heterodimer between HIF-α and HIF-1β. The heterodimer translocates into the nucleus and binds to the consensus enhancer via hypoxia-responsive elements (HREs), which then upregulates downstream target genes. The representative downstream genes include vascular endothelial growth factor (VEGF), erythropoietin (EPO), glucose transporter 1, and heme oxygenase 1, which protect the cell from hypoxia by promoting neovascularization, erythropoiesis, and glycolysis and by decreasing oxidative stress, respectively. There are three isoforms of HIF-α: HIF-1α, HIF-2α, and HIF-3α. In the kidney, HIF-1α is dominantly expressed in tubular cells, whereas HIF-2α accumulates in interstitial and endothelial cells (Rosenberger et al., 2002). The expression and function of HIF-3α remains elusive. Full-length HIF-3α works as a transcriptional factor with HIF-1β; however, some of its splice variants work as dominant negative forms against HIF-1α and HIF-2α (Duan, 2016).

## RENAL HYPOXIA PATHOPHYSIOLOGY

The oxygen tension in the kidney is relatively lower in healthy individuals, even though the kidneys receive approximately 20% of the blood pumped out from the heart. One explanation is the oxygen shunt between the arterial and venous vessels that run parallel in the kidney, as proven by oxygen electrodes (Schurek et al., 1990). Recently, it has been actively debated whether an arteriovenous oxygen shunt affects renal oxygenation based on results from a three-dimensional computational model. To obtain a clear answer, the quantification of the geometry of artery–vein pairs in the kidney may be needed as results from the three-dimensional computational model vary with the assumption of background vascular networks (Ngo et al., 2014; Evans et al., 2015; Olgac and Kurtcuoglu, 2015). An oxygen shunt supposedly affects renal oxygenation and is likely accountable for the higher oxygen tension in renal veins than in efferent arterioles (Welch et al., 2001) and for the oxygen gradient in the kidney, i.e., the oxygen tension decreases deeper in the renal surface. The oxygen tension in the renal surface is approximately 50 mmHg, whereas the tension in the renal medulla is approximately 30 mmHg, as detected by microelectrodes (Friederich-Persson et al., 2013; Ow et al., 2014; Nordquist et al., 2015). A lower oxygen tension in normal kidneys has also been shown in a study that visualized HIF activity in transgenic mice (Safran et al., 2006). In these mice, the luciferase enzyme was fused to the oxygen-dependent degradation domain of HIF-1α. Thus, luciferase activity simulated HIF-α expression. Under normoxic conditions, the kidneys were the only organ that expressed sufficient luminescence that could be observed in the *in vivo* system.

In addition to its innate low oxygen tension, the kidneys suffer from severe hypoxia as CKD progresses. Renal hypoxia pathophysiology in CKD includes a decrease in oxygen supply and an increase in oxygen consumption. Loss of peritubular capillaries (PTCs) (Kang et al., 2001b; Ohashi et al., 2002), reduction in PTC flow (Matsumoto et al., 2004), and renal anemia (Astor et al., 2002) account for insufficient oxygen supply. Increases in oxygen demand in renal tubules have been shown in a reduced renal mass model (Harris et al., 1988; Nath and Paller, 1990), hypertensive model (Adler and Huang, 2002), and diabetes mellitus model (Korner et al., 1994), and this increase in the reduced renal mass model is corrected by renin–angiotensin–aldosterone axis blockade or HIF activation (Deng et al., 2009, 2010). These hypoxic changes likely exacerbate renal tubular damage. Outer medullary areas, including the S3 segment of the proximal tubules, medullary thick ascending limbs, and medullary collecting ducts, are considered to be most susceptible to hypoxia because

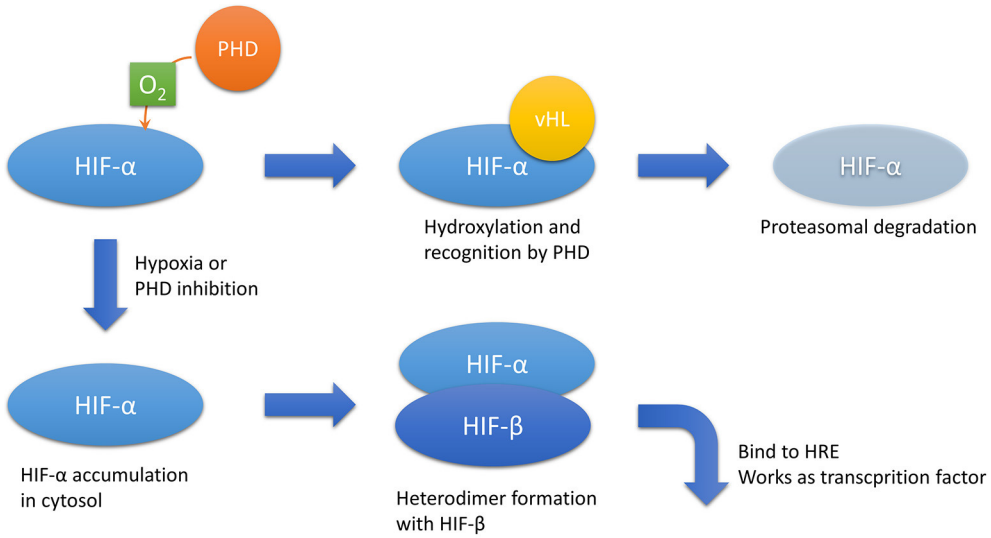


**FIGURE 1 | HIF-α regulation.** In the presence of sufficient oxygen, HIF-α is hydroxylated by PHD. Hydroxylated HIF-α is recognized by vHL, which results in proteasomal degradation. In hypoxic conditions or PHD inhibition, HIF-α accumulates in the cytosol and forms a heterodimer with HIF-β, the hypoxia-insensitive unit. The heterodimer translocates to the nucleus and acts as a transcriptional factor that binds to HREs. Abbreviations: HIF, hypoxia-inducible factor; HREs, hypoxia-responsive elements; PHD, prolyl hydroxylase domain; vHL, von Hippel–Lindau disease tumor suppressor.

histological changes are obvious in these segments of human kidneys with ischemia (Heyman et al., 2010). Differences in several features, including mitochondrial density and transport activity, account for the susceptibility to hypoxic insults. The medullary thick ascending limbs and medullary collecting ducts become more susceptible to hypoxic insults with forced tubular transport (Shanley et al., 1986; Brezis and Rosen, 1995; Epstein, 1997).

## HYPOXIA-ORIENTED THERAPY AGAINST CKD

Renal hypoxia accelerates CKD progression, and in turn, CKD exacerbates renal hypoxia. Therefore, eliminating this cycle is a promising strategy against CKD. One approach is HIF activation via PHD inhibition. Cobalt chloride is a classical PHD inhibitor, and it ameliorates CKD progression in a model of STZ-induced type 1 diabetes and Thy-1 nephritis and a remnant kidney model (Tanaka et al., 2005a,b; Nordquist et al., 2015). However, this treatment cannot be used in CKD patients because of severe adverse effects. PHD inhibitors that specifically inhibit HIF-α hydroxylation have recently been synthesized. These compounds are currently in clinical trials for renal anemia because the EPO gene is markedly upregulated by HIF-α stabilization (Fraisl et al., 2009; Maxwell and Eckardt, 2016), and several drugs show positive outcomes in clinical trials in non-dialysis CKD patients and dialysis patients (Besarab et al., 2016; Brigandi et al., 2016; Holdstock et al., 2016; Pergola et al., 2016; Provenzano et al., 2016). These drugs are expected to have protective effects against CKD.

## OXIDATIVE STRESS-ORIENTED THERAPY AGAINST CKD

Another treatment approach is the enhancement of the anti-oxidant response because hypoxia is closely related to increased oxidative stress. One relevant transcriptional factor for this approach is NF-E2 related factor 2 (Nrf2). Nrf2 is degraded via recognition by Kelch-like ECH-associated protein 1 (Keap1) in the cytosol under normal conditions. When certain chemical stresses, such as oxidative stress, are induced, Nrf2 escapes degradation, translocates into the nucleus, binds to anti-oxidant responsive elements (AREs), and upregulates downstream genes (Bryan et al., 2013; **Figure 2**). Nrf2–ARE axis activation induces strong anti-oxidative effects; therefore, the pharmacological activation of the Nrf2–ARE pathway is a promising target for various diseases, including kidney diseases. Bardoxolone methyl, an Nrf2 activator via Keap1 inhibition, increases eGFR in CKD patients with diabetes mellitus; however, the change in eGFR is not considered primary or secondary outcomes, and hypertension and an increased urinary albumin-to-creatinine ratio was seen in the bardoxolone group (Pergola et al., 2011; de Zeeuw et al., 2013). However, a high frequency of cardiovascular events in the bardoxolone methyl group led to the termination of the phase III trial (de Zeeuw et al., 2013). A subsequent analysis revealed that most of these patients suffered from excessive fluid retention at the early stage. Considering that these clinical signs can be predicted under close follow-up of the patients and that diabetic kidney disease is major cause of end-stage renal disease, the potential benefit of this drug was reconsidered and a new phase II trial that excludes patients with a high risk of cardiovascular disease is ongoing in Japan.

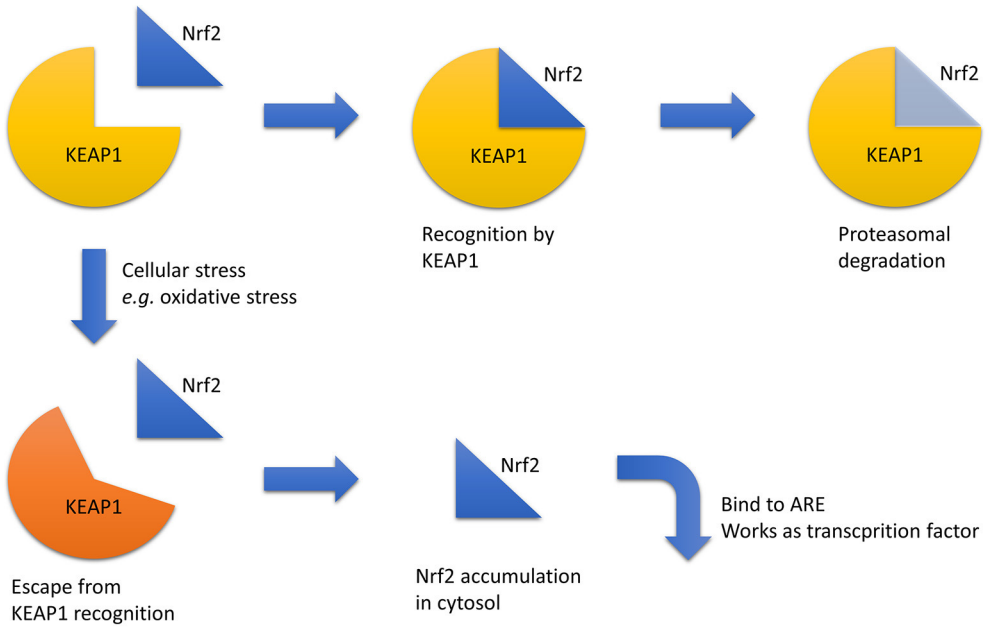


**FIGURE 2 | Nrf2 regulation.** Under normal conditions, Nrf2 is recognized by KEAP1, which triggers its proteasomal degradation. In contrast, under stressful conditions, such as increased oxidative stress, Nrf2 recognition by KEAP1 is disturbed, and Nrf2 accumulates in the cytosol and acts as a transcriptional factor via ARE binding. Abbreviations: ARE, anti-oxidant responsive element; KEAP1, Kelch-like ECH-associated protein 1; Nrf2, NF-E2 related factor 2.

These hypoxia-targeting pharmaceutical therapies are promising. Theoretically, these therapies are effective only on patients whose kidneys are truly hypoxic. The renal oxygen state widely varies in CKD patients (Michaely et al., 2012). Thus, it is important to identify patients whose kidneys are sufficiently hypoxic, i.e., more responsive to hypoxia-oriented therapies. However, the currently available hypoxia detection methods have serious disadvantages. Thus, there is a compelling need for a better understanding of hypoxia detection methods.

## GENERAL PRINCIPLES OF OXYGEN TENSION ASSESSMENT

The most important function of oxygen molecules is their action as an oxidant. In addition, oxygen can bind to hemoglobin to increase its solubility in blood. A lower oxygen tension results in HIF–HRE axis activation. Thus, we consider that methods to measure the oxygen tension can be divided into four groups: (i) assessment of the oxidative power of oxygen molecules (Clark, 1956; Arteel et al., 1995), (ii) measurement of the oxyhemoglobin/total hemoglobin ratio (Prasad et al., 1996), (iii) detection of HIF activity (Safran et al., 2006), and (iv) direct measurement of oxygen molecules by the assessment of fluorescence or phosphorescence quenching rate (Rumsey et al., 1988; Mik et al., 2006). Although these four methods unequivocally depend on the oxygen tension, there are some confounding factors in their interpretation. For example, when the oxidative power of oxygen molecules is measured, other oxidants or reductants can influence the result. Notably, oxidative stress levels increase in CKD patients (Himmelfarb et al., 2002). Although the oxyhemoglobin/total hemoglobin ratio is clinically used to determine a patient's general oxygenation state, this value can be affected by the partial pressures of oxygen and carbon dioxide, changes in pH, and other micro-environmental changes (Bohr effect). Blood oxygen level-dependent magnetic resonance imaging (BOLD-MRI) employs hemoglobin as an oxygen sensor; however, this method only measures the deoxyhemoglobin concentration and not the deoxyhemoglobin/total hemoglobin ratio. Thus, this method is influenced by the hemoglobin concentration, which cannot be precisely measured in small veins (Prasad et al., 1996). Renal anemia and acid–base disorders frequently occur in CKD patients, which may explain why the use of renal BOLD-MRI in CKD patients remains controversial (Inoue et al., 2011; Michaely et al., 2012; Pruijm et al., 2014). HIF activation may be influenced by factors other than oxygen molecules, such as erythropoietin and indoxyl sulfate (Chiang et al., 2011). Indoxyl sulfate, a representative uremic toxin, suppresses *EPO* gene transcription in hypoxic HepG2 cells in an HIF-dependent manner, and the oral administration of indole, a precursor of indoxyl sulfate, decreases the serum erythropoietin concentration in rats.

Another important consideration is whether the method employed reflects the intracellular or extracellular oxygen tension. As previously noted, the HIF-mediated cellular response against hypoxia is regulated by the hydroxylation of HIF-α, which uses oxygen as a substrate. Thus, the intracellular oxygen tension is important. For example, anemia can cause dissociation between the intracellular and extracellular oxygen tensions because anemia does not change the partial pressure of oxygen,

but rather changes the total oxygen amount in arterial blood (i.e., decrease in hemoglobin concentration). This condition should not be overlooked because renal anemia development is associated with renal hypoxia in CKD patients.

Another important aspect to consider is the generation of quantitative or qualitative data. Microelectrodes, BOLD-MRI, pimonidazole protein adduct immunohistochemistry, and HIF activation detection are frequently used as hypoxia detection methods (Heyman et al., 2008). Phosphorescence lifetime measurement is a relatively novel intravital oxygen sensing technique; thus, we have included this technique in our review (Parpaleix et al., 2013; Spencer et al., 2014; Hirakawa et al., 2015). The characteristics of these methods are summarized in **Table 1**. For clinical applications, BOLD-MRI is the only appropriate method. For animal experiments, microelectrodes are a gold standard for oxygen tension measurement, although the specific measurement site is unclear. Pimonidazole staining and HIF activation detection can be used for paraffin sections and has the advantage of spatial resolution. Phosphorescence lifetime measurement is a highly sensitive method, but it requires special instrumentation.

Comparison of results obtained via different methods is attractive, and there is a report that compared $pO_2$ measured by a microelectrode with that measured by a fluorescence needle probe in the kidney and which mentions that there is a slight difference in outcomes between these two methods (O'Connor et al., 2006). However, this comparison cannot determine which of the two methods is reliable; the calibration method of each method differs, and the measurement site is not always the same. Therefore, the comparison of $pO_2$ obtained via different techniques needs to be interpreted with that consideration in mind.

# HYPOXIA DETECTION METHODS

## Microelectrodes

The use of microelectrodes is a classical technique and the gold standard for determining the oxygen tension in living cells and animals. The principle of this technique is based on oxidation–reduction reactions. The reaction for a silver electrode is shown below:

$$4Ag + 4Cl^- \rightarrow 4AgCl + 4e^- \cdots \quad (1)$$

$$4H^+ + 4e^- + O_2 \rightarrow 2H_2O \cdots \quad (2)$$

This reaction contains an oxygen molecule as a reactant in Equation 2; thus, the electric current is dependent on the oxygen concentration, assuming that the voltage is constant. This method is widely used to determine renal oxygenation as well as other visceral organ oxygenation, such as the liver. The kidney has a natural oxygen gradient; therefore, data obtained from a microelectrode is dependent on depth. Typically, representative oxygen tensions in the renal cortex and medulla are 50 and 30 mmHg, respectively. This ability to distinguish between the renal cortex and the medulla is an advantage of the microelectrode; however, technical proficiency is required to accurately measure medullary oxygen tension. This technique has two major disadvantages, in addition to its non-applicability in humans. First, this method is highly invasive. The technique requires renal capsule removal and needle insertion into the renal tissue, which results in microbleeding. This method intrinsically hinders repeat measurements within an individual. The second disadvantage is that microelectrodes measure the partial pressure of oxygen from both microcirculation and microbleeding based on the fact that a microelectrode is slightly pulled after insertion to prevent compression. Despite these disadvantages, the use of microelectrodes remains the gold standard for determining tissue oxygen tension because of its superior quantitative performance.

To overcome the disadvantages of this established method, novel modifications have been developed. The first involves the use of telemetry (Koeners et al., 2013; Emans et al., 2016). For oxygen tension telemetry, carbon paste electrodes are used to avoid surface poisoning (Bolger et al., 2011). Once the electrodes are implanted, renal oxygenation can be monitored for 2 weeks without anesthesia. This technique resolves the two major disadvantages inherent to the conventional microelectrode method, including the continuous measurement within an individual and the avoidance of acute effects from general anesthesia. Another approach is urinary oxygen tension measurement (Evans et al., 2014). Urinary oxygen tension reflects renal medullary oxygen tension and is useful for monitoring renal oxygenation in critically ill patients (Kainuma et al., 1996; Morelli et al., 2003). This technique does not require intervention other than the insertion of electrode-equipped bladder catheters; thus, it has the advantage of being easily applied in clinical settings. One disadvantage is the general lack of proof of this in smaller animals. However, a recent study in rabbits reported the ability of urinary oxygen tension measurements to reflect renal medullary oxygen tension (Sgouralis et al., 2016).

## Nitroimidazole Probes

Pimonidazole is a nitroimidazole. Nitroimidazoles are hypoxic markers that were initially used to detect hypoxic tumors, which are frequently resistant to radiotherapy. Pimonidazole was used to detect tissue hypoxia in a physiological range (Arteel et al., 1995). Under normoxic conditions, pimonidazole is oxidized by oxygen molecule, whereas pimonidazole is reductively activated under hypoxic conditions. Reduced pimonidazole binds to intracellular thiol-containing proteins. Pimonidazole protein adducts are only detected in hypoxic cells after systemic administration. The detection of pimonidazole protein adducts is typically achieved by immunohistochemistry. Thus, this technique requires the systemic administration of pimonidazole and the preparation of paraffin-embedded sections or frozen sections, which prohibits its use in living animals. Another disadvantage is that this technique reflects the redox state; thus, a redox imbalance independent of the oxygen tension can influence the result. In the kidneys, pimonidazole-positive areas are naturally observed in the medulla and corticomedullar junction (Manotham et al., 2004; Fong et al., 2016), which supports the idea that these areas are more hypoxic than the superficial cortex. In CKD models, the pimonidazole-positive area expands (Manotham et al., 2004; Tanaka et al., 2006). This technique can only detect areas with oxygen tensions lower than

**TABLE 1 | Comparison of hypoxia detection methods.**

| Method | What is measured? | Intracellular/extracellular | Qualitative/quantitative | Clinical applicability |
|---|---|---|---|---|
| Pimonidazole staining | Oxidative power of $O_2$ | Intracellular | Qualitative | PET probe only |
| Microelectrode | Oxidative power of $O_2$ | Extracellular | Quantitative | No |
| Detection of the activated HIF–HRE axis | Activation of the HIF–HRE axis | Intracellular | Qualitative | No |
| BOLD-MRI | Deoxyhemoglobin concentration | Extracellular | Quantitative | Yes |
| Phosphorescence lifetime measurement | Quenching by an oxygen molecule | Depends on dyes | Quantitative | No |

*BOLD-MRI, blood oxygen level-dependent magnetic resonance imaging; HIF, hypoxia-inducible factor; HRE, hypoxia-responsive element.*

a certain threshold (approximately below 10 mmHg); thus, it is neither quantitative nor indicative of the oxygen tension.

To overcome the disadvantage of paraffin-embedded sections, several positron emission tomography (PET) tracers with nitroimidazoles have been studied. For example, $^{18}$F-fluoroazomycin arabinoside ($^{18}$F-FAZA) (Piert et al., 2005) was found to accumulate in hypoxic tumors. This probe can be administered in clinical settings, and several papers have proved that it is useful for prognostic prediction in non-small-cell lung cancer (Saga et al., 2015; Kinoshita et al., 2016). It remains unclear if this method can successfully detect renal hypoxia in healthy individuals or CKD patients. The difficulty in detecting renal hypoxia is based on the fact that the oxygen tension of non-tumorous organs, including the kidney, is likely to be much milder than that of tumor tissues, even in pathological conditions (Handley et al., 2011). Pimonidazole binds to intracellular thiols at oxygen tensions below 10 mmHg, which is frequently lower than the tensions found in non-tumorous tissues. Another disadvantage is that $^{18}$F-FAZA is physiologically distributed to even normal kidneys and is excreted from the kidney like other PET tracers (Koh et al., 1992). In PET imaging, there is limited resolution with which to distinguish PET probes in the urinary space and intracellular PET probes. However, PET tracing using nitroimidazoles is potentially preferred because this technique is less invasive and suitable for use in CKD patients. Furthermore, this probe reflects the intracellular rather than the extracellular oxygen tension. The optimization of the oxygen tension threshold and biokinetics of PET tracers may overcome the disadvantages listed above and result in new information on renal hypoxia in CKD patients.

## HIF Activation Detection

The cellular response against hypoxia is mainly regulated by HIF; therefore, HIF activation can be used as evidence on tissue hypoxia. One detection method assesses HRE-downstream genes or proteins in tissues. The advantage of this method is that several HIF target proteins are hypoxia markers and affect CKD progression. An example of one of these targets is VEGF. The transcription of the *VEGF* gene is strongly enhanced under hypoxic conditions. Exogenous VEGF administration ameliorates renal fibrosis in a remnant kidney model, whereas sunitinib administration, a VEGF receptor inhibitor, worsens renal injury in this model (Kang et al., 2001a; Machado et al., 2012), although sunitinib also blocks the platelet-derived growth factor receptor. The expression of HIF target genes can be affected by other transcriptional factors and thus is not always affected by the oxygen tension alone. The protein level of VEGF can remain unchanged in some CKD models despite renal hypoxia (Futatsugi et al., 2016).

Classical techniques, such as reverse transcription PCR and immunohistochemistry, require tissue sample preparation. Another method is the *in vivo* imaging of HIF activity using luciferase. Our group established hypoxia-sensing transgenic rats, in which the luciferase gene was controlled by tandem repeats of HREs located in the 5′ UTR of the *VEGF* gene (Tanaka et al., 2004). A similar approach was employed by Safran et al. who established a hypoxia-sensing mouse strain that expressed firefly luciferase fused to the HIF-1α protein (Safran et al., 2006). These animals emit luminescence after the administration of a systemic chemiluminescent substrate, and the luminescence can be measured from outside the body. This strain was used to detect a decrease in HIF-α hydroxylation induced by hypoxemia and pharmacological PHD inhibition. The advantage of this technique is the lack of autoluminescence in the body, whereas a disadvantage is the reabsorption of luminescence. The kidney contains a significant amount of blood; thus, it can absorb light at an optical wavelength. It is unclear if luminescence from the kidney truly reflects total renal luciferase activity or only superficial activity. Kuchimaru et al. may have overcome this disadvantage (Kuchimaru et al., 2016). They succeeded in synthesizing a novel luminescent substrate whose wavelength was considerably longer ($\lambda_{max}$ = 677 nm) than classical luciferins. Owing to its near-infrared wavelength, this substrate can be used to observe deeper tissue and will definitely aid in the intravital imaging of HIF activity.

## MRI-Based Assessment

BOLD-MRI is a useful tool to evaluate renal oxygenation. Here, the spin–spin relaxation rate R2∗ is measured, which reflects the deoxyhemoglobin concentration in veins (Prasad et al., 1996). To use this technique for tissue oxygenation approximation, we must speculate three proportional relationships: the deoxyhemoglobin concentration and deoxyhemoglobin/total hemoglobin ratio, deoxyhemoglobin/total hemoglobin ratio and partial pressure of oxygen in veins, and partial pressure of oxygen in veins and tissue oxygen level. These three proportional relationships are confounded by the hemoglobin concentration in veins, change in the oxygen affinity of hemoglobin, and intracellular/extracellular oxygen tension

dissociation, respectively. Renal anemia and systemic acid–base disorders frequently occur in CKD patients, which may change the oxygen affinity of hemoglobin. The existence of an oxygen shunt in renal arterial and venous vessels suggests that the oxygenation of renal venous vessels is independent of tissue oxygenation. These disadvantages must be taken into account when interpreting data from BOLD-MRI of the kidney.

Despite these disadvantages, BOLD-MRI is a promising method because it is a non-invasive technique, particularly when applied in humans. A previous report has shown that the renal R2∗ value correlated with eGFR in CKD patients without diabetes (Inoue et al., 2011), whereas another report did not find this correlation in CKD patients (Michaely et al., 2012). The discrepancy between these two reports may be due to differences in patient backgrounds. Another report has indicated there are several factors other than the oxygen tension, such as blood glucose and uric acid levels, that influence the result of BOLD-MRI, whether directly or indirectly (Pruijm et al., 2014). It is debatable whether BOLD-MRI can properly address the heterogeneity of CKD patients.

BOLD-MRI, an R2∗-based technique, employs hemoglobin as an oxygen sensor. However, another MRI-based technique that directly measures oxygen molecules has been recently reported (O'Connor et al., 2009; Winter et al., 2011). In this technique, the relaxation rate of the T1 signal (R1) is measured, which is related to the oxygen molecule itself. One report has suggested that R1 in lipids changes with the oxygen tension in mice tumors, whereas another report has shown that the R1-based technique is less sensitive in detecting renal hypoxia in hypoxemia than the R2∗-based technique (Jordan et al., 2013; Ganesh et al., 2016). Together with the low invasiveness of MRI-based techniques and the limitation of BOLD-MRI, R1-based measurement is a potentially viable method because it directly determines the oxygen tension.

## Phosphorescence

Phosphorescence is a type of light emitted from a molecule in the triplet excited state. Molecules in this state can lose their energy by being hit by oxygen molecules. Phosphorescence intensity and phosphorescence lifetime depend on the oxygen concentration (Rumsey et al., 1988). Thus, this technique can directly measure the oxygen tension. Substances that emit phosphorescence are limited, and exogenous phosphorescence dyes are used to measure phosphorescence. Notably, the phosphorescence lifetime is far longer than the fluorescence lifetime. Both phosphorescence intensity and phosphorescence lifetime can be quantitatively measured. However, phosphorescence dye concentrations in the target organ are required to determine the oxygen tension *in vivo* using the phosphorescence intensity. Therefore, phosphorescence lifetime measurements are frequently used to determine the oxygen tension *in vivo* (Mik et al., 2008; Parpaleix et al., 2013; Spencer et al., 2014; Hirakawa et al., 2015). The phosphorescence lifetime does not depend on dye concentration as long as it sufficiently accumulates. In phosphorescence lifetime measurements, the Stern–Volmer equation is used:

$$[O_2] = \frac{1}{k_q}\left(\frac{1}{\tau} - \frac{1}{\tau_0}\right)\cdots \quad (3)$$

where $k_q$ is the rate constant, $\tau$ is the phosphorescence lifetime at the oxygen concentration of $[O_2]$, and $\tau_0$ is the phosphorescence lifetime in an anoxic condition (Vanderkooi et al., 1987). These two constants, $k_q$ and $\tau_0$, depend on the phosphorescence dye and circumstantial microcondition, such as solvent. Thus, the determination of these parameters is problematic.

The oxygen dependence of the phosphorescence lifetime was established in the 1980s. It is utilized with fluorescence needle probes, which contain an oxygen-sensitive fluorescence dye, such as protoporphyrin IX (PpIX) described below, which has similar characteristics against oxygen. Several studies have employed this fluorescence needle probe because of its high sensitivity to the oxygen tension (O'Connor et al., 2006; dos Santos et al., 2007). However, this method cannot overcome the two major disadvantages of microelectrodes: unclear measurement site and high invasiveness. Thus, another way to apply phosphorescence lifetime measurement to *in vivo* $O_2$ measurement is warranted, and currently, the administration of phosphorescence dyes that are distributed in a certain tissue or cell is frequently used. One research milestone was the report by Spencer et al. (2014). They employed a water-soluble phosphorescence dye, PtP-C343, to measure the oxygen tension in arterioles penetrating cortical bones and showed that the oxygen tension decreased when the arteriole entered the medullary canal in mice. This research directly proved the lower oxygen tension in the bone marrow, which was hypothesized based on the unique vasculature system in the marrow and pimonidazole protein adduct immunohistochemistry (Suda et al., 2011; Nombela-Arrieta et al., 2013).

Powerful research on the kidney was published by Mik et al. (2008). They used Oxyphor G2 as a water-soluble phosphorescence dye and proved that oxygen tension in renal vein was decreased after endotoxin shock in rats. This work clarified where the oxygen tension should be measured (i.e., in renal veins). The phosphorescence dye is excited only in blood in renal vein. In this study, there is no phosphorescence signal from arterial blood, capillary blood, or interstitial fluid, which is problematic in the study of solid organs.

The aforementioned phosphorescence dyes are distributed in the extracellular fluid, mainly in the blood; thus, these dyes cannot directly determine the intracellular oxygen tension. Our group recently reported a novel technique for measuring the intracellular oxygen tension using BTPDM1, a cationic lipophilic phosphorescence dye (Yoshihara et al., 2015). In the kidney, this dye is found only inside tubular cells. Thus, phosphorescence lifetime imaging reflects only the intracellular oxygen tension in tubules. Using this method, phosphorescence lifetime measurement revealed renal hypoxia in CKD, and the phosphorescence lifetime was successfully converted to the partial pressure of oxygen using the calibration curve obtained

from a cultured tubular cell line. One disadvantage of this technique is dye toxicity when applied in human beings because BTPDM1 contains iridium, a heavy metal. Another dye that may overcome this disadvantage is PpIX (Mik et al., 2006). PpIX is a precursor of heme and is unique in that it can emit delayed fluorescence. This delayed fluorescence is similar to phosphorescence in terms of oxygen sensitivity, i.e., its phosphorescence lifetime depends on the oxygen tension. PpIX localizes to the mitochondria, and its physiological concentration is so low that it cannot be used as an endogenous oxygen sensor. However, when a large amount of 5-aminolevulinic acid (5-ALA), a PpIX precursor, is administered, the cellular synthesis of PpIX sufficiently increases to allow its use as an oxygen sensor via delayed fluorescence lifetime measurements. Using this method, the topical application of 5-ALA enables PpIX accumulation in the skin of healthy human volunteers and the oxygen tension estimate in human skin (Harms et al., 2013). Thus, this technique can be applied to abdominal organs, such as the liver (Bodmer et al., 2012). These phosphorescence or delayed fluorescence lifetime measurement techniques have the advantage of direct oxygen measurements and a superior quantitative performance. In contrast, these techniques cannot be used for assessing the deeper portion of the kidney, such as the outer medullary region, because phosphorescence is absorbed in tissues, particularly by hemoglobin.

## CONCLUSION AND FUTURE PERSPECTIVES

In this review, we addressed the pathophysiological importance of renal hypoxia with a focus on hypoxia detection. Although oxygen tension determination has been studied for a long time, recent advances have made it possible to achieve continuous measurements, non-invasive oxygen assessments, and intracellular oxygen assessments. All these methods have their advantages and disadvantages; therefore, a comprehensive understanding and proper selection of the available methods are required to assess renal hypoxia and identify the final common pathway in individual hypoxia patients. Thus, a sufficient understanding of oxygen detection techniques will help researchers develop new drugs against CKD and renal hypoxia.

## AUTHOR CONTRIBUTIONS

YH wrote the manuscript and TT and MN edited the manuscript.

## ACKNOWLEDGMENTS

This study was supported by the Grant-in-Aid for Scientific Research on Innovative Areas (26111003 to MN)

## REFERENCES

Adler, S., and Huang, H. (2002). Impaired regulation of renal oxygen consumption in spontaneously hypertensive rats. *J. Am. Soc. Nephrol.* 13, 1788–1794. doi: 10.1097/01.ASN.0000019781.90630.0F

Arteel, G. E., Thurman, R. G., Yates, J. M., and Raleigh, J. A. (1995). Evidence that hypoxia markers detect oxygen gradients in liver: pimonidazole and retrograde perfusion of rat liver. *Br. J. Cancer* 72, 889–895. doi: 10.1038/bjc.1995.429

Astor, B. C., Muntner, P., Levin, A., Eustace, J. A., and Coresh, J. (2002). Association of kidney function with anemia: the third national health and nutrition examination survey (1988-1994). *Arch. Intern. Med.* 162, 1401–1408. doi: 10.1001/archinte.162.12.1401

Besarab, A., Chernyavskaya, E., Motylev, I., Shutov, E., Kumbar, L. M., Gurevich, K., et al. (2016). Roxadustat (FG-4592): correction of anemia in incident dialysis patients. *J. Am. Soc. Nephrol.* 27, 1225–1233. doi: 10.1681/ASN.2015030241

Bodmer, S. I., Balestra, G. M., Harms, F. A., Johannes, T., Raat, N. J., Stolker, R. J., et al. (2012). Microvascular and mitochondrial $PO_2$ simultaneously measured by oxygen-dependent delayed luminescence. *J. Biophotonics* 5, 140–151. doi: 10.1002/jbio.201100082

Bolger, F. B., McHugh, S. B., Bennett, R., Li, J., Ishiwari, K., Francois, J., et al. (2011). Characterisation of carbon paste electrodes for real-time amperometric monitoring of brain tissue oxygen. *J. Neurosci. Methods* 195, 135–142. doi: 10.1016/j.jneumeth.2010.11.013

Brezis, M., and Rosen, S. (1995). Hypoxia of the renal medulla–its implications for disease. *N. Engl. J. Med.* 332, 647–655. doi: 10.1056/NEJM199503093321006

Brigandi, R. A., Johnson, B., Oei, C., Westerman, M., Olbina, G., de Zoysa, J., et al. (2016). A novel hypoxia-inducible factor-prolyl hydroxylase inhibitor (GSK1278863) for anemia in CKD: a 28-day, phase 2A randomized trial. *Am. J. Kidney Dis.* 67, 861–871. doi: 10.1053/j.ajkd.2015.11.021

Bryan, H. K., Olayanju, A., Goldring, C. E., and Park, B. K. (2013). The Nrf2 cell defence pathway: keap1-dependent and -independent mechanisms of regulation. *Biochem. Pharmacol.* 85, 705–717. doi: 10.1016/j.bcp.2012.11.016

Chen, C. Y., and Liao, K. M. (2016). Chronic obstructive pulmonary disease is associated with risk of chronic kidney disease: a nationwide case-cohort study. *Sci. Rep.* 6:25855. doi: 10.1038/srep25855

Chiang, C. K., Tanaka, T., Inagi, R., Fujita, T., and Nangaku, M. (2011). Indoxyl sulfate, a representative uremic toxin, suppresses erythropoietin production in a HIF-dependent manner. *Lab. Invest.* 91, 1564–1571. doi: 10.1038/labinvest.2011.114

Clark, L. C. J. (1956). Monitor and control of blood and tissue oxygen tensions. *Trans. Am. Soc. Artif. Intern. Organ.* 2, 41–48.

Collins, A. J., Foley, R. N., Gilbertson, D. T., and Chen, S. C. (2015). United states renal data system public health surveillance of chronic kidney disease and end-stage renal disease. *Kidney Int. Suppl.* (2011) 5, 2–7. doi: 10.1038/kisup.2015.2

Deng, A., Arndt, M. A., Satriano, J., Singh, P., Rieg, T., Thomson, S., et al. (2010). Renal protection in chronic kidney disease: hypoxia-inducible factor activation vs. angiotensin II blockade. *Am. J. Physiol. Renal Physiol.* 299, F1365–F1373. doi: 10.1152/ajprenal.00153.2010

Deng, A., Tang, T., Singh, P., Wang, C., Satriano, J., Thomson, S. C., et al. (2009). Regulation of oxygen utilization by angiotensin II in chronic kidney disease. *Kidney Int.* 75, 197–204. doi: 10.1038/ki.2008.481

de Zeeuw, D., Akizawa, T., Audhya, P., Bakris, G. L., Chin, M., Christ-Schmidt, H., et al. (2013). Bardoxolone methyl in type 2 diabetes and stage 4 chronic kidney disease. *N. Engl. J. Med.* 369, 2492–2503. doi: 10.1056/NEJMoa1306033

Duan, C. (2016). Hypoxia-inducible factor 3 biology: complexities and emerging themes. *Am. J. Physiol. Cell Physiol.* 310, C260–C269. doi: 10.1152/ajpcell.00315.2015

Emans, T. W., Janssen, B. J., Pinkham, M. I., Ow, C. P., Evans, R. G., Joles, J. A., et al. (2016). Exogenous and endogenous angiotensin-II decrease renal cortical oxygen tension in conscious rats by limiting renal blood flow. *J. Physiol.* 594, 6287–6300. doi: 10.1113/JP270731

Epstein, F. H. (1997). Oxygen and renal metabolism. *Kidney Int.* 51, 381–385. doi: 10.1038/ki.1997.50

Evans, R. G., Smith, D. W., Khan, Z., Ngo, J. P., and Gardiner, B. S. (2015). Letter to the editor: "The plausibility of arterial-to-venous oxygen shunting in

the kidney: it all depends on radial geometry." *Am. J. Physiol. Renal Physiol.* F179–F180. doi: 10.1152/ajprenal.00094.2015

Evans, R. G., Smith, J. A., Wright, C., Gardiner, B. S., Smith, D. W., and Cochrane, A. D. (2014). Urinary oxygen tension: a clinical window on the health of the renal medulla? *Am. J. Physiol. Regul. Integr. Comp. Physiol.* 306, R45–R50. doi: 10.1152/ajpregu.00437.2013

Fine, L. G., Bandyopadhay, D., and Norman, J. T. (2000). Is there a common mechanism for the progression of different types of renal diseases other than proteinuria? Towards the unifying theme of chronic hypoxia. *Kidney Int. Suppl.* 75, S22–S26. doi: 10.1046/j.1523-1755.57.s75.12.x

Fong, D., Ullah, M. M., Lal, J. G., Abdelkader, A., Ow, C. P., Hilliard, L. M., et al. (2016). Renal cellular hypoxia in adenine-induced chronic kidney disease. *Clin. Exp. Pharmacol. Physiol.* 43, 896–905. doi: 10.1111/1440-1681.12621

Fraisl, P., Aragones, J., and Carmeliet, P. (2009). Inhibition of oxygen sensors as a therapeutic strategy for ischaemic and inflammatory disease. *Nat. Rev. Drug Discov.* 8, 139–152. doi: 10.1038/nrd2761

Friederich-Persson, M., Thorn, E., Hansell, P., Nangaku, M., Levin, M., and Palm, F. (2013). Kidney hypoxia, attributable to increased oxygen consumption, induces nephropathy independently of hyperglycemia and oxidative stress. *Hypertension* 62, 914–919. doi: 10.1161/HYPERTENSIONAHA.113.01425

Futatsugi, K., Tokuyama, H., Shibata, S., Naitoh, M., Kanda, T., Minakuchi, H., et al. (2016). Obesity-induced kidney injury is attenuated by amelioration of aberrant PHD2 activation in proximal tubules. *Sci. Rep.* 6:36533. doi: 10.1038/srep36533

Ganesh, T., Estrada, M., Duffin, J., and Cheng, H. L. (2016). T2∗ and T1 assessment of abdominal tissue response to graded hypoxia and hypercapnia using a controlled gas mixing circuit for small animals. *J. Magn. Reson. Imaging* 44, 305–316. doi: 10.1002/jmri.25169

Handley, M. G., Medina, R. A., Nagel, E., Blower, P. J., and Southworth, R. (2011). PET imaging of cardiac hypoxia: opportunities and challenges. *J. Mol. Cell. Cardiol.* 51, 640–650. doi: 10.1016/j.yjmcc.2011.07.005

Hanly, P. J., and Ahmed, S. B. (2014). Sleep apnea and the kidney: is sleep apnea a risk factor for chronic kidney disease? *Chest* 146, 1114–1122. doi: 10.1378/chest.14-0596

Harms, F. A., Voorbeijtel, W. J., Bodmer, S. I., Raat, N. J., and Mik, E. G. (2013). Cutaneous respirometry by dynamic measurement of mitochondrial oxygen tension for monitoring mitochondrial function *in vivo*. *Mitochondrion* 13, 507–514. doi: 10.1016/j.mito.2012.10.005

Harris, D. C., Chan, L., and Schrier, R. W. (1988). Remnant kidney hypermetabolism and progression of chronic renal failure. *Am. J. Physiol.* 254, F267–F276.

Heyman, S. N., Khamaisi, M., Rosen, S., and Rosenberger, C. (2008). Renal parenchymal hypoxia, hypoxia response and the progression of chronic kidney disease. *Am. J. Nephrol.* 28, 998–1006. doi: 10.1159/000146075

Heyman, S. N., Rosenberger, C., and Rosen, S. (2010). Experimental ischemia-reperfusion: biases and myths-the proximal vs. distal hypoxic tubular injury debate revisited. *Kidney Int.* 77, 9–16. doi: 10.1038/ki.2009.347

Himmelfarb, J., Stenvinkel, P., Ikizler, T. A., and Hakim, R. M. (2002). The elephant in uremia: oxidant stress as a unifying concept of cardiovascular disease in uremia. *Kidney Int.* 62, 1524–1538. doi: 10.1046/j.1523-1755.2002.00600.x

Hirakawa, Y., Yoshihara, T., Kamiya, M., Mimura, I., Fujikura, D., Masuda, T., et al. (2015). Quantitating intracellular oxygen tension *in vivo* by phosphorescence lifetime measurement. *Sci. Rep.* 5:17838. doi: 10.1038/srep17838

Holdstock, L., Meadowcroft, A. M., Maier, R., Johnson, B. M., Jones, D., Rastogi, A., et al. (2016). Four-Week studies of oral hypoxia-inducible factor-prolyl hydroxylase inhibitor GSK1278863 for treatment of anemia. *J. Am. Soc. Nephrol.* 27, 1234–1244. doi: 10.1681/ASN.2014111139

Inoue, T., Kozawa, E., Okada, H., Inukai, K., Watanabe, S., Kikuta, T., et al. (2011). Non-invasive evaluation of kidney hypoxia and fibrosis using magnetic resonance imaging. *J. Am. Soc. Nephrol.* 22, 1429–1434. doi: 10.1681/ASN.2010111143

Iseki, K., Tohyama, K., Matsumoto, T., and Nakamura, H. (2008). High Prevalence of chronic kidney disease among patients with sleep related breathing disorder (SRBD). *Hypertens. Res.* 31, 249–255. doi: 10.1291/hypres.31.249

Jordan, B. F., Magat, J., Colliez, F., Ozel, E., Fruytier, A. C., Marchand, V., et al. (2013). Mapping of oxygen by imaging lipids relaxation enhancement: a potential sensitive endogenous MRI contrast to map variations in tissue oxygenation. *Magn. Reson. Med.* 70, 732–744. doi: 10.1002/mrm.24511

Kainuma, M., Yamada, M., and Miyake, T. (1996). Continuous urine oxygen tension monitoring in patients undergoing cardiac surgery. *J. Cardiothorac. Vasc. Anesth.* 10, 603–608.

Kang, D. H., Hughes, J., Mazzali, M., Schreiner, G. F., and Johnson, R. J. (2001a). Impaired angiogenesis in the remnant kidney model: II. Vascular endothelial growth factor administration reduces renal fibrosis and stabilizes renal function. *J. Am. Soc. Nephrol.* 12, 1448–1457.

Kang, D. H., Joly, A. H., Oh, S. W., Hugo, C., Kerjaschki, D., Gordon, K. L., et al. (2001b). Impaired angiogenesis in the remnant kidney model: I. Potential role of vascular endothelial growth factor and thrombospondin-1. *J. Am. Soc. Nephrol.* 12, 1434–1447.

Kinoshita, T., Fujii, H., Hayashi, Y., Kamiyama, I., Ohtsuka, T., and Asamura, H. (2016). Prognostic significance of hypoxic PET using $^{18}$F-FAZA and $^{62}$Cu-ATSM in non-small-cell lung cancer. *Lung Cancer* 91, 56–66. doi: 10.1016/j.lungcan.2015.11.020

Koeners, M. P., Ow, C. P., Russell, D. M., Abdelkader, A., Eppel, G. A., Ludbrook, J., et al. (2013). Telemetry-based oxygen sensor for continuous monitoring of kidney oxygenation in conscious rats. *Am. J. Physiol. Renal Physiol.* 304, F1471–F1480. doi: 10.1152/ajprenal.00662.2012

Koh, W. J., Rasey, J. S., Evans, M. L., Grierson, J. R., Lewellen, T. K., Graham, M. M., et al. (1992). Imaging of hypoxia in human tumors with [F-18]fluoromisonidazole. *Int. J. Radiat. Oncol. Biol. Phys.* 22, 199–212.

Korner, A., Eklof, A. C., Celsi, G., and Aperia, A. (1994). Increased renal metabolism in diabetes. Mechanism and functional implications. *Diabetes* 43, 629–633.

Kuchimaru, T., Iwano, S., Kiyama, M., Mitsumata, S., Kadonosono, T., Niwa, H., et al. (2016). A luciferin analogue generating near-infrared bioluminescence achieves highly sensitive deep-tissue imaging. *Nat. Commun.* 7:11856. doi: 10.1038/ncomms11856

Liyanage, T., Ninomiya, T., Jha, V., Neal, B., Patrice, H. M., Okpechi, I., et al. (2015). Worldwide access to treatment for end-stage kidney disease: a systematic review. *Lancet* 385, 1975–1982. doi: 10.1016/S0140-6736(14)61601-9

Machado, F. G., Kuriki, P. S., Fujihara, C. K., Fanelli, C., Arias, S. C., Malheiros, D. M., et al. (2012). Chronic VEGF blockade worsens glomerular injury in the remnant kidney model. *PLoS ONE* 7:e39580. doi: 10.1371/journal.pone.0039580

Manotham, K., Tanaka, T., Matsumoto, M., Ohse, T., Miyata, T., Inagi, R., et al. (2004). Evidence of tubular hypoxia in the early phase in the remnant kidney model. *J. Am. Soc. Nephrol.* 15, 1277–1288. doi: 10.1097/01.ASN.0000125614.35046.10

Matsumoto, M., Tanaka, T., Yamamoto, T., Noiri, E., Miyata, T., Inagi, R., et al. (2004). Hypoperfusion of peritubular capillaries induces chronic hypoxia before progression of tubulointerstitial injury in a progressive model of rat glomerulonephritis. *J. Am. Soc. Nephrol.* 15, 1574–1581. doi: 10.1097/01.ASN.0000128047.13396.48

Maxwell, P. H., and Eckardt, K. U. (2016). HIF prolyl hydroxylase inhibitors for the treatment of renal anaemia and beyond. *Nat. Rev. Nephrol.* 12, 157–168. doi: 10.1038/nrneph.2015.193

Michaely, H. J., Metzger, L., Haneder, S., Hansmann, J., Schoenberg, S. O., and Attenberger, U. I. (2012). Renal BOLD-MRI does not reflect renal function in chronic kidney disease. *Kidney Int.* 81, 684–689. doi: 10.1038/ki.2011.455

Mik, E. G., Johannes, T., and Ince, C. (2008). Monitoring of renal venous $PO_2$ and kidney oxygen consumption in rats by a near-infrared phosphorescence lifetime technique. *Am. J. Physiol. Renal Physiol.* F676–F681. doi: 10.1152/ajprenal.00569.2007

Mik, E. G., Stap, J., Sinaasappel, M., Beek, J. F., Aten, J. A., van Leeuwen, T. G., et al. (2006). Mitochondrial $PO_2$ measured by delayed fluorescence of endogenous protoporphyrin IX. *Nat. Methods* 3, 939–945. doi: 10.1038/nmeth940

Mimura, I., and Nangaku, M. (2010). The suffocating kidney: tubulointerstitial hypoxia in end-stage renal disease. *Nat. Rev. Nephrol.* 6, 667–678. doi: 10.1038/nrneph.2010.124

Morelli, A., Rocco, M., Conti, G., Orecchioni, A., Alberto De Blasi, R., Coluzzi, F., et al. (2003). Monitoring renal oxygen supply in critically-ill patients using urinary oxygen tension. *Anesth. Analg.* 97, 1764–1768. doi: 10.1213/01.ANE.0000087037.41342.4F

Nangaku, M. (2006). Chronic hypoxia and tubulointerstitial injury: a final common pathway to end-stage renal failure. *J. Am. Soc. Nephrol.* 17, 17–25. doi: 10.1681/ASN.2005070757

Nath, K. A., and Paller, M. S. (1990). Dietary deficiency of antioxidants exacerbates ischemic injury in the rat kidney. *Kidney Int.* 38, 1109–1117.

Ngo, J. P., Kar, S., Kett, M. M., Gardiner, B. S., Pearson, J. T., Smith, D. W., et al. (2014). Vascular geometry and oxygen diffusion in the vicinity of artery-vein pairs in the kidney. *Am. J. Physiol. Renal Physiol.* 307, F1111–F1122. doi: 10.1152/ajprenal.00382.2014

Nombela-Arrieta, C., Pivarnik, G., Winkel, B., Canty, K. J., Harley, B., Mahoney, J. E., et al. (2013). Quantitative imaging of haematopoietic stem and progenitor cell localization and hypoxic status in the bone marrow microenvironment. *Nat. Cell Biol.* 15, 533–543. doi: 10.1038/ncb2730

Nordquist, L., Friederich-Persson, M., Fasching, A., Liss, P., Shoji, K., Nangaku, M., et al. (2015). Activation of hypoxia-inducible factors prevents diabetic nephropathy. *J. Am. Soc. Nephrol.* 26, 328–338. doi: 10.1681/ASN.2013090990

O'Connor, J. P., Naish, J. H., Parker, G. J., Waterton, J. C., Watson, Y., Jayson, G. C., et al. (2009). Preliminary study of oxygen-enhanced longitudinal relaxation in MRI: a potential novel biomarker of oxygenation changes in solid tumors. *Int. J. Radiat. Oncol. Biol. Phys.* 75, 1209–1215. doi: 10.1016/j.ijrobp.2008.12.040

O'Connor, P. M., Kett, M. M., Anderson, W. P., and Evans, R. G. (2006). Renal medullary tissue oxygenation is dependent on both cortical and medullary blood flow. *Am. J. Physiol. Renal Physiol.* 290, F688–F694. doi: 10.1152/ajprenal.00275.2005

Ohashi, R., Shimizu, A., Masuda, Y., Kitamura, H., Ishizaki, M., Sugisaki, Y., et al. (2002). Peritubular capillary regression during the progression of experimental obstructive nephropathy. *J. Am. Soc. Nephrol.* 13, 1795–1805. doi: 10.1097/01.ASN.0000018408.51388.57

Olgac, U., and Kurtcuoglu, V. (2015). Renal oxygenation: preglomerular vasculature is an unlikely contributor to renal oxygen shunting. *Am. J. Physiol. Renal Physiol.* 308, F671–F688. doi: 10.1152/ajprenal.00551.2014

Ow, C. P., Abdelkader, A., Hilliard, L. M., Phillips, J. K., and Evans, R. G. (2014). Determinants of renal tissue hypoxia in a rat model of polycystic kidney disease. *Am. J. Physiol. Regul. Integr. Comp. Physiol.* 307, R1207–R1215. doi: 10.1152/ajpregu.00202.2014

Parpaleix, A., Goulam Houssen, Y., and Charpak, S. (2013). Imaging local neuronal activity by monitoring $PO_2$ transients in capillaries. *Nat. Med.* 19, 241–246. doi: 10.1038/nm.3059

Pergola, P. E., Raskin, P., Toto, R. D., Meyer, C. J., Huff, J. W., Grossman, E. B., et al. (2011). Bardoxolone methyl and kidney function in CKD with type 2 diabetes. *N. Engl. J. Med.* 365, 327–336. doi: 10.1056/NEJMoa1105351

Pergola, P. E., Spinowitz, B. S., Hartman, C. S., Maroni, B. J., and Haase, V. H. (2016). Vadadustat, a novel oral HIF stabilizer, provides effective anemia treatment in non-dialysis-dependent chronic kidney disease. *Kidney Int.* 90, 1115–1122. doi: 10.1016/j.kint.2016.07.019

Piert, M., Machulla, H. J., Picchio, M., Reischl, G., Ziegler, S., Kumar, P., et al. (2005). Hypoxia-specific tumor imaging with 18F-fluoroazomycin arabinoside. *J. Nucl. Med.* 46, 106–113.

Prasad, P. V., Edelman, R. R., and Epstein, F. H. (1996). Non-invasive evaluation of intrarenal oxygenation with BOLD MRI. *Circulation* 94, 3271–3275.

Provenzano, R., Besarab, A., Sun, C. H., Diamond, S. A., Durham, J. H., Cangiano, J. L., et al. (2016). Oral hypoxia-inducible factor prolyl hydroxylase inhibitor roxadustat (FG-4592) for the treatment of anemia in patients with CKD. *Clin. J. Am. Soc. Nephrol.* 11, 982–991. doi: 10.2215/CJN.06890615

Pruijm, M., Hofmann, L., Piskunowicz, M., Muller, M. E., Zweiacker, C., Bassi, I., et al. (2014). Determinants of renal tissue oxygenation as measured with BOLD-MRI in chronic kidney disease and hypertension in humans. *PLoS ONE* 9:e95895. doi: 10.1371/journal.pone.0095895

Rosenberger, C., Mandriota, S., Jurgensen, J. S., Wiesener, M. S., Horstrup, J. H., Frei, U., et al. (2002). Expression of hypoxia-inducible factor-1alpha and -2alpha in hypoxic and ischemic rat kidneys. *J. Am. Soc. Nephrol.* 13, 1721–1732. doi: 10.1097/01.ASN.0000017223.49823.2A

Rumsey, W. L., Vanderkooi, J. M., and Wilson, D. F. (1988). Imaging of phosphorescence: a novel method for measuring oxygen distribution in perfused tissue. *Science* 241, 1649–1651.

Safran, M., Kim, W. Y., O'Connell, F., Flippin, L., Gunzler, V., Horner, J. W., et al. (2006). Mouse model for non-invasive imaging of HIF prolyl hydroxylase activity: assessment of an oral agent that stimulates erythropoietin production. *Proc. Natl. Acad. Sci. U.S.A.* 103, 105–110. doi: 10.1073/pnas.0509459103

Saga, T., Inubushi, M., Koizumi, M., Yoshikawa, K., Zhang, M. R., Tanimoto, K., et al. (2015). Prognostic value of $^{18}$F-fluoroazomycin arabinoside PET/CT in patients with advanced non-small-cell lung cancer. *Cancer Sci.* 106, 1554–1560. doi: 10.1111/cas.12771

dos Santos, E. A., Li, L. P., Ji, L., and Prasad, P. V. (2007). Early changes with diabetes in renal medullary hemodynamics as evaluated by fiberoptic probes and BOLD magnetic resonance imaging. *Invest. Radiol.* 42, 157–162. doi: 10.1097/01.rli.0000252492.96709.36

Schurek, H. J., Jost, U., Baumgartl, H., Bertram, H., and Heckmann, U. (1990). Evidence for a preglomerular oxygen diffusion shunt in rat renal cortex. *Am. J. Physiol.* 259, F910–F915.

Semenza, G. L. (2014). Oxygen sensing, hypoxia-inducible factors, and disease pathophysiology. *Ann. Rev. Pathol.* 9, 47–71. doi: 10.1146/annurev-pathol-012513-104720

Sgouralis, I., Kett, M. M., Ow, C. P., Abdelkader, A., Layton, A. T., Gardiner, B. S., et al. (2016). Bladder urine oxygen tension for assessing renal medullary oxygenation in rabbits: experimental and modeling studies. *Am. J. Physiol. Regul. Integr. Comp. Physiol.* 311, R532–R544. doi: 10.1152/ajpregu.00195.2016

Shanley, P. F., Brezis, M., Spokes, K., Silva, P., Epstein, F. H., and Rosen, S. (1986). Transport-dependent cell injury in the S3 segment of the proximal tubule. *Kidney Int.* 29, 1033–1037.

Spencer, J. A., Ferraro, F., Roussakis, E., Klein, A., Wu, J., Runnels, J. M., et al. (2014). Direct measurement of local oxygen concentration in the bone marrow of live animals. *Nature* 508, 269–273. doi: 10.1038/nature13034

Suda, T., Takubo, K., and Semenza, G. L. (2011). Metabolic regulation of hematopoietic stem cells in the hypoxic niche. *Cell Stem Cell* 9, 298–310. doi: 10.1016/j.stem.2011.09.010

Tanaka, T., Kato, H., Kojima, I., Ohse, T., Son, D., Tawakami, T., et al. (2006). Hypoxia and expression of hypoxia-inducible factor in the aging kidney. *J. Gerontol. A Biol. Sci. Med. Sci.* 61, 795–805. doi: 10.1093/gerona/61.8.795

Tanaka, T., Kojima, I., Ohse, T., Ingelfinger, J. R., Adler, S., Fujita, T., et al. (2005a). Cobalt promotes angiogenesis via hypoxia-inducible factor and protects tubulointerstitium in the remnant kidney model. *Lab. Invest.* 85, 1292–1307. doi: 10.1038/labinvest.3700328

Tanaka, T., Matsumoto, M., Inagi, R., Miyata, T., Kojima, I., Ohse, T., et al. (2005b). Induction of protective genes by cobalt ameliorates tubulointerstitial injury in the progressive Thy1 nephritis. *Kidney Int.* 68, 2714–2725. doi: 10.1111/j.1523-1755.2005.00742.x

Tanaka, T., Miyata, T., Inagi, R., Fujita, T., and Nangaku, M. (2004). Hypoxia in renal disease with proteinuria and/or glomerular hypertension. *Am. J. Pathol.* 165, 1979–1992. doi: 10.1016/S0002-9440(10)63249-X

Tsubakihara, Y., Gejyo, F., Nishi, S., Iino, Y., Watanabe, Y., Suzuki, M., et al. (2012). High target hemoglobin with erythropoiesis-stimulating agents has advantages in the renal function of non-dialysis chronic kidney disease patients. *Ther. Apher. Dial.* 16, 529–540. doi: 10.1111/j.1744-9987.2012.01082.x

Vanderkooi, J. M., Maniara, G., Green, T. J., and Wilson, D. F. (1987). An optical method for measurement of dioxygen concentration based upon quenching of phosphorescence. *J. Biol. Chem.* 262, 5476–5482.

Welch, W. J., Baumgartl, H., Lubbers, D., and Wilcox, C. S. (2001). Nephron $pO_2$ and renal oxygen usage in the hypertensive rat kidney. *Kidney Int.* 59, 230–237. doi: 10.1046/j.1523-1755.2001.00483.x

Winter, J. D., Estrada, M., and Cheng, H. L. (2011). Normal tissue quantitative T1 and T2∗ MRI relaxation time responses to hypercapnic and hyperoxic gases. *Acad. Radiol.* 18, 1159–1167. doi: 10.1016/j.acra.2011.04.016

Yoshihara, T., Hosaka, M., Terata, M., Ichikawa, K., Murayama, S., Tanaka, A., et al. (2015). Intracellular and *in vivo* oxygen sensing using phosphorescent Ir(III) complexes with a modified acetylacetonato ligand. *Anal. Chem.* 87, 2710–2717. doi: 10.1021/ac5040067

**Conflict of Interest Statement:** The authors declare that the research was conducted in the absence of any commercial or financial relationships that could be construed as a potential conflict of interest.

frontiers in Physiology

MINI REVIEW
published: 08 February 2017
doi: 10.3389/fphys.2017.00074

# Stress Signal Network between Hypoxia and ER Stress in Chronic Kidney Disease

*Hiroshi Maekawa*[1] *and Reiko Inagi*[2]*

[1] Division of Nephrology and Endocrinology, University of Tokyo Graduate School of Medicine, Tokyo, Japan, [2] Division of Chronic Kidney Disease Pathophysiology, University of Tokyo Graduate School of Medicine, Tokyo, Japan

Chronic kidney disease (CKD) is characterized by an irreversible decrease in kidney function and induction of various metabolic dysfunctions. Accumulated findings reveal that chronic hypoxic stress and endoplasmic reticulum (ER) stress are involved in a range of pathogenic conditions, including the progression of CKD. Because of the presence of an arteriovenous oxygen shunt, the kidney is thought to be susceptible to hypoxia. Chronic kidney hypoxia is induced by a number of pathogenic conditions, including renal ischemia, reduced peritubular capillary, and tubulointerstitial fibrosis. The ER is an organelle which helps maintain the quality of proteins through the unfolded protein response (UPR) pathway, and ER dysfunction associated with maladaptive UPR activation is named ER stress. ER stress is reported to be related to some of the effects of pathogenesis in kidney, particularly in the podocyte slit diaphragm and tubulointerstitium. Furthermore, chronic hypoxia mediates ER stress in blood vessel endothelial cells and tubulointerstitium via several mechanisms, including oxidative stress, epigenetic alteration, lipid metabolism, and the AKT pathway. In summary, a growing consensus considers that these stresses interact via complicated stress signal networks, which leads to the exacerbation of CKD (**Figure 1**). This stress signal network might be a target for interventions aimed at ameliorating CKD.

**Keywords: hypoxia, er stress, chronic kidney disease, stress signal network, UPR signaling pathways**

OPEN ACCESS

***Edited by:***
*Maarten Koeners,*
*University of Bristol, UK*

***Reviewed by:***
*Zhanjun Jia,*
*Nanjing Medical University, China*
*Jaap Joles,*
*Utrecht University, Netherlands*

***Correspondence:**
*Reiko Inagi*
*inagi-npr@umin.ac.jp*

***Specialty section:***
*This article was submitted to Renal and Epithelial Physiology, a section of the journal Frontiers in Physiology*

***Received:*** *28 October 2016*
***Accepted:*** *26 January 2017*
***Published:*** *08 February 2017*

***Citation:***
*Maekawa H and Inagi R (2017) Stress Signal Network between Hypoxia and ER Stress in Chronic Kidney Disease. Front. Physiol. 8:74. doi: 10.3389/fphys.2017.00074*

## INTRODUCTION

CKD is a global public health problem which has substantial impact on morbidity, mortality, and health resource utilization. The progression of CKD is defined as a decrease in glomerular filtration rate regardless of primary disease. CKD is related to a variety of metabolic abnormalities including acidosis, hypertension, anemia, and mineral bone disease (Collister et al., 2016). Chronic hypoxia of the tubulointerstitium is the common pathway that leads to end stage renal disease (Mimura and Nangaku, 2010). Hypoxia also triggers ER stress, which further contributes to the progression of CKD (Inagi et al., 2014). In this review article, we summarize the crosstalk between hypoxia and ER stress in CKD and explore possible targets for intervention.

## PATHOPHYSIOLOGY OF HYPOXIA AND ER STRESS IN KIDNEY DISEASE

### Physiological Hypoxia in Kidney

Hypoxia is a pathologic condition which is characterized by an insufficient supply of oxygen to meet demand. The blood supply to the kidneys is very large, accounting for roughly 25% of cardiac

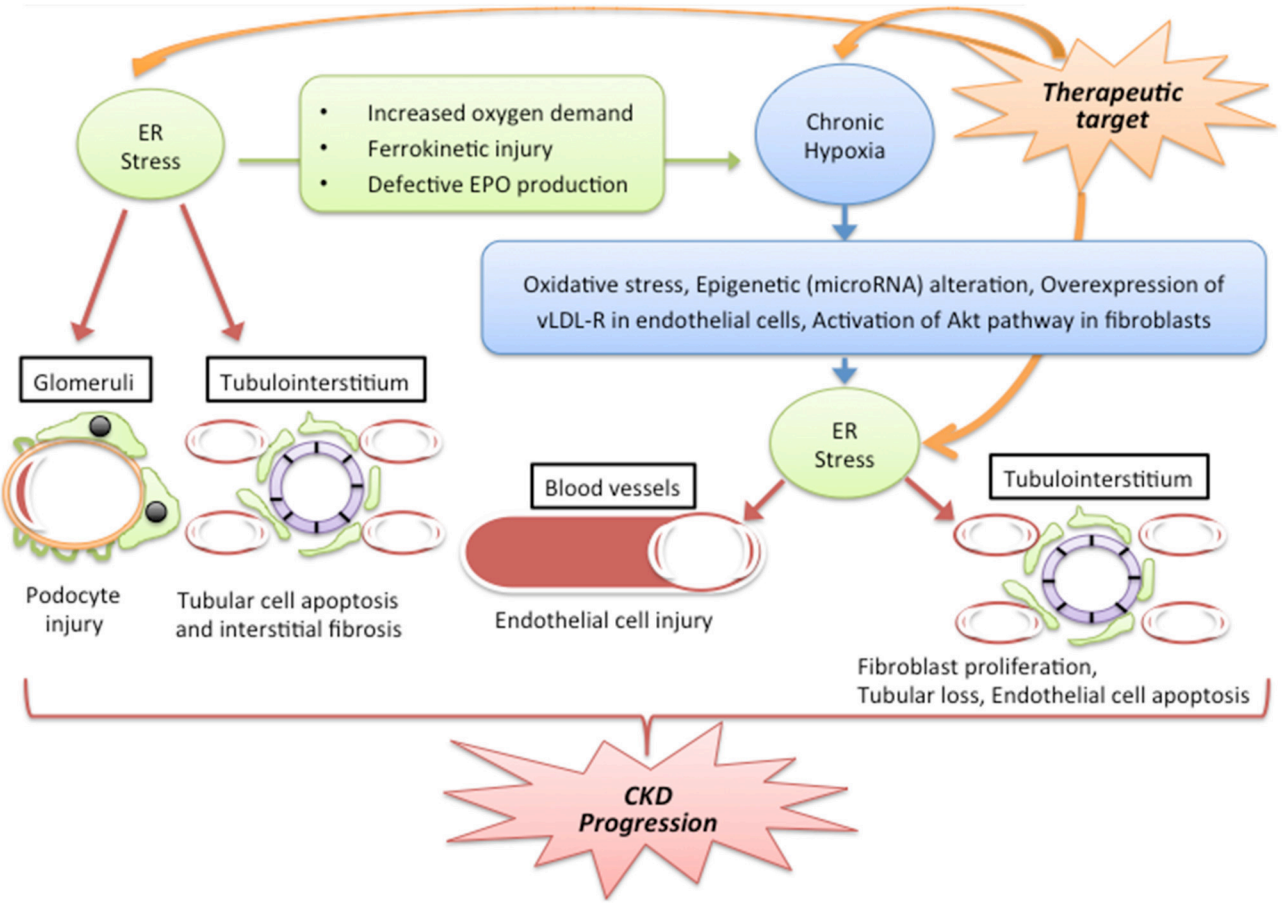


**FIGURE 1 | Putative stress signal network between ER stress and hypoxia in CKD.** Abbreviations: Epo, erythropoietin; ER, endoplasmic reticulum CKD: chronic kidney disease; vLDL-R, very low lipoprotein receptor. Hypoxia and ER stress interact through a number of complicated pathways and lead to the exacerbation of CKD. The progression of CKD is caused via vascular damage, glomerular damage and tubulointerstitial injury. The mechanisms by which ER stress induces hypoxia include a change of oxygen demand in tissue, dysfunction of iron metabolism and reduction in EPO production. By contrast, chronic hypoxia induces ER stress through oxidative stress, epigenetic regulation by microRNA, overexpression of vLDL-R and the Akt pathway. These pathogenic factors could be targets for CKD therapy.

output. However, owing to the presence of an arteriovenous oxygen shunt in the kidney (Schurek et al., 1990; Welch et al., 2001), no more than 10% of the oxygen delivered through the renal artery is utilized (Evans et al., 2008). Oxygen utilization by the kidney therefore appears to be inefficient, suggesting in turn that the kidney might be particularly susceptible to hypoxia.

## How Kidneys Survive the Hypoxic State

When the kidney is exposed to hypoxia, the expression of some genes changes. The master regulator of the adaptation to hypoxia is hypoxia inducible factor (HIF), a transcription factor. HIF is composed of an α-subunit (HIF-1α,2α,3α) and β-subunit [HIF-1β/AhR nuclear translocator (ARNT)]. Although HIF-1β is constitutively expressed, HIF-α members are degraded in normoxic conditions. HIF-α is hydroxylated by a prolyl hydroxylase domain-containing protein (PHD), and the binding of HIF–α protein to the von Hippel Lindau protein (pVHL) results in ubiquitination and degradation. Under hypoxia, HIF-α escapes this degradation and dimerizes with HIF-1β. The dimer translocates into the nucleus and binds to the hypoxia-response element (HRE) of HIF-target genes. This results in the activation of target genes involved in angiogenesis, erythropoiesis, and glycolysis (Mimura and Nangaku, 2010; Shoji et al., 2014).

## Pathogenic Hypoxia in the Kidney

Various pathogenic conditions induce chronic kidney hypoxia, including hypertension and diabetes. Some studies have shown that following renal ischemia, density of the peritubular capillaries decreases, as does oxygen tension in the kidney (Basile et al., 2001, 2003). Furthermore, the systemic hemodynamic changes and vasoconstriction associated with the renin-angiotensin system result in a decrease in peritubular capillary flow (Korner et al., 1994). Hypoxia might also be induced via tubulointerstitium fibrosis, in which the distance between

the capillary and tubular cells is extended, leading to further impairment of oxygen delivery (Norman and Fine, 2006). In addition, some conditions increase oxygen demand, including glomerular hyperfiltration induced by hyperglycemia, (Korner et al., 1994), and anemia decreases oxygen delivery to the kidney (Johannes et al., 2007).

## ER Stress and Its Stress Signal UPR Pathway

The ER is the main organelle involved in the quality control of proteins. This process, termed proteostasis, involves protein synthesis, protein folding, and the degradation of malfolded proteins. The quality of proteins is maintained through the UPR pathway, an integrated pathway which transduces information about protein folding conditions from the ER to the nucleus by controlling the activity of specific downstream transcription factors (Inagi et al., 2014; Rivas et al., 2015). The adaptive UPR pathway is regulated by the three major pathway transducers present in the ER lumen, named inositol-requiring protein 1 (IRE1), pancreatic eukaryotic translation initiation factor 2α (eIF2α) kinase (PERK) and activating transcription factor 6 (ATF6). These transducers are kept in an inactive state in normal conditions via binding to the ER chaperon GRP78 (78 kD glucose-regulated protein). However, the maintenance of protein metabolism is disturbed under various pathogenic stresses, including hypoxia. This disturbance results in the accumulation of unfolded proteins through ER dysfunction, which in turn causes cell damage. This series of events is termed ER stress. Under ER stress, GRP78 is dissociated from transducers and binds to unfolded proteins. The free transducers are thus activated, causing the UPR transcription factors, including X-box-binding protein 1 (XBP1) and ATF4, to translocate into the nucleus. This translation leads to up-regulation of the expression of UPR-target genes involved in protein folding and ER-associated protein degradation (ERAD). Activated ATF6 translocates into the Golgi apparatus and is cleaved to form ATFp50, a transcription factor which activates the expression of the UPR-target gene related to ERAD. However, if the adaptive UPR pathway is overcome by chronic or severe ER stress and proteostasis cannot be maintained, the predominant outcome is the induction of ER stress-related apoptosis, which occurs via the activation of C/EBP homologous protein (CHOP) (Kimata et al., 2004; Inagi, 2010; Pincus et al., 2010). ER stress is associated with many diseases, including diabetes (Rivas et al., 2015), chronic heart failure (Cominacini et al., 2015) and some neurodegenerative diseases (Soto, 2003). Moreover, many recent studies have reported a relationship between the UPR pathway and glomerular and tubular cell damage in various kidney diseases (Inagi et al., 2014).

### Pathophysiology of ER Stress in Kidney Disease

Many studies have revealed the effects of the pathogenesis of the UPR pathway in the kidney. The podocyte slit diaphragm is important as a glomerular filtration barrier. The structural components of the slit diaphragm [nephrin, alpha-actinin-4, and CD2-associated protein (CD2AP)] are subject to a mutation which causes defective protein folding in the ER of podocytes. The accumulation of malfolded proteins of the slit diaphragm induces structural and functional damage associated with ER stress and subsequent proteinuria (Cybulsky et al., 2009; Chiang and Inagi, 2010; He et al., 2011). Various pathogenic factors also trigger ER stress in podocytes, including complement complex (Cybulsky, 2013) and calcium entry via transient receptor protein 6 (TRPC6) (Chen et al., 2011). ER stress also injures podocytes via increased expression of monocyte chemoattractant protein 1 (MCP-1), which plays a central role in the inflammation associated with diabetic nephropathy. The structural and functional properties of tubular epithelial cells are closely dependent on ER proteostasis. Exposure of tubular cells to severe or long-term stress induces UPR pathway-mediated apoptosis and leads to the progression of CKD. Well-known examples of adverse factors that induce UPR pathway-related cell apoptosis, reduce the repair capacity of tubular cells and accelerate the progression of kidney disease include proteinuria (Ohse et al., 2006), hyperglycemia (Lindenmeyer et al., 2008), uremic toxins (Kawakami et al., 2010), and nephrotoxins, including cisplatin (Ozkok and Edelstein, 2014). Furthermore, ER stress has also been demonstrated in a unilateral ureteral obstruction tubulointerstitial fibrosis rat model (Chiang et al., 2011), in which excessive UPR activation over the adaptive UPR pathway contributed to tubular cell apoptosis and the resulting fibrosis.

# INTERACTION OF HYPOXIA AND ER STRESS

## Hypoxia to ER Stress

Chronic hypoxia triggers ER stress. Hypoxia induces cell stress, which leads the production of reactive oxygen species (ROS), a situation termed oxidative stress. ROS are produced in several organelles, including the ER. Altered redox homeostasis in the ER cause ER stress. These findings indicate a close link between hypoxia, oxidative stress, and ER stress (Sena and Chandel, 2012; Cao and Kaufman, 2014; Inagi et al., 2014). For example, we previously reported the epigenetic regulation of the cross-talk of hypoxia-oxidative stress-ER stress by microRNA. We found that miR-205, a microRNA which is predominantly expressed in kidney tubular cells, maintains tubular homeostasis by regulating the expression of PHD1, which negatively controls HIF1α and ATF4. HIF1α is a transcription factor of the HIF pathway and ATF4 is a transcription factor of the URP pathway, and the two act together to regulate antioxidant enzyme expression (Muratsu-Ikeda et al., 2012). Furthermore, hypoxia results in activation of the PERK/eIF2α axis of the UPR pathway by Akt (also known as protein kinase B or PKB), a serine/threonine kinase member of the AGC family of protein kinases which is involved in cell growth, proliferation, protein translation, and cell survival. Cells without Akt isoform 1 and 2 do not induce either PERK or eIF2α phosphorylation, even in hypoxic conditions, demonstrating that Akt mediates PERK/eIF2α activation during hypoxia (Blaustein et al., 2013). In addition, hypoxia triggers ER stress and induces very low density lipoprotein receptors (vLDL-R) in vessel endothelial cells. Knockdown or overexpression of

vLDL-R improves or exacerbates hypoxia-induced ER stress, demonstrating that vLDL-R induces endothelial cell apoptosis via ER stress (Yang et al., 2014). Thus, these mechanisms might be targets for interventions aimed at preventing the CKD progression associated with vessel and tubulointerstitial damage.

## ER Stress to Hypoxia

ER stress is reported to suppress the production of erythropoietin (EPO), a hematopoietic hormone regulated by the HIF pathway. This suppression of EPO by ER stress is inversely correlated with ATF4 expression, and the binding of ATF4 to the 3′ enhancer region of EPO gene abolished the enhancer activity (Chiang et al., 2013). ER stress also changes ferrokinetics. Hepcidin is a peptide hormone secreted by the liver which controls iron homeostasis. The production of Hepcidin is mediated by inflammation and iron. The overproduction of hepcidin causes anemia, but its deficiency leads to hemochromatosis. One report revealed that ER stress also induces hepcidin expression and causes hypoferremia in mice. CREBH (cyclic AMP response element–binding protein H), an ER stress–activated transcription factor, binds to and trans-activates the hepcidin promoter. Hepcidin induction in response to exogenously administered toxins or the accumulation of unfolded proteins in the ER is defective in CREBH knockout mice, indicating a role for CREBH in ER stress–regulated hepcidin expression (Vecchi et al., 2009). These reports indicate that ER stress is related to hematopoiesis and iron metabolism, and that ER stress might therefore be related to hypoxia via the mediation of anemic conditions.

The mechanisms described above could lead to a decrease in kidney function via deteriorating hypoxia by induction of anemia. In turn, a decrease in kidney function results in the accumulation of uremic toxins. Indoxyl sulfate (IS), a representative uremic toxin, induces ER stress in cultured human proximal tubular cells, as demonstrated by an increase in CHOP, and inhibits the proliferation/repair of tubular cells (Kawakami et al., 2010). Moreover, IS also increases oxygen consumption in kidney proximal tubular cells and decreases renal oxygenation. On the other hand, IS suppresses mRNA expression of EPO, demonstrating a link between IS and hypoxia as well as ER stress (Chiang et al., 2011). In fact, IS suppresses the induction of HIF-1 target gene expression in hypoxic conditions through dysfunction of the HIF-1α C-terminal transactivation domain (CTAD). The suppression of HIF-1 activity by IS is correlated with up-regulation of CBP/p300-interacting transactivator with the Glu/Asp-rich carboxy-terminal domain 2 (CITED2), which is a negative regulator of HIF-1 activity. Namely, IS increases CITED2 expression via post-transcriptional mRNA stabilization (Tanaka et al., 2013). Asai et al have shown that IS suppresses HIF activation, and subsequent EPO production via AhR activation, and that AhR blockade improves IS-induced suppression of HIF activation (Asai et al., 2016). These findings suggest that IS may be a pathogen that perturbs cross-talk between the UPR pathway of ER stress and the HIF pathway of hypoxia. Taken together, these findings indicate that the removal of IS, blockage of AhR, inhibition of hepcidin production and mediation of the UPR pathway, including ATF4, might be therapeutic targets in ameliorating hypoxia and subsequent CKD progression.

# CONCLUSION

Hypoxia and ER stress act together to induce a deterioration in kidney function. This adverse effect is mediated by the formation of a complicated signal network between them. Furthermore, uremic toxins such as IS also induce ER stress and subsequent hypoxia through suppression of erythropoiesis and the exacerbation of tubular fibrosis. These pathogenic factors could be targets for CKD therapy.

# AUTHOR CONTRIBUTIONS

This manuscript was written by HM and edited by RI.

# FUNDING

This work was supported by the Japan Society for the Promotion of Science Grants-in-Aid for Scientific Research (25461207, 15KT0088, and 16K15465 to RI), Yakult Bio-Science Foundation (to RI), and a research grant from Kyowa Hakko Kirin Co., Ltd (to RI).

# REFERENCES

Asai, H., Hirata, J., Hirano, A., Hirai, K., Seki, S., and Watanabe-Akanuma, M. (2016). Activation of aryl hydrocarbon receptor mediates suppression of hypoxia-inducible factor-dependent erythropoietin expression by indoxyl sulfate. *Am. J. Physiol. Cell Physiol.* 310, C142–C150. doi: 10.1152/ajpcell.00172.2015

Basile, D. P., Donohoe, D. L., Roethe, K., and Mattson, D. L. (2003). Chronic renal hypoxia after acute ischemic injury: effects of L-arginine on hypoxia and secondary damage. *Am. J. Physiol. Renal Physiol.* 284, F338–F348. doi: 10.1152/ajprenal.00169.2002

Basile, D. P., Donohoe, D., Roethe, K., and Osborn, J. L. (2001). Renal ischemic injury results in permanent damage to peritubular capillaries and influences long-term function. *Am. J. Physiol. Renal Physiol.* 281, F887–F899. doi: 10.1152/ajprenal.0050.2001

Blaustein, M., Perez-Munizaga, D., Sanchez, M. A., Urrutia, C., Grande, A., Risso, G., et al. (2013). Modulation of the Akt pathway reveals a novel link with PERK/eIF2α, which is relevant during hypoxia. *PLoS ONE* 8:e69668. doi: 10.1371/journal.pone.0069668

Cao, S. S., and Kaufman, R. J. (2014). Endoplasmic reticulum stress and oxidative stress in cell fate decision and human disease. *Antioxid. Redox Signal.* 21, 396–413. doi: 10.1089/ars.2014.5851

Chen, S., He, F. F., Wang, H., Fang, Z., Shao, N., Tian, X. J., et al. (2011). Calcium entry via TRPC6 mediates albumin overload-induced endoplasmic reticulum stress and apoptosis in podocytes. *Cell Calcium* 50, 523–529. doi: 10.1016/j.ceca.2011.08.008

Chiang, C. K., Hsu, S. P., Wu, C. T., Huang, J. W., Cheng, H. T., Chang, Y. W., et al. (2011). Endoplasmic reticulum stress implicated in the development of renal fibrosis. *Mol. Med.* 17, 1295–1305. doi: 10.2119/molmed.2011.00131

Chiang, C. K., and Inagi, R. (2010). Glomerular diseases: genetic causes and future therapeutics. *Nat. Rev. Nephrol.* 6, 539–554. doi: 10.1038/nrneph.2010.103

Chiang, C. K., Nangaku, M., Tanaka, T., Iwawaki, T., and Inagi, R. (2013). Endoplasmic reticulum stress signal impairs erythropoietin

production: a role for ATF4. *Am. J. Physiol. Cell Physiol.* 304, C342–C353. doi: 10.1152/ajpcell.00153.2012

Collister, D., Ferguson, T., Komenda, P., and Tangri, N. (2016). The patterns, risk factors, and prediction of progression in chronic kidney disease: a narrative review. *Semin. Nephrol.* 36, 273–282. doi: 10.1016/j.semnephrol.2016.05.004

Cominacini, L., Mozzini, C., Garbin, U., Pasini, A., Stranieri, C., Solani, E., et al. (2015). Endoplasmic reticulum stress and Nrf2 signaling in cardiovascular diseases. *Free Radic. Biol. Med.* 88, 233–242. doi: 10.1016/j.freeradbiomed.2015.05.027

Cybulsky, A. V. (2013). The intersecting roles of endoplasmic reticulum stress, ubiquitin- proteasome system, and autophagy in the pathogenesis of proteinuric kidney disease. *Kidney Int.* 84, 25–33. doi: 10.1038/ki.2012.390

Cybulsky, A. V., Takano, T., Papillon, J., Bijian, K., Guillemette, J., and Kennedy, C. R. (2009). Glomerular epithelial cell injury associated with mutant α-actinin-4. *Am. J. Physiol. Renal Physiol.* 297, F987–F995. doi: 10.1152/ajprenal.00055.2009

Evans, R. G., Gardiner, B. S., Smith, D. W., and O'connor, P. M. (2008). Intrarenal oxygenation: unique challenges and the biophysical basis of homeostasis. *Am. J. Physiol. Renal Physiol.* 295, F1259–F1270. doi: 10.1152/ajprenal.90230.2008

He, F., Chen, S., Wang, H., Shao, N., Tian, X., Jiang, H., et al. (2011). Regulation of CD2-associated protein influences podocyte endoplasmic reticulum stress-mediated apoptosis induced by albumin overload. *Gene* 484, 18–25. doi: 10.1016/j.gene.2011.05.025

Inagi, R. (2010). Endoplasmic reticulum stress as a progression factor for kidney injury. *Curr. Opin. Pharmacol.* 10, 156–165. doi: 10.1016/j.coph.2009.11.006

Inagi, R., Ishimoto, Y., and Nangaku, M. (2014). Proteostasis in endoplasmic reticulum–new mechanisms in kidney disease. *Nat. Rev. Nephrol.* 10, 369–378. doi: 10.1038/nrneph.2014.67

Johannes, T., Mik, E. G., Nohe, B., Unertl, K. E., and Ince, C. (2007). Acute decrease in renal microvascular $PO_2$ during acute normovolemic hemodilution. *Am. J. Physiol. Renal Physiol.* 292, F796–F803. doi: 10.1152/ajprenal.00206.2006

Kawakami, T., Inagi, R., Wada, T., Tanaka, T., Fujita, T., and Nangaku, M. (2010). Indoxyl sulfate inhibits proliferation of human proximal tubular cells via endoplasmic reticulum stress. *Am. J. Physiol. Renal Physiol.* 299, F568–F576. doi: 10.1152/ajprenal.00659.2009

Kimata, Y., Oikawa, D., Shimizu, Y., Ishiwata-Kimata, Y., and Kohno, K. (2004). A role for BiP as an adjustor for the endoplasmic reticulum stress-sensing protein Ire1. *J. Cell Biol.* 167, 445–456. doi: 10.1083/jcb.200405153

Korner, A., Eklof, A. C., Celsi, G., and Aperia, A. (1994). Increased renal metabolism in diabetes. Mechanism and functional implications. *Diabetes* 43, 629–633. doi: 10.2337/diab.43.5.629

Lindenmeyer, M. T., Rastaldi, M. P., Ikehata, M., Neusser, M. A., Kretzler, M., Cohen, C. D., et al. (2008). Proteinuria and hyperglycemia induce endoplasmic reticulum stress. *J. Am. Soc. Nephrol.* 19, 2225–2236. doi: 10.1681/ASN.2007121313

Mimura, I., and Nangaku, M. (2010). The suffocating kidney: tubulointerstitial hypoxia in end-stage renal disease. *Nat. Rev. Nephrol.* 6, 667–678. doi: 10.1038/nrneph.2010.124

Muratsu-Ikeda, S., Nangaku, M., Ikeda, Y., Tanaka, T., Wada, T., and Inagi, R. (2012). Downregulation of miR-205 modulates cell susceptibility to oxidative and endoplasmic reticulum stresses in renal tubular cells. *PLoS ONE* 7:e41462. doi: 10.1371/journal.pone.0041462

Norman, J. T., and Fine, L. G. (2006). Intrarenal oxygenation in chronic renal failure. *Clin. Exp. Pharmacol. Physiol.* 33, 989–996. doi: 10.1111/j.1440-1681.2006.04476.x

Ohse, T., Inagi, R., Tanaka, T., Ota, T., Miyata, T., Kojima, I., et al. (2006). Albumin induces endoplasmic reticulum stress and apoptosis in renal proximal tubular cells. *Kidney Int.* 70, 1447–1455. doi: 10.1038/sj.ki.5001704

Ozkok, A., and Edelstein, C. L. (2014). Pathophysiology of cisplatin-induced acute kidney injury. *Biomed. Res. Int.* 2014:967826. doi: 10.1155/2014/967826

Pincus, D., Chevalier, M. W., Aragon, T., Van Anken, E., Vidal, S. E., El-Samad, H., et al. (2010). BiP binding to the ER-stress sensor Ire1 tunes the homeostatic behavior of the unfolded protein response. *PLoS Biol.* 8:e1000415. doi: 10.1371/journal.pbio.1000415

Rivas, A., Vidal, R. L., and Hetz, C. (2015). Targeting the unfolded protein response for disease intervention. *Expert Opin. Ther. Targets* 19, 1203–1218. doi: 10.1517/14728222.2015.1053869

Schurek, H. J., Jost, U., Baumgartl, H., Bertram, H., and Heckmann, U. (1990). Evidence for a preglomerular oxygen diffusion shunt in rat renal cortex. *Am. J. Physiol.* 259, F910–F915.

Sena, L. A., and Chandel, N. S. (2012). Physiological roles of mitochondrial reactive oxygen species. *Mol. Cell* 48, 158–167. doi: 10.1016/j.molcel.2012.09.025

Shoji, K., Tanaka, T., and Nangaku, M. (2014). Role of hypoxia in progressive chronic kidney disease and implications for therapy. *Curr. Opin. Nephrol. Hypertens.* 23, 161–168. doi: 10.1097/01.mnh.0000441049.98664.6c

Soto, C. (2003). Unfolding the role of protein misfolding in neurodegenerative diseases. *Nat. Rev. Neurosci.* 4, 49–60. doi: 10.1038/nrn1007

Tanaka, T., Yamaguchi, J., Higashijima, Y., and Nangaku, M. (2013). Indoxyl sulfate signals for rapid mRNA stabilization of Cbp/p300-interacting transactivator with Glu/Asp-rich carboxy-terminal domain 2 (CITED2) and suppresses the expression of hypoxia-inducible genes in experimental CKD and uremia. *FASEB J.* 27, 4059–4075. doi: 10.1096/fj.13-231837

Vecchi, C., Montosi, G., Zhang, K., Lamberti, I., Duncan, S. A., Kaufman, R. J., et al. (2009). ER stress controls iron metabolism through induction of hepcidin. *Science* 325, 877–880. doi: 10.1126/science.1176639

Welch, W. J., Baumgartl, H., Lubbers, D., and Wilcox, C. S. (2001). Nephron $pO_2$ and renal oxygen usage in the hypertensive rat kidney. *Kidney Int.* 59, 230–237. doi: 10.1046/j.1523-1755.2001.00483.x

Yang, D., Gao, L., Wang, T., Qiao, Z., Liang, Y., and Zhang, P. (2014). Hypoxia triggers endothelial endoplasmic reticulum stress and apoptosis via induction of VLDL receptor. *FEBS Lett.* 588, 4448–4456. doi: 10.1016/j.febslet.2014.09.046

**Conflict of Interest Statement:** The authors declare that the research was conducted in the absence of any commercial or financial relationships that could be construed as a potential conflict of interest.

frontiers in Physiology

MINI REVIEW
published: 05 January 2017
doi: 10.3389/fphys.2016.00667

# Blood Oxygenation Level-Dependent MRI to Assess Renal Oxygenation in Renal Diseases: Progresses and Challenges

*Menno Pruijm *, Bastien Milani and Michel Burnier*

*Service of Nephrology and Hypertension, Department of Medicine, Centre Hospitalier Universitaire Vaudois, Lausanne, Switzerland*

BOLD-MRI (blood oxygenation-level dependent magnetic resonance imaging) allows non-invasive measurement of renal tissue oxygenation in humans, without the need for contrast products. BOLD-MRI uses the fact that magnetic properties of hemoglobin depend of its oxygenated state:: the higher local deoxyhemoglobin, the higher the so called apparent relaxation rate R2* ($sec^{-1}$), and the lower local tissue oxygen content. Several factors other than deoxyhemoglobin (such as hydration status, dietary sodium intake, and susceptibility effects) influence the BOLD signal, and need to be taken into account when interpreting results. The last 5 years have witnessed important improvements in the standardization of these factors, and the appearance of new, highly reproducible analysis techniques of BOLD-images, that are reviewed in this article. Using these new BOLD-MRI analysis techniques, it has recently been shown that persons suffering from chronic kidney diseases (CKD) have lower cortical oxygenation than normotensive controls, thus confirming the chronic hypoxia hypothesis. The acute alterations in R2* after the administration of furosemide are smaller in CKD, and represent an estimate of the oxygen-dependent tubular transport of sodium. BOLD-MRI-alone or in combination with other functional MRI methods- can be used to monitor the renal effects of drugs, and is increasingly used in the preclinical setting. The near future will tell whether or not BOLD-MRI represents a new tool to predict renal function decline an adverse renal outcome.

**Keywords: BOLD-MRI, chronic kidney disease, renal artery stenosis, furosemide, TLCO-technique**

OPEN ACCESS

***Edited by:***
*Maarten Koeners,*
*University of Bristol, UK*

***Reviewed by:***
*Kirk L. Hamilton,*
*University of Otago, New Zealand*
*Christoffer Laustsen,*
*Aarhus University, Denmark*

****Correspondence:***
*Menno Pruijm*
*menno.pruijm@chuv.ch*

***Specialty section:***
*This article was submitted to Renal and Epithelial Physiology, a section of the journal Frontiers in Physiology*

***Received:*** *01 November 2016*
***Accepted:*** *19 December 2016*
***Published:*** *05 January 2017*

***Citation:***
*Pruijm M, Milani B and Burnier M (2017) Blood Oxygenation Level-Dependent MRI to Assess Renal Oxygenation in Renal Diseases: Progresses and Challenges. Front. Physiol. 7:667. doi: 10.3389/fphys.2016.00667*

## INTRODUCTION

Chronic kidney disease (CKD), defined as an estimated glomerular filtration rate below 60 ml/min/1.73 $m^2$ and/or the presence of (micro) albuminuria, has become a major public health problem with a global prevalence in the general population of ∼10% (Ponte et al., 2013). CKD is an independent cardiovascular risk factor and associated with increased mortality (Astor et al., 2011). The pathophysiology of CKD and its progression to end stage renal disease is complex and incompletely understood, but mounting evidence from animal studies suggests that renal tissue hypoxia is the final and common pathway, irrespective of etiology (Alberti and Zimmet, 1998; Fine and Norman, 2008). According to this "chronic hypoxia hypothesis," loss of peritubular capillaries induces interstitial hypoxia which triggers local inflammation and fibrosis. This leads in turn to

further obliteration and loss of capillaries, thus completing the vicious circle. So far, evidence for the chronic hypoxia hypothesis in humans has been sparse, mainly because of the lack of methods to assess renal tissue oxygenation in a reliable, non-invasive manner.

A technique to measure tissue oxygenation in humans would be a valuable tool for several reasons. First of all, such a technique could be used to confirm or reject the chronic hypoxia hypothesis. Secondly, ideally it would allow to identify CKD patients at increased risk for rapid renal function decline and end-stage renal disease, since according to the chronic hypoxia hypothesis, those with the lowest degree of oxygenation have the highest renal risk. Finally, drugs that chronically increase renal tissue oxygenation would have the potential to retard the progression of CKD. Thus, a method capable of measuring renal tissue oxygenation could identify at an early stage drugs with oxygen-increasing and possibly nephroprotective potential.

Since its first description in 1996 (Prasad et al., 1996), renal blood oxygenation-level dependent MRI (BOLD-MRI) is seen by many as the most promising method to assess renal oxygenation non-invasively in humans. In brief, BOLD-MRI uses the paramagnetic properties of deoxyhemoglobin to assess tissue oxygenation: the higher local deoxyhemoglobin, the higher the apparent relaxation rate R2* ($sec^{-1}$), and the lower local tissue oxygen content, assuming that blood $pO_2$ is in equilibrium with tissue $pO_2$. BOLD-MRI does not require the administration of (possibly nephrotoxic) contrast media, making it an interesting tool for CKD patients. BOLD-MRI is fast and can be repeated many times in short time intervals without side-effects.

Despite these advantages, BOLD-MRI is for the moment mainly used in research settings and not yet fully integrated in clinical practice. The initial enthusiasm was tempered by studies who failed to demonstrate with BOLD-MRI that chronic hypoxia is indeed present in humans. Besides, we have learned that factors other than oxygenation (such as blood pH, hematocrite, hydration status, and susceptibility effects, see below) influence the BOLD-signal (Prasad and Epstein, 1999; Pruijm et al., 2010; Neugarten, 2012). However, progress has been made in the standardization of these factors, as well as in data acquisition and analysis, which has recently lead to interesting results and will possibly lead to new applications for this technique. In this article, we review the technical hurdles that had to be overcome, others that still need to be resolved, the main results of clinical studies and the perspectives of BOLD-MRI.

## BOLD-MRI: TECHNIQUE AND PITFALLS

The basic principle of Magnetic Resonance Imaging (MRI) can be summarized as follows: when atomic nuclei with non-zero angular momentum (like hydrogen) are placed in a magnetic field and reach thermal equilibrium, an excess of nuclei lying in the low energy state appears. This excess of nuclei can be brought to some higher energy state when excited by an electromagnetic wave (pulse). The nuclei return to equilibrium after the excitation while emitting back a radiation; this takes a certain time, measured as the so called relaxation times (T1 and T2). These parameters provide information about the density and localization of (hydrogen or other) nuclei, and allow the construction of an image.

BOLD-MRI measures the apparent relaxation rate R2* (or decay rate, defined as 1/T2* and expressed in $sec^{-1}$) for each voxel located in the kidney. This parameter is influenced by any kind of inhomogeneity in the static magnetic field, in particular by the effect of deoxyhemoglobin, which has a strong positive magnetic susceptibility due to its central iron atom. The susceptibility difference between deoxyhemoglobin and surrounding tissues will generate intra-voxel magnetic field inhomogeneities. As such, the decay rate R2* will be enhanced when the local deoxyhemoglobin concentration is increased. Assuming that blood pO2 is in equilibrium with tissue pO2, R2* values allows to qualitatively compare tissue oxygenation between different voxel of the same subject and between subjects: low R2* values indicates high tissue oxygenation, and vice versa (Prasad, 2006). BOLD-MRI has been validated in animal studies, showing that R2* correlates negatively with directly measured pO2 (Pedersen et al., 2005). However, several points merit attention in the interpretation of R2* values. First, factors that affect the oxygen dissociation curve (which describes the relationship between de(oxy)Hb and pO2) such as blood pH, body temperature, and hematocrite alter the equilibrium described above, and should be taken into account when performing BOLD-MRI (Neugarten, 2012). Second, the BOLD-signal is sensitive to an acute water load (Prasad and Epstein, 1999). This sensitivity is partly explained by the water-induced reduction in oxygen-consuming tubular transport, but an increase in tubular volume after water intake will also reduce the local deoxyhemoglobin volume fraction and thus further decrease R2*. Standardization of water intake is therefore warranted. Because tubular sodium reabsorption is a major driver of oxygen consumption, short-term alterations in dietary sodium intake influence significantly medullary R2* values, and urinary sodium excretion (as a proxy of sodium intake) should therefore be measured whenever possible (Pruijm et al., 2010).

While the acquisition of BOLD-MRI is performed in many centers worldwide, no general consensus exists on how to analyze the BOLD-images, and many methods are in use (see **Figure 1** for a few examples). In the oldest and most frequently used method, the ROI technique, small circles each containing a collection of voxels -called regions of interest (ROI's)- are placed manually in the cortex and in the medulla of each slice (**Figure 1**, left image). This allows the calculation of the average cortical and medullary R2* values, per kidney or for both kidneys together (Simon-Zoula et al., 2006). Placement of ROIs is easy in kidneys with preserved renal function, but difficult in patients with advanced CKD due to the lack of cortico-medullary differentiation in the latter (e.g., the human eye is no longer capable of differentiating the cortex from the medulla purely based on radiological contrast differences). A second, recent method called the TLCO (12 layers concentric objects) technique is a semi-automatic procedure that divides the kidney in 12 layers of equal thickness. The mean R2* values of all layers can be plotted as a curve (the R2* radial profile) with a certain slope (**Figure 1**, middle image). The steepness of the slope is associated with the degree of CKD: the higher the eGFR, the steeper the slope (Milani et al., 2016). The R2* profile has a

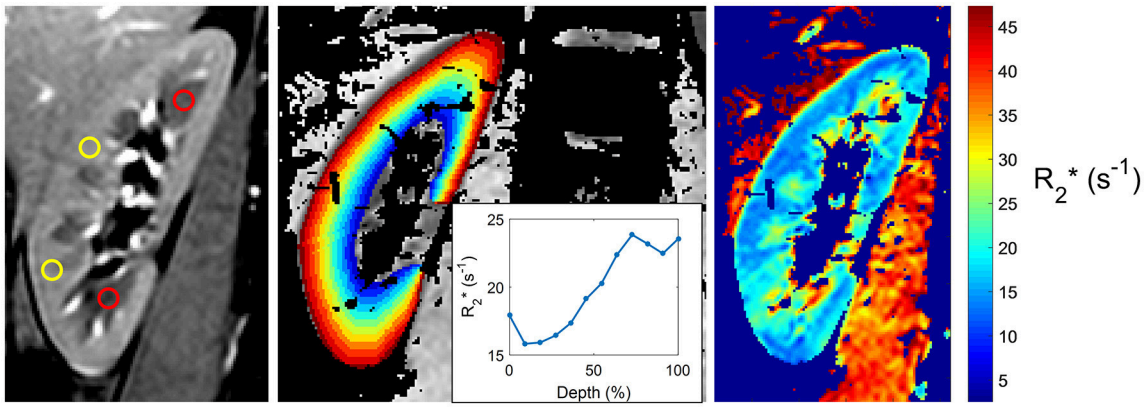


**FIGURE 1 | Three currently used techniques to analyze BOLD-MRI. (Left)** Classical ROI-based technique, with placement of circle-shaped regions of interest (ROIs) in the renal cortex (yellow) and medulla (red); **(Middle)** Twelve-Layer Concentric Objects (TLCO) technique, which divides the renal parenchyma in 12 layers of equal thickness; **(Right)** Fractional hypoxia technique, which counts the percentage of voxels with an R2* value >30 $sec^{-1}$.

low inter-observer variability and can visualize layer by layer the effect of external stimuli, making it an interesting tool to study the effects of drugs, as recently demonstrated (Vakilzadeh et al., 2015).

Since the BOLD-signal is influenced by many factors, of which some are scanner related, absolute R2* values are not comparable across sites. The steepness of the R2* slopes less of the R2* values, but merely of their intra-compartmental distribution. This observable may therefore be more suitable for comparisons across centers, which would be a huge advantage for eventual future integration in clinical practice. Another way to overcome this hurdle is to perform a dynamic test (such as the administration of IV furosemide or 100% oxygen breathing), and to assess the percentage change in R2*.

In a third method called the fractional tissue hypoxia-technique, the whole renal parenchyma is selected, and the percentage of R2* values above a certain threshold (usually 30 $s^{-1}$ or >2.5 standard deviations of the average R2* value) is reported (Saad et al., 2013). This technique provides a variable—the percentage of hypoxic tissue- that can be easily interpreted by clinicians, but it does not differentiate between cortex and medulla (**Figure 1**, right image).

Taken together, each technique has his advantages and disadvantages. The most promising and reproducible technique for CKD patients is at the moment, to our opinion, the TLCO method; international efforts are ongoing and necessary to standardize analysis methods in the years to come.

## BOLD-MRI IN CKD

Surprisingly, BOLD-MRI studies have not uniformly demonstrated that renal tissue oxygenation is reduced in CKD patients as compared with controls. Some studies reported higher R2* values suggesting lower renal oxygenation at lower eGFR, whereas other studies did not find any correlation between CKD status and R2* (**Table 1**). Unfortunately, many of the "early" studies lacked information on drug-or sodium intake, did not standardize water intake, or did not differentiate between the underlying causes of CKD. However, even well-designed studies failed to show differences in R2* between persons with and without CKD (Khatir et al., 2015). It has become clear that the analysis technique has a large impact on the results. Our research group has recently demonstrated that the ROI technique is highly observer-dependent in advanced CKD, and should therefore not be used in these patients (Piskunowicz et al., 2015). The importance of the used analysis technique is further illustrated by the fact that our research group did not find any differences in R2* with the ROI technique, whereas the use of the TLCO technique in the same patient cohort showed significant differences in R2* between the cortical layers of CKD patients and controls (Milani et al., 2016).

As can be appreciated in **Table 1**, recent BOLD-MRI studies have actually demonstrated that CKD patients have higher R2* values (corresponding to lower renal tissue oxygenation) as compared to controls, thus confirming the findings of animal studies. Differences in R2* were mainly confined to the cortex, which is somewhat surprising, since the cortex has higher pO2 values than the medulla (50 vs. 10–20 mmHg), receives 90% of the renal blood flow, and has relatively lower oxygen consumption than the medulla (Aukland and Krog, 1960; Heyman et al., 2008). In theory, the cortex should therefore be better protected against hypoxia. Whether this is explained by glomerular hyperfiltration in residual glomeruli, altered diffusive shunting pathways or reduced metabolic efficiency of solute transport in tubular cells is actually unclear. Of note, although the mean R2* is higher in CKD patients, differences are small, and according to some authors mainly driven by a minority of CKD patients with high R2* values (Prasad et al., 2015). This finding illustrates that renal tissue oxygenation is rather tightly controlled in the majority of individuals. In this respect, some have stated that interstitial fibrosis- the consequence of hypoxia and one of the hallmarks of advanced kidney disease- might be a way to maintain to a certain degree renal oxygenation, by decreasing local oxygen-consuming

**TABLE 1 | Overview of the studies that have used BOLD-MRI to assess renal tissue oxygenation in CKD patients as compared with controls.**

| Author | | *N* | Design | Field strength (Tesla) | Analysis method | R2* cortex | R2* medulla | Remark |
|---|---|---|---|---|---|---|---|---|
| Inoue | 2011 | 119 | CKD-control | 1.5 | ROI | No difference | Not available | Only DM |
| Wang | 2011 | 27 | CKD-control | 1.5 | ROI | No difference | Lower in CKD | Only DM |
| Michaely | 2012 | 280 | Observational | 1.5 and 3 | ROI | No difference | No difference | |
| Xin-Long | 2012 | 26 | CKD-control | 3 | ROI | Higher in CKD | Higher in CKD | |
| Yin | 2012 | 115 | CKD-control | 3 | ROI | Higher in CKD | Higher in CKD | Only DM |
| Pruijm | 2014 | 195 | CKD-control | 3 | ROI | No difference | No difference | |
| Vink | 2015 | 75 | Hypertensives | 1.5 and 3 | Fractional and Compartmental | No difference | Higher at lower eGFR | eGFR 75 ± 18 ml/min |
| Thacker | 2015 | 47 | CKD-control | 3 | Large ROI-entire parenchyma | Higher in CKD | No difference | |
| Prasad | 2015 | 59 | CKD-control | 3 | ROI | Higher in CKD | No difference | |
| Khatir | 2015 | 86 | CKD-control | 1.5 | ROI | No difference | No difference | |
| Milani | 2016 | 207 | CKD-control | 3 | TLCO | Higher in CKD | Lower in CKD | |

active transport. Long-term 5/6 nephrectomy models in the rat have indeed reported maintained pO2 levels in remnant kidneys (Priyadarshi et al., 2002). In humans, this hypothesis has not been confirmed so far; one study reported no correlation between R2* values and the degree of fibrosis (Ries et al., 2003), another found higher R2* values at increasing degrees of biopsy-proven fibrosis (Inoue et al., 2011). Finally, it is actually unknown whether CKD patients with high R2* values have more progressive disease than those with lower R2* values, and longitudinal follow-up studies are therefore eagerly awaited.

## BOLD-MRI AND DRUGS

As stated in the introduction, BOLD-MRI can be repeated many times without side effects, making it an interesting tool to study the effect of drugs. On this behalf, the loop diuretic furosemide has been the most investigated. Blocking the $Na^+$-$K^+$-$2Cl^-$ transporter in the thick ascending loop of Henle with an IV bolus of furosemide leads to an acute decrease in active oxygen-consuming sodium transport, and increases local pO2 (Liss et al., 1999). As a proof of concept, acute furosemide-induced decreases in medullary R2* have been reported in both animals and humans (Brezis et al., 1994; Epstein and Prasad, 2000). Of interest, the medulla of CKD patients shows smaller decreases in R2* in response to furosemide than controls, and the furosemide-induced R2* change correlates well with the eGFR (Pruijm et al., 2014). This is explained by some as purely a dose effect due to the reduced renal function. Indeed, in order to exert its natriuretic action, furosemide has to be secreted by the proximal tubular cells, which is less the case at lower eGFR. Others see the R2* response as an indicator of tubular function and transport. For example, hypertensive individuals show, as CKD patients, a blunted R2* response to furosemide, although their eGFR is preserved, an observation that possibly refers to altered tubular sodium handling in hypertensives. Whether the R2* response to furosemide is indeed a marker of tubular function and mass, and has prognostic potential to predict adverse renal outcome, is currently unknown.

Few studies have tested other drugs with regard to their effect on R2*. One of the earliest studies reported acute increases in medullary and cortical R2* after iodinated contrast products, which is in line with their well-known vasoconstrictive and nephrotoxic potential (Hofmann et al., 2006). Inversely, acute decreases in R2* (within 1 h) have been described after the administration of blockers of the renin-angiotensin system in small studies that included hypertensive or CKD patients (Djamali et al., 2007; Siddiqi et al., 2014). This is in line with the nephroprotective properties of these drugs, that lower intraglomerular pressure, tubular sodium transport, local inflammation, and oxidative stress (Tocci and Volpe, 2011). In contrast, chronic intake of renin-angiotensin system inhibitors did not alter renal R2* values (Pruijm et al., 2013), although a small decrease in cortical R2* values was found in hypertensive patients after 2 months of aliskiren (Vakilzadeh et al., 2015). These studies show that acute alterations in R2* occur, but they also illustrate once more that chronic renal tissue oxygenation is rather tightly controlled. The acute, drug induced- alterations in R2* offer insights in the mechanism of action and possibly nephroprotective potential of drugs in a preclinical setting. BOLD-MRI can be combined with other MRI methods such as arterial spin labeling, capable of measuring localrenal blood flow, or dynamic contrast enhanced-imaging that can directly measure glomerular filtration rate (Ebrahimi et al., 2014). Therefore, functional MRI can provide a wealth of information in the renal mechanisms of action of drugs, and possibly indicate renal side effects or benefits long before clinical outcome studies. Considering animal studies, functional MRI also has the potential to reduce animal usage. For these reasons, we expect functional MRI to play an increasingly important role in drug research.

## BOLD-MRI AND RENAL ARTERY STENOSIS

As any organ, renal tissue oxygenation depends not only of local oxygen consumption (mainly active tubular sodium-dependent transport), but also of oxygen delivery (renal blood flow and hemoglobin level). Renal artery stenosis (RAS) is the classic example of ischemic nephropathy, and one would expect to find cortical and medullary hypoxia in this patient group. Animal

studies have indeed reported acute increases in R2* after clipping of the renal artery (Juillard et al., 2004). However, no hypoxia could be detected with BOLD-MRI 4 weeks after clipping of the renal artery (Rognant et al., 2010). As in the remnant kidney model, the kidneys at the side of the clipped renal artery were atrophic and non-functional, and this study therefore does not necessarily reflect the situation as often encountered in the clinic when RAS kidneys are (slightly) reduced in size, but not atrophic.

In humans, BOLD-MRI has, to the best of our knowledge, not been used in situations of acute renal artery occlusion. In chronic RAS, increases in R2* have been reported in patients with severe RAS (>90%), but not in those with less severe RAS (Gloviczki et al., 2011a). Hence, renal tissue oxygenation seems to be relatively independent from global renal blood flow. Of note, kidneys have the particularity that increases in RBF do not necessarily increase local pO2. Indeed, an increase in RBF leads, at constant filtration fraction, also to a higher GFR which on its term will increase the amount of filtered sodium, and thus the tubular sodium load and oxygen consumption (Hansell et al., 2013).

Some investigators have used the R2* response to furosemide as a marker of viability of renal tissue (Gloviczki et al., 2011b). In unilateral RAS, the eGFR does not provide information on the relative function of each kidney, whereas BOLD-MRI allows per-kidney analysis. The research group from the Mayo Clinic has demonstrated that the change in R2* after IV furosemide is smaller in those with severe RAS and reduced renal volume than in those with moderate RAS, and that non-viable renal tissue is therefore possibly defined as tissue that does not exhibit any change in R2* after furosemide (Gloviczki et al., 2011a).

# CLINICAL APPLICATIONS AND PERSPECTIVES

## Renal Artery Stenosis

Large randomized trials such as the Angioplasty and Stenting for Renal Artery Lesions trial (ASTRAL) have tempered the enthusiasm of clinicians to perform renal artery angioplasty ± stenting in RAS patients (Investigators et al., 2009). Nevertheless, it is well known that some patients definitely benefit from angioplasty, and the main question remains how to predict the outcome of this procedure. The studies outlined above show that renal oxygenation can be maintained over a wide range of stenosis, but that above a certain individual threshold, chronic ischemia occurs, leading to inflammation, and decline of renal function, and diminished response to furosemide (Gloviczki et al., 2011a,b). This suggests that patients who will most likely benefit from angioplasty present chronic ischemia and a maintained response to furosemide, but this has not been tested in clinical practice. Hermann et al. recently reported that fractional hypoxia was higher in the stenotic kidneys of patients with high-grade RAS than in patients with essential hypertension (22.1 ± 20 vs. 9.6 ± 7%). Fractional hypoxia diminished (from 22.1 ± 20 to 14.9 ± 18.3%) after renal stenting (Herrmann et al., 2016). In a similar way, an English research group showed that those with higher overall R2* levels and preserved renal volume and function had favorable outcomes after revascularization (Chrysochou et al., 2012). The integration of functional BOLD-MRI in the workup and decision process of RAS opens new perspectives, but this needs further validation in clinical studies.

## Chronic Kidney Disease

Ideally, BOLD-MRI should identify patients at increased risk of CKD progression, expecting that those with the lowest renal oxygenation, or the lowest R2* change after furosemide, have the highest risk of progression. So far, these data are lacking, hampering the introduction of BOLD-MRI in clinical practice.

Another issue is the fact that BOLD-MRI alone cannot establish whether a high R2* value is the result of low oxygen delivery (low RBF, extended renal fibrosis), high oxygen consumption (glomerular hyperfiltration, enhanced tubular absorption), or both. CKD is characterized by increased fibrosis, which on the one hand limits oxygen diffusion out of capillaries into renal cells, yet on the other hand also limits oxygen consumption. Quantifying fibrosis and regional blood flow, in combination with BOLD-MRI, could therefore provide useful information. Apart from $T_1$mapping, so-called diffusion-weighted MRI (DW-MRI) offers a non-invasive way to quantify renal fibrosis and microcirculation. DW-MRI collects images with and without diffusion weighted gradients, and expresses molecular diffusion as the apparent diffusion coefficient (ADC) Liss et al., 2013. The total ADC can be separated in a perfusion fraction ($F_p$) and perfusion-free diffusion ($ADC_D$), as measures of local microcirculation and fibrosis. A reduction in ADC has been shown to correlate with CKD staging and the degree of fibrosis (Xu et al., 2010; Zhao et al., 2014), and a reduction in $F_p$ has been demonstrated in renal allografts suffering from acute rejection (Eisenberger et al., 2010). Whether a combination of BOLD-MRI and diffusion MRI is capable of predicting renal function decline is not yet known, and subject of active research.

# CONCLUSION

BOLD-MRI is an exciting technique to assess renal oxygenation non-invasively in humans. Increased knowledge of factors that influence the BOLD-signal has lead to better standardization, and refinements in the analysis technique to highly reproducible results. BOLD-MRI is a powerful tool to detect the influence of altered hemodynamics, drugs, or dietary factors on renal oxygenation. The near future will tell if BOLD-MRI (alone or in combination with other MRI modalities) allows the selection of RAS patients who will benefit from revascularization, and/or early identification of CKD patients at high risk for renal function decline.

# AUTHOR CONTRIBUTIONS

MP: Drafting the article, final approval of the version to be published, agrees to be accountable for all aspects of the work in ensuring that questions related to the accuracy or integrity of any part of the work are appropriately investigated and resolved. BM and MB: Revising the article critically for important intellectual

content, final approval of the submitted version, both agree to be accountable for all aspects of the work in ensuring that questions related to the accuracy or integrity of any part of the work are appropriately investigated and resolved.

## FUNDING

This work was supported by grants from the Swiss National Science Fondation (FN 32003B-149309 and 320030-169191).

## REFERENCES

Alberti, K. G., and Zimmet, P. Z. (1998). Definition, diagnosis and classification of diabetes mellitus and its complications. Part 1: diagnosis and classification of diabetes mellitus provisional report of a WHO consultation. Diabetic medicine: a journal of the British Diabetic Association. 15, 539–553. doi: 10.1002/(SICI)1096-9136(199807)15:7<539::AID-DIA668>3.0.CO;2-S

Astor, B. C., Matsushita, K., Gansevoort, R. T., van der Velde, M., Woodward, M., Levey, A. S., et al. (2011). Lower estimated glomerular filtration rate and higher albuminuria are associated with mortality and end-stage renal disease. A collaborative meta-analysis of kidney disease population cohorts. *Kidney Int.* 79, 1331–1340. doi: 10.1038/ki.2010.550

Aukland, K., and Krog, J. (1960). Renal oxygen tension. *Nature* 188:671. doi: 10.1038/188671a0

Brezis, M., Agmon, Y., and Epstein, F. H. (1994). Determinants of intrarenal oxygenation. I. Effects of diuretics. *Am. J. Physiol.* 267, F1059–F1062.

Chrysochou, C., Mendichovszky, I. A., Buckley, D. L., Cheung, C. M., Jackson, A., and Kalra, P. A. (2012). BOLD imaging: a potential predictive biomarker of renal functional outcome following revascularization in atheromatous renovascular disease. *Nephrol. Dial Transplant.* 27, 1013–1019. doi: 10.1093/ndt/gfr392

Djamali, A., Sadowski, E. A., Muehrer, R. J., Reese, S., Smavatkul, C., Vidyasagar, A., et al. (2007). BOLD-MRI assessment of intrarenal oxygenation and oxidative stress in patients with chronic kidney allograft dysfunction. *Am. J. Physiol. Renal Physiol.* 292, F513–F522. doi: 10.1152/ajprenal.00222.2006

Ebrahimi, B., Textor, S. C., and Lerman, L. O. (2014). Renal relevant radiology: renal functional magnetic resonance imaging. *Clin. J. Am. Soc. Nephrol.* 9, 395–405. doi: 10.2215/CJN.02900313

Eisenberger, U., Thoeny, H. C., Binser, T., Gugger, M., Frey, F. J., Boesch, C., et al. (2010). Evaluation of renal allograft function early after transplantation with diffusion-weighted MR imaging. *Eur. Radiol.* 20, 1374–1383. doi: 10.1007/s00330-009-1679-9

Epstein, F. H., and Prasad, P. (2000). Effects of furosemide on medullary oxygenation in younger and older subjects. *Kidney Int.* 57, 2080–2083. doi: 10.1046/j.1523-1755.2000.00057.x

Fine, L. G., and Norman, J. T. (2008). Chronic hypoxia as a mechanism of progression of chronic kidney diseases: from hypothesis to novel therapeutics. *Kidney Int.* 74, 867–872. doi: 10.1038/ki.2008.350

Gloviczki, M. L., Glockner, J. F., Crane, J. A., McKusick, M. A., Misra, S., Grande, J. P., et al. (2011a). Blood oxygen level-dependent magnetic resonance imaging identifies cortical hypoxia in severe renovascular disease. *Hypertension* 58, 1066–1072. doi: 10.1161/HYPERTENSIONAHA.111.171405

Gloviczki, M. L., Lerman, L. O., and Textor, S. C. (2011b). Blood oxygen level-dependent (BOLD) MRI in renovascular hypertension. *Curr. Hypertens. Rep.* 13, 370–377. doi: 10.1007/s11906-011-0218-7

Hansell, P., Welch, W. J., Blantz, R. C., and Palm, F. (2013). Determinants of kidney oxygen consumption and their relationship to tissue oxygen tension in diabetes and hypertension. *Clin. Exp. Pharmacol. Physiol.* 40, 123–137. doi: 10.1111/1440-1681.12034

Herrmann, S. M., Saad, A., Eirin, A., Woollard, J., Tang, H., McKusick, M. A., et al. (2016). Differences in GFR and tissue oxygenation, and interactions between stenotic and contralateral kidneys in unilateral atherosclerotic renovascular disease. *Clin. J. Am. Soc. Nephrol.* 11, 458–469. doi: 10.2215/CJN.036 20415

Heyman, S. N., Khamaisi, M., Rosen, S., and Rosenberger, C. (2008). Renal parenchymal hypoxia, hypoxia response and the progression of chronic kidney disease. *Am. J. Nephrol.* 28, 998–1006. doi: 10.1159/000146075

Hofmann, L., Simon-Zoula, S., Nowak, A., Giger, A., Vock, P., Boesch, C., et al. (2006). BOLD-MRI for the assessment of renal oxygenation in humans: acute effect of nephrotoxic xenobiotics. *Kidney Int.* 70, 144–150. doi: 10.1038/sj.ki.5000418

Inoue, T., Kozawa, E., Okada, H., Inukai, K., Watanabe, S., Kikuta, T., et al. (2011). Noninvasive evaluation of kidney hypoxia and fibrosis using magnetic resonance imaging. *J. Am. Soc. Nephrol.* 22, 1429–1434. doi: 10.1681/ASN.2010111143

Investigators, A., Wheatley, K., Ives, N., Gray, R., Kalra, P. A., Moss, J. G., et al. (2009). Revascularization versus medical therapy for renal-artery stenosis. *N. Engl. J. Med.* 361, 1953–1962. doi: 10.1056/NEJMoa0905368

Juillard, L., Lerman, L. O., Kruger, D. G., Haas, J. A., Rucker, B. C., Polzin, J. A., et al. (2004). Blood oxygen level-dependent measurement of acute intra-renal ischemia. *Kidney Int.* 65, 944–950. doi: 10.1111/j.1523-1755.2004.00469.x

Khatir, D. S., Pedersen, M., Jespersen, B., and Buus, N. H. (2015). Evaluation of renal blood flow and oxygenation in CKD using magnetic resonance imaging. *Am. J. Kidney Dis.* 66, 402–411. doi: 10.1053/j.ajkd.2014.11.022

Liss, P., Cox, E. F., Eckerbom, P., and Francis, S. T. (2013). Imaging of intrarenal haemodynamics and oxygen metabolism. *Clin. Exp. Pharmacol. Physiol.* 40, 158–167. doi: 10.1111/1440-1681.12042

Liss, P., Nygren, A., Ulfendahl, H. R., and Erikson, U. (1999). Effect of furosemide or mannitol before injection of a non-ionic contrast medium on intrarenal oxygen tension. *Adv. Exp. Med. Biol.* 471, 353–359. doi: 10.1007/978-1-4615-4717-4_42

Milani, B., Ansaloni, A., Sousa-Guimaraes, S., Piskunowicz, M., Vogt, B., Stuber, M., et al. (2016). [Op.4d.06] reduction of cortical oxygenation in chronic kidney disease: evidence obtained with bold-mri and a new analytic technique. *J. Hypertens.* 34(Suppl. 2):e52. doi: 10.1097/01.hjh.0000491472.37273.d4

Neugarten, J. (2012). Renal BOLD-MRI and assessment for renal hypoxia. *Kidney Int.* 81, 613–614. doi: 10.1038/ki.2011.462

Pedersen, M., Dissing, T. H., Mørkenborg, J., Stødkilde-Jorgensen, H., Hansen, L. H., Pedersen, L. B., et al. (2005). Validation of quantitative BOLD MRI measurements in kidney: application to unilateral ureteral obstruction. *Kidney Int.* 67, 2305–2312. doi: 10.1111/j.1523-1755.2005.00334.x

Piskunowicz, M., Hofmann, L., Zuercher, E., Bassi, I., Milani, B., Stuber, M., et al. (2015). A new technique with high reproducibility to estimate renal oxygenation using BOLD-MRI in chronic kidney disease. *Magn. Reson. Imaging* 33, 253–261. doi: 10.1016/j.mri.2014.12.002

Ponte, B., Pruijm, M., Marques-Vidal, P., Martin, P. Y., Burnier, M., Paccaud, F., et al. (2013). Determinants and burden of chronic kidney disease in the population-based CoLaus study: a cross-sectional analysis. *Nephrol. Dial. Transplant.* 28, 2329–2339. doi: 10.1093/ndt/gft206

Prasad, P. V. (2006). Evaluation of intra-renal oxygenation by BOLD MRI. *Nephron Clin. Pract.* 103, c58–c65. doi: 10.1159/000090610

Prasad, P. V., Edelman, R. R., and Epstein, F. H. (1996). Noninvasive evaluation of intrarenal oxygenation with BOLD MRI. *Circulation* 94, 3271–3275. doi: 10.1161/01.CIR.94.12.3271

Prasad, P. V., and Epstein, F. H. (1999). Changes in renal medullary $pO_2$ during water diuresis as evaluated by blood oxygenation level-dependent magnetic resonance imaging: effects of aging and cyclooxygenase inhibition. *Kidney Int.* 55, 294–298. doi: 10.1046/j.1523-1755.1999.00237.x

Prasad, P. V., Thacker, J., Li, L. P., Haque, M., Li, W., Koenigs, H., et al. (2015). Multi-parametric evaluation of chronic kidney disease by mri: a preliminary cross-sectional study. *PLoS ONE* 10:e0139661. doi: 10.1371/journal.pone.0139661

Priyadarshi, A., Periyasamy, S., Burke, T. J., Britton, S. L., Malhotra, D., and Shapiro, J. I. (2002). Effects of reduction of renal mass on renal oxygen tension and erythropoietin production in the rat. *Kidney Int.* 61, 542–546. doi: 10.1046/j.1523-1755.2002.00140.x

Pruijm, M., Hofmann, L., Maillard, M., Tremblay, S., Glatz, N., Wuerzner, G., et al. (2010). Effect of sodium loading/depletion on renal oxygenation in young normotensive and hypertensive men. *Hypertension* 55, 1116–1122. doi: 10.1161/HYPERTENSIONAHA.109.149682

Pruijm, M., Hofmann, L., Piskunowicz, M., Muller, M. E., Zweiacker, C., Bassi, I., et al. (2014). Determinants of renal tissue oxygenation as measured with

BOLD-MRI in chronic kidney disease and hypertension in humans. *PLoS ONE* 9:e95895. doi: 10.1371/journal.pone.0095895

Pruijm, M., Hofmann, L., Zanchi, A., Maillard, M., Forni, V., Muller, M. E., et al. (2013). Blockade of the renin-angiotensin system and renal tissue oxygenation as measured with BOLD-MRI in patients with type 2 diabetes. *Diabetes Res. Clin. Pract.* 99, 136–144. doi: 10.1016/j.diabres.2012.11.004

Ries, M., Basseau, F., Tyndal, B., Jones, R., Deminiere, C., Catargi, B., et al. (2003). Renal diffusion and BOLD MRI in experimental diabetic nephropathy. Blood oxygen level-dependent. *J. Magn. Reson. Imaging* 17, 104–113. doi: 10.1002/jmri.10224

Rognant, N., Rouviere, O., Janier, M., Le, Q. H., Barthez, P., Laville, M., et al. (2010). Hemodynamic responses to acute and gradual renal artery stenosis in pigs. *Am. J. Hypertens.* 23, 1216–1219. doi: 10.1038/ajh.2010.147

Saad, A., Crane, J., Glockner, J. F., Herrmann, S. M., Friedman, H., Ebrahimi, B., et al. (2013). Human renovascular disease: estimating fractional tissue hypoxia to analyze blood oxygen level-dependent MR. *Radiology* 268, 770–778. doi: 10.1148/radiol.13122234

Siddiqi, L., Hoogduin, H., Visser, F., Leiner, T., Mali, W. P., and Blankestijn, P. J. (2014). Inhibition of the renin-angiotensin system affects kidney tissue oxygenation evaluated by magnetic resonance imaging in patients with chronic kidney disease. *J. Clin. Hypertens.* 16, 214–218. doi: 10.1111/jch.12263

Simon-Zoula, S. C., Hofmann, L., Giger, A., Vogt, B., Vock, P., Frey, F. J., et al. (2006). Non-invasive monitoring of renal oxygenation using BOLD-MRI: a reproducibility study. *NMR Biomed.* 19, 84–89. doi: 10.1002/nbm.1004

Tocci, G., and Volpe, M. (2011). End-organ protection in patients with hypertension: focus on the role of angiotensin receptor blockers on renal function. *Drugs* 71, 1003–1017. doi: 10.2165/11591350-000000000-00000

Vakilzadeh, N., Muller, M. E., Forni, V., Milani, B., Hoffman, L., Piskunowicz, M., et al. (2015). Comparative effect of a renin inhibitor and a thiazide diuretic on renal tissue oxygenation in hypertensive patients. *Kidney Blood Press. Res.* 40, 542–554. doi: 10.1159/000368530

Xu, X., Fang, W., Ling, H., Chai, W., and Chen, K. (2010). Diffusion-weighted MR imaging of kidneys in patients with chronic kidney disease: initial study. *Eur. Radiol.* 20, 978–983. doi: 10.1007/s00330-009-1619-8

Zhao, J., Wang, Z. J., Liu, M., Zhu, J., Zhang, X., Zhang, T., et al. (2014). Assessment of renal fibrosis in chronic kidney disease using diffusion-weighted MRI. *Clin. Radiol.* 69, 1117–1122. doi: 10.1016/j.crad.2014.06.011

**Conflict of Interest Statement:** The authors declare that the research was conducted in the absence of any commercial or financial relationships that could be construed as a potential conflict of interest.

frontiers in Physiology

MINI REVIEW
published: 01 March 2016
doi: 10.3389/fphys.2016.00072

# Hyperpolarized Renal Magnetic Resonance Imaging: Potential and Pitfalls

*Christoffer Laustsen* *

*Department of Clinical Medicine, MR Research Centre, Aarhus University, Aarhus, Denmark*

The introduction of dissolution dynamic nuclear polarization (d-DNP) technology has enabled a new paradigm for renal imaging investigations. It allows standard magnetic resonance imaging complementary renal metabolic and functional fingerprints within seconds without the use of ionizing radiation. Increasing evidence supports its utility in preclinical research in which the real-time interrogation of metabolic turnover can aid the physiological and pathophysiological metabolic and functional effects in *ex vivo* and *in vivo* models. The method has already been translated to humans, although the clinical value of this technology is unknown. In this paper, I review the potential benefits and pitfalls associated with dissolution dynamic nuclear polarization in preclinical research and its translation to renal patients.

**Keywords: dynamic nuclear polarization, hyperpolarization, magnetic resonance imaging, renal metabolism**

OPEN ACCESS

***Edited by:***
*Maarten Koeners,*
*University of Bristol, UK*

***Reviewed by:***
*Rajesh Mohandas,*
*University of Florida, USA*
*Paul Hockings,*
*Antaros Medical, Sweden*
*Menno Pruijm,*
*University Hospital Lausanne (CHUV), Switzerland*

***Correspondence:**
*Christoffer Laustsen*
*cl@clin.au.dk*

***Specialty section:***
*This article was submitted to Renal and Epithelial Physiology, a section of the journal Frontiers in Physiology*

***Received:*** *14 December 2015*
***Accepted:*** *15 February 2016*
***Published:*** *01 March 2016*

***Citation:***
*Laustsen C (2016) Hyperpolarized Renal Magnetic Resonance Imaging: Potential and Pitfalls. Front. Physiol. 7:72. doi: 10.3389/fphys.2016.00072*

## RENAL MAGNETIC RESONANCE IMAGING

Magnetic resonance imaging (MRI) is a harmless, non-ionizing imaging modality that provides excellent soft tissue contrast. Although this technique has been used successfully in several applications, its full potential is seldom utilized *in vivo* because of its limited sensitivity. This low sensitivity increases the acquisition times beyond acceptable time scales for detecting metabolically active molecules and substrates in low concentrations. To date, renal MRI is used primarily for morphological examinations in clinical practice. However, for renal functional imaging, several potentially important alternatives exist, which can provide information on renal physiological status in terms of fibrosis, oxygenation, and glomerular filtration. These methods have yet to be translated to clinical practice (Prasad, 2006; Notohamiprodjo et al., 2010). Preclinical and clinical studies have indicated that these methods hold promise for improving the management and outcome of patients with renal diseases (Prasad, 2006; Notohamiprodjo et al., 2010).

The complex pathophysiology of renal disease is closely associated with metabolic alterations that contribute to the disease or are caused as a result of disease progression. Despite tremendous achievements in understanding the basic mechanism of renal disease, scientists still have poor insight into the metabolic link between the development and treatment of renal disease. This is partly because the methods employed to investigate these mechanisms are often destructive *ex vivo* methods or *in vivo* radiolabeled tracer techniques.

Advances in hyperpolarization technology have opened up new avenues for increasing the sensitivity of diagnostic imaging in humans using both spin exchange optical pumping (SEOP) and dissolution dynamic nuclear polarization (d-DNP) hyperpolarization. SEOP enables hyperpolarization of noble gases such as Xenon-129 and Helium-3, while d-DNP enables

**Abbreviations:** d-DNP, dissolution dynamic nuclear polarization; MRI, magnetic resonance imaging.

hyperpolarization of carbon-13 in solution (Ardenkjaer-Larsen et al., 2003). This review focuses on d-DNP for renal imaging applications.

## DISSOLUTION DYNAMIC NUCLEAR POLARIZATION

Dissolution dynamic nuclear polarization (d-DNP) is a method that extends the already vast applicability of MRI to provide real time *in situ* cellular metabolic information (Ardenkjaer-Larsen et al., 2003, 2011). The method relies on the generation of a transient artificial high signal 10,000-fold greater than the thermal signal at room temperature at clinical MR magnetic field strengths. This is achieved by placing the sample in a high magnetic field (typically 3–5 T) at low temperature (typically 1.3–0.8 K), and irradiating it with microwaves to transfer energy from electron spins to nuclear spins (typically carbon-13), creating the hyperpolarized sample. The hyperpolarized sample is then rapidly dissolved to obtain a liquid solution retaining the transient hyperpolarized signal (**Figure 1**).

d-DNP MRI relies on an intravenous bolus injection of carbon-13 ($^{13}$C)-enriched biomarkers. Thus, high renal perfusion, metabolic activity, and altered metabolic and functional status in renal diseases makes this technology useful for renal investigations (Johansson et al., 2004; Golman and Petersson, 2006; Leupold et al., 2009). Hyperpolarized biomarkers enable direct quantification of tracer movement, as visible on positron emission tomography (PET). Similar to PET, the hyperpolarized tracer, and not modulation of the surrounding tissue, is the origin of the signal, as seen on standard contrast MRI. This allows for background-free images with high temporal resolution without the use of harmful radiation. The hyperpolarized signal is typically only observable within 1–2 min after dissolution, similar to the fast decaying PET tracers. The chemical structure dictates the signal decay rate and thus the usability of a given molecule, which leads to only small molecules being candidates for d-DNP imaging *in vivo*. The use of very small molecules ensures that bio-probes such as pyruvate, urea, and fumarate are typically freely filtered by the glomerulus and reabsorbed in the proximal tubule.

Compared to existing diagnostic tools, hyperpolarized MRI has a clear advantage in that it detects the metabolic conversion of $^{13}$C-labeled endogenous biomarkers into metabolic derivatives within the cells *in vivo*. Thus, it detects physiological and pathophysiological changes without the need for invasive biopsies and allows characterization of the entire parenchyma over time. This factor potentially enables separate assessment of individual kidneys, the cortex, and medulla, functional heterogeneity, and focal deficits.

Renal d-DNP MR has received increased attention because it illustrates the dynamic renal status in normal and diseased kidneys in a harmless manner (Leupold et al., 2009; Clatworthy et al., 2012; Laustsen et al., 2013, 2014a,b; Reed et al., 2014). For patients at risk of developing kidney disease, progressive knowledge of *in vivo* renal substrate selection and functional alterations may help to clarify the mechanisms that cause the kidney to fail.

The potential of d-DNP MR for metabolic and functional investigations of the kidneys was recognized early on by Golman et al. using hyperpolarized renal renograms and perfusion assessment (Golman et al., 2001; Johansson et al., 2004; Golman and Petersson, 2006); more importantly, they showed that hyperpolarized [1-$^{13}$C]pyruvate could be used for real-time metabolic imaging *in vivo*. The localization and metabolic rate of pyruvate conversion may be important for diagnosis and for monitoring treatment in renal ischemia reperfusion (Leupold et al., 2009). It can thus serve as a marker of early renal dysfunction to guide therapeutic interventions (Laustsen et al., 2013, 2014b, 2015; Keshari et al., 2015), and highlight potential targets of therapy so as to prevent progression toward chronic kidney disease. An increasing amount of evidence supports the claim of [1-$^{13}$C] pyruvate as a renal biomarker in diabetic nephropathy and in ischemia/reperfusion injury.

Although no alterations in renal pyruvate metabolism were detected in mice with folic acid-induced acute kidney injury, early tubular necrosis can be detected using fumarate-to-malate conversion. Fumarate does not readily enter healthy cells, and therefore, its conversion is observed only when the cell membrane is permeable. Hence, only early tubular necrosis is detectable *via* a positive malate signal (Clatworthy et al., 2012). In addition to a severely deranged pyruvate metabolism profile in the early diabetic nephropathic kidney, Keshari et al. (2015) recently showed increased oxidative stress in diabetic mouse kidneys by using the novel redox sensor, hyperpolarized [1-$^{13}$C] dehydroascorbate. The Keshari study interestingly highlighted the potential of interrogating oxidative stress modulations, which showed that angiotensin II treatment reversed the renal redox status in the diabetic kidney. A particularly interesting alternative bioprobe for renal investigations—$^{13}$C-urea—is sensitive to the intra-renal osmolality gradient—a hallmark of tubular function. Measuring the intrarenal distribution and perfusion of urea has been demonstrated to detect alterations in the distribution between hydration and diuresis (von Morze et al., 2012). Improved relaxation (decay rate) properties are easily incorporated by utilizing [$^{13}$C,$^{15}$N] urea as the bioprobe. This avoids the fast relaxation of quadrupolar nitrogen 14 ($^{14}$N), which reduces the lifetime of the hyperpolarized sample (Reed et al., 2014). Hyperpolarized urea may ultimately reveal pathological changes in the diseased kidney. Recent novel methods that utilize the relaxation contrast mechanisms of urea are able to identify increased oxygen consumption in the early diabetic kidney and during diuresis and antidiuresis with high resolution (Reed et al., 2015; Laustsen et al., 2016). Urea shows a major potential for clinical translation as a single metabolite bioprobe, and provides simple, intuitive, and quantifiable information on the renal status. These studies together highlight the potential of a conceptual new framework for future research and drug discovery for renal diseases.

## POTENTIAL AND PITFALLS

Growing evidence supports hyperpolarized MRI as an excellent research tool in specialized centers; however, several potential pitfalls exist for its translation into widespread use and clinical

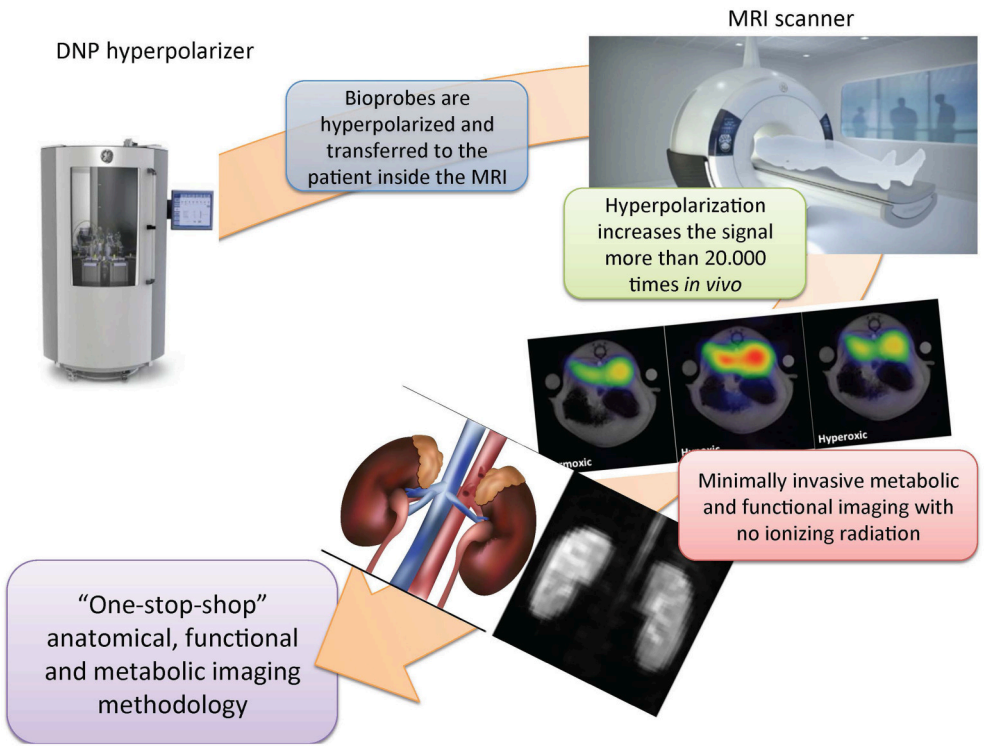


**FIGURE 1 | Dissolution dynamic nuclear polarization magnetic resonance imaging—a "one-stop-shop" methodology.** The biomarker is hyperpolarized and transferred by intravenous injection to the patient inside the clinical scanner. This procedure increases the sensitivity of the measurements by more than 20,000 times, and enables the direct interrogation of renal uptake and metabolic turnover. Standard clinical magnetic resonance imaging (MRI) capabilities are simultaneously available and provide a very versatile and sensitive diagnostic modality that is free of ionizing radiation and thereby ensures patient safety. DNP, dissolution dynamic nuclear polarization.

practice. Most noteworthy are the use of apparent rate constants rather than the "true" rate constants, which would require significant invasive information on the cellular distribution of enzymes, cosubstrates, pH, temperature, and the pool sizes of the substrates for the reactions. This limitation can be partly overcome by introducing an intervention in the examination, similar to the furosemide challenge in blood oxygenation level-dependent (BOLD) MRI, which promotes a change in oxygen utilization because the required energy need is halted; however, a quantifiable measure would significantly increase the impact of the methods. The acquisition and following reconstruction strategies can also significantly impact the quantification of the experiments by imposing compromises on the available information. Hyperpolarized MRI inherently spans a five-dimensional space (i.e., three spatial, one temporal, and one spectral dimension); thus, the acquisition of the transient signal (signal decay due to image acquisition and relaxation decay) is a compromise between signal availability and the information needed to answer a particular question. Several advanced methods have thus been developed for obtaining metabolic and functional information in d-DNP experiments (Cunningham et al., 2007, 2008; Leupold et al., 2009; Mayer et al., 2009; Schmidt et al., 2014). However, this factor limits the reproducibility and comparability of the results. It is also imperative to align acquisition, reconstruction, and analysis protocols to increase the impact in research and in clinical practice, including standardization of supporting information, such as oxygenation status, heart rate, and perfusion.

Non-metabolic biomarkers such as urea for renal functional imaging can be readily quantified *via* perfusion mapping similar to positron emission tomography and relaxation mapping. This allows easier translation and interpretation of the results.

Most renal investigations have been performed in rodent models, which have unipapillary kidneys, in contrast to the multipapillary human kidney. Thus, rodent metabolism is highly elevated in comparison to that of humans. This difference between the physiology of the rat and human kidneys imposes limitations on the interpretation and translatability of the results. A limited number of studies have been performed in porcine models, which resemble the human physiology and show good agreement with the findings in rodents, along with high intra-animal reproducibility (Laustsen et al., 2015). The limited resolution often utilized in rodent studies imposes significant challenges in differentiating the cortical signal from the medullary signal. This limitation is less pronounced in large animal models; however, improved resolution is still needed.

## HUMAN TRANSLATION IN RENAL PATIENTS

A critical point is patient safety. The current clinically ready d-DNP system relies on closed sterile samples, denoted fluid paths, and a non-contact quality control system, which ensures patient safety. The general tolerability of the pyruvate injection is high, which showed no adverse events in humans in an initial human study (Nelson et al., 2013). The production utilizes stable isotopes and requires only increased capacities of the vendors, which makes the method an already affordable technology. [1-$^{13}$C] Pyruvate is the first bioprobe in the market, but several other candidates are in the clinical pipeline such as [2-$^{13}$C]pyruvate, [1,4-$^{13}C_2$]fumarate, $^{13}$C-urea, and [1-$^{13}$C]lactate.

The initial human study (Nelson et al., 2013) was performed on cancer patients. However, the biomarkers and procedures are similar for renal investigations, and thereby reduce the transfer time between patient groups. Hyperpolarized MRI shows great potential for generating new and translational insights, and thereby advances the basic understanding of renal pathophysiology and improves the basal needs for treating renal disease, even without clinical translation. To realize the clinical potential of renal hyperpolarized MRI, it is essential to improve the general availability and reproducibility of the method, to generate strong evidence of its clinical utility by performing multicenter trials, and to demonstrate the warranted evidence by comparing it to gold standard methods in patients. An especially critical point in the translation of the method is the standardization of the patient with respect to hydration and metabolic status, as illustrated by the preclinical studies. This is critical to ensure reproducibility and to maximize the sensitivity to both disease and interventions.

Although d-DNP has a few but significant pitfalls, it has great potential as a medical imaging modality. Dissolution-DNP can potentially change the medical imaging paradigm by allowing a harmless, so-called "one-stop-shop" imaging methodology. In this paper, I reviewed the advantages and the pitfalls associated with dissolution dynamic nuclear polarization in preclinical research and its translation to renal patients. The findings of this review suggest that this technology may generate new and translational insights, advance the basic understanding of renal pathophysiology, and improve the treatment of renal disease, even without clinical translation.

## AUTHOR CONTRIBUTIONS

All authors listed, have made substantial, direct and intellectual contribution to the work, and approved it for publication.

## FUNDING

The study was supported by The Danish Research Council, The Danish Kidney Foundation, Helen and Ejnar Bjørnows Foundation.

## REFERENCES

Ardenkjaer-Larsen, J. H., Fridlund, B., Gram, A., Hansson, G., Hansson, L., Lerche, M. H., et al. (2003). Increase in signal-to-noise ratio of > 10,000 times in liquid-state NMR. *Proc. Natl. Acad. Sci. U.S.A.* 100, 10158–10163. doi: 10.1073/pnas.1733835100

Ardenkjaer-Larsen, J. H., Leach, A. M., Clarke, N., Urbahn, J., Anderson, D., and Skloss, T. W. (2011). Dynamic nuclear polarization polarizer for sterile use intent. *NMR Biomed.* 24, 927–932. doi: 10.1002/nbm.1682

Clatworthy, M. R., Kettunen, M. I., Hu, D. E., Mathews, R. J., Witney, T. H., Kennedy, B. W., et al. (2012). Magnetic resonance imaging with hyperpolarized [1,4-$^{13}C_2$]fumarate allows detection of early renal acute tubular necrosis. *Proc. Natl. Acad. Sci. U.S.A.* 109, 13374–13379. doi: 10.1073/pnas.1205539109

Cunningham, C. H., Chen, A. P., Albers, M. J., Kurhanewicz, J., Hurd, R. E., Yen, Y. F., et al. (2007). Double spin-echo sequence for rapid spectroscopic imaging of hyperpolarized $^{13}$C. *J. Magn. Reson.* 187, 357–362. doi: 10.1016/j.jmr.2007.05.014

Cunningham, C. H., Chen, A. P., Lustig, M., Hargreaves, B. A., Lupo, J., Xu, D., et al. (2008). Pulse sequence for dynamic volumetric imaging of hyperpolarized metabolic products. *J. Magn. Reson.* 193, 139–146. doi: 10.1016/j.jmr.2008.03.012

Golman, K., Axelsson, O., Jóhannesson, H., Månsson, S., Olofsson, C., and Petersson, J. S. (2001). Parahydrogen-induced polarization in imaging: subsecond $^{13}$C angiography. *Magn. Reson. Med.* 46, 1–5. doi: 10.1002/mrm.1152

Golman, K., and Petersson, J. S. (2006). Metabolic imaging and other applications of hyperpolarized $^{13}$C. *Acad. Radiol.* 13, 932–942. doi: 10.1016/j.acra.2006.06.001

Johansson, E., Olsson, L. E., Månsson, S., Petersson, J. S., Golman, K., Ståhlberg, F., et al. (2004). Perfusion assessment with bolus differentiation: a technique applicable to hyperpolarized tracers. *Magn. Reson. Med.* 52, 1043–1051. doi: 10.1002/mrm.20247

Keshari, K. R., Wilson, D. M., Sai, V., Bok, R., Jen, K. Y., Larson, P., et al. (2015). Noninvasive *in vivo* imaging of diabetes-induced renal oxidative stress and response to therapy using hyperpolarized $^{13}$C dehydroascorbate magnetic resonance. *Diabetes* 64, 344–352. doi: 10.2337/db13-1829

Laustsen, C., Hansen, E. S., Kjaergaard, U., Bertelsen, L. B., Ringgaard, S., and Stødkilde-Jørgensen, H. (2015). Acute porcine renal metabolic effect of endogastric soft drink administration assessed with hyperpolarized [1-(13)C]pyruvate. *Magn. Reson. Med.* 74, 558–563. doi: 10.1002/mrm.25692

Laustsen, C., Østergaard, J. A., Lauritzen, M. H., Nørregaard, R., Bowen, S., Søgaard, L. V., et al. (2013). Assessment of early diabetic renal changes with hyperpolarized [1-$^{13}$C]pyruvate. *Diabetes Metab. Res. Rev.* 29, 125–129. doi: 10.1002/dmrr.2370

Laustsen, C., Lipsø, K., Ostergaard, J. A., Nørregaard, R., Flyvbjerg, A., Pedersen, M., et al. (2014b). Insufficient insulin administration to diabetic rats increases substrate utilization and maintains lactate production in the kidney. *Physiol. Rep.* 2:e12233. doi: 10.14814/phy2.12233

Laustsen, C., Lycke, S., Palm, F., Østergaard, J. A., and Bibby, B. M., Nørregaard, R., et al. (2014a). High altitude may alter oxygen availability and renal metabolism in diabetics as measured by hyperpolarized [1-$^{13}$C]pyruvate magnetic resonance imaging. *Kidney Int.* 86, 67–74. doi: 10.1038/ki.2013.504

Laustsen, C., Stokholm Nørlinger, T., Christoffer Hansen, D., Qi, H., Mose Nielsen, P., Bonde Bertelsen, L., et al. (2016). Hyperpolarized $^{13}$C urea relaxation mechanism reveals renal changes in diabetic nephropathy. *Magn. Reson. Med.* 75, 515–518. doi: 10.1002/mrm.26036

Leupold, J., Månsson, S., Petersson, J. S., Hennig, J., and Wieben, O. (2009). Fast multiecho balanced SSFP metabolite mapping of 1H and hyperpolarized $^{13}$C compounds. *MAGMA* 22, 251–256. doi: 10.1007/s10334-009-0169-z

Mayer, D., Yen, Y. F., Tropp, J., Pfefferbaum, A., Hurd, R. E., and Spielman, D. M. (2009). Application of subsecond spiral chemical shift imaging to real-time multislice metabolic imaging of the rat *in vivo* after injection

of hyperpolarized $^{13}C_1$-pyruvate. *Magn. Reson. Med.* 62, 557–564. doi: 10.1002/mrm.22041

Nelson, S. J., Kurhanewicz, J., Vigneron, D. B., Larson, P. E., Harzstark, A. L., Ferrone, M., et al. (2013). Metabolic imaging of patients with prostate cancer using hyperpolarized [1-$^{13}$C] pyruvate. *Sci. Transl. Med.* 5:198ra108. doi: 10.1126/scitranslmed.3006070

Notohamiprodjo, M., Reiser, M. F., and Sourbron, S. P. (2010). Diffusion and perfusion of the kidney. *Eur. J. Radiol.* 76, 337–347. doi: 10.1016/j.ejrad.2010.05.033

Prasad, P. V. (2006). Functional MRI of the kidney: tools for translational studies of pathophysiology of renal disease. *Am. J. Physiol. Renal Physiol.* 290, F958–F974. doi: 10.1152/ajprenal.00114.2005

Reed, G. D., von Morze, C., Bok, R., Koelsch, B. L., van Criekinge, M., Smith, K. J., et al. (2014). High resolution (13)C MRI with hyperpolarized urea: *in vivo* T(2) mapping and (15)N labeling effects. *IEEE Trans. Med. Imaging* 33, 362–371. doi: 10.1109/TMI.2013.2285120

Reed, G. D., von Morze, C., Verkman, A. S., Koelsch, B. L., Chaumeil, M. M., Lustig, M., et al. (2015). Imaging renal urea handling in rats at millimeter resolution using hyperpolarized magnetic resonance relaxometry. arXiv:1511.00200.

Schmidt, R., Laustsen, C., Dumez, J. N., Kettunen, M. I., Serrao, E. M., Marco-Rius, I., et al. (2014). *In vivo* single-shot $^{13}$C spectroscopic imaging of hyperpolarized metabolites by spatiotemporal encoding. *J. Magn. Reson.* 240, 8–15. doi: 10.1016/j.jmr.2013.12.013

von Morze, C., Bok, R. A., Sands, J. M., Kurhanewicz, J., and Vigneron, D. B. (2012). Monitoring urea transport in rat kidney *in vivo* using hyperpolarized $^{13}$C magnetic resonance imaging. *Am. J. Physiol. Renal Physiol.* 302, F1658–F1662. doi: 10.1152/ajprenal.00640.2011

**Conflict of Interest Statement:** The author declares that the research was conducted in the absence of any commercial or financial relationships that could be construed as a potential conflict of interest.

# Advantages of publishing in Frontiers

**OPEN ACCESS**
Articles are free to read for greatest visibility and readership

**FAST PUBLICATION**
Around 90 days from submission to decision

**HIGH QUALITY PEER-REVIEW**
Rigorous, collaborative, and constructive peer-review

**TRANSPARENT PEER-REVIEW**
Editors and reviewers acknowledged by name on published articles

**Frontiers**
Avenue du Tribunal-Fédéral 34
1005 Lausanne | Switzerland

**Visit us:** www.frontiersin.org
**Contact us:** info@frontiersin.org | +41 21 510 17 00

**REPRODUCIBILITY OF RESEARCH**
Support open data and methods to enhance research reproducibility

**DIGITAL PUBLISHING**
Articles designed for optimal readership across devices

**FOLLOW US**
@frontiersin

**IMPACT METRICS**
Advanced article metrics track visibility across digital media

**EXTENSIVE PROMOTION**
Marketing and promotion of impactful research

**LOOP RESEARCH NETWORK**
Our network increases your article's readership